

RESEARCH ARTICLE

Epidemiology of capybara-associated Brazilian spotted fever

Hermes R. Luz^{1,2*}, Francisco B. Costa^{1,3}, Hector R. Benatti¹, Vanessa N. Ramos^{1,4}, Maria Carolina de A. Serpa¹, Thiago F. Martins¹, Igor C. L. Acosta¹, Diego G. Ramirez^{1,5}, Sebastián Muñoz-Leal¹, Alejandro Ramirez-Hernandez¹, Lina C. Binder¹, Marcio Port Carvalho⁶, Vlamir Rocha⁷, Thiago C. Dias^{7,8}, Camila L. Simeoni⁷, José Brites-Neto⁹, Jardel Brasil⁹, Ana Maria Nieves¹⁰, Patricia Ferreira Monticelli¹⁰, Maria Estela G. Moro¹¹, Beatriz Lopes¹², Daniel M. Aguiar¹³, Richard C. Pacheco¹³, Celso Eduardo Souza¹⁴, Ubiratan Piovezan^{15,16}, Raquel Juliano¹⁵, Katia Maria P. M. B. Ferraz¹², Matias P. J. Szabó¹⁷, Marcelo B. Labruna^{1*}



1 Departamento de Medicina Veterinária Preventiva e Saúde Animal, Faculdade de Medicina Veterinária e Zootecnia, Universidade de São Paulo, São Paulo, SP, Brazil, **2** Departamento de Patologia, Programa de Pós Graduação em Biotecnologia do Renorbio, Ponto Focal Maranhão, Universidade Federal do Maranhão, São Luís, MA, Brazil, **3** Departamento de Patologia, Faculdade de Medicina Veterinária, Universidade Estadual do Maranhão, São Luís, MA, Brazil, **4** Pós-Doutorado em Ciências Veterinárias, Faculdade de Medicina Veterinária, Universidade Federal de Uberlândia, Uberlândia, MG, Brazil, **5** Departamento de Parasitologia Animal, Instituto de Medicina Veterinária, Universidade Federal Rural do Rio de Janeiro, Seropédica, RJ, Brazil, **6** Instituto Florestal, São Paulo, SP, Brazil, **7** Centro de Ciências Agrárias, Universidade Federal de São Carlos, Araras, SP, Brazil, **8** Programa de Pós-graduação em Ecologia e Recursos Naturais, Centro de Ciências Biológicas e da Saúde, Universidade Federal de São Carlos, São Carlos, SP, Brazil, **9** Departamento de Vigilância Epidemiológica, Secretaria Municipal de Saúde, Americana, SP, Brazil, **10** Departamento de Psicologia, Faculdade de Filosofia, Ciências e Letras de Ribeirão Preto, Universidade de São Paulo, Ribeirão Preto, SP, Brazil, **11** Departamento de Zootecnia, Faculdade de Zootecnia e Engenharia de Alimentos, Universidade de São Paulo, Pirassununga, SP, Brazil, **12** Departamento de Ciências Florestais, Escola Superior de Agricultura Luiz de Queiroz, Universidade de São Paulo, Piracicaba, SP, Brazil, **13** Programa de Pós-graduação em Ciências Veterinárias, Faculdade de Medicina Veterinária, Universidade Federal de Mato Grosso, Cuiabá, MT, Brazil, **14** Laboratório de Carrapatos, Superintendência de Controle de Endemias, Mogi Guaçu, SP, Brazil, **15** Embrapa Pantanal, Corumbá, MS, Brazil, **16** Embrapa Tabuleiros Costeiros, Aracaju, SE, Brazil, **17** Laboratório de Ixodologia, Faculdade de Medicina Veterinária, Universidade Federal de Uberlândia, Uberlândia, MG, Brazil

OPEN ACCESS

Citation: Luz HR, Costa FB, Benatti HR, Ramos VN, de A. Serpa MC, Martins TF, et al. (2019) Epidemiology of capybara-associated Brazilian spotted fever. *PLoS Negl Trop Dis* 13(9): e0007734. <https://doi.org/10.1371/journal.pntd.0007734>

Editor: Job E Lopez, Baylor College of Medicine, UNITED STATES

Received: June 6, 2019

Accepted: August 26, 2019

Published: September 6, 2019

Copyright: © 2019 Luz et al. This is an open access article distributed under the terms of the [Creative Commons Attribution License](https://creativecommons.org/licenses/by/4.0/), which permits unrestricted use, distribution, and reproduction in any medium, provided the original author and source are credited.

Data Availability Statement: All relevant data are within the manuscript and its Supporting Information files.

Funding: Funding of this study was supported by Fundação de Amparo a Pesquisa do Estado de São Paulo. www.fapesp.br (MBL: FAPESP grant 2013/18046-7). Funder had no role in the study design, data collection and analysis, decision to publish, or preparation of the manuscript.

Competing interests: The authors have declared that no competing interests exist.

* hermesluz@usp.br (HRL); labruna@usp.br (MBL)

Abstract

Background

Brazilian spotted fever (BSF), caused by the bacterium *Rickettsia rickettsii*, has been associated with the transmission by the tick *Amblyomma sculptum*, and one of its main hosts, the capybara (*Hydrochoerus hydrochaeris*).

Methods

During 2015–2019, we captured capybaras and ticks in seven highly anthropic areas of São Paulo state (three endemic and four nonendemic for BSF) and in two natural areas of the Pantanal biome, all with established populations of capybaras.

Results

The BSF-endemic areas were characterized by much higher tick burdens on both capybaras and in the environment, when compared to the BSF-nonendemic areas. Only two tick

species (*A. sculptum* and *Amblyomma dubitatum*) were found in the anthropic areas; however, with a great predominance of *A. sculptum* ($\approx 90\%$ of all ticks) in the endemic areas, in contrast to a slight predominance of *A. dubitatum* ($\approx 60\%$) in the nonendemic areas. Tick species richness was higher in the natural areas, where six species were found, albeit with a predominance of *A. sculptum* ($\approx 95\%$ of all ticks) and environmental tick burdens much lower than in the anthropic areas. The BSF-endemic areas were characterized by overgrowth populations of *A. sculptum* that were sustained chiefly by capybaras, and decreased populations of *A. dubitatum*. In contrast, the BSF-nonendemic areas with landscape similar to the endemic areas differed by having lower tick burdens and a slight predominance of *A. dubitatum* over *A. sculptum*, both sustained chiefly by capybaras. While multiple medium- to large-sized mammals have been incriminated as important hosts for *A. sculptum* in the natural areas, the capybara was the only important host for this tick in the anthropic areas.

Conclusions

The uneven distribution of *R. rickettsii* infection among *A. sculptum* populations in highly anthropic areas of São Paulo state could be related to the tick population size and its proportion to sympatric *A. dubitatum* populations.

Author summary

Brazilian spotted fever (BSF), caused by the bacterium *Rickettsia rickettsii*, is the deadliest tick-borne disease of the New World. In southeastern Brazil, where 489 patients succumbed to the disease from 2001 to 2018, *R. rickettsii* is transmitted to humans mainly by the tick *Amblyomma sculptum*, which uses the capybara (*Hydrochoerus hydrochaeris*) as its main host. During 2015–2019, we captured capybaras and ticks in seven highly anthropic areas of São Paulo state (three endemic and four nonendemic for BSF) and in two natural areas of the Pantanal biome. The BSF-endemic areas were characterized by much higher tick burdens on both capybaras and in the environment, with a predominance of *Amblyomma sculptum*. In the BSF-nonendemic areas, another tick species, *Amblyomma dubitatum*, outnumbered *A. sculptum*. In the natural areas, six tick species were found; however, with much lower numbers than in the anthropic areas. The BSF-endemic areas were characterized by overgrowth populations of *A. sculptum* that were sustained chiefly by capybaras, and decreased populations of *A. dubitatum*. Results of this study support the idea that any intervention resulting in a drastic reduction of the *A. sculptum* population shall eliminate the *R. rickettsii* infection from the tick population, and consequently, prevent new BSF cases.

Introduction

Brazilian spotted fever (BSF), caused by the bacterium *Rickettsia rickettsii*, is the deadliest tick-borne disease of the New World. The disease is endemic in many parts of southeastern Brazil, especially in the state of São Paulo, where 978 laboratory-confirmed cases were recorded from 2001 to 2018, of which 489 (50%) had a fatal outcome (official data from the São Paulo State Health Secretary). In North America, where the *R. rickettsii*-caused disease is known as Rocky Mountain spotted fever (RMSF), multiple strains of *R. rickettsii* (including less virulent ones)

are known to occur. In contrast, a highly virulent strain prevails in Central and South America, which has been linked to the higher fatality rates of BSF, when compared to RMSF [1]. In addition, the greatest fatality of BSF is also evidenced by its neglected status in Brazil, such as the unavailability in the country of parenteral doxycycline, considered the first-choice medication to treat severe BSF or RMSF presenting vomiting or altered mental status [2, 3].

During this century, several studies have elucidated key factors in the epidemiology of BSF in southeastern Brazil, where *R. rickettsii* is transmitted to humans mainly by the tick *Amblyomma sculptum*. Besides being a competent vector, *A. sculptum* larvae, nymphs and adults are partially refractory to *R. rickettsii* infection, and less than half of the infected females transmit *R. rickettsii* to their offspring (transovarial transmission) [4–6]. This fact, associated to the higher mortality and lower reproductive performance of infected ticks, when compared to uninfected mates (5, 6), causes infection of *A. sculptum* by *R. rickettsii* in BSF-endemic areas to be very low, usually <1% [7–10]. Within this scenario, mathematical models have indicated that an *A. sculptum* population is not able to sustain a *R. rickettsii* infection for successive tick generations without the creation of new cohorts of infected ticks via horizontal transmission on vertebrate rickettsemic hosts (amplifying hosts) [11, 12]. In this case, the capybara (*Hydrochoerus hydrochaeris*), the largest living rodent in the world, has been pointed out as the major amplifying host of *R. rickettsii* for *A. sculptum* in most of the BSF-endemic areas of southeastern Brazil [11, 13, 14]. However, it is important to note that the tick *Amblyomma dubitatum* has also been frequently found infesting capybaras in southeastern Brazil, albeit with no direct role on BSF-epidemiology [7–10, 14, 15].

During the last four decades, the state of São Paulo has undergone extensive anthropogenic modifications in its landscape due to a rapid expansion of agricultural crops (especially sugar cane), deforestation, and creation of artificial water bodies [16, 17]. Such modifications have favored capybara reproduction primarily by higher food availability by agriculture (e.g., sugar cane, corn fields) and because of the local extinction of natural predators (e.g., the jaguar *Panthera onca*), in human-modified landscapes, leading to an increment on the extension and density of its populations [17–19]. Because capybara is considered to be the main host for *A. sculptum* in such landscapes [10, 15, 20], and at the same time an efficient *R. rickettsii* amplifying host [13], the increase of BSF incidence in the state of São Paulo during the last three decades has been associated to the afore mentioned anthropogenic modifications [11, 14, 21].

While the expansion of capybaras and their ticks have been well recognized in the state of São Paulo during the last decades, many of these human-modified landscapes have remained free of *R. rickettsii* circulation, despite of the established presence of capybaras and *A. sculptum* [22–24]. Since the reasons determining the establishment of *R. rickettsii* in a capybara-sustained *A. sculptum* population are not well understood, the present study aimed to characterize and to quantify in time and space the tick fauna in capybaras and in the habitats where these rodents occur among different human-modified landscapes in the state of São Paulo, either endemic or nonendemic for BSF. Differences in the tick fauna composition could be one of the possible multiple reasons driving the uneven distribution of *R. rickettsii* among different *A. sculptum* populations. In order to confirm the endemic or nonendemic status of each area, we determined the serological profile of the capybaras against a battery of rickettsial antigens, including *R. rickettsii*. For comparison purposes, we performed the same capybara and tick evaluations in pristine areas of the Pantanal biome of Brazil, where capybaras live in natural habitats in which landscape has suffered only minimal anthropogenic alterations and from where BSF has never been reported. Our results might provide some clues for a better understanding on the main epidemiological characteristics of the BSF-endemic areas associated to capybaras.

Methods

Ethical statements

This study has been approved by the Institutional Animal Care and Use Committee (IACUC) of the Faculty of Veterinary Medicine of the University of São Paulo (approval number 5948070314), in accordance with the regulations/guidelines of the Brazilian National Council of Animal Experimentation (CONCEA). Field capture of capybaras and collections of ticks were authorized by the Brazilian Ministry of the Environment (permit SISBIO Nos. 43259–6) and by the São Paulo Forestry Institute (Cotec permit 260108–000.409/2015).

Study areas

All study areas were inhabited by capybaras, and were classified into the following three epidemiological categories: (i) BSF-endemic areas—highly anthropic areas (human-modified landscape) in the state of São Paulo, where human cases of BSF have been recently confirmed and the transmissions have been epidemiologically associated with *A. sculptum*. Three BSF-endemic areas were sampled: Area 1 in the municipality of Piracicaba, Area 2 in the municipality of Americana, Area 3 in the municipality of Araras, all located in transition areas of the biomes Savannah and Atlantic Forest; (ii) BSF-nonendemic areas—highly anthropic areas (human-modified landscape) in the state of São Paulo, however, with no history of BSF. Four BSF-nonendemic areas were sampled: Areas 4 and 5 in the municipality of Pirassununga, located in a transition area of the biomes Savannah and Atlantic Forest, Area 6 in the municipality of Ribeirão Preto, located in the Savannah biome, and Area 7 in São Paulo municipality, in the Atlantic Forest biome; and (iii) natural areas—low anthropic areas (natural landscape) in the Pantanal biome, with no history of BSF. Two natural areas were sampled: Area 8 in Poconé municipality, state of Mato Grosso, and Area 9 in Corumbá municipality, state of Mato Grosso do Sul. We sampled capybaras and ticks in 3 BSF-endemic areas, 4 BSF-nonendemic areas, and 2 natural areas (S1 Table, Fig 1 and S1 Text).

Capybara sampling

During 2015–2018, we performed capture of capybaras in all study areas by using 16 to 20 m²–corrals baited with sugar cane and green corn. Once closed in the corral, every animal was physically restrained by a net catcher and anaesthetized with an intramuscular injection of a combination of ketamine (10 mg/kg) and xylazine (0.2 mg/kg). Under anesthesia, animals were weighed in an electronic balance (Pesola model PCS0300, Hatton Rock, UK) and identified with a subcutaneous microchip (Alflex model P/N 860005–001, Capalaba, Australia). In Mato Grosso do Sul, corrals were not effective, thus capybaras were captured by anesthetic darting via a CO₂-injection rifle (Dan-Inject model JM Standard, Denmark) by injecting the same chemicals above. Capybaras were sexed and aged as follows: young (<10 Kg), juvenile (10–35 Kg), and adult (>35 Kg), following Vargas et al. [25]. From each capybara, we collected blood samples through the femoral artery or cranial vena cava, and the serum was separated by centrifugation and stored frozen at -20°C until serological analysis (described below). Because many capybaras were heavily infested by ticks, we standardized a 3-min random collection of ticks from the entire body of every capybara. During the 3-min period, any tick on sight was collected, regardless of the size or part of capybara body. These ticks were brought to the laboratory, where they were identified to species following current literature [20, 26, 27]. After recovering from anesthesia, capybaras were released at the same capture site.

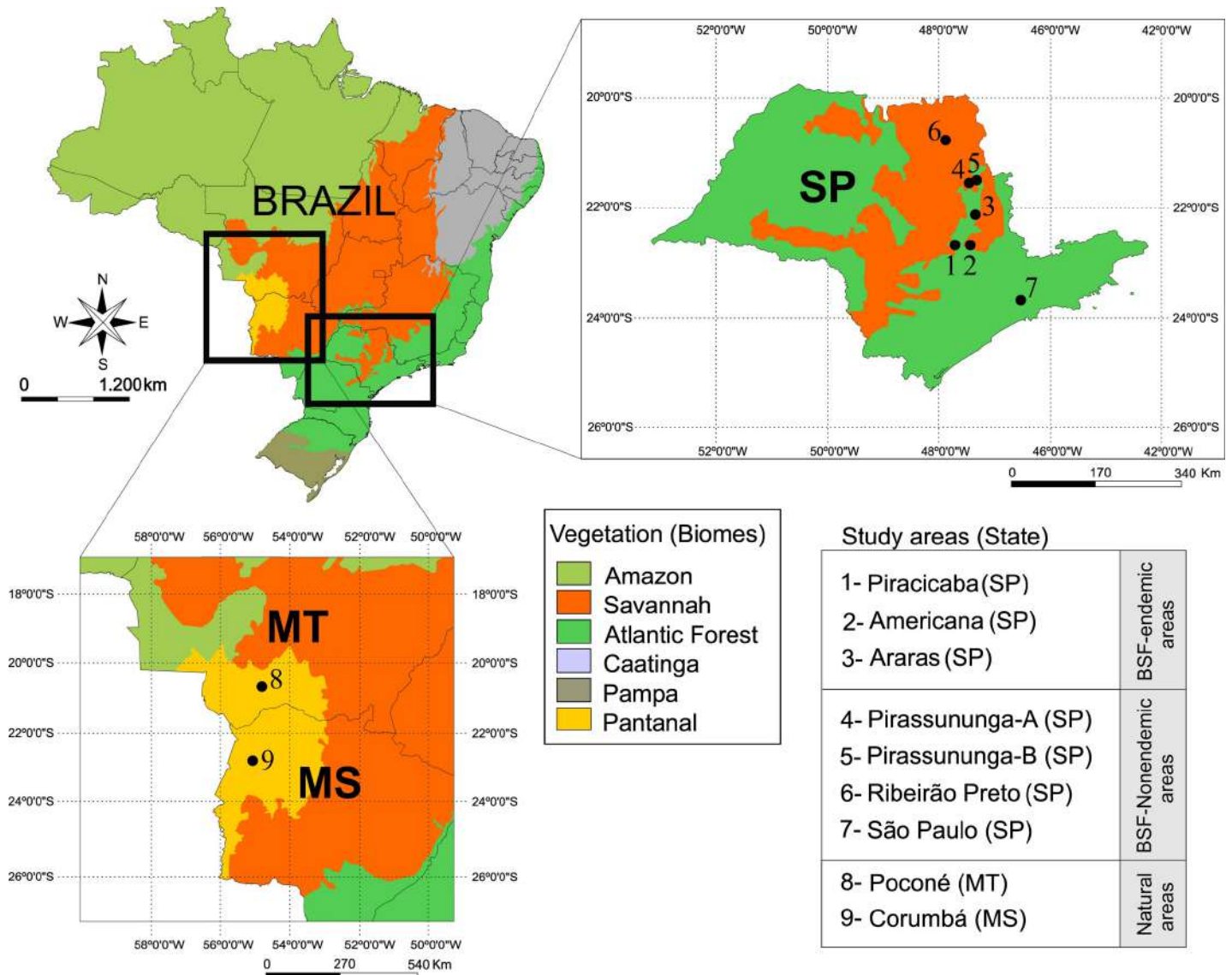


Fig 1. Areas where capybaras and ticks were sampled in the state of São Paulo (SP) (highly anthropic, low diversity areas), and in the states of Mato Grosso (MT) and Mato Grosso do Sul (MS) (low anthropic, high diversity areas). Map source was obtained from the “Instituto Brasileiro de Geografia e Estatística”(IBGE) website (www.ibge.gov.br) and the final figure was constructed with the use of CorelDraw Graphics Suite 2017.

<https://doi.org/10.1371/journal.pntd.0007734.g001>

Serological analysis

Capybara sera were tested by immunofluorescence assay (IFA) as described elsewhere [22] using rickettsial crude antigens derived from Vero cells (provided by the Instituto Adolfo Lutz, São Paulo, Brazil) infected with each of the following five *Rickettsia* species known to infect ticks in Brazil: *R. rickettsii* strain Taiacu [28], *Rickettsia parkeri* strain At24 [29], *Rickettsia amblyommatis* strain Ac37 [30], *Rickettsia rhipicephali* strain HJ5 [31], and *Rickettsia bellii* strain Mogi [28]. In addition, a sixth rickettsial antigen consisted of C6/36 cells (provided by the Instituto Adolfo Lutz, São Paulo, Brazil) infected with *Rickettsia felis* strain Pedreira, was also implemented [32]. In each slide, a serum previously shown to be non-reactive (negative control) and a known reactive serum (positive control) from a previous study [13] were included. Slides were incubated with fluorescein isothiocyanate-labeled sheep anti-capybara

IgG (produced by the Centro de Controle de Zoonoses, São Paulo City). For each sample, the endpoint titer reacting with each of the six *Rickettsia* antigens was determined. Sera showing an antibody titer to a *Rickettsia* species at least fourfold higher than the titers observed for the other *Rickettsia* species were supposed to be homologous to the first *Rickettsia* species or to a very closely related genotype, as previously determined for several animal species [33–35], including capybaras [22].

Collection of host-questing ticks

Host questing ticks were collected in each of the nine study areas (Fig 1, S1 Table) during four consecutive years. Our schedule for collection of free-living ticks was based on the seasonal dynamics of *A. sculptum*, which is known to complete one generation per year, with larvae peaking during autumn, nymphs during spring, and adults during summer [36–38]. Therefore, between May 2015 and January 2019, ticks were collected in each area during the larval peak (May–June), nymphal peak (August–September) and adult peak (January–February) of every year. In each area at each time point, a 1 m² white flannel was dragged over 800 m of animal trails. With this procedure, every dragging event on a given area represented the number of ticks for an 800 m²-sampled area. Collected nymphs and adults were immediately put in plastic vials containing 70% ethanol, except for a few adult ticks that were placed in dry plastic vials and taken alive to the laboratory, where they were kept frozen at -80°C until molecular analysis for *Rickettsia* (described below). Every time a larval cluster was captured by dragging, the cluster was immediately picked up with a 5 cm-large transparent plastic adhesive tape, which was then stuck on a white paper that was put within a sealed plastic bag and taken to the laboratory. Adult and nymphal ticks were counted individually and identified to species according to [20, 26, 27]. Larvae were counted as number of clusters, since it was assumed that each larval cluster represented the offspring of one engorged female [38, 39]. Larval taxonomic identification consisted of comparing side-by-side individuals of a larval cluster with laboratory-reared larvae of *A. sculptum* and *A. dubitatum*, following established criteria [40, 41].

Host-questing ticks were also collected by dry ice traps following Szabó et al. [39]; however, this method was used only at one time point (August 2015) in each area, and had to be discontinued due to logistic difficulties. In each area, 20 to 40 dry ice traps were set at 10 m intervals along the same trails that were sampled by dragging. Collected ticks were immediately placed in 70% ethanol, and taken to the laboratory for taxonomic identification as described above.

Rickettsial detection in ticks

Frozen unfed adult ticks, previously collected by dragging in each area, were thawed and individually submitted to DNA extraction by the guanidine isothiocyanate-phenol technique [42]. Extracted DNA samples were firstly tested by a conventional PCR protocol targeting the tick mitochondrial 16S rRNA gene, as previously described [43], in order to certify successful DNA extraction. Then, viable DNA samples (those positive by the tick 16S rRNA PCR assay) were tested by a Taqman real-time PCR assay targeting the rickettsial *gltA* gene, as described [5]. The sensitivity of this PCR assay was determined to be 1 DNA copy of *R. rickettsii* [44]. Positive samples by this Taqman real-time PCR were tested by two protocols of conventional PCR, one targeting a 401-bp fragment of the rickettsial *gltA* gene [44], and one heminested PCR assay targeting the *ompA* gene; this latter protocol consisted of a first reaction targeting a 631-bp fragment, and a second targeting a 532-bp fragment, as described [45]. PCR products were DNA-sequenced and the resultant sequences were submitted to BLASTn analyses (www.ncbi.nlm.nih.gov/blast) in order to confirm the identity of the *Rickettsia* species.

Data analyses

The proportions of seroreactive capybaras for *R. rickettsii* were compared between the nine sampled areas by the Chi-square test. Endpoint titers for the six *Rickettsia* species were compared between BSF-endemic and BSF-nonendemic areas by the Mann-Whitney test. For the ticks collected on capybaras, we calculated the prevalence (No. infested hosts / No. examined capybaras x 100), and the mean abundance of tick infestation (total number of collected ticks / number of examined capybaras) according to [46] in each of the 9 study areas.

Density of host-questing ticks was calculated for the total dragged area (TDA). For this purpose, TDA = number of dragging events performed in one area during the four years of study x 800m² (considering that each dragging event encompassed an 800m² area in each of the study areas). Then, the tick density (TD), represented by number of host-questing ticks per 1,000 m², was calculated by: TD = total number of collected ticks / TDA x 1,000 m². These calculations were applied to the two most abundant tick species, *A. sculptum* and *A. dubitatum*. TD was calculated separately for larvae, nymphs, and adult ticks for the whole study period, as well as for the period of larval peak (all collections during autumn), nymphal peak (all collections during winter), and adult peak (all collections during summer).

For statistical analyses, we pooled the tick data for each of the three epidemiological categories: (i) BSF-endemic areas, (ii) BSF-nonendemic areas, and (iii) natural areas. The Chi-square test was used to compare the differences between the proportions of ticks on capybaras or host-questing ticks between the three epidemiological categories (BSF-endemic, BSF-nonendemic, natural areas). The Lilliefors test implemented in the PAST 3.19 program was used to analyze the normality of the data in order to choose the appropriate statistical test for each situation. Values of mean abundance of tick infestation were analyzed using the Kruskal-Wallis non-parametric test. For all tests, the level of significance was 5%. Analyses were performed by using PAST Version 3.19 and BioEstat 5.0.

Results

Captured capybaras

A total of 347 capybaras were captured during the 2015–2018 period. The number of captured capybaras per each of the nine areas varied from 14 to 73 (mean: 38.6). Since we sampled during four consecutive years, some individuals were captured twice among different years; recaptured capybaras represented 0 to 50% of the total number of captures in each area (Table 1). Removing recaptured animals, the total number of different individuals sampled in this study was 287; however, we considered all recaptures as different units for our analyses of serology and tick infestations (described below), since recaptures occurred in years different from the first capture. The 347 captured capybaras were represented by 94 (27%) males and 253 (73%) females. They were aged as 27 (7.8%) young, 70 (20.2%) juvenile, and 250 (72%) adults (Table 1).

Serology of capybaras

Among the 347 captured capybaras, sera were collected from 337, which were tested by IFA against six *Rickettsia* species (Table 2). Considering the three epidemiological categories, the proportions of seropositive capybaras for *R. rickettsii* in the 3 BSF-endemic areas (88 to 98%) were significantly higher ($P < 0.05$) than the proportions in the 4 BSF-nonendemic areas (14 to 38%) and in the natural area of Corumbá (47%); the proportions for *R. rickettsii* in the later 5 areas were statistically similar ($P > 0.05$). While the proportion of seropositive capybaras in the natural area of Poconé (100%) was similar ($P > 0.05$) to the BSF-endemic areas, the endpoint

Table 1. Capybaras captured in nine areas during 2015–2018.

Areas	Captured capybaras			Gender		Age		
	Total No. captures	No. different individuals	No. recaptures (%)	Males	Females	Young	Juvenile	Adult
BSF-endemic areas								
1-Piracicaba	65	48	17 (26)	9	56	3	10	52
2-Americana	23	20	3 (13)	12	11	0	7	16
3-Araras	41	36	5 (12)	7	34	8	7	26
BSF-nonendemic areas								
4-Pirassununga-A	26	22	4 (15)	10	16	1	4	21
5-Pirassununga-B	73	68	5 (7)	19	54	8	9	56
6-Ribeirão Preto	48	37	11 (23)	16	32	4	24	20
7-São Paulo	14	14	0 (0)	4	10	2	1	11
Natural areas								
8-Poconé	26	13	13 (50)	9	17	0	6	20
9-Corumbá	31	29	2 (6)	8	23	1	2	28
TOTAL	347	287	60 (17)	94 (27%)	253 (73%)	27 (7.8%)	70 (20.2%)	250 (72.0%)

<https://doi.org/10.1371/journal.pntd.0007734.t001>

titers to *R. rickettsii* were quite different, with much higher values for the BSF-endemic areas (S2 Table). In fact, 56 capybaras of the 3 BSF-endemic areas had endpoint titers for *R. rickettsii* at least fourfold higher than the titers for the remaining five *Rickettsia* species, indicating that these capybaras were likely infected by *R. rickettsii* (Table 2). Using these same criteria, no

Table 2. Results of immunofluorescence assay for six *Rickettsia* species in capybaras from 9 localities, being 3 Brazilian spotted fever (BSF)-endemic areas, 4 BSF-nonendemic areas, and 2 natural areas.

Areas	No. capybaras tested	No. seroreactive capybaras to each of the <i>Rickettsia</i> species (% seroreactivity for the area)						No. capybaras with determined homologous reaction (PAIHR in parentheses) ^a
		<i>Rickettsia rickettsii</i> ^b	<i>Rickettsia parkeri</i>	<i>Rickettsia amblyommatis</i>	<i>Rickettsia rhipicephali</i>	<i>Rickettsia bellii</i>	<i>Rickettsia felis</i>	
BSF-endemic areas								
1-Piracicaba	64	63 (98) a	62 (97)	56 (87)	55 (86)	54 (84)	27 (42)	35 (<i>R. rickettsii</i>), 4 (<i>R. bellii</i>), 2 (<i>R. amblyommatis</i>)
2-Americana	23	22 (97) a	21 (91)	15 (65)	14 (61)	20 (87)	11 (48)	8 (<i>R. rickettsii</i>), 1 (<i>R. bellii</i>)
3-Araras	33	29 (88) a	25 (76)	18 (55)	19 (58)	24 (73)	9 (27)	13 (<i>R. rickettsii</i>), 7 (<i>R. bellii</i>)
BSF-nonendemic areas								
4-Pirassununga-A	26	10 (38) b	8 (31)	9 (35)	10 (38)	14 (54)	6 (23)	9 (<i>R. bellii</i>)
5-Pirassununga-B	73	26 (36) b	14 (19)	11 (15)	13 (18)	32 (44)	10 (14)	11 (<i>R. bellii</i>)
6-Ribeirão Preto	48	14 (29) b	9 (19)	13 (27)	9 (19)	25 (52)	4 (8)	10 (<i>R. bellii</i>), 1 (<i>R. amblyommatis</i>)
7-São Paulo	14	2 (14) b	1 (7)	2 (14)	4 (26)	7 (50)	0 (0)	6 (<i>R. bellii</i>)
Natural areas								
8-Poconé	26	26 (100) a	26 (100)	24 (92)	23 (88)	25 (96)	20 (77)	7 (<i>R. amblyommatis</i>), 5 (<i>R. parkeri</i>), 1 (<i>R. bellii</i>)
9-Corumbá	30	14 (47) b	11 (37)	11 (37)	7 (23)	17 (57)	0 (0)	10 (<i>R. bellii</i>), 2 (<i>R. amblyommatis</i>)

^a homologous reaction was determined when an endpoint titer to a *Rickettsia* species was at least 4-fold higher than those observed for the other *Rickettsia* species. In this case, the *Rickettsia* species involved in the highest endpoint titer was considered the possible antigen involved in a homologous reaction (PAIHR).

^b different letters in this column mean significantly different ($P < 0.05$) proportions of seroreactive capybaras for *R. rickettsii*.

<https://doi.org/10.1371/journal.pntd.0007734.t002>

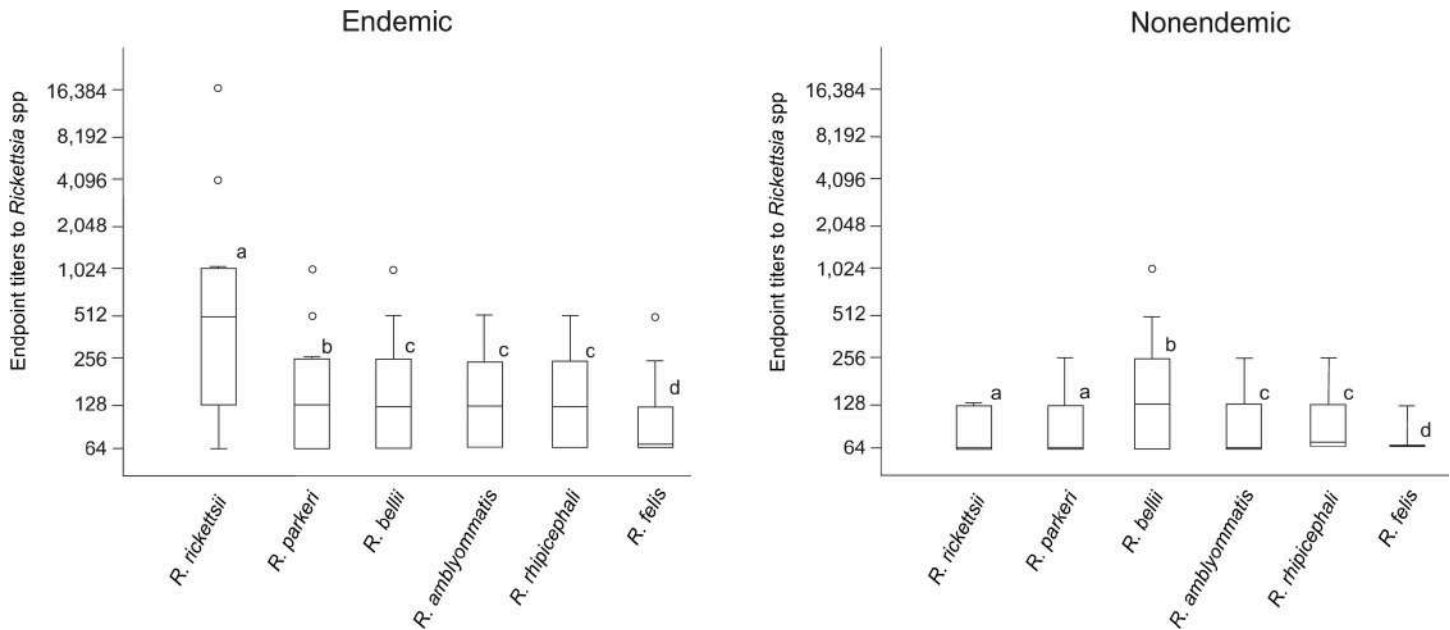


Fig 2. Boxplot representing the serological endpoint titers for six *Rickettsia* species of capybaras from Brazilian spotted fever (BSF)-endemic areas and BSF-nonendemic areas. Different lower case letters mean statistically different ($P < 0.05$) endpoint titers between *Rickettsia* species in endemic or nonendemic areas.

<https://doi.org/10.1371/journal.pntd.0007734.g002>

capybara from either BSF-nonendemic or natural areas were considered to have been infected by *R. rickettsii*, whereas 12, 36, and 11 capybaras from BSF-endemic, BSF-nonendemic, and natural areas, respectively, were probably infected by *R. bellii*; and two, one and nine capybaras from BSF-endemic, BSF-nonendemic, and natural areas, respectively, were probably infected by *R. amblyommatis*. In addition, five capybaras from the natural area of Poconé were likely infected by *R. parkeri* (Table 2). While the endpoint titers of the capybaras from the BSF-endemic areas were significantly higher for *R. rickettsii* than for the remaining five *Rickettsia* species, in the BSF-nonendemic areas the endpoint titers were significantly higher for *R. bellii* (Fig 2).

Ticks on capybaras

Capybaras in the seven anthropic areas of the state of São Paulo (BSF-endemic and BSF-nonendemic areas) were infested by two tick species, *A. sculptum* and *A. dubitatum*. Among the two natural areas in the Pantanal biome, *A. sculptum* was the only species infesting capybaras in the Corumbá area, while *A. sculptum*, *A. dubitatum* and *Amblyomma triste* were found on capybaras in the Poconé area. Tick prevalence on capybaras was 100% in all seven anthropic areas, and 95% in natural areas, where only three capybaras did not have any tick. For data comparison, we excluded the 27 young capybaras (Table 1) because they were usually infested by low number of ticks (mean abundance: 15.3 ticks/capybara), when compared to the overall mean abundance of 31.8 ticks/capybara among adults and juveniles. The overall mean abundance of ticks was significantly higher ($P < 0.05$) in the BSF-endemic areas (40.9 ticks/capybara) than in the BSF-nonendemic areas (33.7 ticks/capybara), which was also significantly higher ($P < 0.05$) than the mean abundance in the natural areas (7.7 ticks/capybara) (Table 3 and Fig 3). *Amblyomma sculptum* was the dominant tick species in the BSF-endemic areas, where they represented 85% (4,091/4,821) of all ticks collected from capybaras (Table 3) and had the highest mean abundance values (Fig 4). In contrast, *A. dubitatum* was the

Table 3. Ticks collected on capybaras in 9 localities, being 3 Brazilian spotted fever (BSF)-endemic areas, 4 BSF-nonendemic areas, and 2 natural areas during 2015–2018.

Areas	N	P	MA ^a	No. ticks according to species and stage									Total
				<i>Amblyomma sculptum</i>			<i>Amblyomma dubitatum</i>			<i>Amblyomma triste</i>		<i>Amblyomma</i> sp.	
				nymphs	females	males	nymphs	females	males	females	males	larvae	
BSF-endemic areas													
1-Piracicaba	62	100	39.7	987	665	491	191	76	32			17	2,459
2-Americana	23	100	44.1	325	216	250	137	60	26			1	1,015
3-Araras	33	100	40.8	705	265	187	114	58	18				1,347
Total	118	100	40.9 a	2,017	1,146	928	442	194	76			18	4,821
BSF-nonendemic areas													
4-Pirassununga-A	25	100	33.7	75	147	106	382	70	43			19	842
5-Pirassununga-B	65	100	30.1	197	145	187	720	369	338				1,956
6-Ribeirão Preto	44	100	37.6	410	110	85	671	239	135			4	1,654
7-São Paulo	12	100	38.5	31	5	3	198	103	122				462
Total	146	100	33.7 b	713	407	381	1,971	781	638			23	4,914
Natural areas													
8-Poconé	26	92	10.9	53	72	109	3	17	18	2	9		283
9-Corumbá	30	97	4.9	88	28	30							146
Total	56	95	7.7 c	141	100	139	3	17	18	2	9		429
Total (9 areas)	320	99	31.8	2,871	1,653	1,448	2,416	992	732	2	9	41	10,164

N: Number of examined capybaras; P: prevalence = No. infested capybaras / No. examined capybaras x 100; MA: mean abundance of tick infestation = total No. collected ticks / No. examined capybaras.

^a different letters in this column mean significantly different ($P < 0.05$) MA values between the three epidemiological categories.

<https://doi.org/10.1371/journal.pntd.0007734.t003>

dominant species in the BSF-nonendemic areas, where they encompassed 69% (3390/4914) of all ticks collected on capybaras (Table 3) and had the highest mean abundance values (Fig 4). Mean abundance values of either *A. sculptum* or *A. dubitatum* were significantly different ($P < 0.05$) between BSF-endemic and BSF-nonendemic areas (Fig 5). In the natural areas, *A. sculptum* was the dominant tick species (88%; 380/429); however, with a mean abundance of only 6.8 *A. sculptum* ticks/capybara, contrasting to the mean abundance of 34.7 and 10.2 *A. sculptum* ticks/capybara in the BSF-endemic and BSF-nonendemic areas, respectively.

Host-questing ticks

Host questing ticks were collected along four consecutive years, during the activity peaks of larvae (autumn), nymphs (winter) and adults (summer) of *A. sculptum* in each year. In the anthropic area of São Paulo (area no. 7), dragging was performed only at two instances during the first year (2015); thereafter, this area had to be discontinued from the study due to a highly fatal outbreak of fascioliasis that decimated the capybara population of the area [47], what certainly impacted the environmental tick burdens in the subsequent years. In the remaining six anthropic areas of the state of São Paulo (areas no 1 to 6), dragging was not possible only during the adult tick season of the 2016 summer, due to personal problems beyond our control. In the two natural areas (Poconé and Corumbá), dragging was not possible at two occasions in each area due to logistic problems related to road conditions and access to both areas. Overall, dragging was performed at 11 occasions in each of the three BSF-endemic areas, at 11 occasions in two BSF-nonendemic areas (Pirassununga A and Pirassununga B), at 20 occasions in the BSF-nonendemic area of Ribeirão Preto, at 19 occasions in the natural area of Poconé, and at 16 occasions in the natural area of Corumbá.

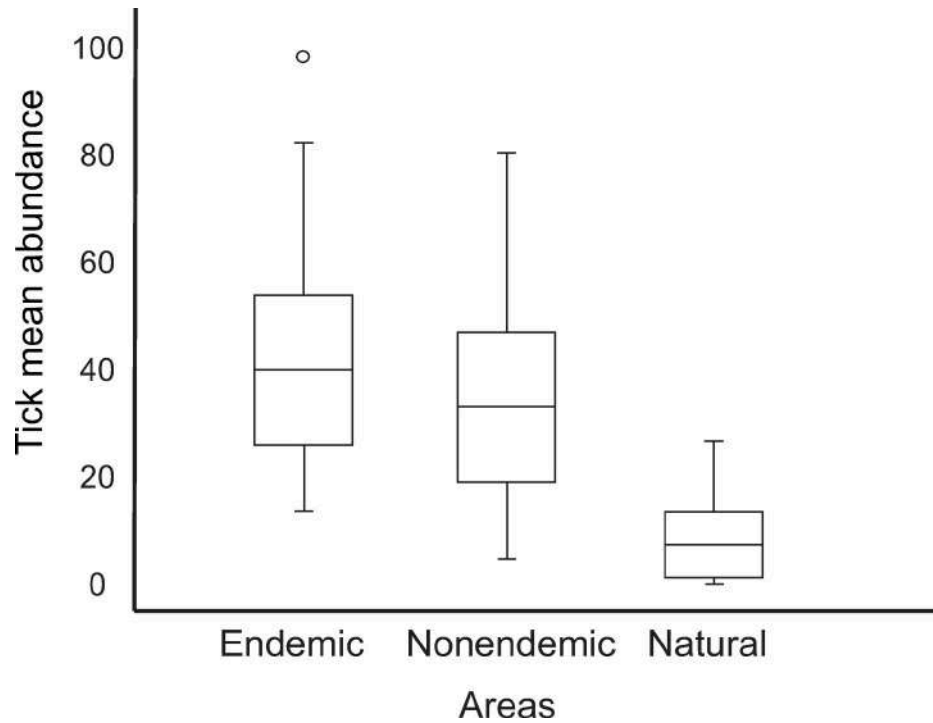


Fig 3. Boxplot representing the mean abundance of total tick infestations of capybaras from Brazilian spotted fever (BSF)-endemic areas, BSF-nonendemic areas, and natural areas.

<https://doi.org/10.1371/journal.pntd.0007734.g003>

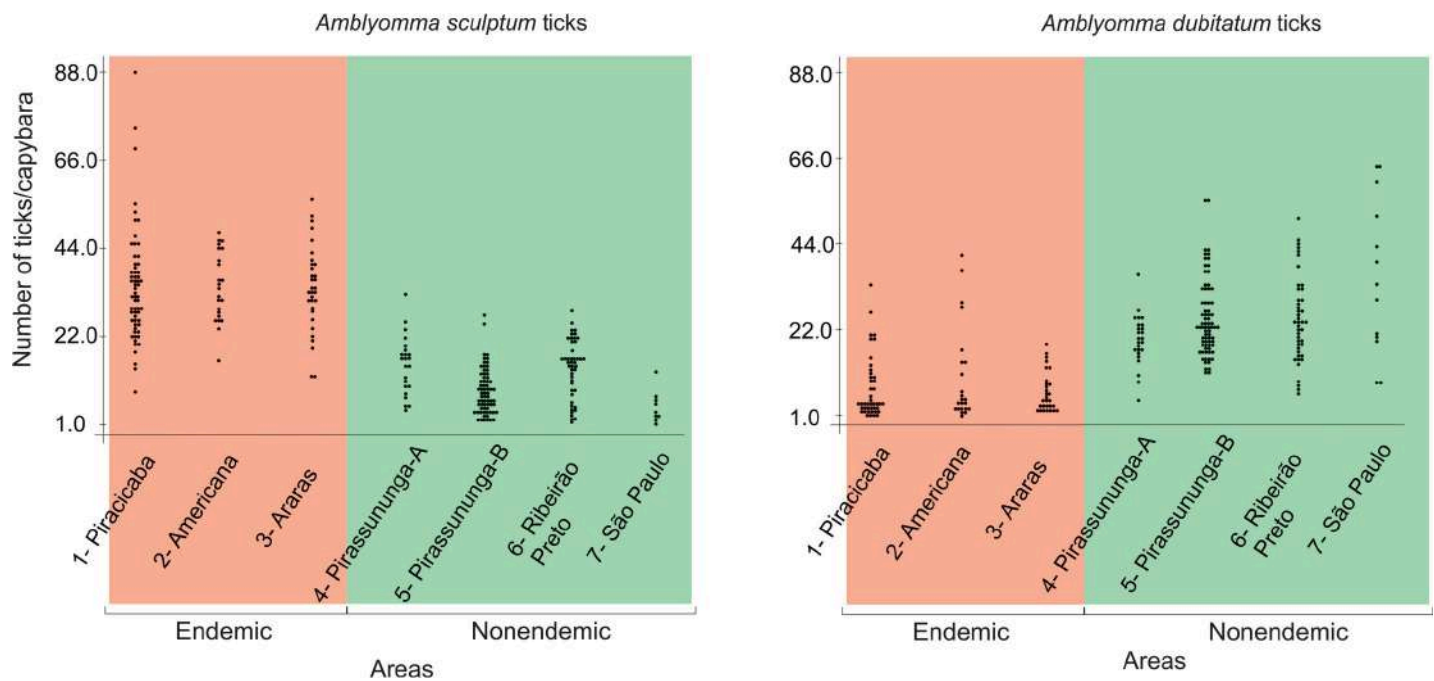


Fig 4. Dotplot representing the number of *Amblyomma sculptum* and *Amblyomma dubitatum* ticks per capybara among 3 Brazilian spotted fever (BSF)-endemic areas, and 4 BSF-nonendemic areas.

<https://doi.org/10.1371/journal.pntd.0007734.g004>

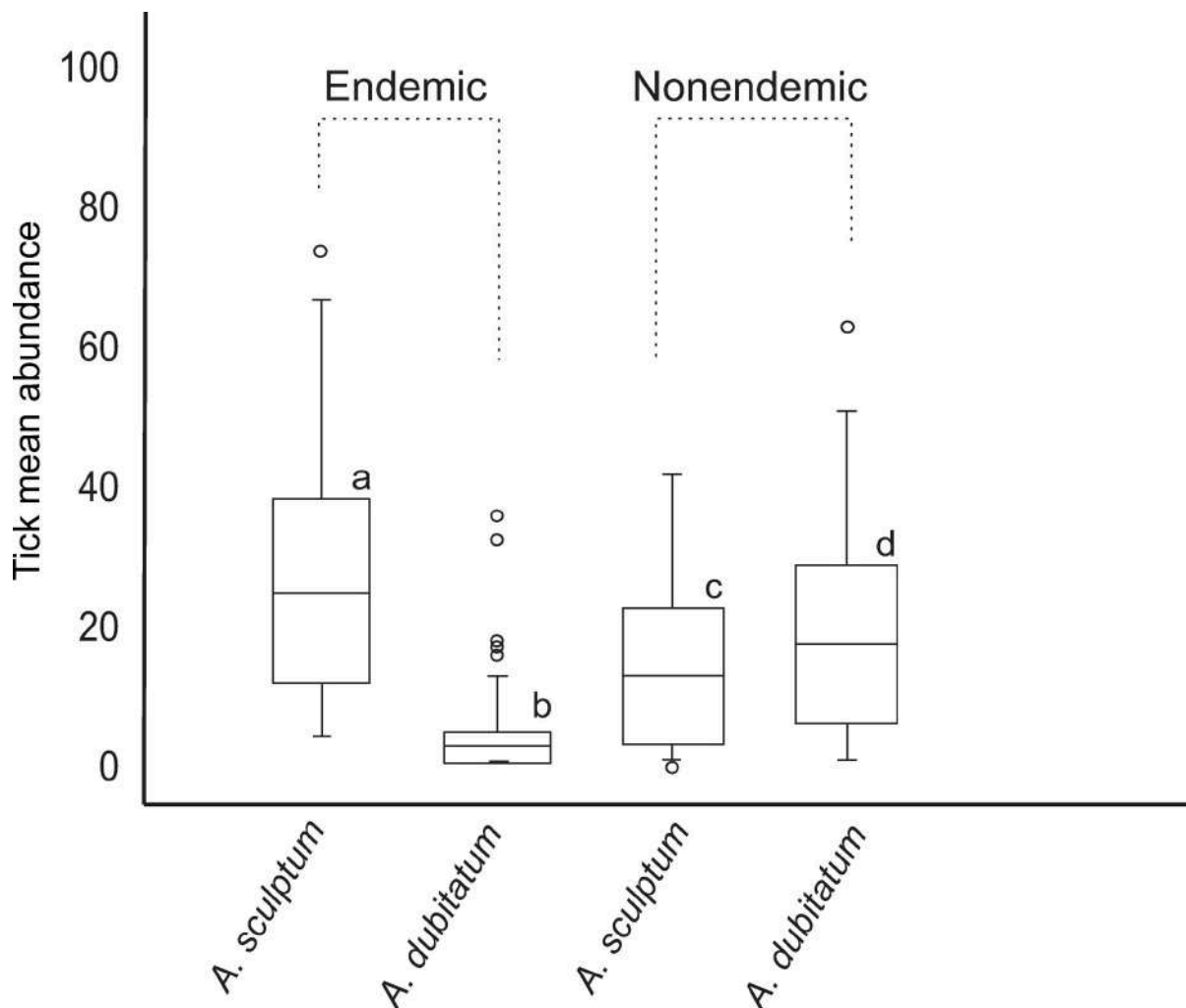


Fig 5. Boxplot representing the mean abundance of *Amblyomma sculptum* and *Amblyomma dubitatum* infestations of capybaras from Brazilian spotted fever (BSF)-endemic areas and BSF-nonendemic areas. Different lower case letters mean statistically different ($P < 0.05$) mean abundance values of either *A. sculptum* or *A. dubitatum* between endemic and nonendemic areas.

<https://doi.org/10.1371/journal.pntd.0007734.g005>

A total of 21,670 ticks were collected by dragging in all areas during the study. In the anthropic areas, only two tick species were identified, *A. sculptum* and *A. dubitatum*. In the natural areas, the following six tick species were collected: *A. sculptum*, *A. dubitatum*, *Amblyomma parvum*, *A. triste*, *Amblyomma ovale*, and *Ornithodoros rostratus* (Table 4). In the BSF-endemic areas, the proportions of *A. sculptum* and *A. dubitatum* were 92% (10,425/11,305) and 8% (880/11,305), respectively. In contrast, the proportions of *A. sculptum* and *A. dubitatum* in the BSF-nonendemic areas were 43% (3,688/8,633) and 57% (4,945/8,633), respectively. These proportions were significantly different ($P < 0.05$) between the two epidemiological categories. In the natural areas, *A. sculptum* represented 98% (1,694/1,732) of all collected ticks, a proportion significantly different ($P < 0.05$) from the two categories of anthropic areas.

Tick density (TD) values, represented by the number of host-questing ticks per 1,000 m², were calculated for the two most abundant tick species, *A. sculptum* and *A. dubitatum*, in all areas. Grouping all dragging occasions during the four years, TD of *A. sculptum* larvae,

Table 4. Host-questing ticks collected by dragging during 2015–2019 in 9 localities, being 3 Brazilian spotted fever (BSF)-endemic areas, 4 BSF-nonendemic areas, and 2 natural areas.

Areas	No. ticks according to species and stage											Total
	<i>Amblyomma sculptum</i>			<i>Amblyomma dubitatum</i>			<i>Amblyomma parvum</i>		<i>Amblyomma triste</i>	<i>Amblyomma ovale</i>	<i>Ornithodoros rostratus</i>	
	Larval clusters	nymphs	adults	Larval clusters	nymphs	adults	nymphs	adults	adults	adults	nymphs	
BSF-endemic areas												
1-Piracicaba	131	1,646	887	10	196	49						2,919
2-Americana	119	2,781	1,464	11	288	27						4,690
3-Araras	117	2,576	704	9	261	29						3,696
Total	367	7,003	3,055	30	745	105						11,305
BSF-nonendemic areas												
4-Pirassununga-A	48	461	132	61	276	221						1,199
5-Pirassununga-B	56	1,143	118	81	1,464	151						3,013
6-Ribeirão Preto	159	1,218	342	161	2,143	351						4,374
7-São Paulo		5	6		15	21						47
Total	263	2,827	598	303	3,898	744						8,633
Natural areas												
8-Poconé	48	618	139		2				12	2		821
9-Corumbá	65	672	152				15	2		1	4	911
Total	113	1,290	291		2		15	2	12	3	4	1,732
Total (9 areas)	743	11,120	3,944	333	4,645	849	15	2	12	3	4	21,670

<https://doi.org/10.1371/journal.pntd.0007734.t004>

nymphs and adults were higher in BSF-endemic areas than in BSF-nonendemic and natural areas, with some significant ($P < 0.05$) differences (Table 5 and Fig 6). Comparisons of TD values of *A. sculptum* with those of *A. dubitatum* revealed significantly higher values ($P < 0.05$) for larvae, nymphs and adults of the former species in the BSF-endemic areas. On the other hand, *A. sculptum* and *A. dubitatum* had similar ($P > 0.05$) larval, nymphal and adult TD among the BSF-nonendemic areas (S2 Table). Because only two *A. dubitatum* nymphs were collected by dragging in the natural areas (Table 4), TD values were not statistically compared with *A. sculptum* in these areas.

Grouping the dragging occasions that were performed during only the autumn season (larval peak) of the four years, larval TD of *A. sculptum* in the BSF-endemic areas (31.8 larval clusters/1,000 m²) was ≈ 2 times higher ($P < 0.05$) than in the BSF-nonendemic areas (15.1 larval clusters/1,000 m²), and ≈ 3 times higher ($P < 0.05$) than in the natural areas (9.1 larval clusters/1,000 m²). On the other hand, larval TD of *A. dubitatum* in the BSF-endemic areas (2.7 larval clusters/1,000 m²) was about ≈ 4 times lower ($P < 0.05$) than in the BSF-nonendemic areas (13.8 larval clusters/1,000 m²) (Table 6 and Fig 6).

During the winter season (nymphal peak) of the four years, nymphal TD of *A. sculptum* in the BSF-endemic areas (703.9 nymphs/1,000 m²) was ≈ 3.5 times higher ($P < 0.05$) than in the BSF-nonendemic areas (199.6 nymphs/1,000 m²), and ≈ 9 times higher ($P < 0.05$) than in the natural areas (86.7 nymphs/1,000 m²). On the other hand, nymphal TD of *A. dubitatum* in the BSF-endemic areas (72.1 nymphs/1,000 m²) was about ≈ 3.5 times lower ($P < 0.05$) than in the BSF-nonendemic areas (262.3 nymphs/1,000 m²) (Table 7 and Fig 6).

During the summer season (adult peak) of the four years, adult TD of *A. sculptum* in the BSF-endemic areas (311.8 adults/1,000 m²) was ≈ 6 times higher ($P < 0.05$) than in the BSF-nonendemic areas (52.3 adults/1,000 m²), and ≈ 14 times higher ($P < 0.05$) than in the natural

Table 5. Density of host-questing ticks in 9 localities [3 Brazilian spotted fever (BSF)-endemic areas, 4 BSF-nonendemic areas, and 2 natural areas] during 2015–2019. In each area, dragging was performed up to three times a year, each at autumn, winter and summer seasons.

Areas	Total area dragged (m ²)	Tick density (per 1,000 m ²) ^a					
		<i>Amblyomma sculptum</i>			<i>Amblyomma dubitatum</i>		
		Adults	nymphs	Larvae	Adults	Nymphs	Larvae
BSF-endemic areas							
1-Piracicaba	8,800	100.8	187.1	14.9	5.6	22.3	1.1
2-Americana	8,800	166.4	316.0	13.5	3.1	32.7	1.3
3-Araras	8,800	80.0	292.7	13.3	3.3	29.7	1.0
Total	26,400	115.7^{A,a}	265.3^{A,a}	13.9^{A,a}	4.0^{A,b}	28.2^{A,b}	1.1^{A,b}
BSF-nonendemic areas							
4-Pirassununga-A	8,800	15.0	52.4	5.5	25.1	31.4	6.9
5-Pirassununga-B	8,800	13.4	129.9	6.4	17.2	166.4	9.2
6-Ribeirão Preto	16,000	21.4	76.1	9.9	21.9	133.9	10.1
7-São Paulo	1,600	3.8	3.1	0.0	13.1	9.4	0.0
Total	35,200	17.0^{B,a}	80.3^{A,a}	7.5^{A,a}	21.1^{B,a}	110.4^{B,a}	8.6^{B,a}
Natural areas							
8-Poconé	15,200	9.1	40.7	3.2	0	0.1	0
9-Corumbá	12,800	11.9	52.5	5.1			
Total	28,000	10.4^B	46.1^A	4.0^B	0	0.1	0

^a different capital letters in each column mean significantly different ($P < 0.05$) tick density values between the three epidemiological categories (BSF-endemic areas, BSF-nonendemic areas, Natural area); different lowercase letters in each line mean significantly different ($P < 0.05$) tick density values of adults or nymphs or larvae between *A. sculptum* and *A. dubitatum*.

<https://doi.org/10.1371/journal.pntd.0007734.t005>

areas (22 adults/1,000 m²). On the other hand, adult TD of *A. dubitatum* in the BSF-endemic areas (12.1 adults/1,000 m²) was about ≈4 times lower ($P < 0.05$) than in the BSF-nonendemic areas (50.9 adults/1,000 m²) (Table 8 and Fig 6).

During autumn, winter and summer, TD values of larvae, nymphs and adults, respectively, were always higher ($P < 0.05$) for *A. sculptum* than for *A. dubitatum* in the BSF-endemic areas, but at the same time similar ($P > 0.05$) between the two tick species in the BSF-nonendemic areas (Tables 6–8).

A total of 8,790 ticks were collected by 220 dry ice traps during August 2015 in all areas of the study (S3 Table). In the BSF-endemic areas, the mean number of *A. sculptum* ticks per trap was 35.4, ≈3.5 times higher than the mean number of *A. dubitatum* ticks per trap (9.4). In the BSF-nonendemic areas, the mean numbers of *A. sculptum* and *A. dubitatum* per trap were similar, 25.2 and 23.8, respectively. In the natural areas, we collected on average 6.3 *A. sculptum*/trap and 0.3 *A. dubitatum*/trap, in addition to two other species, *A. parvum* (0.1 ticks/trap) and *O. rostratus* (0.2 ticks/trap).

Rickettsial detection in ticks

A total of 216 host-questing adults of *A. sculptum* [24 from each of 8 sampled areas (ticks from the BSF-nonendemic area of São Paulo were not included)] were tested individually for the presence of rickettsial DNA, but none of them contained rickettsia. On the other hand, rickettsial DNA was successfully amplified in 4 (29%) out of 14 *A. parvum* ticks from Corumbá, and in 2 (17%) out of 12 *A. triste* from Poconé. The rickettsial DNA amplified from all four *A. parvum* ticks was identified as ‘*Candidatus Rickettsia andeanae*’; i.e., their *gltA* and *ompA* partial sequences were 100% identical to the corresponding sequences of this agent in GenBank (KF030931 and KF030932, respectively). The *gltA* and *ompA* partial sequences generated from

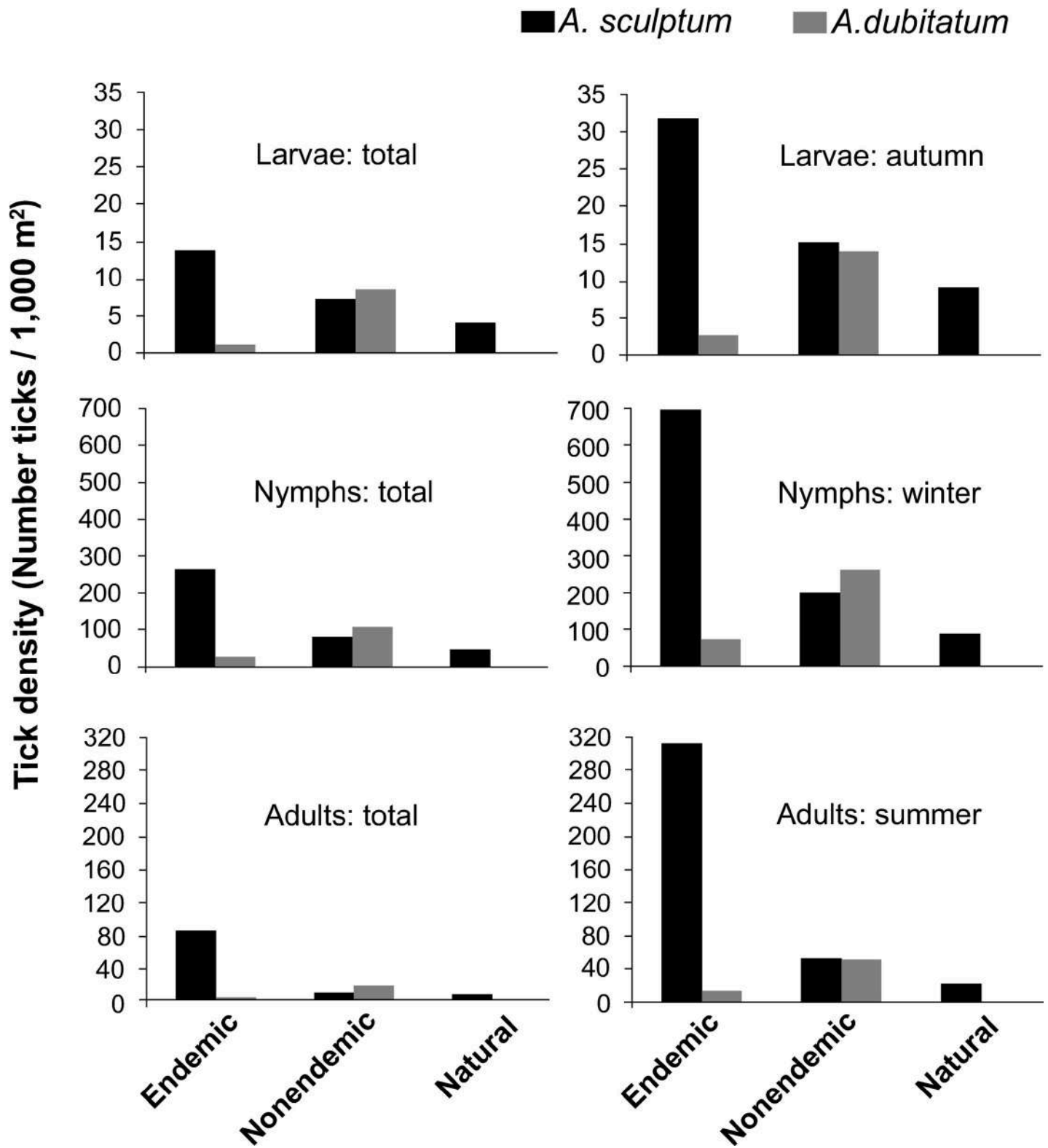


Fig 6. Density of host-questing larvae, nymphs and adult ticks (*Amblyomma sculptum* and *Amblyomma dubitatum*) collected during all seasons of the study period (total) or during the larval (autumn), nymphal (winter) or adult (summer) seasons during 2015–2019 in Brazilian spotted fever (BSF)-endemic areas, BSF-nonendemic areas, and natural areas.

<https://doi.org/10.1371/journal.pntd.0007734.g006>

Table 6. Density of host-questing ticks in 9 localities [3 Brazilian spotted fever (BSF)-endemic areas, 4 BSF-nonendemic areas, and 2 natural areas] for ticks collected only during autumn (May or June) of the years 2015–2018.

Areas	Total area dragged (m ²)	Tick density per 1,000 m ²					
		<i>Amblyomma sculptum</i>			<i>Amblyomma dubitatum</i>		
		Adults	nymphs	Larvae	Adults	Nymphs	Larvae
BSF-endemic areas							
1-Piracicaba	3,200	10.9	5.9	35.9	0.3	4.1	2.8
2-Americana	3,200	0	15.6	29.7	0	1.3	3.1
3-Araras	3,200	0.3	5.6	29.7	0	0.6	2.2
Total	9,600	3.8	9.1	31.8 ^{A,a}	0.1	2.0	2.7 ^{A,b}
BSF-nonendemic areas							
4-Pirassununga-A	3,200	0	3.1	10.9	4.7	6.3	12.2
5-Pirassununga-B	3,200	0	5.6	11.9	0	18.8	15.9
6-Ribeirão Preto	4,800	1.3	3.1	22.5	1.3	15.8	15.6
7-São Paulo	800	5.0	3.8	0	11.3	13.8	0
Total	12,000	0.8	3.8	15.1 ^{B,a}	2.5	13.9	13.8 ^{B,a}
Natural areas							
8-Poconé	4,000	1.3	2.8	3.0	0	0	0
9-Corumbá	1,600	11.9	17.5	24.4			
Total	5,600	4.3	7.0	9.1 ^C	0	0	0

^a different capital letters in each column mean significantly different ($P < 0.05$) tick density values of larvae between the three epidemiological categories (BSF-endemic areas, BSF-nonendemic areas, Natural area); different lowercase letters in each line mean significantly different ($P < 0.05$) tick density values of larvae between *A. sculptum* and *A. dubitatum*.

<https://doi.org/10.1371/journal.pntd.0007734.t006>

Table 7. Density of host-questing ticks in 9 localities [3 Brazilian spotted fever (BSF)-endemic areas, 4 BSF-nonendemic areas, and 2 natural areas] for ticks collected only during winter (August or September) of the years 2015–2018.

Areas	Total area dragged (m ²)	Tick density per 1,000 m ²					
		<i>Amblyomma sculptum</i>			<i>Amblyomma dubitatum</i>		
		Adults	Nymphs	Larvae	Adults	Nymphs	Larvae
BSF-endemic areas							
1-Piracicaba	3,200	85.3	480.9	4.4	5.0	52.5	0.3
2-Americana	3,200	130.3	847.2	7.2	0.3	82.8	0.3
3-Araras	3,200	26.3	783.4	6.6	0.0	80.9	0.6
Total	9,600	80.6	703.9 ^{A,a}	6.0	1.8	72.1 ^{A,b}	0.4
BSF-nonendemic areas							
4-Pirassununga-A	3,200	3.8	137.2	4.1	24.1	57.2	3.8
5-Pirassununga-B	3,200	11.9	338.8	5.6	16.3	422.5	5.0
6-Ribeirão Preto	6,400	5.3	185.8	5.6	13.1	316.9	12.5
7-São Paulo	800	2.5	2.5	0.0	15.0	5.0	0.0
Total	13,600	6.3	199.6 ^{B,a}	4.9	16.5	262.3 ^{B,a}	7.9
Natural areas							
8-Poconé	6,400	5.8	86.4	5.6	0	0.3	0
9-Corumbá	6,400	3.0	87.0	1.4			
Total	12,800	4.4	86.7 ^C	3.5	0	0.3	0

^a different capital letters in each column mean significantly different ($P < 0.05$) tick density values of nymphs between the three epidemiological categories (BSF-endemic areas, BSF-nonendemic areas, Natural area); different lowercase letters in each line mean significantly different ($P < 0.05$) tick density values of nymphs between *A. sculptum* and *A. dubitatum*.

<https://doi.org/10.1371/journal.pntd.0007734.t007>

Table 8. Density of host-questing ticks in 9 localities [3 Brazilian spotted fever (BSF)-endemic areas, 4 BSF-nonendemic areas, and 2 natural areas] for ticks collected only during summer (January or February) of the years 2015–2019.

Areas	Total area dragged (m ²)	Tick density per 1,000 m ²					
		<i>Amblyomma sculptum</i>			<i>Amblyomma dubitatum</i>		
		Adults	Nymphs	Larvae	Adults	Nymphs	Larvae
BSF-endemic areas							
1-Piracicaba	2,400	241.3	36.7	0.8	13.3	6.3	0
2-Americana	2,400	436.3	8.3	0.4	10.8	7.9	4.6
3-Araras	2,400	257.9	21.3	0.4	12.1	0.0	0
Total	7,200	311.8^{A,a}	22.1	0.6	12.1^{A,b}	4.7	1.5
BSF-nonendemic areas							
4-Pirassununga-A	2,400	50.0	5.0	0	53.8	30.4	4.2
5-Pirassununga-B	2,400	33.3	17.1	0	41.3	21.7	5.8
6-Ribeirão Preto	4,800	62.9	2.9	3.1	54.4	8.1	1.3
7-São Paulo	Not done						
Total	9,600	52.3^{B,a}	7.0	1.6	50.9^{B,a}	17.1	3.1
Natural areas							
8-Poconé	4,800	20.2	11.3	0	0	0	0
9-Corumbá	4,800	23.8	18.1	3.5			
Total	9,600	22.0^C	14.7	1.8	0	0	0

^a different capital letters in each column mean significantly different ($P < 0.05$) tick density values of adults between the three epidemiological categories (BSF-endemic areas, BSF-nonendemic areas, Natural area); different lowercase letters in each line mean significantly different ($P < 0.05$) tick density values of adults between *A. sculptum* and *A. dubitatum*.

<https://doi.org/10.1371/journal.pntd.0007734.t008>

the two *A. triste* ticks were 100% identical to the corresponding sequences of *R. parkeri* strain Portsmouth (CP003341). Tick mitochondrial 16S rRNA gene-DNA was successfully amplified from all *Rickettsia*-negative samples, validating our PCR-negative results.

Discussion

A four-year field evaluation demonstrated marked differences of capybara and environmental tick burdens between the three epidemiological classifications of the sampled areas, namely BSF-endemic, BSF-nonendemic, and natural areas. Among the nine sampled areas, only three were classified as BSF-endemic, based primarily on recent records of human cases of the disease (S1 Table). In order to certify on the presence/absence of *R. rickettsii* circulation between capybaras and ticks in all nine study areas, we performed serological analyses of capybaras against antigens of the most frequent *Rickettsia* species that have been reported in Brazil. While cross-reactive antibodies between *Rickettsia* species are often observed, testing a vertebrate serum against the possible *Rickettsia* species known to occur in a given area is ideal because often homologous antibody titers are higher than heterologous antibody titers. In some cases, the differences in titers may be great enough (\geq fourfold higher) to differentiate among the rickettsial species potentially stimulating the immune response [33, 48]. Based on these criteria, the BSF endemic status of areas no. 1 to 3 (Piracicaba, Americana, and Araras) was corroborated by endpoint titers at least fourfold higher for *R. rickettsii* than for other *Rickettsia* species in many of the tested capybaras. In fact, we have just reported a successful isolation of *R. rickettsii* from *A. sculptum* ticks that were parasitizing one of the capybaras that were captured in the BSF-endemic area of Piracicaba, corroborating local circulation of *R. rickettsii* between ticks and capybaras [10].

As expected, we had no serological evidence of *R. rickettsii* infection in the four BSF-nonendemic areas of São Paulo state. Actually, what we observed in these areas was serological

evidence of other *Rickettsia* species, especially *R. bellii*. This result should be related to the predominance of *A. dubitatum* ticks in these areas, since it has been reported that most of the *A. dubitatum* populations are infected by *R. bellii* (usually at high infection rates) in multiple areas in the state of São Paulo, including some of the present study [40, 44, 49, 50].

Similarly to the BSF-nonendemic areas, we did not find serological evidence of *R. rickettsii* circulation in the two natural areas; however, it was interesting to note that 100% of the capybaras from Poconé were seroreactive to both *R. rickettsii* and *R. parkeri*, with endpoint titers generally higher for the later. Our findings of *R. parkeri*-infected *A. triste* ticks in Poconé supports the serological evidence that some of the capybaras from this area have been infected by *R. parkeri*, since *A. triste* ticks were found infesting capybaras in that area. Finally, the few serological evidence of capybara exposure to *R. amblyommatis* could be related to the recent reports of *R. amblyommatis* infecting *A. sculptum* ticks [38, 51], including the Poconé area [52], where we found seven capybaras with endpoint titers fourfold higher for *R. amblyommatis*.

Our tick surveys clearly demonstrated that the BSF-endemic areas were characterized by tick burdens much higher than in the BSF-nonendemic areas, with *A. sculptum* encompassing the vast majority of the ticks on either capybaras or in the environment. In contrast, there was a predominance of *A. dubitatum* over *A. sculptum* in the BSF-nonendemic areas. Considering that both BSF-endemic and BSF-nonendemic areas had similar landscapes, one of the reasons driving the two distinct tick scenarios could be the size of the capybara population of each area. This hypothesis relies on a recent study performed within another highly anthropic area of the state of São Paulo, which in 2006 was not endemic for BSF, had 78 capybaras, and dry ice traps captured a mean of 0.7 *A. sculptum*/trap and 3.3 *A. dubitatum*/trap; in 2012, the same area had become endemic for BSF, had 230 capybaras (≈ 3 times higher than in 2006), and dry ice traps captured a mean of 33 *A. sculptum*/trap (≈ 47 times higher than in 2006) and 2.1 *A. dubitatum*/trap (≈ 0.3 times lower than in 2006) [53]. The authors concluded that the emergence of BSF in the area in 2012 was a consequence of the increase of the local capybara population, which in turn, provided the increment of the *A. sculptum* population. Unfortunately, the numbers of capybaras among the BSF-endemic and BSF-nonendemic areas were not available for comparisons during the present study. Indeed, further studies should be done in order to verify capybara demographic differences among the areas here prospected. Moreover, these studies should also focus on the reproduction rates of capybara groups, since recent mathematical models have proposed that the establishment of *R. rickettsii* in a capybara-sustained *A. sculptum* population is dependent on a high reproduction rate of this host species [11, 54].

The predominance of *A. dubitatum* over *A. sculptum* could also have direct implications on the absence of *R. rickettsii* in BSF-non endemic areas, especially because populations of *A. dubitatum* have been found naturally infected by *R. bellii* throughout the state of São Paulo, usually at high infection rates [40, 44, 49, 50]. One study showed that *R. bellii*-infected *A. dubitatum* ticks were partially refractory to *R. rickettsii*, and were not competent to pass *R. rickettsii* transovarially [55]. Thus, as long as *A. dubitatum* prevails in one area, *R. rickettsii* might not be able to establish an infection in either *A. dubitatum* or *A. sculptum*. In the case of *A. sculptum*, our results and the study of [53] showed that *R. rickettsii* was established only when there was an overgrowth population of *A. sculptum*, possibly because the proportion of *R. rickettsii*-infected *A. sculptum* ticks under natural conditions is always very low ($< 1\%$) [7–10]. Such assumption might allow us to speculate that any intervention resulting in a drastic reduction of the *A. sculptum* population would eliminate the *R. rickettsii* infection from the tick population.

Different from the highly anthropic areas of the state of São Paulo, as much as six tick species were collected in the natural areas of the Pantanal biome. Such species richness was

somewhat expected in pristine areas of this biome, where several species of medium- to large-sized mammals act as major hosts for ticks, including *A. sculptum* [20, 56–60]. While *A. sculptum* was the dominant tick species in the natural areas, tick burdens were much lower than in the anthropic areas. Such findings highlight the ecological disequilibrium of the anthropic areas, where much higher tick burdens were associated to a single major host species, the capybara.

Other factors that could be contributing for the BSF endemic or nonendemic status in *A. sculptum*-capybara associated areas in southeastern Brazil are inherent to the *A. sculptum* populations, namely their susceptibilities to *R. rickettsii* infection. This hypothesis relies on a recent study that compared the susceptibility of *R. rickettsii* infection among six populations of *A. sculptum* [61]. The authors showed that there were significant differences among the susceptibilities of the six tick populations, and suggested that it could be another factor driving the uneven distribution of *R. rickettsii* among the wide distribution of *A. sculptum* in southeastern Brazil. However, the mechanisms driving these different susceptibilities are yet to be determined.

The relatively low number of sampled areas (nine) distributed among three contiguous biomes could be considered a main drawback of this study. Indeed, higher number of areas per epidemiological category would imply greater robustness to our results. However, the high similarity of our observations by epidemiological category supports our results. Actually, sampling of areas within three different biomes was chosen for their strong relation with spotted fever core features; capybaras and *A. sculptum* ticks. In fact, the endemic and non-endemic areas in São Paulo State were intensely anthropized green areas. Although they might have originally been rainforests or savannahs, their natural phytophysiognomies vanished and now share common environmental features characterized by a water source and low grassy areas with relatively few trees, all adequate for capybaras. Similar natural areas maintaining capybara populations had to be found for the control groups as well. Such pristine areas are non-existent in São Paulo State, and the Pantanal biome was the one that provided the most similar features, for example abundant water source and widespread capybara populations. More importantly, all the nine sampled areas are around the center of the wide range of *A. sculptum* [20] and away from the geographic boundaries of this tick species, precluding negative effects of extreme weather on our results for ticks.

Conclusions

The BSF-endemic areas of the state of São Paulo were characterized by overgrowth populations of *A. sculptum* that were sustained chiefly by capybaras, and decreased populations of *A. dubitatum*. In contrast, the BSF-nonendemic areas with landscape similar to the endemic areas differed by having lower tick burdens and a slight predominance of *A. dubitatum* over *A. sculptum*, both sustained chiefly by capybaras. Higher species richness of ticks (six species) was found in the natural areas of Pantanal, although environmental tick burdens were lower than in the anthropic areas of São Paulo. While multiple medium- to large-sized mammals have been pointed out as important hosts for *A. sculptum* in the Pantanal, the capybara was the only important host for this tick species in the anthropic areas of the present study. The uneven distribution of the presence of *R. rickettsii* infection among *A. sculptum* populations in highly anthropic areas of the state of São Paulo could be related to the tick population size and its proportion in relation to sympatric *A. dubitatum* populations.

Supporting information

S1 Text. General overview of the nine areas (1 to 9) where capybaras and host-questing ticks were sampled in this study. Satellite images were obtained from Google Earth Pro

version 7.3, and the final figure was constructed with the use of Microsoft Power Point 2010, version 14.0.7232.5000.

(PDF)

S1 Table. Areas where capybaras and ticks were sampled in the present study.

(PDF)

S2 Table. Antibody endpoint titers determined by immunofluorescence assays (IFA) against antigens of six *Rickettsia* species in sera of capybaras captured in 9 localities, being 3 Brazilian spotted fever (BSF)-endemic areas, 4 BSF-nonendemic areas, and 2 natural areas of Brazil, during 2015–2018.

(PDF)

S3 Table. Host-questing ticks collected by dry-ice traps in 9 localities [3 Brazilian spotted fever (BSF)-endemic areas, 4 BSF-nonendemic areas, and 2 natural areas] during 2015–2019.

(PDF)

Acknowledgments

This work is dedicated to Danilo Gonçalves Saraiva, who gave his life in January 2016, while doing field work for this project. We are very grateful to the SESC Pantanal, UFMT, Embrapa Pantanal, and Alegria and São José Farms (Corumbá) for their logistic support during our field work in the Pantanal areas. We are also grateful to the “Departamento de Água e Esgoto de Americana (DAE)” for allowing us to work at the “Estação de Tratamento de Esgoto (ETE) de Carioba”, Americana municipality.

Author Contributions

Conceptualization: Ubiratan Piovezan, Katia Maria P. M. B. Ferraz, Matias P. J. Szabó, Marcelo B. Labruna.

Data curation: Hermes R. Luz, Francisco B. Costa, Hector R. Benatti, Vanessa N. Ramos, Thiago F. Martins, Ana Maria Nieves, Richard C. Pacheco, Ubiratan Piovezan, Marcelo B. Labruna.

Formal analysis: Hermes R. Luz, Marcelo B. Labruna.

Funding acquisition: Vlamir Rocha, José Brites-Neto, Patricia Ferreira Monticelli, Ubiratan Piovezan, Katia Maria P. M. B. Ferraz, Matias P. J. Szabó, Marcelo B. Labruna.

Investigation: Hermes R. Luz, Francisco B. Costa, Hector R. Benatti, Vanessa N. Ramos, Maria Carolina de A. Serpa, Thiago F. Martins, Igor C. L. Acosta, Diego G. Ramirez, Sebastián Muñoz-Leal, Alejandro Ramirez-Hernandez, Lina C. Binder, Thiago C. Dias, Camila L. Simeoni, Jardel Brasil, Ana Maria Nieves, Beatriz Lopes, Daniel M. Aguiar, Richard C. Pacheco, Ubiratan Piovezan, Matias P. J. Szabó, Marcelo B. Labruna.

Methodology: Ubiratan Piovezan, Katia Maria P. M. B. Ferraz, Matias P. J. Szabó, Marcelo B. Labruna.

Project administration: Marcelo B. Labruna.

Resources: Marcio Port Carvalho, Vlamir Rocha, José Brites-Neto, Patricia Ferreira Monticelli, Maria Estela G. Moro, Daniel M. Aguiar, Richard C. Pacheco, Celso Eduardo Souza, Ubiratan Piovezan, Raquel Juliano, Katia Maria P. M. B. Ferraz, Marcelo B. Labruna.

Software: Hermes R. Luz, Marcelo B. Labruna.

Supervision: Marcelo B. Labruna.

Validation: Hermes R. Luz, Francisco B. Costa, Marcelo B. Labruna.

Visualization: Marcelo B. Labruna.

Writing – original draft: Hermes R. Luz, Marcelo B. Labruna.

Writing – review & editing: Hermes R. Luz, Francisco B. Costa, Hector R. Benatti, Vanessa N. Ramos, Maria Carolina de A. Serpa, Thiago F. Martins, Igor C. L. Acosta, Diego G. Ramirez, Sebastián Muñoz-Leal, Alejandro Ramirez-Hernandez, Lina C. Binder, Marcio Port Carvalho, Vlamir Rocha, Thiago C. Dias, Camila L. Simeoni, José Brites-Neto, Jardel Brasil, Ana Maria Nievas, Patricia Ferreira Monticelli, Maria Estela G. Moro, Beatriz Lopes, Daniel M. Aguiar, Richard C. Pacheco, Celso Eduardo Souza, Ubiratan Piovezan, Raquel Juliano, Katia Maria P. M. B. Ferraz, Matias P. J. Szabó, Marcelo B. Labruna.

References

1. Labruna MB, Santos FC, Ogrzewalska M, Nascimento EM, Colombo S, Marcili A, et al. Genetic identification of rickettsial isolates from fatal cases of Brazilian spotted fever and comparison with *Rickettsia rickettsii* isolates from the American continents. *J Clin Microbiol*. 2014; 52: 3788–3791. <https://doi.org/10.1128/JCM.01914-14> PMID: 25078908
2. Chapman AS, Bakken JS, Folk SM, Paddock CD, Bloch KC, Krusell A, et al. Diagnosis and management of tickborne rickettsial diseases: Rocky Mountain spotted fever, ehrlichioses, and anaplasmosis—United States: a practical guide for physicians and other health-care and public health professionals. *MMWR Recomm Rep*. 2006; 55:1–27
3. Oliveira SV, Willemann MCA, Gazeta GS, Angerami RN, Gurgel-Gonçalves R. Predictive factors for fatal tick-borne spotted fever in Brazil. *Zoo Pub Health*. 2017; 64:44–50. <https://doi.org/10.1111/zph.12345>
4. Labruna MB, Ogrzewalska M, Martins TF, Pinter A, Horta MC. Comparative susceptibility of larval stages of *Amblyomma aureolatum*, *Amblyomma cajennense*, and *Rhipicephalus sanguineus* to infection by *Rickettsia rickettsii*. *J Med Entomol*. 2008; 45: 1156–1159. PMID: 19058642
5. Soares JF, Soares HS, Barbieri AM, Labruna MB. Experimental infection of the tick *Amblyomma cajennense*, Cayenne tick, with *Rickettsia rickettsii*, the agent of Rocky Mountain spotted fever. *Med Vet Entomol*. 2012; 26: 139–151. <https://doi.org/10.1111/j.1365-2915.2011.00982.x> PMID: 22007869
6. Gerardi M, Ramírez-Hernández A, Binder LC, Krawczak FS, Gregori F, Labruna MB. Comparative susceptibility of different populations of *Amblyomma sculptum* to *Rickettsia rickettsii*. *Front Physiol*. 2019. <https://doi.org/10.3389/fphys.2019.00653> PMID: 31191350
7. Guedes E, Leite RC, Pacheco RC, Silveira I, Labruna MB. *Rickettsia* species infecting *Amblyomma* ticks from an area endemic for Brazilian spotted fever in Brazil. *Rev Bras Parasitol Vet*. 2011; 20: 308–311. <http://dx.doi.org/10.1590/S1984-29612011000400009> PMID: 22166385
8. Krawczak FS, Nieri-Bastos FA, Nunes FP, Soares JF, Moraes-Filho J, Labruna MB. Rickettsial infection in *Amblyomma cajennense* ticks and capybaras (*Hydrochoerus hydrochaeris*) in a Brazilian spotted fever-endemic area. *Parasites & Vectors*. 2014; 7: 1–7. <https://doi.org/10.1186/1756-3305-7-7>
9. Labruna MB, Krawczak FS, Gerardi M, Binder LC, Barbieri ARM, Paz GF, et al. Isolation of *Rickettsia rickettsii* from the tick *Amblyomma sculptum* from a Brazilian spotted fever-endemic area in the Pampulha Lake region, southeastern Brazil. *Vet Parasitol: Regional Studies and Reports*. 2017; 8: 82–85. <https://doi.org/10.1016/j.vprsr.2017.02.007>
10. Costa FB, Gerardi M, Binder LC, Benatti HR, Serpa MC, Lopes B, et al. *Rickettsia rickettsii* (Rickettsiales: Rickettsiaceae) infecting *Amblyomma sculptum* (Acari: Ixodidae) ticks and capybaras in a Brazilian spotted fever-endemic area of Brazil. *J Med Entomol*. 2019 (in press) <https://doi.org/10.1093/jme/tjz141>
11. Polo G, Mera Acosta C, Labruna MB, Ferreira F. Transmission dynamics and control of *Rickettsia rickettsii* in populations of *Hydrochoerus hydrochaeris* and *Amblyomma sculptum*. *PLoS Neglected Tropical Dis*. 2017; 11:e0005613. <https://doi.org/10.1371/journal.pntd.0005613>
12. Polo G, Mera Acosta C, Labruna MB, Ferreira F, Brockmann D. Hosts mobility and spatial spread of *Rickettsia rickettsii*. *PLoS Comput Biol*. 2018a; 14:e1006636. <https://doi.org/10.1371/journal.pcbi.1006636> PMID: 30586381

13. Souza CE, Moraes-Filho J, Ogrzewalska M, Uchoa FC, Horta MC, Souza SS, et al. Experimental infection of capybaras *Hydrochoerus hydrochaeris* by *Rickettsia rickettsii* and evaluation of the transmission of the infection to ticks *Amblyomma cajennense*. *Vet Parasitol*. 2009; 161: 116–121. <https://doi.org/10.1016/j.vetpar.2008.12.010> PMID: 19147293
14. Labruna M B. Brazilian spotted fever: the role of capybaras. In: Moreira JR, Ferraz KMPMB, Herrera EA, Macdonald DW (Eds.), *Capybara: biology, use and conservation of an exceptional neotropical species* (p. 371–383). New York: Springer Science Business Media; 2013. p. 175.
15. Perez CA, Almeida AF, Almeida A, Carvalho VHB, Balestrin DC, Guimarães MS, et al. Carrapatos do gênero *Amblyomma* (acarí: ixodidae) e suas relações com os hospedeiros em área endêmica para febre maculosa no estado de São Paulo. *Rev Bras Parasitol Vet*. 2008; 17: 210–217. PMID: 19265580
16. Verdade LM, Gheler-Costa C, Penrado M, Dotta G. The impacts of sugarcane expansion on wildlife in the state of São Paulo, Brazil. *J Sust Bioe Syst*. 2012; 2: 138–144.
17. Bovo AAA, Ferraz KMPMB, Verdade LM, Moreira JR. Capybaras (*Hydrochoerus hydrochaeris*) in Anthropogenic Environments: Challenges and Conflicts. In Gheler-Costa Carla, Lyra-Jorge Maria Carolina, Verdade Luciano Martins (Eds.), *Biodiversity in Agricultural Landscapes of Southeastern Brazil* Warsaw, Poland: De Gruyter Open; 2016. p. 178–189. <https://doi.org/10.1515/9783110480849-013>
18. Verdade LM, Ferraz KMPMB. Capybaras in an anthropogenic habitat in southeastern Brazil *Braz J Biol*. 2006; 66: 371–378. PMID: 16710529
19. Ferraz KMPMB Ferraz SFB, Moreira JR, Couto HT, Verdade LM. Capybara (*Hydrochoerus hydrochaeris*) distribution in agroecosystems: a cross-scale habitat analysis. *J Biogeogr*. 2007; 34: 223–230. <https://doi.org/10.1111/j.1365-2699.2006.01568.x>
20. Martins TF, Barbieri AR, Costa FB, Terrasini FA, Camargo LM, Peterka CR, et al. Geographical distribution of *Amblyomma cajennense* (sensu lato) ticks (Parasitiformes: Ixodidae) in Brazil, with description of the nymph of *A. cajennense* (sensu stricto). *Parasit Vectors*, 2016; 9: 1–14. <https://doi.org/10.1186/s13071-016-1460-2> <https://doi.org/10.1186/s13071-015-1291-6> PMID: 26728523
21. Souza CE, Pinter A, Donalisio MR. Risk factors associated with the transmission of Brazilian spotted fever in the Piracicaba river basin, State of São Paulo, Brazil. *Rev Soc Bras Med Trop*. 2015; 48:11–17. <https://doi.org/10.1590/0037-8682-0281-2014> PMID: 25860458
22. Pacheco RC, Horta MC, Moraes-Filho J, Ataliba AC, Pinter A, Labruna MB. Rickettsial infection in capybaras (*Hydrochoerus hydrochaeris*) from São Paulo, Brazil: serological evidence for infection by *Rickettsia bellii* and *Rickettsia parkeri*. *Biomedica*. 2007; 27: 364–371. PMID: 18320102
23. Souza CE, Souza SSL, Lima VLC, Calic SB, Camargo MCGO, Savani ESMM, et al. Serological identification of *Rickettsia* spp from the spotted fever group in capybaras in the region of Campinas—SP—Brazil. *Ciênc Rur Santa Maria*. 2008; 38: 1694–1699. <http://dx.doi.org/10.1590/S0103-84782008000600031>
24. Mazzei K, Rosa AR, Arromba AL, Duarte AMC, Barleta C, Waldman CCS, et al. Levantamento e propostas de ação para as principais zoonoses dos parques estaduais Alberto Löffgren e da Cantareira. *IF Sér. Reg.*, São Paulo, 2009. p. 25–41.
25. Vargas FC, Vargas SC, Moro MEG, Silva V, Carrer CRO. Monitoramento populacional de capivaras (*Hydrochoerus hydrochaeris* Linnaeus, 1776) em Pirassununga, SP, Brasil. *Ciênc Rural*. 2007; 37: 1104–1108.
26. Barros-Battesti D, Arzua M, Bechara GH. Carrapatos de importância médico veterinária da região neotropical. Um guia ilustrado para identificação de espécies. *Vox/ICTTD-3/Butantan*, São Paulo/BR; 2006. p. 223.
27. Martins TF, Onofrio VC, Barros-Battesti DM, Labruna MB. Nymphs of the genus *Amblyomma* (Acari: Ixodidae) of Brazil: descriptions, redescription, and identification key. *Ticks and Tick-Borne Dis*. 2010; 1: 75–99. <https://doi.org/10.1016/j.ttbdis.2010.03.002>
28. Pinter A. and Labruna MB. Isolation of *Rickettsia rickettsii* and *Rickettsia bellii* in cell culture from the tick *Amblyomma aureolatum* in Brazil. *Ann N Y Acad Sci*. 2006; 1078: 523–529. <https://doi.org/10.1196/annals.1374.103> PMID: 17114770
29. Silveira I, Pacheco RP, Szabó MPJ, Ramos HGC, Labruna MB. *Rickettsia parkeri* in Brazil. *Emerg Infect Dis*. 2007; 13: 1111–1113. <https://doi.org/10.3201/eid1307.061397> PMID: 18214195
30. Labruna MB, Whitworth T, Bouyer DH, McBride JW, Camargo LM, Camargo EP, et al. *Rickettsia bellii* and *Rickettsia amblyommii* in *Amblyomma* ticks from the state of Rondonia, Western Amazon, Brazil. *J Med Entomol*. 2004a; 41:1073–1081. <https://doi.org/10.1603/0022-2585-41.6.1073> PMID: 15605647
31. Labruna MB, Pacheco RC, Richtzenhain LJ, Szabó MP. Isolation of *Rickettsia rhipicephali* and *Rickettsia bellii* from *Haemaphysalis juxtakochi* ticks in the state of São Paulo, Brazil. *Appl Environ Microbiol*. 2007; 73:869–873. <https://doi.org/10.1128/AEM.02249-06> PMID: 17142361

32. Horta MC, Labruna MB, Durigon EL, Schumaker TT. Isolation of *Rickettsia felis* in the mosquito cell line C6/36. *Appl Environ Microbiol*. 2006; 72:1705–1707. <https://doi.org/10.1128/AEM.72.2.1705-1707>. 2006 PMID: 16461734
33. Horta MC, Labruna MB, Sangioni LA, Vianna MCB, Gennari SM, Galvão MA, Mafra CL, et al. Prevalence of antibodies to spotted fever group rickettsiae in humans and domestic animals in a Brazilian Spotted fever endemic area in the state of São Paulo, Brazil: serological evidence for infection by *Rickettsia rickettsii* and another spotted fever group rickettsia. *Am J Trop Med Hyg* 2004; 71:93–97. PMID: 15238696
34. Horta MC, Sabatini GS, Moraes-Filho J, Ogrzewalska M, Canal RB, Pacheco RC, et al. Experimental infection of the opossum *Didelphis aurita* by *Rickettsia felis*, *Rickettsia bellii*, and *Rickettsia parkeri* and evaluation of the transmission of the infection to ticks *Amblyomma cajennense* and *Amblyomma dubitatum*. *Vector Borne Zoonotic Dis*. 2010; 10:959–967. <https://doi.org/10.1089/vbz.2009.0149> PMID: 20455783
35. Ueno TE, Costa FB, Moraes-Filho J, Agostinho WC, Fernandes WR, Labruna MB. Experimental infection of horses with *Rickettsia rickettsii*. *Parasit Vectors*. 2016; 13: 1–11. <https://doi.org/10.1186/s13071-016-1784-y> PMID: 27624315
36. Oliveira PR, Borges LM, Lopes CM, Leite RC: Population dynamics of the free-living stages of *Amblyomma cajennense* (Fabricius, 1787) (Acari: ixodidae) on pastures of Pedro Leopoldo, Minas Gerais State, Brazil. *Vet Parasitol*. 2000; 92: 295–301. [https://doi.org/10.1016/S0304-4017\(00\)00322-8](https://doi.org/10.1016/S0304-4017(00)00322-8) PMID: 10996741
37. Labruna MB, Kasai N, Ferreira F, Faccini JL, Gennari SM. Seasonal dynamics of ticks (Acari Ixodidae) on horses in the state of São Paulo, Brazil. *Vet Parasitol*. 2002; 105: 65–77. [https://doi.org/10.1016/S0304-4017\(01\)00649-5](https://doi.org/10.1016/S0304-4017(01)00649-5) PMID: 11879967
38. Barbieri ARM, Szabó MPJ, Costa FB, Martins TF, Soares HS, et al. Species richness and seasonal dynamics of ticks with notes on rickettsial infection in a Natural Park of the Cerrado biome in Brazil. *Ticks Tick Borne Dis*. 2019; 10: 442–453. <https://doi.org/10.1016/j.ttbdis.2018.12.010> PMID: 30611725
39. Szabó MP, Labruna MB, Garcia MV, Pinter A, Castagnolli KC, Pacheco RC, et al. Ecological aspects of the free-living ticks (Acari: Ixodidae) on animal trails within Atlantic rainforest in south-eastern Brazil. *Ann Trop Med Parasitol*. 2009; 103: 57–72. <https://doi.org/10.1179/136485909X384956> PMID: 19173777
40. Brites-Neto J, Nieri-Bastos FA, Brasil J, Duarte KMR, Martins TF, Veríssimo CJ, et al. Environmental infestation and rickettsial infection in ticks in a Brazilian spotted fever-endemic area. *Rev Bras Parasitol Vet*. 2013; 22: 367–372. <https://doi.org/10.1590/S1984-29612013000300008> PMID: 24142167
41. Brites-Neto J, Brasil J, Takeda GACG, Guillen AC, Labruna MB, Pinter A. Diferenciação morfológica entre larvas de *Amblyomma sculptum* Berlese, 1888 e *Amblyomma dubitatum* Neumann, 1899. *Arq Bras Med Vet Zootec*. 2018; 70: 1521–1528. <http://dx.doi.org/10.1590/1678-4162-9774>
42. Sangioni LA, Horta MC, Vianna MCB, Gennari SM, Soares RS, Galvão MAM, et al. Rickettsial infection in animals and Brazilian spotted fever endemicity. *Emerg Infect Dis*. 2005; 11: 265–270. <https://doi.org/10.3201/eid1102.040656> PMID: 15752445
43. Mangold AJ, Barges MD, Mas-Coma S. Mitochondrial 16SrDNA sequences and phylogenetic relationships of species of *Rhipicephalus* and other tick genera among Metastrata (Acari: Ixodidae). *Parasitol Res*. 1998; 84: 478–484. PMID: 9660138
44. Labruna MB, Whitworth T, Horta MC, Bouyer DH, McBride JW, Pinter A, et al. *Rickettsia* species infecting *Amblyomma cooperi* ticks from an area in the state of São Paulo, Brazil, where Brazilian spotted fever is endemic. *J Clin Microbiol*. 2004b; 42: 90–98. <https://dx.doi.org/10.1128/JCM.42.1.90-98>
45. Eremeeva ME, Bosserman EA, Demma LJ, Zambrano ML, Blau DM, Dasch GA. Isolation and identification of *Rickettsia massillae* from *Rhipicephalus sanguineus* ticks collected in Arizona. *Appl Environ Microbiol*. 2006; 72: 5569–5577. <https://doi.org/10.1128/AEM.00122-06> PMID: 16885311
46. Bush AO, Lafferty KD, Lotz JM, Shostak AW. Parasitology meets ecology on its own terms: margolis et al. Revisited *J Parasitol*. 1997; 83: 575–583. PMID: 9267395
47. Labruna MB, Costa FB, Port-Carvalho M, Oliveira AS, Souza SLP, Castro MB. Lethal Fascioliasis in Capybaras (*Hydrochoerus hydrochaeris*) in Brazil. *J Parasitol*. 2018; 104:173–176. <https://doi.org/10.1645/17-114> PMID: 29185852
48. LaScola B, Raoult D. Laboratory diagnosis of rickettsioses: current approaches to diagnosis of old and new rickettsial diseases. *J Clin Microbiol*. 1997; 35: 2715–2727. PMID: 9350721
49. Horta MC, Labruna MB, Pinter A, Linardi PM, Schumaker TT. Rickettsia infection in five areas of the state of São Paulo, Brazil. *Mem Inst Oswaldo Cruz*. 2007; 102: 793–801. <http://dx.doi.org/10.1590/S0074-02762007000700003> PMID: 18094887
50. Pacheco RC, Horta MC, Pinter A, Moraes-Filho J, Martins TF, Nardi MS, et al. Pesquisa de *Rickettsia* spp. em carrapatos *Amblyomma cajennense* e *Amblyomma dubitatum* no Estado de São Paulo. *Rev*

- Soc Bras Med Trop. 2009; 42: 351–353. <http://dx.doi.org/10.1590/S0037-86822009000300023> PMID: 19684990
51. Nunes EDC, Vizzoni VF, Navarro DL, Iani FCDM, Durães LS, Daemon E, et al. *Rickettsia amblyommii* infecting *Amblyomma sculptum* in endemic spotted fever area from southeastern Brazil. Mem Inst Oswaldo Cruz 2015; 110: 1058–1061. <https://doi.org/10.1590/0074-02760150266> PMID: 26676317
 52. Alves AS, Melo AL, Amorim MV, Borges AM, Gaíva e Silva L, Martins TF, et al. Seroprevalence of *Rickettsia* spp. in Equids and Molecular Detection of 'Candidatus *Rickettsia amblyommii*' in *Amblyomma cajennense* Senu Lato Ticks From the Pantanal Region of Mato Grosso, Brazil. J Med Entomol. 2014; 1; 51:1242–1247. <https://doi.org/10.1603/ME14042> PMID: 26309313
 53. Passos Nunes FB, Silva SC, Cieto AD, Labruna MB. The dynamics of ticks and capybaras in a residential park area in southeastern Brazil: implications for the risk of *Rickettsia rickettsii* infection. Vector-Borne Zoonotic Dis. 2019 (in press) <https://doi.org/10.1089/vbz.2019.2479>
 54. Polo G, Labruna MB, Ferreira F. Basic reproduction number for the Brazilian Spotted Fever. J T Biol, 2018b; 458: 119–124. <https://doi.org/10.1016/j.jtbi.2018.09.011>.
 55. Sakai RK, Costa FB, Ueno TE, Ramirez DG, Soares JF, Fonseca AH, et al. Experimental infection with *Rickettsia rickettsii* in an *Amblyomma dubitatum* tick colony, naturally infected by *Rickettsia bellii*. Ticks Tick Borne Dis. 2014; 9:17–923. <https://doi.org/10.1016/j.ttbdis.2014.07.003> PMID: 25108783
 56. Pereira MC, Szabó MP, Bechara GH, Matushima ER, Duarte JM, Rechav Y, et al. Ticks (Acari: Ixodidae) associated with wild animals in the Pantanal region of Brazil. J Med Entomol. 2000; 37: 979–83. PMID: 11126563
 57. Cançado PH, Piranda EM, Mourão GM, Faccini JL. Spatial distribution and impact of cattle-raising on ticks in the Pantanal region of Brazil by using the CO(2) tick trap. Parasitol Res. 2008; 103: 371–377. <https://doi.org/10.1007/s00436-008-0982-8> PMID: 18454288
 58. Ramos VN, Piovezan U, Franco AH, Osava CF, Herrera HM, Szabó MP. Feral pigs as hosts for *Amblyomma sculptum* (Acari: Ixodidae) populations in the Pantanal, Mato Grosso do Sul, Brazil. Exp Appl Acarol. 2014; 64: 393–406. <https://doi.org/10.1007/s10493-014-9832-9> PMID: 25037743
 59. Melo AL, Alves AS, Nieri-Bastos FA, Martins TF, Witter R, Pacheco TA, et al. *Rickettsia parkeri* infecting free-living *Amblyomma triste* ticks in the Brazilian Pantanal. Ticks Tick Borne Dis. 2015; 6: 237–41. <https://doi.org/10.1016/j.ttbdis.2015.01.002> PMID: 25650348
 60. de Sousa KCM, Herrera HM, Rocha FL, Costa FB, Martins TF, Labruna MB, et al. *Rickettsia* spp. among wild mammals and their respective ectoparasites in Pantanal wetland, Brazil. Ticks Tick Borne Dis. 2018; 9:10–17. <https://doi.org/10.1016/j.ttbdis.2017.10.015> PMID: 29111373
 61. Gerardi M, Ramírez-Hernández A, Binder LC, Krawczak FS, Gregori F, Labruna MB. Comparative susceptibility of different populations of *Amblyomma sculptum* to *Rickettsia rickettsii*. Front Physiol. 2019; 10:653. <https://doi.org/10.3389/fphys.2019.00653> PMID: 31191350



Bovine Genital Leptospirosis and reproductive disorders of live subfertile cows under field conditions

Luiza Aymée^a, Wilmara Rampinelli Reuter Gregg^b, Ana Paula Loureiro^{a,c},
 Maria Isabel Nogueira Di Azevedo^a, Juliana de Souza Pedrosa^a,
 Juliana dos Santos Loria de Melo^a, Filipe Anibal Carvalho-Costa^d,
 Guilherme Nunes de Souza^{a,e}, Walter Lilenbaum^{a,*}

^a Laboratory of Veterinary Bacteriology, Biomedical Institute, Federal Fluminense University, Niterói, Rio de Janeiro, Brazil

^b Practitioner, Brazil

^c Estácio de Sá University, Rio de Janeiro, Brazil

^d Laboratory of Epidemiology and Molecular Systematics, Oswaldo Cruz Institute, Rio de Janeiro, Brazil

^e Brazilian Agricultural Research Corporation (Embrapa), Juiz de Fora, Minas Gerais, Brazil

ARTICLE INFO

Keywords:

Leptospira
 cattle
 reproductive disease
 uterine infection
 PCR

ABSTRACT

Bovine genital leptospirosis (BGL) is characterized by silent chronic reproductive disorders, most related to early embryonic death leading to estrus repetition, subfertility and abortions. However, most studies were conducted in slaughterhouses, which lacks reproductive and sanitary history of the studied animals. This study aimed to evaluate the occurrence of *Leptospira* sp. infection in live cows with history of low reproductive efficiency. Blood, urine, cervico-vaginal mucus and uterine fragment were collected from nine cows of the same herd presenting reproductive failure (abortions, estrus repetition and chronic infertility). Serology (MAT) and molecular analysis (PCR and nucleotide sequencing) were performed. Serology showed three (33.3%) seroreactive cows, two to Sejroe and one to Icterohaemorrhagiae serogroups. Six cows (66.7%) presented leptospiral DNA on genital samples, while all urine samples were negative. *L. interrogans* was identified in five samples, very closely related to strains from Sejroe (n = 3) and Icterohaemorrhagiae (n = 2) serogroups, while *L. noguchii* was identified in one sample. Results from this preliminary study demonstrates the presence of leptospires on uterus and reinforces the negative impact of leptospiral infection on reproductive tract, highlighting its association with reproductive failures on live animals.

1. INTRODUCTION

Leptospirosis in cattle is a main concern, since it leads to reproductive disorders, resulting in economic losses (Ellis, 1985; Libonati et al., 2018). Recently, a distinct syndrome named as Bovine Genital Leptospirosis (BGL) was described (Loureiro and Lilenbaum, 2020). BGL represents a silent and chronic reproductive disease characterized by embryonic death (ED) leading to estrus repetition and subfertility (Libonati et al., 2018; Pimenta et al., 2019; Loureiro and Lilenbaum, 2020). Although BGL is the most common form of leptospirosis in cattle, its subclinical characteristic makes it a neglected syndrome (Loureiro and Lilenbaum, 2020). *Leptospira interrogans* serovar Hardjoprajitno, *L. borgpetersenii* sv. Hardjobovis and *L. santarosai* sv. Guaricura, all

belonging to Sejroe serogroup, are primary causative agents of BGL (Ellis, 2015; Loureiro et al., 2017).

Maintenance of *Leptospira* in the reproductive tract is the key of genital leptospirosis. Paradoxically, most of studies concerning to *Leptospira* infections in bovine aimed the detection of renal carriers (Loureiro and Lilenbaum, 2020). Uterus has been reported as an important extra-renal site of *Leptospira* infection in cows and ewes (Pires et al., 2018; Silva et al., 2019; Di Azevedo et al., 2020). However, the association between the presence of leptospires in uterus and low reproductive efficiency is scarcely established, since most of these studies were conducted in slaughterhouses and it lacks history of reproductive data. Based on this, the present study aimed to evaluate the occurrence of *Leptospira* sp. infection in live cows with clinical history of low

* Corresponding author at: Prof. Hernani Pires de Mello street, number 101, 3rd floor, Niterói, Rio de Janeiro state, Brazil.

E-mail address: wlilenbaum@id.uff.br (W. Lilenbaum).

reproductive efficiency.

2. MATERIAL AND METHODS

2.1. Animals and samples

This research was approved by Ethical Committee for Animal Use of Federal Fluminense University (protocol 1025/2017). We performed our study in a beef cattle herd (Tabapuã, Nelore or Tabanel breeds) located in northeast region of Rio de Janeiro state, Brazil. Due to the high frequency of reproductive failures, this herd's practitioner contacted our group to perform the screening diagnoses by Microscopic Agglutination Test (MAT). From 30 bovine sera received, 10 (33.3%) were reactive to Sejroe serogroup with titres above 200. The herd had not been vaccinated against leptospirosis. Only cows destined to culling due to low reproductive performance without a definitive diagnosis were included. Reproductive management was conducted by a veterinarian who provided reproductive data: date of artificial insemination or natural breeding, pregnancy confirmation, date of calving or abortion episodes. The animals used in this study were not the same animals of the screening MAT samples, which was used as collective (herd) diagnoses.

After proper physical contention, blood, urine, cervico-vaginal mucus (CVM) and uterine fragment (UF) were collected of each animal. Blood was obtained by venipuncture of coccygeal vein in recipients without anticoagulants. After asepsis procedures of perineal and vulva, urine was collected using Levin nasogastric tube (16 FR) as a urethral probe and suction with a syringe attached in the other extremity. CVM collection was performed with cytology brush following Loureiro and Lilenbaum (2020) recommendations. After urine and CVM collection, low epidural anesthesia with lidocaine 2% and epinephrine (Bravet Inc, Brazil) was applied. Biopsy were conducted using Yeoman forceps through the cervix to obtain fragments from the uterus corpus. Fragments of approximately five millimeters were obtained and deposited in sterile Petri dish to be fractionated. Samples were kept frozen (-20 °C) until molecular analysis.

2.2. Reproductive parameters

Reproductive examinations were performed through transrectal palpation and ultrasonography (Aloka SSD-500; Wallingford, CT, USA). Cows were monitored as needed, during the breeding season. Absence of pregnancy given by two consecutive negative results for more than a year was interpreted as chronic infertility. Reproductive disorders as embryonic death - ED (≤ 45 days of pregnancy), abortions (≥ 45 days of pregnancy), stillbirth and birth of weak calves were recorded. Embryonic death was detected by the absence of embryo in transrectal ultrasonography after confirmation of pregnancy.

2.3. Serology

Serum samples were tested for antibodies against leptospirosis by microscopic agglutination test (MAT) using an antigen panel composed by six reference strains: *Leptospira interrogans* serovar Copenhageni (strain M20), Hardjoprajitno (strain OMS), Pomona, (strain Pomona), Icterohaemorrhagiae (strain Icterohaemorrhagiae) and Grippityphosa (strain Moskva V); *Leptospira borgpetersenii* serovar Hardjobovis (strain Sponselee), all originated from Institut Pasteur, Paris, France; and *Leptospira santarosai* serovar Guaricura (strain U140) from Universidade de São Paulo, São Paulo, Brazil. The strains selected to the antigen panel were known to be the predominant in cattle in the region of the herd (Pinto et al. 2016). A cut-off titer of 100 was considered for positivity (OIE, 2018).

2.4. Molecular analysis

DNA extraction from urine and CVM samples was proceeded with Wizard SV Genomic DNA Purification System Kit (Promega, Madison, USA), while DNA from uterine fragment was extracted using commercial DNeasy Blood and Tissue Kit (QIAamp, Qiagen, Courtaboeuf, France). Polymerase chain reaction (PCR) was conducted targeting *lipL32* (242bp) (Stoddard et al., 2009), according to Hamond et al. (2014). Amplicons obtained were submitted to a nested PCR procedure targeting partial *secY* gene (411bp), following recommendations (Di Azevedo and Lilenbaum, 2021). Ultrapure water and 10 fg of DNA extracted from *Leptospira interrogans* serovar Copenhageni (Fiocruz L1-130) were employed as negative and positive control, respectively. Electrophoresis in 1.5-2% agarose gel and visualized under UV light, was performed to PCR products analysis.

Nucleotide sequencing was performed in amplicons obtained in *secY* PCR. This procedure was carried out using Big Dye Terminator v.3.1 Cycle Sequencing Ready Reaction Kit (Applied Biosystems) in a 3100 automated DNA sequencer according to the manufacturer's instructions. Nucleotide sequences were deposited in GenBank under accession numbers MZ099639 - MZ099644". Regarding phylogenetic analysis, Pairwise/Blast/NCBI, SeqMan v. 7.0, ClustalW v. 1.3512 and BioEdit v. 7.0.1 (Hall, 1999) softwares were used for the editing and sequence analysis. A maximum likelihood (ML) tree was constructed using the Tamura-Nei model with the gamma distribution (TN + G) in MEGA X software, as it was determined to be the best-fitting model of DNA substitution using the Bayesian information criterion.

3. RESULTS

All animals presented infertility, since it was an inclusion criterion, and none of the included cows had clinical signs of acute systemic leptospirosis. Abortion episodes was recorded in 3/9 (33.3%) cows, while 4/9 (44.4%) presented embryonic death (ED) ranging from one to two embryos lost per reproductive season (Table 1). Serology showed three (33.3%) seroreactive cows, two to Sejroe and one to Icterohaemorrhagiae serogroups.

Regarding to molecular tests, six out of nine (66.6%) samples were positive for *lipL32*-PCR, producing amplicons with the expected size, confirming the presence of leptospiral DNA in the genital tract of the animals. In two cows, *Leptospira* spp. was detected in CVM, while in four it was detected in uterine fragment (Table 1). All urine samples were *lipL32*-PCR negative. Complementary, *lipL32*-PCR positive samples were submitted to *secY* amplification and sequencing (Table 2). Pairwise/Blast/NCBI comparisons with the GenBank *secY* gene dataset identified them as *L. interrogans* (n = 5) and *L. noguchii* (n = 1) with a 100% of identity. Phylogenetic analysis based on ML TN + G confirmed the species identification (Fig. 1). Additionally, sequences from UF 3, UF 4 and CVM 1 grouped with high support (bootstrap = 98%) with *L. interrogans* serogroup Sejroe serovar Hardjo strains from the same host and geographical location, i.e. cows from Brazil (Fig. 1). Two sequences (UF 10 and CVM 2) were very closely related to *L. interrogans* serovar Icterohaemorrhagiae, included in a group with high bootstrap value (97%) (Fig. 1). Sequences from this clade were from different hosts, but from the same geographical area. The sequence identified as *L. noguchii* clustered in a high supported group (bootstrap = 99%) with sequences from the same host, all from South America (Fig. 1).

4. DISCUSSION

Silent reproductive failures characterize the main manifestation of BGL. Despite previous studies have shown the presence of *Leptospira* DNA in CVM and uterus, they could not complement the outcomes with reproductive data, since they were conducted in slaughtered cows with no available records (Loureiro et al., 2017; Pires et al., 2018; Di Azevedo et al., 2020). The herd herein studied presented, as main reproductive

Table 1
Leptospira infection status (PCR of *lipL32* and Serology by MAT) in live cows from a herd with low reproductive efficiency.

Cow	PCR Urine	PCR Genital		MAT Serogroup (Titre)	Reproductive History
		Uterus	CVM		
1	Negative	Negative	Positive	Icterohaemorrhagiae (200)	Infertility for two years
2	Negative	Negative	Positive	Sejroe (100)	Infertility for two years
3	Not available	Positive	Negative	Negative	Abortion two years ago. Infertility since then
4	Negative	Positive	Negative	Negative	Abortion four years ago. Estrus repetition. Infertility for two years
5	Negative	Positive	Negative	Sejroe (100)	Infertility for two years
6	Negative	Positive	Negative	Negative	Abortion one year ago. Estrus repetition. Infertility for two years
7	Negative	Negative	Negative	Negative	Estrus repetition. Infertility for three years
8	Negative	Negative	Negative	Negative	Estrus repetition. Infertility for two years
9	Negative	Negative	Negative	Negative	Infertility for two years

MAT – Microscopic Agglutination Test; CVM – Cervico-vaginal mucus.

Table 2
 Results from nucleotide sequencing of *secY* gene from genital samples of cows with reproductive disorders:

Cow	Sample	Nucleotide Sequencing
1	CVM	<i>L. interrogans</i> sg Sejroe
2	CVM	<i>L. interrogans</i> sg Icterohaemorrhagiae
3	Uterus	<i>L. interrogans</i> sg Sejroe
4	Uterus	<i>L. interrogans</i> sg Sejroe
5	Uterus	<i>L. noguchii</i> sg Australis
6	Uterus	<i>L. interrogans</i> sg Icterohaemorrhagiae

CVM – Cervico-vaginal mucus. Sg - Serogroup.

disorder, recurrent estrus repetition leading to chronic infertility, as a consequence of ED, what was confirmed by ultrasonography. Although ED has been previously associated to leptospirosis (Libonati et al., 2018), on that study the authors did not use ultrasonography on all the cows. It has been suggested that ED probably occurs as result of uterine

inflammation in response to leptospiral colonization, impairing implantation; and/or by direct embryo damage by this pathogen (Loureiro and Lilenbaum, 2020).

Unsurprisingly, some of infected cows had episode of abortion in the course of their reproductive life. Abortion is one of the most classical signs of bovine leptospirosis and can be caused by a range of leptospires, both adapted or incidental (Ellis, 2015; Gregoire et al., 2020). The abortion episodes described in each animals' history occurred a long time ago and the infection status back then is unknown. It is possible that abortion occurred during an acute phase in the beginning of the leptospiral infection. As already suggested by Ellis (2015), after an acute phase, the infection becomes chronic and reproductive signs could evolve to a prolonged subfertility. We believe that abortions happened at the early moments of the leptospiral infection on that herd, and has chronicized onto a silent BGL, mainly characterized by ED and subfertility.

Only half of the PCR-positive cows (n = 3) presented positive results in MAT, what reinforces that MAT fails for individual diagnosis, being

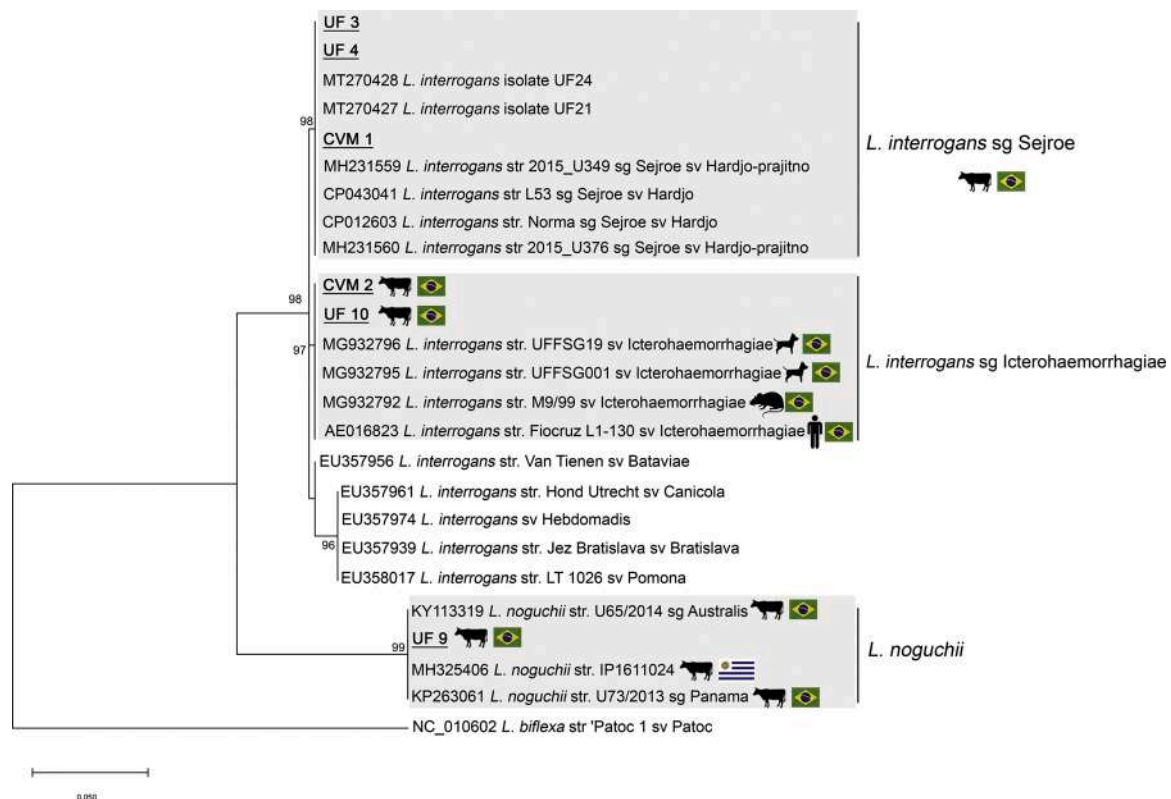


Fig. 1. Maximum likelihood phylogenetic tree inferred from partial *secY* gene sequences of *L. interrogans* and *L. noguchii* from this study (UF and CVM) and GenBank sequences (accession numbers, strain and serovar are shown). Hosts and location are indicated. Numbers at nodes are bootstrap values greater than 50%. *Leptospira biflexa* strain Patoc is the outgroup taxa.

preferentially indicated for screening of positive herds and also to define circulant leptospires serogroup (Otaka et al., 2012; OIE, 2018). Seroreactivity against Sejroe corroborates to BGL hypothesis, since strains of this serogroup are adapted to bovine (Ellis, 2015), and high association of those strains with estrus repetition was previously established (Libonati et al., 2018).

Three strains showed high association with *L. interrogans* from Sejroe serogroup. This is in agreement with BGL hypothesis that indicates that Hardjo (from Sejroe serogroup) preferably colonizes the reproductive tract (Ellis et al., 1986; Ellis, 2015) and is associated to chronic reproductive form of bovine leptospirosis (Loureiro and Lilenbaum, 2020; Di Azevedo et al., 2020). *Leptospira interrogans* Icterohaemorrhagiae serogroup and *L. noguchii* are incidental to cattle, but the present study demonstrates that those strains cannot be neglected in cows with reproductive disorders. Incidental strains have been recovered from urine and vaginal fluid from asymptomatic cows, suggesting that, in some conditions, cattle could also harbor and shed incidental strains (Pinto et al., 2017). *L. interrogans*, particularly those from Icterohaemorrhagiae serogroup similar to the strain Fiocruz L1-130, is widely distributed in Brazil in different hosts, including bovine (Jaeger et al., 2018). Similarly, *L. noguchii* has been previously identified in a great variety of hosts, including cows (Martins et al., 2015; Hamond et al., 2016) and was reported as the second more recovered leptospires in culture of urine and CVM (Loureiro et al., 2017). In the present study, cows with chronic infertility history presented *L. noguchii* in uterus, what indicates that that species might also play a role in chronic reproductive failures in bovines.

The main limitation of the present study is the small number of studied cows. Despite this, outcomes are encouraging and complement the limitation brought in a recent study conducted on uteri from slaughtered cows (Di Azevedo et al., 2020). Noteworthy that leptospiral DNA was detected in most genital samples of cows with chronic subfertility, while none of the urine samples were positive. The absence of leptospiral DNA in urine highlights that reproductive tract is a primary site of leptospiral colonization (Pinto et al., 2020; Di Azevedo et al., 2020). The presence of leptospires in the genital tract of cows with reproductive problems was shown to be more frequent than in the urinary tract. Pimenta et al. (2019) reported 8/24 positive cows in CVM in contrast to only one in urine. These outcomes and the fact that bovine leptospirosis is mainly related to reproductive failure emphasize the importance of diagnosing genital carriers and how this infection may have been misdiagnosed when only urine samples were analyzed.

Although uterine biopsy has been an ordinary tool to assess endometrial health, it has never been used for the diagnosis of leptospirosis in live cows before. It is important to mention that biopsy has some limitations: it is a relatively difficult to proceed and must be executed by an experienced practitioner; and the fragment obtained is slight and may not represent the whole organ (Chapwanya et al., 2010). Besides, the exact localization of the leptospiral infection on uterus is unknown; thus, although positive results are very reliable, negative results may not reflect that the whole uterus is indeed free of infection (Loureiro and Lilenbaum, 2020). For that reason, we could not affirm that cows # 7, 8 and 9 were really free of infection.

In conclusion, this study reinforces data obtained in slaughtered cows about genital colonization by leptospires. Besides the detection of leptospiral DNA on genital samples of live subfertile cows and not in urine, the outcomes could be associated to embryonic death and chronic subfertility.

Funding: This work was supported by the Fundação de Amparo à Pesquisa do Estado do Rio de Janeiro (FAPERJ) and Conselho Nacional de Desenvolvimento Científico e Tecnológico (CNPq).

Declaration of Competing Interest

The authors declare that they have no known competing financial interests or personal relationships that could have appeared to influence the work reported in this paper.

References

- Chapwanya, A., Meade, K., Narciandi, F., Stanley, P., 2010. Endometrial biopsy: a valuable clinical and research tool in bovine reproduction. *Theriogenology* 73, 988–994.
- Di Azevedo, M.I.N., Lilenbaum, W., 2021. An overview on the molecular diagnosis of animal leptospirosis. *Lett Appl Microbiol* 72, 496–508.
- Di Azevedo, M.I.N., Pires, B.C., Libonati, H., Pinto, P.S., Barbosa, L.F.C., Carvalho-Costa, F.A., Lilenbaum, W., 2020. Extra-renal bovine leptospirosis: Molecular characterization of the *Leptospira interrogans* Sejroe serogroup on the uterus of non-pregnant cows. *Vet. Microbiol.* 250, e108869.
- Ellis, W.A., 1985. Bovine leptospirosis in the tropics: prevalence, pathogenesis and control. *Prev. Vet. Med.* 2, 411–442.
- Ellis, W.A., 2015. Animal Leptospirosis. *Cur Top Microbiol. Immunol.* 387, 99–137.
- Gregoire, F., Bakinahe, R., Petitjean, T., Boarbi, S., Delooz, L., Fretin, D., Saulmont, M., Mori, M., 2020. Laboratory Diagnosis of Bovine Abortions Caused by Non-Maintenance Pathogenic *Leptospira* spp.: Necropsy, Serology and Molecular Study Out of a Belgian Experience. *Pathogens* 9, 413.
- Hamond, C., Pestana, C.P., Medeiros, M.A., Lilenbaum, W., 2016. Genotyping of *Leptospira* directly in urine samples of cattle demonstrates a diversity of species and strains in Brazil. *Epidemiol. Infect.* 144, 72–75.
- Jaeger, L.H., Loureiro, A.P., Lilenbaum, W., 2018. VNTR analysis demonstrates new patterns and high genetic diversity of *Leptospira* sp. of animal origin in Brazil. *Lett Appl Microbiol.* 67, 183–189.
- Libonati, H.A., Santos, G.B., Souza, G.N., Brandão, F.Z., Lilenbaum, W., 2018. Leptospirosis is strongly associated to estrus repetition on cattle. *Trop. Anim. Health Prod.* 50, 1625–1629.
- Loureiro, A.P., Pestana, C., Medeiros, M.A., Lilenbaum, W., 2017. High frequency of leptospiral vaginal carriers among slaughtered cows. *Anim. Reprod. Sci.* 178, 50–54.
- Loureiro, A.P., Lilenbaum, W., 2020. Genital bovine leptospirosis: a new look to an old disease. *Theriogenology* 141, 41–47.
- Martins, G., Loureiro, A.P., Hamond, C., Pinna, M.H., Bremont, S., Bourhy, P., Lilenbaum, W., 2015. First isolation of *Leptospira noguchii* serogroups Panama and Autumnalis from cattle. *Epidemiol. Infect.* 143, 1538–1541.
- OIE, 2018. Manual of Diagnostic Tests and Vaccine for Terrestrial Animals. World Organisation for Animal Health.
- Otaka, D.Y., Martins, G., Hamond, C., Penna, B., Medeiros, M.A., Lilenbaum, W., 2012. Serology and PCR for bovine leptospirosis: herd and individual approaches. *Vet. Rec.* 170, 338.
- Pimenta, C.L.R.M., Costa, D.F., Silva, M.L.C.R., Pereira, H.D., Júnior, J.P.A., Malossi, C. D., Ullmann, L.S., Alves, C.J., Azevedo, S.S., 2019. Strategies of the control of an outbreak of leptospiral infection in dairy cattle in Northeastern Brazil. *Trop Anim Health Prod.* 51, 237–241.
- Pinto, P.S., Libonati, H., Penna, B., Lilenbaum, W., 2016. A systematic review on the microscopic agglutination test seroepidemiology of bovine leptospirosis in Latin America. *Trop Anim Health Prod.* 48, 239–248.
- Pinto, P.S., Pestana, C., Medeiros, M.A., Lilenbaum, W., 2017. Plurality of *Leptospira* strains on slaughtered animals suggest a broader concept of adaptability of leptospires to cattle. *Acta Trop.* 172, 156–159.
- Pinto, P.S., Barbosa, C., Ferreira, A.M.R., Lilenbaum, W., 2020. Uterine leptospiral infection is strongly associated to strains of serogroup Sejroe on experimentally infected hamsters. *Microb. Pathog.* 104030
- Pires, B.C., Berzin Grapiglia, J., Moreira, L., Jaeger, L.H., Carvalho-Costa, F.A., Lilenbaum, W., 2018. Occurrence of uterine carriers for *Leptospira interrogans* on slaughtered cows. *Microb. Pathog.* 114, 163–165.
- Silva, A.F., Farias, P.J.A., Silva, M.L.C.R., Araújo Junior, J.P., Malossi, C.D., Ullmann, L. S., Costa, D.F., Higino, S.S.S., Azevedo, S.S., Alves, C.J., 2019. High frequency of genital carriers of *Leptospira* sp. in sheep slaughtered in the semi-arid region of northeastern Brazil. *Trop. Anim. Health Prod.* 51, 43–47.
- Stoddard, R.A., Gee, J.E., Wilkins, P.P., McCaustland, K., Hoffmaster, A.R., 2009. Detection of pathogenic *Leptospira* spp. through TaqMan polymerase chain reaction targeting *LipL32* gene. *Diagn. Microbiol. Infect. Dis.* 64, 247–255.



Reproductive seasonality of hair rams under tropical conditions: an alternative for non-seasonal lamb production?

Arnaldo de Sá Geraldo¹ · Pedro Henrique Nicolau Pinto¹ · Ana Beatriz da Silva Carvalho¹ ·
Marta Maria Campos Pereira da Costa¹ · Juliana Dantas Rodrigues Santos¹ · Augusto Ryonosuke Taira¹ ·
Isabel Oliveira Cosentino¹ · Bruna Ramalho Rigaud de Figueiredo¹ · Mário Felipe Alvarez Balaro¹ ·
Rodolfo Ungerfeld² · Felipe Zandonadi Brandão¹

Received: 9 July 2023 / Accepted: 27 November 2023
© The Author(s), under exclusive licence to Springer Nature B.V. 2023

Abstract

Reproductive seasonality limits the periods of breeding on the year and, therefore, productive output. However, some breeds appear as probably non-seasonal. The aim of the study was to characterize the seasonal pattern of Santa Inês rams, including an ultrasound characterization of the reproductive tract, testosterone concentrations, and semen characteristics. Fifteen Santa Inês rams remained in a grazing system with concentrate supplementation, and measurements of the reproductive tract and ultrasound evaluation (biometrics and pixel intensity) of the testicles and accessory sex glands were monthly recorded. Computerized seminal evaluations were also performed monthly, and serum testosterone concentration was measured every 15 days. Body weight and condition remained stable throughout the year. In general, reproductive traits varied along the year and reached maximum values during autumn and minimum in spring. Despite that, as fresh semen remained with enough quality to breed all along the year, seasonality does not appear as a limiting factor to breed along the year. Therefore, Santa Inês rams can be used for all-year-round breeding or for crossbreeding when rams from other breeds decrease their fertilizing ability.

Keywords Breeding period · Seasonality · Photoperiod · Hair sheep

Introduction

Most small ruminants are classified as short-day seasonal polyestrous animals, which implies that their reproductive activity increases when the day time length decreases (summer to autumn). The intensity of the changes in photoperiod along the year is greater at higher latitudes, therefore making more pronounced the reproductive changes in sheep throughout the year (Fraser and Lincoln, 1980). However, as domestication has reduced the environmental influences on seasonality, currently, there are other factors influencing the length and intensity of reproductive activity in livestock

during the photoperiod season (Lincoln et al., 1990). However, in many regions of the world, the sheep industry is limited by the seasonality of its products (Chemineau et al. 2007) as lambs can be only delivered to the market according to the seasonal period of births. The spermatogenic process limits the reproductive ability in males to breed, so there is a lack between male and female seasonal patterns. In general, males increase their reproductive activity 2 or 3 months before the onset of the female breeding season. (Ungerfeld et al., 2020).

Several reproductive biotechnologies including hormonal treatments have been explored to overcome the seasonal barrier to induce estrus and ovulation in the ewe and to stimulate the ram reproductive activity (Amiridis and Cseh, 2012; Espírito-Santo et al. 2021). However, new consumers demand hormone-free products (Scaramuzi and Martin, 2008), so the interest in the development of natural strategies to modify or even switch seasonal reproduction is increasing (Martin and Kadokawa, 2006). This implies a deeper knowledge of the physiological mechanisms involved in the

✉ Felipe Zandonadi Brandão
fzbrandao@id.uff.br

¹ Faculdade de Veterinária, Universidade Federal Fluminense, Niterói, RJ, Brazil

² Departamento de Biociencias Veterinarias, Facultad de Veterinaria, Universidad de La República, Ruta 8 Km 18, 13000 Montevideo, Uruguay

regulation of the reproductive pattern, especially in understand how breeds and their evolution are related to their seasonal pattern. In this sense, searching for less or non-seasonal biotypes breeds is an alternative to mitigate the seasonal lamb production. From this perspective, hair sheep breeds are considered non-seasonal or light seasonal breeds (Balara et al. 2014), although there are scarce systematic studies in the ram focused on the breeding activity and changes of the reproductive tract throughout the year. Moreover, seasonality can be affecting in different intensities on some traits, disturbing the effectiveness of rams for breeding purposes. Although in some studies the hair sheep breeds are considered as non-seasonal (Cerna et al., 2000; Arroyo et al., 2007), the reproductive development of Saint Croix male lambs differs according to the birth season (Sánchez-Dávila et al. 2019).

In this context, Santa Inês is a hair sheep breed locally originated in Brazil, adapted to tropical climate (Rocha et al 2004), which presents maternal ability, prolificacy, early puberty (Silva et al., 2011), and resistance to parasitic infections (Amarante et al., 2004). Moreover, this breed is adapted to tropical conditions. Therefore, the aim of this study was to characterize the seasonal pattern of Santa Inês rams, including an ultrasound characterization of the reproductive tract, testosterone levels, and semen traits.

Materials and methods

This study was approved by the Ethics Committee for Use of Animals (CEUA no. 5526080119) of Universidade Federal Fluminense, following the guidelines of the “Brazilian Society of Science in Laboratory Animal” and the “Animal Research: Report of In vivo Experiences” (ARRIVE).

Location and animals

The study was performed at the Unidade de Pesquisa Experimental em Caprinos e Ovinos (UNIPECO) in Cachoeiras de Macacu (22°27' SL), Rio de Janeiro, Brazil, from June 2019 to May 2020. Fifteen Santa Inês rams of 1.2 ± 0.2 years old at the beginning of the study, weighing 49.3 ± 1.8 kg and with a body condition score of 2.7 ± 0.4 (1–5 scale) (Suiter, 1994), were used. At the onset of the study, none of the animals had a clinical disorder and were approved in a breeding soundness exam. Animals included had at least 75% progressive motile sperm (subjective evaluation) and 90% of cells with normal morphology, in agreement with the recommendations of the Brazilian College of Animal Reproduction (CBRA, 2013). Rams were allocated in pens with grass (*Brachiaria decumbens*) during the day and sheltered at night when they were fed chopped grass (*Pennisetum purpureum*; 2.0 kg DM/day/ram) and 500 g concentrate each

(18% crude protein). Water and mineral salt (Salminas, Sal Minas, Minas Gerais Brazil) were provided ad libitum.

Biometric variables

Epididymis and testicles' depth, width, and height were monthly determined using a caliper (Levolpe, São Paulo, Brazil). The testicular and the epididymis volume were estimated as $(4 \cdot \pi \cdot \text{testicular or epididymis height} \cdot \text{length} \cdot \text{width})/3$, and a gonadosomatic index expressed as percentage (testicular volume/body weight) was calculated. Scrotal circumference was determined using flexible measuring tape (WalMur, Porto Alegre, Brazil).

Ultrasound evaluation

Ultrasound evaluations of the reproductive tract were monthly performed by the same operator using a portable transrectal B-mode ultrasonography equipment (Sonoscape S6, SonoScape, Shenzhen, China), with a 7.5 MHz linear transducer. Accessory sex glands were scanned through transrectal ultrasound according to Espírito-Santo et al. (2021). The areas of the bulbourethral and vesicular glands (BUG-A and VG-A, respectively) and the prostatic gland diameter (PG-D) were measured.

A pixel evaluation from the images produced during ultrasonography was performed according to Espírito-Santo et al. (2021). For that, one spot in the center of accessory sex glands was selected ($w = 250$; $h = 80$). The pixel intensity ranged from 0 to 255, where 0 was assigned to a black pixel (anechoic) and 255 to a white pixel (hyperechoic). ImageJ software was used to calculate the average number of pixels or their echogenicity. This variable was determined for the vesicular gland, prostate, and bulbourethral gland echogenicity. Mean data was calculated in each variable and used for the analysis.

Testosterone measurement

Blood samples were collected every 15 days for testosterone assessment. Blood was collected by jugular venipuncture, using vacuum tubes without anticoagulant or preservative (Vacutainer, BD, Juiz de Fora, Brazil). Samples were immediately centrifuged at 1500 g for 15 min. Serum was removed and stored in 1.5 mL microtubes and refrigerated (-20°C) until analysis. Serum testosterone was determined by solid-phase radioimmunoassay, using commercial kits (Beckman Coulter, Immunotech, Prague, Czech Republic) following the manufacturer's instructions. The sensitivity was 0.05 ng/mL, and the intra-assay coefficient of variation was 10%. All data were found to be within the minimum and maximum points of the curve.

Semen collection and assessment

Semen was monthly collected for 12 months — except March, due to technical problems — by electro-ejaculator (2–5 V) following the method described by Ungerfeld et al. (2022). The rams were mechanically restrained in a sheep crush, and the prepuce was shaved, and its inner part washed with saline solution. The rectum was emptied of feces, and the electro-ejaculator's (TK800, TK Reprodução Animal, Minas Gerais, Brazil) probe was lubricated with carboxymethyl cellulose and then inserted. Series of 10 electrical pulses were applied, beginning with 2 V and increasing by 1 V every ten pulses until a maximum of 5 V. Each pulse lasted 3–5 s, with resting periods of 2 s. The process was manually controlled. After the semen collection, the volume was measured using graduated micropipettes, and sperm concentration was determined using a Neubauer chamber (1:800 dilution). Vigor (velocity of the sperm cell to cross a visual section under the microscope) was assessed using a subjective 1–5 scale (being, 1 minimum speed and 5 maximum speed) by observing one drop of diluted semen with a coverslip at 400× magnification. The functional integrity of the sperm membrane was evaluated with the hypo-osmotic swelling test (HOST) according to Ramu and Jeyendran (2013).

An aliquot of 10 µL was diluted in 990 µL of saline solution at 37 °C (1:100 dilution) for computer-assisted semen analysis (CASA) using the SCA system (Sperm Class Analyzer – SCA, Microscopic Automatic Diagnostic Systems, Barcelona, Spain). Five fields from each sample were randomly selected and evaluated. Software settings were adjusted to ram spermatozoa. Sperm kinetics variables included the percentage of motile sperm (MS); sperm with progressive motility (SPM); fast, medium, and slow sperm; the average path velocity (VAP); and curvilinear velocity (VCL). CASA analyses were not performed in September due to technical problems the equipment. Observing one drop of diluted semen with a coverslip (400× magnification), and using a subjective 1–5 scale (being, 1 minimum speed and 5 maximum speed) vigor (velocity of the sperm cell to cross a visual section under the microscope), was assessed.

Statistical analysis

Data were analyzed with a mixed model, including time (month) as the main fact, considering it as a repeated measure. All data were analyzed with the SAS on Demand for Academics. Post hoc comparisons were performed with the pdiff tool of SAS. Data are presented as LS mean ± SEM. Differences were considered significant when $P \leq 0.05$ and as tendencies when $0.1 \leq P < 0.05$.

Results

Overall, the reproductive traits varied along the year, with greater development at autumn and worst at spring. In all the figures, the upper panel presents the daylight hours to make it easy to relate it with the different variables.

Biometric variables and testosterone concentrations

During the experimental period, body weight and body condition did not change significantly (body weight, Fig. 1B). Testicular volume and the scrotal circumference changed along the year ($P < 0.0001$ and $P = 0.02$ respectively). Testicular volume increased during winter and showed a significant drop in February. Scrotal circumference increased during the months of July to December, and then it stabilized (Fig. 1C). The relative amount of testes volume (gonadosomatic index) varied along the year ($P < 0.0001$), showed an important drop in February, and remained low until the end of the study (Fig. 1D). Testosterone concentrations varied throughout the year ($P < 0.0001$) and showed higher values from February to April (Fig. 1E).

Epididymis volume varied along the year ($P < 0.0001$), with a significant drop in February, and ended the experimental period at its lowest levels (Fig. 2B). The prostatic gland diameter varied throughout the year ($P < 0.0001$), with lower values from June to August, and a significant increase in March (Fig. 2C). Its pixel intensity also varied throughout the year ($P < 0.0001$), with greater values from November to April (Fig. 2C). The bulbourethral gland area and its' pixel intensity varied with time ($P = 0.001$ and $P < 0.0001$ respectively) and increased from February to March (Fig. 2D). The vesicular gland area increased during the experiment, and its' pixel intensity tended to vary throughout the year ($P = 0.09$) (Fig. 2E).

Spermatic variables

Semen volume varied along the year ($P = 0.02$), with stable values in most months, with a significant increase in February (Fig. 3B). Sperm concentration did not change significantly throughout the year (Fig. 3B). The total number of ejaculated sperm did not change significantly over the year. The total number of sperm with functional membrane ejaculated increased ($P = 0.04$) from January to April (Fig. 3C). The percentage of motile sperm tended to vary along the year ($P = 0.057$). The percentage of sperm with progressive motility showed a punctual decrease in May (Fig. 3D). The total number of motile sperm ejaculated did not vary significantly along the year. The total number of progressive motile sperm ejaculated had a significant peak in April

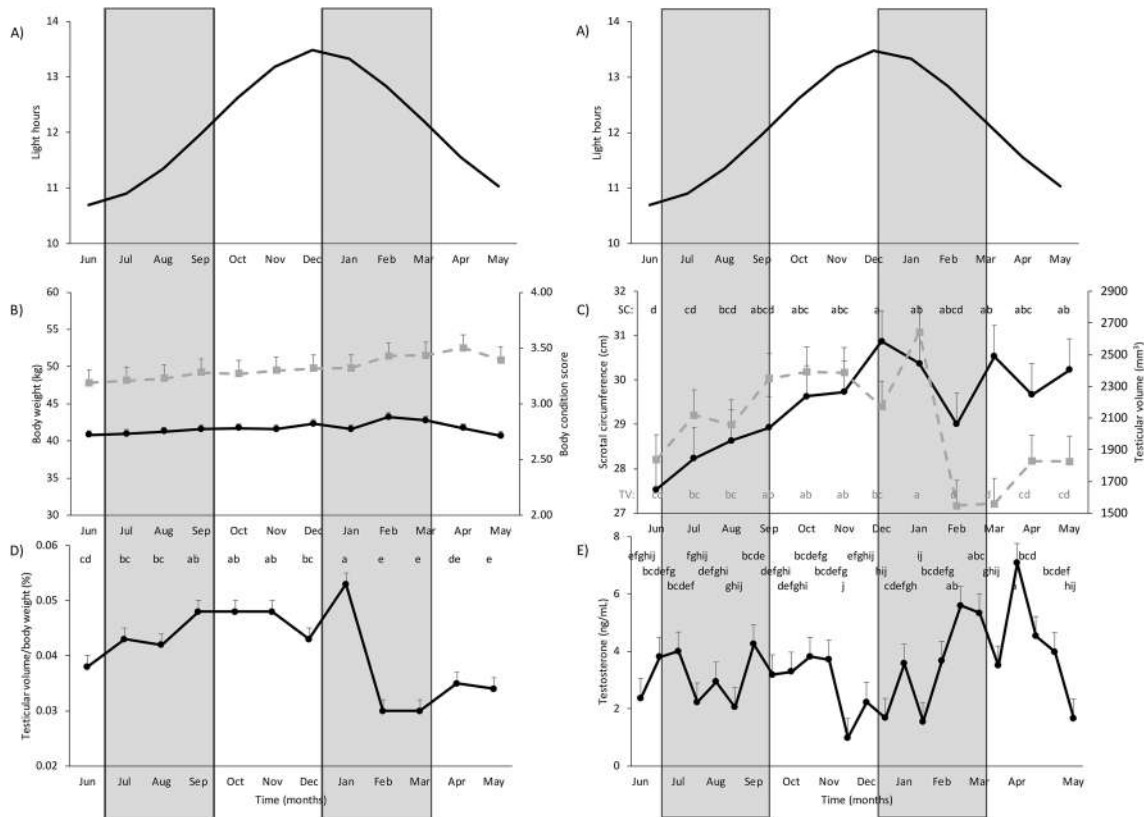


Fig. 1 Seasonal variation in **A** light hours, **B** body weight (solid line) and body condition score (dotted line), **C** scrotal circumference (solid line) and testicular volume (dotted line), **D** testicular volume-to-body

weight ratio, **E** serum testosterone concentrations in Santa Inês rams located at 22°27' SL. Gray bars indicate winter and summer. Different letters in the same line indicate significant differences ($P < 0.05$)

and a decrease in May (Fig. 3E). Vigor varied along the year ($P = 0.01$) and had lower values in July and October to December. The percentage of sperm with integral membrane tended to vary along the year ($P = 0.06$) (Fig. 3F).

The percentage of fast, medium, and slow sperm varied along the year ($P = 0.001$, $P = 0.004$, and $P < 0.0001$, respectively). While the percentage of fast sperm showed a significant drop from April to May, the percentage of medium and slow sperm increased during that period (Fig. 4B). Sperm velocity variables, VCL and VAP, also varied along the year ($P < 0.0001$ for both variables). Both had minimum values in November, January, and May (Fig. 4C).

Discussion

Santa Inês rams have seasonal changes but considering that motile sperm, vigor, and sperm concentration are the main markers used in breeding soundness exams (CBRA, 2013); it appears that these rams are probably able to impregnate ewes at any moment of the year. In this sense, the breed can be characterized as a light seasonal

breed in which ewes are cycling at any moment of the year (Balara et al., 2014), expanding now the knowledge to rams. For example, despite there being variations, the percentage of motile sperm remained above 80% throughout the whole year. This year-long suitability for reproduction was also observed in Pelibuey and Zulu rams in similar latitudes (Aguirre et al., 2007; Ngcobo et al., 2020), with the advantage that Santa Inês sheep are well adapted to local conditions, including low-fat meat and good maternal traits (Paim et al. 2013). Therefore, this breed provides an opportunity for terminal crossbreeding with meat-producing breeds whose rams may be more seasonal (Pool et al., 2020), enhancing production efficiency. However, it should be noted that the success of males is related not only to semen quality but also to the display of a libido enough strong to search for estrous ewes and mate them effectively, a factor that should be studied to have a whole view of the breed. In any case, according to the results of this study, at least fresh semen appears as usable throughout the year, remaining also to determine its' cryoresistance to produce semen from superior breeders all along the year.

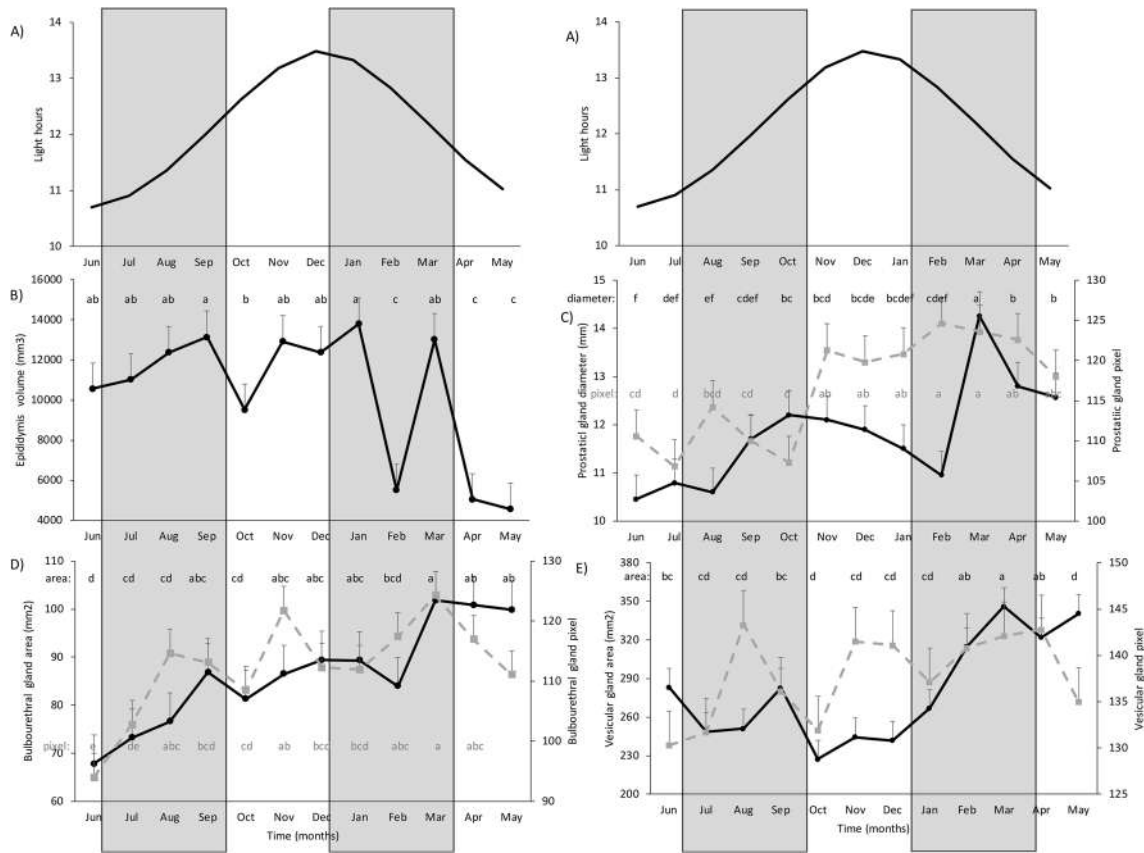


Fig. 2 Seasonal variation in **A** light hours, **B** epididymis volume, **C** prostatic gland diameter (solid line) and echogenicity (dotted line), **D** bulbourethral gland area (solid line) and echogenicity (dotted line), **E** vesicular gland area (solid line) and echogenicity (dotted line) in

Santa Inês rams located at 22°27' SL. Gray bars indicate winter and summer. Different letters in the same line indicate significant differences ($P < 0.05$)

It is important to point out that body weight and body condition had only slight non-significant changes along the year, so the fluctuations reported in most reproductive traits were independent of changes in the general status of the animals and, therefore, dependent on other environmental signals. The changes reported on the testicular volume-to-body weight relationship reinforce this concept, indicating changes in testicular size not associated with changes in rams body weight. However, the annual increase in this trait was delayed from the absolute value of testicular volume and more closely associated with the period in which testosterone concentrations increased. Therefore, it is suggested that the recovery of testicular functionality was delayed in relation to testicular size. In concordance, the period with greater relative testicular size was related with also the greater number of sperm ejaculated and the increase in the size of the accessory glands. Indicating that testicular size is an easy and non-costly trait very practical to evaluate potential performance. However, it should be considered as a dynamic trait with more predictable results if it is evaluated

over time. In this sense, although being able to breed along the year, Santa Inês rams have important variations in their reproductive status, being able therefore to be categorized as a seasonal breed.

As was mentioned, there were not important variations in the metabolic status as body weight and body condition remained stable throughout the year. In general, in small ruminants, it is assumed that photoperiod is the main influence on seasonality (Lincoln and Short, 1980; Bronson, 1990). A reduction in the length of time that light is perceived by the animal leads to a longer period of melatonin secretion, associated with an increase in the production of steroid hormones, such as testosterone (Bhattacharya et al., 2019). Unfortunately, it was not possible to evaluate semen during March, apparently a crucial month in the middle of the negative photoperiod phase, so those data remain to be assessed. However, according to the general trend, it is expected to collect semen with high-quality characteristics, also consistent with what may be expected during that period of the year.

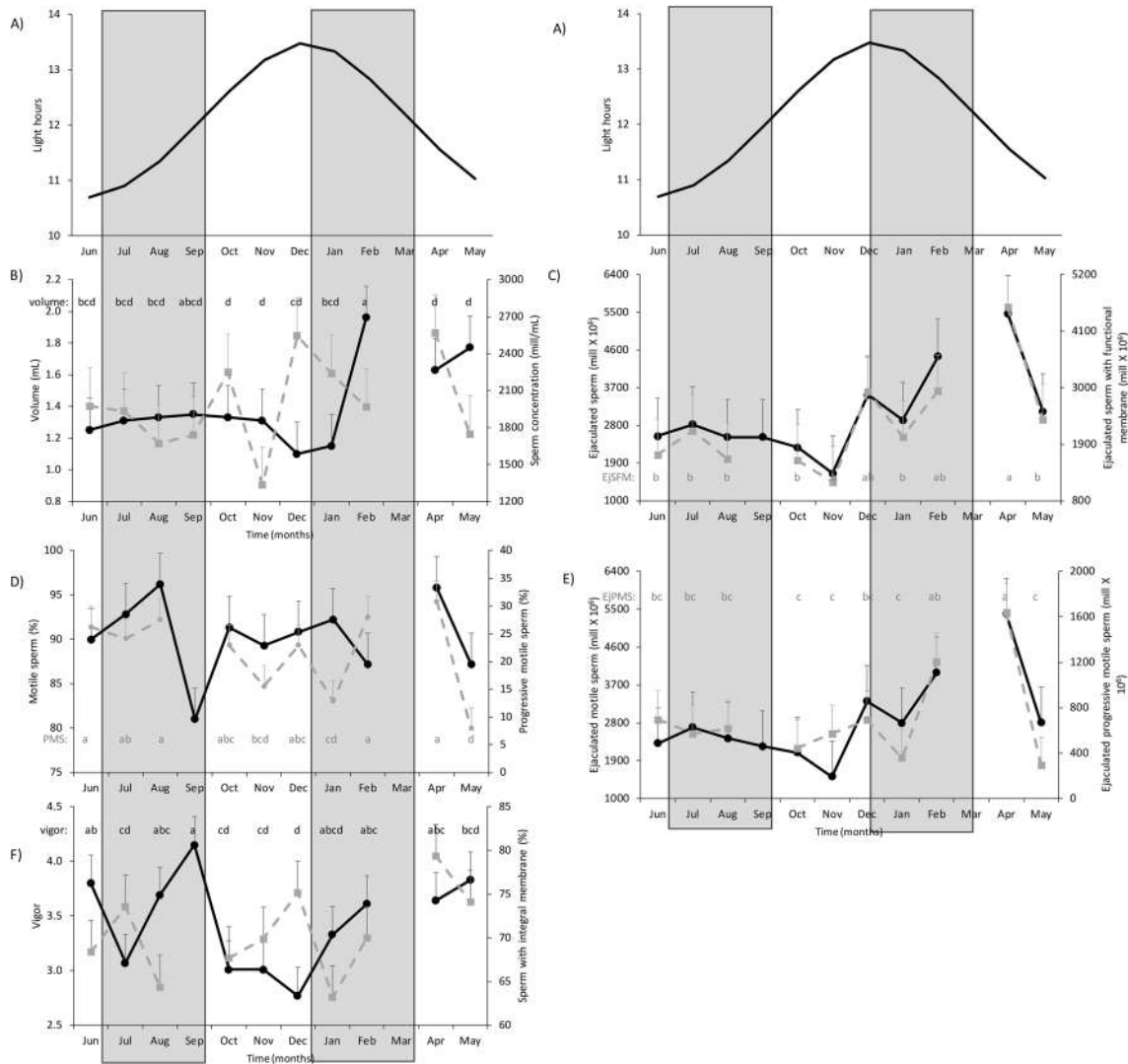


Fig. 3 Seasonal variation in **A** light hours, **B** semen volume (solid line) and sperm concentration (dotted line), **C** ejaculated sperm (solid line) and ejaculated sperm with a functional membrane (dotted line), **D** total motile sperm (solid line) and sperm with progressive motility (dotted line), **E** ejaculated motile sperm (solid line) and ejaculated

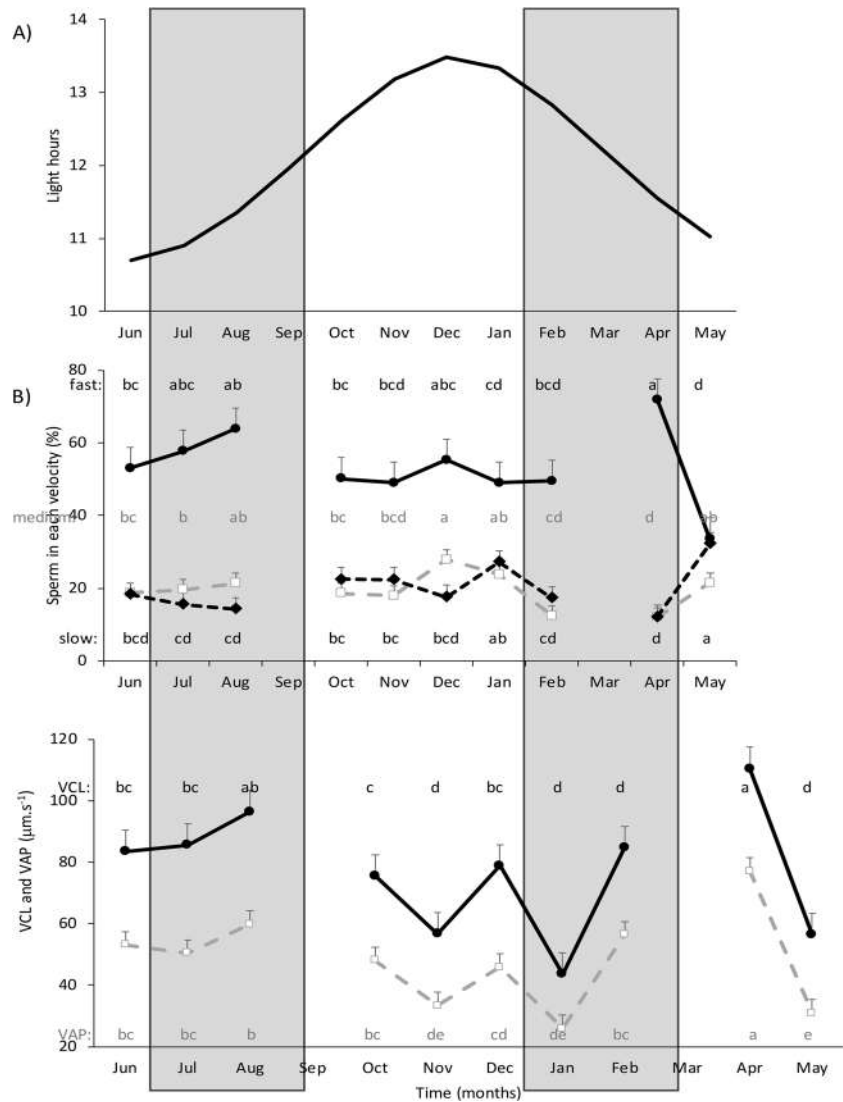
progressive motile sperm (dotted line), **F** vigor (solid line) and sperm with a functional membrane (dotted line) in Santa Inês rams located at 22°27' SL. Gray columns indicate winter and summer. Different letters in the same line indicate significant differences ($P < 0.05$)

In our study, rams received similar amounts of food of stable quality throughout the year, which in concordance, allowed them to maintain their body condition. However, in typical tropical systems, food availability and quality vary along the year, with higher availability of forage in summer (Feitosa et al., 2021), which may also impact testosterone production (Martin et al., 1994; Selvaraju et al., 2012). In our study, testosterone concentration remained during the year in values similar to those reported in summer in this breed (Espírito Santo et al., 2021), which may be related to the breed per se or to the high body condition of these rams. This may be an interesting characteristic of the breed, as there are more strong seasonal breeds in which rams are unresponsive to nutritional “flushing”

stimulation, but rams from less seasonal breeds are more responsive to nutritional stimulus (Hötzel et al., 2003). If so, this would allow managing the reproductive status of the rams according to breeding periods independent of the moment of the year.

In conclusion, Santa Inês rams raise at 22° south latitude do not have slight reproductive changes throughout seasons the year. However, there are seasonal variations with traits reaching greater values in autumn and lower in spring. However, these oscillations appear as non-limiting Santa Inês rams’ ability to impregnate ewes all along the year. Therefore, this breed can be used for all-year-round breeding or for crossbreeding when rams from other breeds decrease their fertilizing ability.

Fig. 4 Seasonal variation in **A** light hours; **B** sperm in each velocity, fast (solid line), medium (gray dotted line), and slow (black dotted line); **C** curvilinear velocity (VCL, solid line) and average path velocity (VAP, dotted line) in Santa Inês rams located at 22°27' SL. Gray columns indicate winter and summer. Different letters in the same line indicate significant differences ($P < 0.05$)



Author contribution A.S.G. and P.H.N.P., data interpretation and first draft production; A.B.S.C., M.M.C.P., J.D.R.S., A.R.T., I.O.C., B.R.R., and M.F.A.B., contributed with data collection and animal handling. R.U. and F.Z.B. participated in the conception of the study, developed the hypothesis, study design, data collection, and draft production. R.U. also performed statistical analysis. In addition, all authors revised and approved the final version of the manuscript.

Funding This work was supported by Universidade Federal Fluminense and FAPERJ (E-26/010.002238/2019). MFAB, BRR, and FZB are fellows of the CNPq and PHNP, ABSC, and JDRS of FAPERJ.

Data availability The data that support our findings are available upon reasonable request.

Declarations

Ethics approval This study was approved by the Ethics Committee for Use of Animals (CEUA no. 5526080119) of Universidade Federal Fluminense, following the guidelines of the “Brazilian Society of Science

in Laboratory Animal” and the “Animal Research: Report of In vivo Experiences” (ARRIVE).

Conflict of interest The authors declare no competing interests.

References

- Aguirre, V., Orihuela, A., Vázquez, R., 2007. Effect of semen collection frequency on seasonal variation in sexual behaviour, testosterone, testicular size and semen characteristics of tropical hair rams (*Ovis aries*), *Tropical Animal Health and Production*, 39, 271–277. <https://doi.org/10.1007/s11250-007-9010-8>
- Amarante, A.F.T., Bricarello, P.A., Rocha, R.A., Gennari, S.M., 2004. Resistance of Santa Inês, Suffolk and Ile de France sheep to naturally acquired gastrointestinal nematode infections, *Veterinary Parasitology*, 120, 91–106. <https://doi.org/10.1016/j.vetpar.2003.12.004>

- Amiridis, G.S, Cseh, S., 2012. Assisted reproductive technologies in the reproductive management of small ruminants. *Animal Reproduction Science*, 130, 152–161. <https://doi.org/10.1016/j.anireprosci.2012.01.009>
- Arroyo, L. J., Gallegos-Sánchez, J., Villa-Godoy, A., Berruecos, J. M., Perera, G., Valencia, J., 2007. Reproductive activity of Pelibuey and Suffolk ewes at 19 north latitude. *Animal Reproduction Science*, 102, 24–30. <https://doi.org/10.1016/j.anireprosci.2006.09.025>
- Balaro, M.F.A., Fonseca, J.F., Oba, E., Cardoso, E.C., Brandão, F.Z., 2014. Is the Santa Inês sheep a typical non-seasonal breeder in the Brazilian Southeast? *Tropical Animal Health and Production*, 46, 1533–1537. <https://doi.org/10.1007/s11250-014-0672-8>
- Bhattacharya, K., Sengupta, P., Dutta, S., 2019. Role of melatonin in male reproduction. *Asian Pacific Journal of Reproduction*, 8, 211.
- Bronson F.H., 1990. *Mammalian reproductive biology*, (The University of Chicago Press, Chicago)
- CBRA, 2013. *Manual para exame andrológico e avaliação de sêmen animal*. (Colégio Brasileiro de Reprodução Animal: Belo Horizonte, MG, Brazil)
- Cerna, C., Porras, A., Valencia, M.J., Perera, G., Zarco, L., 2000. Effect of an inverse subtropical (19° 13' N) photoperiod on ovarian activity, melatonin and prolactin secretion in Pelibuey ewes. *Animal Reproduction Science*, 60/61, 511–525. [https://doi.org/10.1016/s0378-4320\(00\)00127-5](https://doi.org/10.1016/s0378-4320(00)00127-5)
- Chemineau, P., Malpaux, B., Brillard, J.P., Fostier, A., 2007. Seasonality of reproduction and production in farm fishes, birds and mammals, *Animal*, 1, 419–423. <https://doi.org/10.1017/S1751731107691873>
- Espírito-Santo, C.G., Balaro, M.F.A., Santos, J.D.R., Correia, L.F.L., Souza, C.V., Taira, A.R., Costa, M.M.C.P., Carvalho, A.B.S., Ungerfeld, R., Brandão, F.Z., 2021. Semen quality, testosterone values, and testicular and accessory gland parameters in rams receiving sustained stimulation with low doses of buserelin. *Animal Production Science*, 62, 152–162. <https://doi.org/10.1071/AN20679>
- Feitosa, O.S., Leite, R.C., Alexandrino, E., Pires, T.J.S., Oliveira, L.B.T., Neto, J.J.P., Santos, A.C. 2021. Forage performance and cattle production as a function of the seasonality of a Brazilian tropical region. *Acta Scientiarum Animal Science*, 44, 2-11. <https://doi.org/10.4025/actascianimsci.v44i1.53779>
- Fraser, H.M., Lincoln, G.A., 1980. Effects of chronic treatment with an LHRH agonist on the secretion of LH, FSH and testosterone in the ram. *Biology of Reproduction*, 22, 269–276. <https://doi.org/10.1095/biolreprod22.2.269>
- Hötzel, M.J., Walkden-Brown, W.W., Fisher, J.S., Martin, G.B., 2003. Determinants of the annual pattern of reproduction in mature male Merino and Suffolk sheep: responses to a nutritional stimulus in the breeding and non-breeding seasons. *Reproduction and Fertility and Development*, 15, 1-9. <https://doi.org/10.1071/rd02024>
- Lincoln, G.A., Lincoln, C.E., McNeilly, A.S., 1990. Seasonal cycles in the blood plasma concentration of FSH, inhibin and testosterone, and testicular size in rams of wild, feral and domesticated breeds of sheep. *Journal Reproduction and Fertility*, 88, 623–633. <https://doi.org/10.1530/jrf.0.0880623>
- Lincoln G.A, Short R.V., 1980. Seasonal breeding: Nature's contraceptive. *Recent Progress Hormone Research*, 36, 1–52. <https://doi.org/10.1016/B978-0-12-571136-4.50007-3>
- Martin, G.B., Tjondronegor, S., Blackberry, M.A., 1994. Effects of nutrition on testicular size and the concentrations of gonadotrophins, testosterone and inhibin in plasma of mature male sheep. *Journal of Reproduction and Fertility*, 101, 121–128. <https://doi.org/10.1530/jrf.0.1010121>
- Martin G.B., Kadokawa H., 2006. 'Clean, green and ethical' animal production. Case study: Reproductive efficiency in small ruminants. *Journal of Reproduction and Development*, 52, 145–152. <https://doi.org/10.1262/jrd.17086-2>
- Ngcobo, J.N., Nephawe, K.A., Maqhashu, A., Nedanbale, T.L., 2020. Seasonal Variations in Semen Parameters of Zulu Rams Preserved at 10°C for 72 H During Breeding and NonBreeding Season. *American Journal of Animal and Veterinary Sciences*, 15, 226-239. <https://doi.org/10.3844/ajavsp.2020.226.239>
- Paim, T.P., Silva, A.F., Martins, R.F.S., Borges, B.O., Lima, P.M.T., Cardoso, C.C., Esteves, G.I.F., Louvandini, H., McManus, C.M., 2013. Performance, survivability and carcass traits of crossbred lambs from five paternal breeds with local hair breed Santa Inês ewes. *Small Ruminant Research*, 112, 28–34. <http://dx.doi.org/https://doi.org/10.1016/j.smallrumres.2012.12.024>
- Pool, K.R., Rickard, J.P., Pini, T., Graaf, S.P., 2020. Exogenous melatonin advances the ram breeding season and increases testicular function. *Scientific Reports*, 10, 9711. <https://doi.org/10.1038/s41598-020-66594-6>
- Ramu S., Jeyendran R.S., 2013. The hypo-osmotic swelling test for evaluation of sperm membrane integrity. *Methods in Molecular Biology*, 927, 21-25. https://doi.org/10.1007/978-1-62703-038-0_3
- Rocha, R.A., Amarante, A.F.T., Bricarello, P.A., 2004. Influence of reproduction status on susceptibility of Santa Inês and Ile de France ewes to nematode parasitism. *Small Ruminant Research*, 55, 65-75. <https://doi.org/10.1016/j.smallrumres.2003.12.004>
- Sánchez-Dávila F., Ungerfeld, R., Bosque-González A.S.D., Bernal-Barragán H., 2019. Seasonality in Saint Croix male lamb reproductive development in northern Mexico. *Reproduction in Domestic Animals*, 54, 391-400. <https://doi.org/10.1111/rda.13372>
- Scaramuzzi, R.J., Martin G.B., 2008. The Importance of Interactions Among Nutrition, Seasonality and Socio-sexual Factors in the Development of Hormone-free Methods for Controlling Fertility. *Reproduction in Domestic Animals*, 43, 129-136. <https://doi.org/10.1111/j.1439-0531.2008.01152.x>
- Selvajaru, S., Sivasubramani, T., Raghavendra, B.S., Raju, P., Rao, S.B.N., Sineshkumar, D., Ravindra, J.P., 2012. Effect of dietary energy on seminal plasma insulin-like growth factor-I (IGF-I), serum IGF-I and testosterone levels, semen quality and fertility in adult rams. *Theriogenology*, 78, 646-655. <https://doi.org/10.1016/j.theriogenology.2012.03.010>

- Silva B.D.M., Castro E.A., Souza C.J.H., Paiva S.R., Sartori R., Franco M.M., Azevedo, H.C., Silva, T.A.S.N., Vieira, A.M.C., Neves, J.P., Melo, E.O., 2011. A new polymorphism in the Growth and Differentiation Factor 9 (GDF9) gene is associated with increased ovulation rate and prolificacy in homozygous sheep. *Animal Genetics*, 42), 89–92. <https://doi.org/10.1111/j.1365-2052.2010.02078.x>
- Suiter J. 1994. Body condition scoring in sheep and goats. *Farmnote*, 69. <https://www.agric.wa.gov.au/>. Accessed 01/11/2022
- Ungerfeld, R., Villagrán, M., Gil-Laureiro, J., Sestelo, A., Beracochea, F., Fumagalli, F., Bielli, A., 2020. Adult and yearling pampas deer stags (*Ozotoceros bezoarticus*) display mild reproductive seasonal patterns with maximum values in autumn. *Animal Reproduction*, 17, e20200021.
- Ungerfeld, R., Fernandes, D.A.M., Balaro, M.F.A., Taira, A.R., Espírito-Santo, C.G., Santos, J.D.R., Costa, M.M.C.P., Carvalho, A.B.S., Rodrigues, A.L.R., Brandão, F.Z., 2022. Administration of butorphanol with ketamine/xylazine sedation reduces the negative responses to electroejaculation in rams. *Theriogenology*, 191, 96-101. <https://doi.org/10.1016/j.theriogenology.2022.08.008>

Publisher's Note Springer Nature remains neutral with regard to jurisdictional claims in published maps and institutional affiliations.

Springer Nature or its licensor (e.g. a society or other partner) holds exclusive rights to this article under a publishing agreement with the author(s) or other rightsholder(s); author self-archiving of the accepted manuscript version of this article is solely governed by the terms of such publishing agreement and applicable law.



Is it time to reconsider the relative weight of sociosexual relationships compared with photoperiod in the control of reproduction of small ruminant females?

J.A. Delgadillo ^{a,*}, H. Hernández ^a, J.A. Abecia ^b, M. Keller ^c, P. Chemineau ^c

^a Centro de Investigación en Reproducción Caprina (CIRCA), Universidad Autónoma Agraria Antonio Narro, 27054 Torreón, Coahuila, Mexico

^b Departamento de Producción Animal, Instituto de Investigación en Ciencias Ambientales (IUCA), Universidad de Zaragoza, Miguel Servet, 177 Zaragoza 50013, Spain

^c Physiologie de la Reproduction et des Comportements, CNRS, IFCE, INRA, Université de Tours, Agreenium, 37380 Nouzilly, France

ARTICLE INFO

Article history:

Received 31 October 2019

Received in revised form 25 February 2020

Accepted 26 February 2020

Keywords:

Caprine

Ovine

Puberty

Postpartum anestrus

Male effect

ABSTRACT

In goats and sheep from the temperate and subtropical latitudes, the breeding season lasts from early autumn to late winter, whereas the anestrus season lasts from late winter to late summer. In prepubertal or postpartum females, the duration of the quiescent period depends mainly on the season of parturition and of nursing duration. In both situations, the ovulatory activity starts only during the breeding season. Photoperiod has been generally considered as a major regulator of all these periods of reproductive activity/inactivity in female sheep and goats (ie puberty, seasonal anestrus, postpartum anestrus). In particular, regarding seasonal anestrus, the sociosexual interactions between males and females have been considered to have only a modulatory role, limited to few weeks preceding the onset or after the offset of the breeding season. Nonetheless, we recently showed that the use of sexually active males plays a crucial role to trigger ovulatory and estrous activities during the anestrus season and also in prepubertal and postpartum females. In fact, in females exposed to sexually active males, puberty is strikingly advanced in comparison with females exposed to sexually inactive castrated males or to isolated females (6 mo vs 7.5 mo). Most females (>85%) exposed during the anestrus season to sexually active males ovulated, whereas a low proportion of them ovulated when in contact with sexually inactive males (<10%). Interestingly, the presence of these sexually active males allows females to ovulate all the year round and prevents the seasonal decrease of LH plasma concentrations in ovariectomized females treated with an estradiol implant. Finally, the presence of sexually active males triggers ovulation in postpartum anestrus females nursing their offspring. All these findings show that sexually active males can play an important role to reduce anestrus periods. We need, therefore, to reconsider the relative weight of sociosexual relationships, compared with photoperiod, in the management of reproduction of goat does and ewes.

© 2020 Elsevier Inc. All rights reserved.

1. Introduction

Seasonality of birth in sheep and goats is one of the major constraints for farmers in the temperate and subtropical latitudes [1]. This trait has been inherited from their wild ancestors during the domestication process

* Corresponding author. Tel.: 8717297641; fax: 8717297642.

E-mail address: joaldesa@yahoo.com (J.A. Delgadillo).

about 13,000 yr ago [2]. This seasonality of breeding comes from the existence of periods in the year when both sexes are spontaneously sexually active (end of summer-autumn) or sexually inactive (winter-spring, called the anestrus season), conducting to a well-defined season of birth at the end of winter [3]. Durations of prepubertal and postpartum periods of anovulation also depend strongly on the season of birth for puberty and of parturition for postpartum anestrus (PPA). In both instances, sexual activity occurs in the next breeding season after birth or parturition.

Sheep and goats are a model for studying the mechanisms of control of seasonal reproduction, especially the mechanisms by which photoperiod and sociosexual relationships act on the reproductive axis to induce a stable succession of breeding and anestrus seasons. The main conclusions of these studies until recently were that photoperiod is the major environmental cue controlling the onset and end of estrus and ovulatory cyclicity in ewes and does. Similarly, photoperiod controls the increase and decrease of spermatogenic and libidinous activities in males in summer-autumn and winter-spring, respectively. Photoperiod induces changes in estradiol and testosterone negative feedback on LH secretion, constituting the main neuroendocrine mechanism responsible for seasonality. The sociosexual interactions between sexes have been generally considered of minor weight compared with photoperiod, their importance being limited to the few weeks preceding the onset or after the offset of the seasonal cyclicity in females. Many studies were performed using the so-called “male effect” to induce ovulations in anestrus females just before the onset of the sexual season or just after its end [4–6].

However, it is only recently that we realized we may have severely underestimated the full possibility to use sociosexual interactions to manipulate the seasonality of breeding in female sheep and goats. Indeed, recent results indicate that the presence of sexually active males can lead to the total inhibition of seasonality in females. This situation has never been obtained in the aforementioned experiments where the male effect, even when it induced 100% of response in females, triggered only one single ovulation and did not allow ewes or goats to be cyclic. The main reason of this underestimation comes from the fact that males and females are sexually well synchronized over the year: when females are in anestrus season, males are also relatively inactive with a low libido and a poor spermatogenic activity. This is particularly marked in the more seasonal breeds of sheep and goats. Thus, all experiments performed to study sexual seasonality in goats were performed using either females without males or females in contact with sexually inactive males. The same applied in experiments aiming to study the quiescent prepubertal or postpartum periods. Finally, to our knowledge, all experiments conducted to study the male effect in the middle of the anestrus season were performed using males under natural photoperiod, hence showing low sexual activity [4–6].

Using males rendered sexually active during the rest season by an artificial photoperiodic treatment has emerged recently as a promising practice and has led to reconsideration of the relative weight of sociosexual

relationships compared with photoperiod to manipulate goat and sheep reproduction. We will review, in 3 separate sections, the evidence that sociosexual cues play a crucial role to trigger ovulatory and estrous activities in the 3 quiescent periods of the lifetime of goat does and ewes: (i) puberty, (ii) seasonal anestrus, and (iii) PPA.

2. Induction of puberty in female goats and sheep by sexually active males

Puberty is a complex process as it marks the beginning of the reproductive life. During this phase, the individual acquires the physiological capacity of reproduction, exhibiting sexual behaviors. This pubertal transition requires morphological, physiological, and behavioral modifications. During puberty, the hypothalamic-pituitary-gonadal axis, which remains quiescent throughout childhood, is activated leading to the secretion of gonadotropin-releasing hormone (GnRH). Gonadotropin-releasing hormone then stimulates the secretion of gonadotropins, leading to the onset of cyclical ovulatory activity [7].

At the agricultural level, being able to manipulate the age of puberty is important because the time between weaning and puberty is considered as an “unproductive” period. Therefore, the study of the physiological and environmental factors that might reduce this period reasonably or synchronize it with farm management is of interest. Indeed, the management of young females to introduce them in the adult breeding scheme is still an unsolved problem. Finally, the fertility of young females at the first artificial insemination is still low and any early maturation of reproductive function could have a significant impact to improve it.

However, the factors that modulate puberty are far from being understood. It is now clear that various exogenous and endogenous factors modulate puberty onset. Indeed, genetic, metabolic, or environmental signals can all play a role. Among environmental factors, photoperiodic cues are especially of importance in goats as autumn-born females delay their first ovulation to next autumn, when photoperiodic conditions became again favorable [8,9]. Manipulating the photoperiodic environment with a spring-like photoperiod allows counterbalancing this delay in prepubertal ewe lambs [10].

In this context, sociosexual interactions can also modulate puberty. For example, the classical male effect has been used to advance the onset of puberty during the anestrus in ewe lambs/doe kids (see Section 3). Hence, it has been shown that contact with males at the end of the anestrus period advances time of the first estrus by about 2 wk [11–13]. Synchronization of puberty onset or of the first mating occurs after the introduction of a male (ram or buck, respectively) in a group of ewe lambs/doe kids [14], which also stimulated onset of luteal function [15].

However, the only well-documented example of puberty acceleration after male exposure during the sexual season is the prepubertal exposure to an intact male or to its odor that accelerates the onset of puberty in female rodents (the so-called “Vandenbergh” effect) [16]. Until the eighties, only limited reports were documented in domestic ungulates [11,17,18]. More recently, we added

further demonstration that sociosexual contact is important in goats and sheep. In Alpine goats from temperate latitudes, prepubertal females exposed to sexually active males reached puberty 6 wk earlier than prepubertal females exposed to castrated and sexually inactive males or isolated females (6 mo vs 7.5 mo; Fig. 1A) [19]. In this study, females were exposed to males from weaning at 3 mo, starting at the end of June. They reached puberty when they were 6 mo of age, that is when their own sexual season starts in early September. This advance of puberty can be measured by LH pulsatility, progesterone secretion, and by the presence of corpora lutea in the ovary and also through an enhanced development of the reproductive tract [19]. We also showed that when exposing females to sexually active males starting at 3 mo of age, the onset of puberty can even occur as soon as 3.5 to 4 mo, thus highlighting the very early responsiveness of the female gonadotropic axis and the high efficiency of sexually active males [20]. In these experiments, there was a high synchronization of ovarian cyclicity observed in females exposed to sexually active males once they started ovulating. The first ovulation occurred within 2 wk in all females exposed to sexually active males compared with more than 4 wk in the other groups [19,20].

Finally, castrated bucks or bucks used during the nonbreeding season have never produced any effect, thus underlying the role of sensory cues derived from male sexual activity. This suggests that the efficient sensory cues emitted by males are androgen-dependent, as previously

demonstrated in the context of the Vandenberg effect in male mice [21,22]. In addition, we also demonstrated that this effect of puberty acceleration can occur when physical contact between both sexes is prevented, indicating that the somatosensory cues that occur during direct physical interaction are not vital. This result indicates a role of male olfactory cues in this early maturation of female reproductive function, as established in rodents [16,22].

In Aragonesa ewes from Mediterranean latitudes, sexually active males also advance puberty. September-born ewe lambs were housed with vasectomized rams either rendered sexually active by exposure to 2 mo of artificial long days or exposed to the natural photoperiod. Ewe lambs exposed to “activated” rams initiated their ovulatory activity at 27 wk of age, whereas this occurred at 39 wk of age in ewe lambs housed with control rams [23]. Collectively, our results demonstrate the power of sexually active males to initiate and reactivate reproductive function during the quiescent prepubertal period.

3. Suppression of reproductive seasonality in adult female goats and sheep by sexually active males

Seasonality of reproduction is a characteristic of goats and ewes from temperate and subtropical latitudes. For a long time, it was considered that controlling the photoperiod was the main factor if not only means to manipulate seasonality. However, recent studies have shown that sociosexual interactions can be a major tool to override

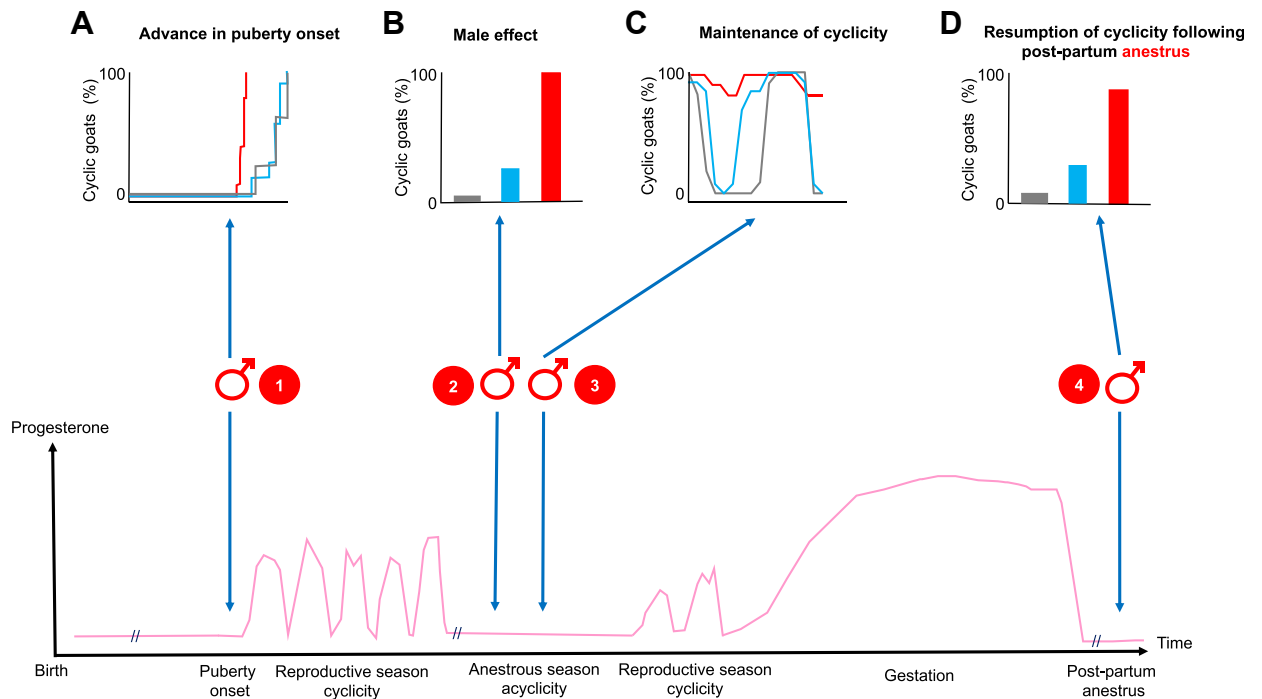


Fig. 1. Schematic representation of the effects of sudden introduction or permanent presence of sexually active bucks on induction and/or maintenance of ovulatory cyclicity in goats in different anovulatory situations (red lines and bars). These sexually active males (A) advance puberty, (B) induce ovulations in seasonally anestrus goats, (C) maintain ovulatory cyclicity over the year in multiparous goats, and (D) induce ovulations in nursing postpartum goats. Note that in each situation, a low percentage of goats ovulated when exposed to sexually inactive bucks (blue lines and bars) or isolated from bucks (gray lines and bars). (For interpretation of the references to color in this figure legend, the reader is referred to the Web version of this article.)

reproductive seasonality. Physiologically, photoperiod induces changes in estradiol and testosterone negative feedback on LH secretion, constituting the main neuroendocrine mechanism responsible of seasonality: estradiol and testosterone negative feedback increases during long days, reducing the secretion of LH, and provoking the anestrus season and sexual rest [24,25]. For decades, therefore, photoperiod has been used to induce reproductive activity during seasonal rest in females and males [26].

Nonetheless, the sociosexual interactions between males and females can also be used to break the natural inhibition of reproductive activity of females during the seasonal rest. Hence, the sudden introduction of a male into a group of seasonal anestrus goats or ewes stimulates within minutes the secretion of LH, as well as estrous behavior (goats), and ovulations within the first 5 days after joining. This phenomenon is known as the “male effect” [27–29]. The sexual response of females to the male effect varies among breeds. In less seasonal breeds, females can respond to the male effect throughout the anestrus season by experiencing generally one single estrous cycle of normal duration after, or if not, a short one [4–6]. By contrast, in strongly seasonal breeds, females respond to the male effect only some weeks preceding the breeding season, but this response is low or null when teasing is performed during midanestrus [4–6]. This low response can be overcome by using males rendered sexually more active during the sexual rest. In Australian cashmere bucks, high-quality diets stimulate their sexual behavior allowing them to induce more females to ovulate than males fed with low-quality diets [30]. However, the sexual behavior of males from some breeds is not improved by nutrition, and photoperiodic treatments must be used. Hence, in Alpine, Payoya, and Mexican bucks, exposure to 2 mo of artificial long days followed by natural photoperiod stimulates their sexual behavior and renders them more efficient to trigger the endocrine and sexual activity in seasonally anestrus goats than untreated bucks (Figs. 1B and 2) [31–33]. Interestingly, in the Mexican goats exposed to sexually active males, LH secretion increased within 15 min after introducing the bucks and remained elevated for 24 h and all females ovulated. On the contrary, in goats exposed to photoperiod-treated males that had been sedated to prevent the display of sexual behavior, LH secretion increased within the first 8 h of exposure but then decreased up to 24 h after the onset of contact and no female ovulated [34,35]. It was also shown that the continued presence of rams is necessary to maintain high rates of LH secretion [36]. These findings indicate that the sexual behavior of males is an important factor to stimulate the endocrine and sexual activity in seasonal anestrus goats.

How the male effect triggers LH secretion and ovulation is not yet fully understood. Estradiol negative feedback on LH secretion was shown in ovariectomized female goats and ewes bearing subcutaneous implants releasing estradiol-17 β (OVX + E). Low and high plasma LH concentrations coincide with the seasonal anovulatory and ovulatory activity in intact does, respectively [37,38]. Merino OVX + E ewes exposed to rams during the anestrus season increased LH secretion [39]. Similarly, Mexican OVX + E goats exposed to sexually active males increased LH

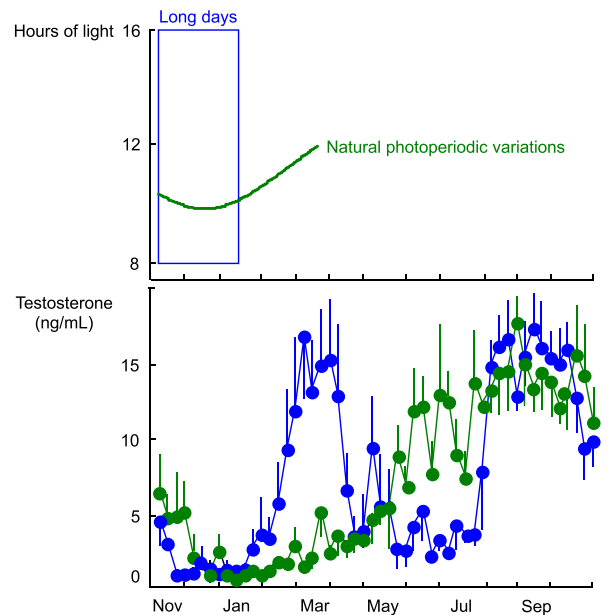


Fig. 2. Photoperiodic treatment applied in open barns (upper panel) and plasma testosterone concentrations (mean \pm SEM; lower panel) in bucks exposed to natural photoperiodic variations (green symbols) or to 2.5 mo of artificial long days from 1 November to 15 January and then exposed to natural day length (blue symbols) [modified from 33]. (For interpretation of the references to color in this figure legend, the reader is referred to the Web version of this article.)

secretion within 15 min of exposure and remained elevated for 12 h. On the contrary, the introduction of sexually inactive males did not stimulate LH secretion [40]. These findings indicate that sexually active males reduce estradiol negative feedback on LH secretion during seasonal anestrus, probably by stimulating kisspeptin neurons located in the arcuate nucleus, which control GnRH secretion [41]. Indeed, in ewes, the introduction of a male stimulated kisspeptin neurons in the hypothalamus, triggering GnRH/LH secretion [42,43]. In goats, a pool of kisspeptin neurons located in the arcuate nucleus acts as a pulse generator controlling GnRH secretion from the median eminence [44], and we showed that neurons of the arcuate nucleus were activated by a sexually active buck but not by a sexually inactive buck [45]. Thus, the stimulus provided by the sexually active males may act via kisspeptin neurons to circumvent estradiol negative feedback on LH secretion during seasonal anestrus, counterbalancing the inhibitory effect of photoperiod.

The continuous presence of control bucks or rams does not prevent females entering seasonal anestrus, even though they increase the duration of the breeding season by delaying its offset and advancing its onset [46]. A first possibility to explain this fact is that the females become refractory to the presence of males [6,46]. A second possibility is that the males in sexual rest are unable to maintain a sufficient stimulation of females during seasonal anestrus [47,48]. Recent results support the second hypothesis. The continuous presence of sexually active males led most Mexican goats to ovulate from April to July (86%), during

their seasonal anestrus. By contrast, the presence of sexually inactive males led to less than 15% females ovulating from April to June (Fig. 1C) [49]. Similarly, at Mediterranean latitudes, Aragonesa ewes exposed to sexually active rams exhibited a higher proportion of monthly estrus and ovulations than ewes exposed to rams in sexual rest [50]. These findings indicate that females do not become refractory to males but, instead, that the continuous presence of sexually active males prevents seasonal anestrus. It appears therefore that in female goats and sheep, the sexual activity of males can be as efficient as photoperiod to manipulate reproductive seasonality.

These findings allowed us to question whether the influences of sexually active males occur at the level of the hypothalamo-pituitary axis or at the level of the gonad. Regarding the classic male effect, it is known that this effect is exerted at the central level to induce synchronous ovulations [43], but the aforementioned effect where males are able to prevent completely the seasonal inhibition of ovulations and are able to prevent any cessation of cyclical activity may be different. To clarify this point, Mexican OVX + E goats were continuously exposed to sexually active or inactive males. In both groups, plasma LH concentrations were high and did not differ from November to February (breeding season). By contrast, from March to May (anestrus season), LH concentrations decreased significantly in goats exposed to sexually inactive males but not in goats exposed to the sexually active males [40]. Similarly, at Mediterranean latitudes, OVX + E Aragonesa ewes maintained high concentrations of plasma LH throughout seasonal anestrus when continuously exposed to photostimulated, sexually active rams. On the contrary, concentrations of plasma LH were reduced from March to May in ewes housed with control rams or in isolated ewes [51]. These findings indicate that the permanent presence of sexually active males prevented the seasonal decrease in LH, probably by reducing estradiol negative feedback on LH secretion. In addition, these findings indicate that stimulation from these sexually active males occurs at the brain level to override the inhibitory effect of photoperiod.

4. Reduction of the duration of PPA in goats and ewes by sexually active bucks

In breeds of goats and sheep showing reproductive seasonality, resumption of sexual activity after parturition depends on several factors, including season of parturition and nursing of offspring. In both species, parturition generally occurs during spring, and resumption of sexual activity after parturition occurs only during the following breeding season. Consequently, the length of PPA is longer in females that give birth in winter than in those that give birth in spring [52,53]. On the other hand, the influence of the duration of nursing on the length of PPA is observed only during the breeding season, and this anestrus is longer in females nursing their offspring than in those not nursing them [52,54].

Interestingly, the sociosexual interactions can reduce the duration of PPA. Indeed, goats kidding in October during the breeding season and nursing their kids for 55 d remained anovulatory up to weaning at 55 d of lactation. In

contrast, the introduction of sexually active bucks at d 30 postpartum induced more than 90% of goats to ovulate (Nandayapa et al unpublished; Fig. 1D). Moreover, the permanent presence of sexually active males reduce the duration of PPA giving birth during seasonal anovulation. Most nursing females kidding in January did not ovulate during the first 55 d postpartum when maintained isolated from bucks or in presence of sexually inactive bucks (<12%); in contrast, most nursing does maintained in contact with sexually active males ovulated during the same period (>80%; Nandayapa et al unpublished). This last study illustrates that when PPA coincides with seasonal anestrus, the presence of sexually active males can override the inhibitory effect of photoperiod and/or lactation on the reactivation of reproductive activity. Therefore, the importance of the biostimulation exerted by sexually active males should be regarded as relevant as suckling of the offspring and season of kidding to control the length of PPA for breeding management. This also applies to sheep because postpartum ewes do not respond to a continuous presence of rams at the time of spring rebreeding [55], but when photoperiodic-treated, sexually active rams are introduced in spring, they advance the resumption of estrous activity in Aragonesa ewes after weaning and, most importantly, this occurred during seasonal anestrus (April to June) [56].

5. Conclusion

It is clear that the power of sexually active bucks and rams on the reproductive activity of does and ewes has been underestimated in the past. We already know by numerous experiments carried out previously that rams and bucks maintained under the same photoperiodic conditions as females are able to induce ovulations when females are anovulatory, but in many cases, when the male effect has succeeded, not all females ovulate and if they do so, they experience only one single cycle of normal duration. We now have a general picture showing that sexually active bucks and rams are able (i) to advance the onset of puberty, (ii) to quite completely suppress seasonal anestrus, and (iii) to reduce the postpartum sexual rest, which are the only 3 quiescent periods in the reproductive life of goats and ewes.

This underestimation probably comes from the close synchronization between sexes: when females are anovulatory, males are sexually quiescent. This observation and the successful experimental use of sexually active males to trigger ovulations in the 3 aforementioned situations has 3 main consequences.

The first one is scientific and incites investigators to reconsider the relative weight of the 2 major cues controlling goats and sheep reproduction: the power of the sociosexual cue is equivalent to that of photoperiod to modulate the central nervous systems and induce LH pulsatility to induce ovulations and maintain cyclicity outside of the annual breeding season. This can be an effective tool to better understand where and how sexually active males act via the different sensory cues, which were demonstrated to be involved in the effect, up to the GnRH neurons themselves in the hypothalamus. Deciphering the pathways from the input of sexually active males into the

olfactory and/or visual and/or tactile systems to the positive control of kisspeptin and their interaction with the negative photoperiodic system could be useful for the future understanding of the seasonal control of reproduction. This is not only true for the 2 species studied here, but we can wonder if more classical models of photoperiodic control of seasonal sexual activity, such as hamsters, would or would not be in the same situation in which sexually active males are able to completely suppress seasonal anovulation. This can be helpful for understanding the underlying mechanisms of photosensitivity in these species.

The second one is also scientific and deals with the other types of sociosexual relationships that may influence reproductive activity in goats and sheep. We have just seen that sexually active males are extremely potent to stimulate female activity, but in the reverse, is intense female sexual activity identically potent for triggering male spermatogenesis and libido? In the same way, are sexually active males able to stimulate other males in the sexual rest as they did to females? These 2 points would be of interest and may help to build a general scheme of how seasonal animals are interacting with their environment and how they integrate the different cues they receive from it.

The third one is more applied and may represent the onset of a new and very useful set of tools to control sheep and goat seasonality on farms, while the future is moving toward more sustainable techniques for controlling reproduction. The use of sexually active males on farms is easy and feasible and presents a much better image of animal production than hormone treatments, which are largely used nowadays for out-of-season breeding and/or artificial insemination. These latter treatments are prohibited in organic farming and are not well thought of by some consumers and citizens. The development of these new and sustainable techniques, that are environmentally friendly, is likely a good avenue to follow in the future.

Acknowledgments

We thank all members of the Centro de Investigación en Reproducción Caprina of the Universidad Autónoma Agraria Antonio Narro, Torreón, Coahuila, Mexico, of the Station de Physiologie de la Reproduction et des Comportements de Nouzilly, France, and of the Departamento de Producción Animal of the Universidad de Zaragoza, Spain, for their dedicated participation in the studies described in this review. Studies performed on goats were conducted as part of the CABRAA International Associated Laboratory between Mexico (UAAAN-CIRCA) and France (INRA-PRC). The authors declare that there are no conflicts of interest.

References

- Chemineau P, Malpoux B, Brillard JP, Fostier A. Seasonality of reproduction and production in farm fishes, birds and mammals. *Animal* 2007;1:419–32.
- Balasse M, Tresset A, Balasescu A, Blaise E, Tornero C, Gandois H, Fiorillo D, Nyerges EA, Fremondeau D, Banffy E, Ivanova M. Animal board invited review: sheep birth distribution in past herds: a review for prehistoric Europe (6th to 3rd millennia BC). *Animal* 2017; 11:2229–36.
- Ortavant R, Pelletier J, Ravault JP, Thimonier J, Volland P. Photoperiod: main proximal and distal factor of the circannual cycle of reproduction in farm mammals. *Oxf Rev Reprod Biol* 1985;7: 305–45.
- Martin GB, Oldham CM, Cognié Y, Pearce DL. The physiological responses of anoovulatory ewes to the introduction of rams—a review. *Livestock Prod Sci* 1986;15:219–47.
- Ungerfeld R, Forsberg M, Rubianes E. Overview of the response of anoestrus ewes to the ram effect. *Reprod Fertil Dev* 2004;16: 479–90.
- Walkden-Brown SW, Martin GB, Restall BJ. Role of male-female interaction in regulating reproduction in sheep and goats. *J Reprod Fertil* 1999;52:243–57.
- Valasi I, Chadio S, Fthenakis GC, Amiridis GS. Management of prepubertal small ruminants: physiological basis and clinical approach. *Anim Reprod Sci* 2012;130:126–34.
- Delgado JA, De Santiago-Miramontes MA, Carrillo E. Season of birth modifies puberty in female and male goats raised under subtropical conditions. *Animal* 2007;1:858–64.
- Papachristoforou C, Koumas A, Pthiouti C. Seasonal effect on puberty and reproductive characteristics of female Chios sheep and Damascus goats born in autumn or in February. *Small Rumin Res* 2000; 38:9–15.
- Foster DL, Ryan KD. Endocrine mechanisms governing transition into adulthood in the female sheep. *J Reprod Fertil* 1981;30:75–90.
- Amoah EA, Bryant MJ. A note on the effect of contact with male goats on occurrence of puberty in female goat kids. *Anim Prod* 1984;38:141–4.
- Kassem R, Owen JB, Fadel I. The effect of pre-mating nutrition and exposure to the presence of rams on the onset of puberty in Awassi Ewe lambs under semi-arid conditions. *Anim Prod* 1989;48:393–7.
- O'Riordan EG, Hanrahan JP. Advancing first estrus in Ewe lambs. *Farm Food Res* 1989;20:25–7.
- Dyrmondsson OR, Lees JL. Attainment of puberty and reproductive performance in Clun Forest Ewe lambs. *J Agric Sci* 1972;78:39–45.
- Bartlewski PM, Beard AP, Cook SJ, Rawlings NC. Ovarian activity during sexual maturation and following introduction of the ram to Ewe lambs. *Small Rumin Res* 2002;43:37–44.
- Vandenbergh JG. Effect of the presence of a male on the sexual maturation of female mice. *Endocrinology* 1967;81:345–9.
- Izard MK, Vandenbergh JG. The effects of bull urine on puberty and calving date in crossbred beef heifers. *J Anim Sci* 1982;55: 1160–8.
- Oldham CM, Gray SJ. The ram effect will advance puberty in 9–10 months old Merino ewes independent of their season of birth. *Proc Aust Soc Anim Prod* 1984;15:727.
- Chasles M, Chesneau D, Moussu C, Poissenot K, Beltramo M, Delgado JA, Chemineau P, Keller M. Sexually active bucks are a critical social cue that activates the gonadotrope axis and early puberty onset in does. *Horm Behav* 2018;106:81–92.
- Chasles M, Chesneau D, Moussu C, Abecia A, Delgado JA, Chemineau P, Keller M. Highly precocious activation of reproductive function in autumn-born goats (*Capra hircus*) by exposure to sexually active bucks. *Domest Anim Endocrinol* 2019;68:100–5.
- Drickamer LC. Contact stimulation, androgenized females and accelerated sexual maturation in female mice. *Behav Biol* 1974;1: 101–10.
- Vandenbergh JG. Male odor accelerates female sexual maturation in mice. *Endocrinology* 1969;84:658–60.
- Abecia JA, Chemineau P, Gomez A, Keller M, Forcada F, Delgado JA. Presence of photoperiod-melatonin-induced, sexually-activated rams in spring advances puberty in autumn-born Ewe lambs. *Anim Reprod Sci* 2016;170:114–20.
- Karsch FJ, Bittman EL, Foster DL, Goodman RL, Legan SJ, Robinson JE. Neuroendocrine basis of seasonal reproduction. *Recent Prog Horm Res* 1984;40:185–232.
- Pelletier J, Ortavant R. Photoperiodic control of LH release in the ram: II. Light-androgens interaction. *Acta Endocrinol (Copenh)* 1975;78:442–50.
- Chemineau P, Pelletier J, Guerin Y, Colas G, Ravault JP, Toure G, Almeida G, Thimonier J, Ortavant R. Photoperiodic and melatonin treatments for the control of seasonal reproduction in sheep and goats. *Reprod Nutr Dev* 1988;28:409–22.
- Underwood EJ, Shier FL, Davenport NJ. Studies in sheep husbandry in Western Australia. V. The breeding season of Merino, crossbred and British breed ewes in agricultural districts. *J Agric* 1944;2:135–43.
- Ungerfeld R, Pinczak A, Forsberg M, Rubianes E. Ovarian responses of anoestrus ewes to the "ram effect". *Can J Anim Sci* 2002;82:599–602.

- [29] Shelton M. The influence of the presence of the male goat on the initiation of oestrous and ovulation in Angora does. *J Anim Sci* 1960; 19:368–75.
- [30] Walkden-Brown SW, Restall BJ, Henniawati. The male effect in Australian cashmere goats. 3: Enhancement with buck nutrition and use of oestrous females. *Anim Reprod Sci* 1993;32:69–84.
- [31] Chasles M, Chesneau D, Moussu C, Delgadillo JA, Chemineau P, Keller M. Sexually active bucks are efficient to stimulate female ovulatory activity during the anestrus season also under temperate latitudes. *Anim Reprod Sci* 2016;168:86–91.
- [32] Zarazaga LA, Gatica MC, Hernández H, Gallego-Calvo L, Delgadillo JA, Guzmán JL. The isolation of females from males to promote a later male effect is unnecessary if the bucks used are sexually active. *Theriogenology* 2017;95:42–7.
- [33] Delgadillo JA, Flores JA, Véliz FG, Hernández HF, Duarte G, Vielma J, Poindron P, Chemineau P, Malpoux B. Induction of sexual activity in lactating anovulatory female goats using male goats treated only with artificially long days. *J Anim Sci* 2002;80:2780–6.
- [34] Vielma J, Chemineau P, Poindron P, Malpoux B, Delgadillo JA. Male sexual behavior contributes to the maintenance of high LH pulsatility in anestrus female goats. *Horm Behav* 2009;56:444–9.
- [35] Martínez-Alfaro JC, Hernández H, Flores JA, Duarte G, Fitz-Rodríguez G, Fernández IG, Bedos M, Chemineau P, Keller M, Delgadillo JA, Vielma J. Importance of intense male sexual behavior for inducing the preovulatory LH surge and ovulation in seasonally anovulatory female goats. *Theriogenology* 2014;82:1028–35.
- [36] Oldham CM, Pearce DT. Mechanism of the ram effect. *Proc Aust Soc Reprod Biol* 1983;15:72–5.
- [37] Duarte G, Flores JA, Malpoux B, Delgadillo JA. Reproductive seasonality in female goats adapted to a subtropical environment persists independently of food availability. *Domest Anim Endocrinol* 2008;35:362–70.
- [38] Legan SJ, Karsch FJ. Photoperiodic control of seasonal breeding in ewes: modulation of the negative feedback action of estradiol. *Biol Reprod* 1980;23:1061–8.
- [39] Martin GB, Scaramuzzi RJ, Lindsay DR. Effect of the introduction of rams during the anoestrus season on the pulsatile secretion of LH in ovariectomized ewes. *J Reprod Fertil* 1983;67:47–55.
- [40] Muñoz AL, Chesneau D, Hernández H, Bedos M, Duarte G, Vielma J, Zarazaga LA, Chemineau P, Keller M, Delgadillo JA. Sexually active bucks counterbalance the seasonal negative feedback of estradiol on LH in ovariectomized goats. *Domest Anim Endocrinol* 2017;60:42–9.
- [41] Caraty A, Lomet D, Sébert ME, Guillaume D, Beltramo M, Evans NP. Gonadotrophin-releasing hormone release into the hypophyseal portal blood of the Ewe mirrors both pulsatile and continuous intravenous infusion of kisspeptin: an insight into kisspeptin's mechanism of action. *J Neuroendocrinol* 2013;25:537–46.
- [42] De Bond JAP, Li Q, Millar RP, Clarke IJ, Smith JT. Kisspeptin signaling is required for the luteinizing hormone response in anestrus ewes. *PLoS One* 2013;8:e57972.
- [43] Fabre-Nys C, Cognié J, Dufourny L, Ghenim M, Martinet S, Lasserre O, Lomet D, Millar RP, Ohkura S, Suetomi Y. The two populations of kisspeptin neurons are involved in the ram-induced LH pulsatile secretion and LH surge in anestrus ewes. *Endocrinology* 2017;158: 3914–28.
- [44] Wakabayashi Y, Nakada T, Murata K, Ohkura S, Mogi K, Navarro VM, Clifton DK, Mori Y, Tsukamura H, Maeda K, Steiner RA, Okamura H. Neurokinin B and dynorphin A in kisspeptin neurons of the arcuate nucleus participate in generation of periodic oscillation of neural activity driving pulsatile gonadotropin-releasing hormone secretion in the goat. *J Neurosci* 2010;30:3124–32.
- [45] Bedos M, Portillo W, Dubois JP, Duarte G, Flores JA, Chemineau P, Keller M, Paredes RG, Delgadillo JA. A high level of male sexual activity is necessary for the activation of the medial preoptic area and the arcuate nucleus during the “male effect” in anestrus goats. *Physiol Behav* 2016;165:173–8.
- [46] Restall BJ. Seasonal variation in reproductive activity in Australian goats. *Anim Reprod Sci* 1992;27:305–18.
- [47] Delgadillo JA, Chemineau P. Abolition of the seasonal release of luteinizing hormone and testosterone in Alpine male goats (*Capra hircus*) by short photoperiodic cycles. *J Reprod Fertil* 1992;94:45–55.
- [48] Rivas-Muñoz R, Fitz-Rodríguez G, Poindron P, Malpoux B, Delgadillo JA. Stimulation of estrous behavior in grazing female goats by continuous or discontinuous exposure to males. *J Anim Sci* 2007;85:1257–63.
- [49] Delgadillo JA, Flores JA, Hernández H, Poindron P, Keller M, Fitz-Rodríguez G, Duarte G, Vielma J, Fernández IG, Chemineau P. Sexually active males prevent the display of seasonal anestrus in female goats. *Horm Behav* 2015;69:8–15.
- [50] Abecia JA, Chemineau P, Flores JA, Keller M, Duarte G, Forcada F, Delgadillo JA. Continuous exposure to sexually active rams extends estrous activity in ewes in spring. *Theriogenology* 2015;84:1549–55.
- [51] Abecia JA, Keller M, Palacios C, Chemineau P, Delgadillo JA. Light-induced sexually active rams prevent the seasonal inhibition of luteinizing-hormone in ovariectomized estradiol-implanted ewes. *Theriogenology* 2019;136:43–6.
- [52] Delgadillo JA, Flores JA, Villarreal O, Flores MJ, Hoyos G, Chemineau P, Malpoux B. Length of postpartum anestrus in goats in subtropical Mexico: effect of season of parturition and duration of nursing. *Theriogenology* 1998;49:1209–18.
- [53] Amir D, Gacitua H. Sexual activity of Assaf ewes after October and February lambings. *Theriogenology* 1987;27:377–82.
- [54] Schirar A, Cognié Y, Louault F, Poulin N, Levasseur MC, Martinet J. Resumption of oestrous behaviour and cyclic ovarian activity in suckling and non-suckling ewes. *J Reprod Fertil* 1989;87:789–94.
- [55] Hamadeh SK, Abi Said M, Tami F, Barbour EK. Weaning and the ram-effect on fertility, serum luteinizing hormone and prolactin levels in spring rebreeding of postpartum Awassi ewes. *Small Rumin Res* 2001;41:191–4.
- [56] Abecia JA, Chemineau P, Gómez A, Palacios C, Keller M, Delgadillo JA. Exposure to photoperiod-melatonin-induced, sexually-activated rams after weaning advances the resumption of sexual activity in post-partum mediterranean ewes lambing in January. *Vet Sci* 2017; 4:4.

Plantas cardiotoxícas para ruminantes no Brasil¹

Naiara C. F. Nascimento², Lorena D.A. Aires³, James A. Pfister⁴,
Rosane M.T. Medeiros⁵, Franklin Riet-Correa⁶ e Fábio S. Mendonça^{7*}

ABSTRACT.- Nascimento N.C.F., Aires L.D.A., Pfister J.A., Medeiros R.M.T., Riet-Correa F. & Mendonça F.S. 2018. [Cardiotoxic plants affecting ruminants in Brazil.] Plantas cardiotoxícas para ruminantes no Brasil. *Pesquisa Veterinária Brasileira* 38(7):1239-1249. Laboratório de Diagnóstico Animal, Universidade Federal Rural de Pernambuco, Rua Dom Manoel de Medeiros s/n, Dois Irmãos, Recife, PE 52171-900, Brazil. E-mail: fabio.mendonca@pq.cnpq.br

This review updates information about cardiotoxic plants affecting ruminants in Brazil. Currently it is known that there are at least 131 toxic plants belonging to 79 genera. Twenty five species affect the heart function. Plants that contain sodium monofluoroacetate (*Palicourea* spp., *Psychotria hoffmannseggiana*, *Amorimia* spp., *Niedenzuella* spp., *Tanaecium bilabiatum* and *Fridericia elegans*) cause numerous outbreaks of poisoning, mainly in cattle, but buffaloes, sheep and goats are occasionally affected. Poisoning by *Palicourea marcgravii* remains the most important due to the wide distribution of this plant in Brazil. New species of the genus *Palicourea* containing sodium monofluoroacetate, such as *Palicourea amapaensis*, *Palicourea longiflora*, *Palicourea barraensis*, *Palicourea macarthurorum*, *Palicourea nigricans*, *Palicourea vacillans* and *Palicourea* aff. *juruaana* were described in the amazon region. In the northeast region, the most important toxic plant for cattle is *Amorimia septentrionalis*. In the midwest, outbreaks of *Niedenzuella stannea* poisoning have been reported in cattle in the Araguaia region and the disease needs to be better investigated for its occurrence and importance. *Tetrapteryx multiglandulosa* and *Tetrapteryx acutifolia*, two plants causing cardiac fibrosis also contain sodium monofluoroacetate and were reclassified to the genus *Niedenzuella*. These two plants and *Ateleia glazioviana*, other plant that causes cardiac fibrosis continues to be important in the southeastern and south of Brazil. Other less important are the plants that contain cardiotoxic glycosides, such as *Nerium oleander* and *Kalanchoe blossfeldiana*, in which poisonings are generally accidental. Recently, several experimental methodologies were successfully employed to avoid poisonings by sodium monofluoroacetate containing plants. These methodologies include the induction of food aversion using lithium chloride, the administration of repeatedly non-toxic doses of leaves to induce resistance, the use of acetamide to prevent poisonings and the intraruminal inoculation of sodium monofluoroacetate degrading bacteria.

INDEX TERMS: Poisonous plants, cardiotoxic plants, cardiotoxic glycosides, sodium monofluoroacetate, plant poisoning, ruminants, toxicoses.

¹ Recebido em 21 de agosto de 2017.

Aceito para publicação em 28 de agosto de 2017.

² Programa de Pós-Graduação em Medicina Veterinária, Universidade Federal Rural de Pernambuco (UFRPE), Rua Dom Manoel de Medeiros s/n, Dois Irmãos, Recife, PE 52171-900, Brasil.

³ Departamento de Medicina Veterinária, Universidade Federal Rural de Pernambuco (UFRPE), Rua Dom Manoel de Medeiros s/n, Dois Irmãos, Recife, PE 52171-900.

⁴ Poisonous Plant Research Laboratory, Agricultural Research Service, United States Department of Agriculture, 1150 E. 1400 N., Logan, UT 84341, USA.

⁵ Hospital Veterinário, Universidade Federal de Campina Grande (UFCG), Patos, PB 58700-000, Brasil.

⁶ Instituto Nacional de Investigación Agropecuaria (INIA), La Estanzuela, Colonia, Uruguay, CP 70.000.

⁷ Laboratório de Diagnóstico Animal, Departamento de Morfologia e Fisiologia Animal, Universidade Federal Rural de Pernambuco (UFRPE), Rua Dom Manoel de Medeiros s/n, Dois Irmãos, Recife, PE 52171-900. *Autor para correspondência: fabio.mendonca@pq.cnpq.br

RESUMO.- Esta revisão atualiza informações sobre plantas cardiotoxícas que afetam os ruminantes no Brasil. Atualmente, sabe-se que existem pelo menos 131 plantas tóxicas pertencentes a 79 gêneros. Vinte e cinco espécies afetam o funcionamento do coração. As plantas que contêm monofluoroacetato de sódio (*Palicourea* spp., *Psychotria hoffmannseggiana*, *Amorimia* spp., *Niedenzuella* spp., *Tanaecium bilabiatum* e *Fridericia elegans*) causam numerosos surtos de intoxicação, principalmente em bovinos, mas búfalos, ovinos e caprinos são ocasionalmente afetados. A intoxicação por *Palicourea marcgravii* continua a ser a mais importante devido à ampla distribuição desta planta no Brasil. Novas espécies do gênero *Palicourea* contendo monofluoroacetato de sódio, como *Palicourea amapaensis*, *Palicourea longiflora*, *Palicourea barraensis*, *Palicourea*

macarthurorum, *Palicourea nigricans*, *Palicourea vacillans* e *Palicourea aff. juruana* foram descritas na região amazônica. Na região nordeste, a planta tóxica mais importante para bovinos é *Amorimia septentrionalis*. No Centro-Oeste, surtos de intoxicação por *Niedenzuella stannea* foram relatados em bovinos na região do Araguaia e a doença precisa ser melhor investigada quanto à sua ocorrência e importância. *Tetrapteryx multiglandulosa* e *Tetrapteryx acutifolia*, duas plantas que causam fibrose cardíaca, também contêm monofluoroacetato de sódio e foram reclassificadas para o gênero *Niedenzuella*. Essas duas espécies e *Ateleia glazioveana*, outra planta que causa fibrose cardíaca, continuam sendo importantes no Sul e Sudeste do Brasil. Outras espécies menos importantes e que ocasionalmente provocam surtos acidentais de intoxicação são as plantas que contêm glicosídeos cardiotoxícos, tais como *Nerium oleander* e *Kalanchoe blossfeldiana*. Recentemente, várias metodologias experimentais foram empregadas para evitar intoxicações por plantas que contêm monofluoroacetato de sódio. Estas metodologias incluem a indução de aversão condicionada utilizando cloreto de lítio, a utilização de doses repetidas não tóxicas de folhas para induzir resistência, o uso de acetamida para prevenir as intoxicações e a inoculação intraruminal de bactérias degradantes de monofluoroacetato de sódio.

TERMOS DE INDEXAÇÃO: Plantas tóxicas, glicosídeos cardiotoxícos, monofluoroacetato de sódio, intoxicação por plantas, ruminantes, toxicoses.

INTRODUÇÃO

No Brasil, plantas pertencentes às famílias Rubiaceae, Malpighiaceae, Bignoniaceae, Fabaceae, Apocynaceae e Crassulaceae constituem um grupo muito importante de plantas tóxicas para animais de produção por afetarem o funcionamento do coração (Tokarnia et al. 2012). De acordo com dados dos laboratórios de diagnóstico de diferentes regiões do país, estima-se que esse grupo de plantas seja responsável pela morte de cerca de 500 mil bovinos por ano. Considerando o preço médio de US\$ 200,00 por animal, as perdas anuais podem ultrapassar a cifra de um milhão de dólares (Riet-Correa & Medeiros 2001, Tokarnia et al. 2012). Considerando a importância econômica desse grupo de plantas no Brasil, este trabalho tem como objetivo atualizar os dados sobre os principais aspectos epidemiológicos, clínicos, patológicos e formas de controle das intoxicações por plantas que afetam o funcionamento do coração de ruminantes.

REVISÃO DE LITERATURA

Plantas que provocam mortes súbitas associadas ao exercício

De uma maneira geral, as plantas que provocam mortes súbitas associadas ao exercício contêm concentrações elevadas de monofluoroacetato de sódio (MFA) e por esse motivo o quadro clínico-patológico apresenta evolução superaguda, sem que se observem lesões cardíacas significantes. Esse grupo de plantas é atualmente representado por 22 espécies pertencentes às três famílias: Rubiaceae (*Palicourea* e *Psychotria*), Malpighiaceae (*Amorimia* e *Niedenzuella*) e Bignoniaceae (*Tanaecium* e *Fridericia*).

Plantas dos gêneros *Palicourea* e *Psychotria*

No gênero *Palicourea*, são importantes as intoxicações por *P. marcgravii*, *P. aeneofusca*, *P. juruana* e *P. grandiflora* (Tokarnia et al. 2012). Porém, em pesquisas recentes detectou-se monofluoroacetato de sódio em mais oito espécies: *P. amapaensis*, *P. longiflora*, *P. barraensis* (anteriormente *P. aff. longiflora*), *P. macarthurorum*, *P. nigricans*, *P. vacillans* e *P. aff. juruana*. No gênero *Psychotria*, só existem relatos de intoxicação por *Psychotria hoffmannseggiana* (Cook et al. 2014, Pedroza 2015, Carvalho et al. 2016).

Desse grupo, *P. marcgravii* é a planta tóxica mais importante devido à sua vasta distribuição no Brasil, ocorrendo nos domínios amazônia, caatinga, cerrado e mata atlântica. Provoca altos índices de mortalidade devido à sua boa palatabilidade, como por exemplo, na região amazônica, onde é responsável por 80% de todas as mortes relacionadas às intoxicações por plantas em bovinos (Tokarnia et al. 2012). *Palicourea aeneofusca* é importante nos estados de Pernambuco, Paraíba, leste da Bahia e Alagoas, onde ocorre em áreas de mata atlântica do litoral e zona da mata e no agreste, em matas de brejo de altitude (Vasconcelos et al. 2008a, Brito et al. 2016). A intoxicação natural é frequente em bovinos e ocasionalmente é relatada em pequenos ruminantes (Albuquerque et al. 2013, Brito et al. 2016, Oliveira-Neto et al. 2017).

Várias espécies que contêm MFA têm sua ocorrência registrada na região amazônica e podem ser encontradas em florestas de terra firme, florestas e campos de várzea, como *P. grandiflora* (Acre, Amazonas, Pará, Rondônia e Mato Grosso), *P. amapaensis* (Amazonas, Amapá e Pará), *P. macarthurorum* (Amazonas), *P. longiflora* (Amazonas, Pará e Rondônia), *P. nigricans* (Acre e Amazonas), *P. barraensis* (Amazonas, Roraima e Rondônia) e *P. aff. juruana* (Maranhão e Tocantins). *Palicourea vacillans* encontra-se distribuída em áreas de cerrado nos estados de Minas Gerais e Bahia (Cook et al. 2014, Taylor 2015a, 2015b, Carvalho et al. 2016). Das espécies acima citadas existem casos registrados de surtos de morte súbita em bovinos associados às intoxicações por *P. grandiflora*, *P. barraensis* e *P. longiflora*. Experimentalmente, *P. longiflora* e *P. barraensis* também causam intoxicação em coelhos (Cook et al. 2014, Carvalho et al. 2016).

A classificação do gênero *Psychotria* é complexa e não está totalmente resolvida, posto que algumas espécies atualmente classificadas como *Psychotria* estão mais intimamente relacionadas com o gênero *Palicourea* (Taylor 1996, Taylor et al. 2010, Taylor & Gereau 2013). Desse gênero, *Psychotria hoffmannseggiana* é provavelmente importante por ser endêmica em todo o país. *Psychotria hoffmannseggiana* é um arbusto que mede de 0,5 a 2 m e pode ser encontrado na mata atlântica, em matas mesófilas, semidecíduas, restingas, matas ciliares e no cerrado (Taylor 2007). No Brasil, há somente dois registros de intoxicação por *P. hoffmannseggiana* em bovinos, nos estados de Minas Gerais e Rondônia (Schons 2011, Pedroza 2015). Nessas regiões, produtores rurais e médicos veterinários relatam há muito tempo surtos de mortes súbitas em bovinos. No Vale do Paraíba, *Palicourea barbiflora* (sinônimo de *P. hoffmannseggiana*) foi relatada como responsável por surtos de mortes súbitas em bovinos em décadas passadas e sua toxicidade foi confirmada experimentalmente em bovinos (Camargo 1962). A concentração de MFA em *P. hoffmannseggiana* ainda não foi determinada (Pedroza 2015).

A concentração de MFA difere entre as espécies do gênero *Palicourea*. Em um estudo mais recente com métodos mais precisos (Lee et al. 2012), as concentrações foram significativamente maiores que as relatadas em estudos anteriores, cujos valores eram de 0.00054% de MFA (Krebs et al. 1994, Tokarnia et al. 2012). No estudo publicado por Cook et al. (2014) as concentrações de MFA nas folhas maduras de *P. marcgravii* foram estabelecidas em $0,24 \pm 0,10\%$ e $0,88 \pm 0,08\%$ nas folhas jovens e em desenvolvimento. Já nas folhas de *P. aeneofusca*, a concentração foi de $0,09 \pm 0,05\%$ (Lee et al. 2012). Nas folhas de *P. longiflora* a concentração variou de 0.006% a 0.16% e nas folhas de *P. barraensis* a concentração foi de 0.01% (Carvalho et al. 2016).

As concentrações de MFA nas folhas de *P. juruana*, *P. grandiflora*, *P. amapaensis*, *P. macarthurorum*, *P. nigricans*, *P. vacillans* e *P. aff. juruana* ainda não foram determinadas. Sugeriu-se, porém, que devem ser similares às encontradas em *marcgravii*, *P. aeneofusca*, *P. barraensis* e *P. longiflora* (Cook et al. 2014, Carvalho et al. 2016). A dose letal das folhas frescas de *P. marcgravii* para bovinos foi estabelecida em 0,6g/kg, sendo similar a dose letal para pequenos ruminantes (Tokarnia et al. 2012). A menor dose de folhas frescas de *P. aeneofusca* capaz de matar um bovino foi de 0,75g/kg (Tokarnia et al. 1983). A dose letal das folhas de *P. juruana* foi estabelecida em 2,0g/kg e de *P. grandiflora* entre 1,0 e 2,0g/kg (Peixoto et al. 2011). Para coelhos, a dose letal das folhas de *P. barraensis* e *P. longiflora* foi de 2g/kg (Carvalho et al. 2016). Assumindo-se que as concentrações de MFA são similares em *Palicourea* spp., é presumível que as doses letais e o quadro clínico-patológico sejam similares. Portanto, são potencialmente tóxicas se as folhas e frutos forem consumidos por animais de fazenda.

Plantas dos gêneros *Amorimia* e *Niendenzuella*

Dentre as Malpighiaceae, são importantes as intoxicações por *A. amazonica*, *A. exotropicalis*, *A. pubiflora*, *A. rigida* e *A. septentrionalis* (Duarte et al. 2013). No gênero *Niendenzuella* são importantes as intoxicações por *N. stannea*, *N. multiglandulosa* e *N. acutifolia*. É importante ressaltar que várias espécies anteriormente classificadas como *Mascagnia* foram reclassificadas como *Amorimia* (Anderson 2006) e que várias espécies anteriormente classificadas como *Tetrapteryx* foram reclassificadas como *Niendenzuella* (Davis & Anderson 2010). As informações sobre as intoxicações por *N. multiglandulosa* e *N. acutifolia* (anteriormente denominadas *Tetrapteryx multiglandulosa* e *Tetrapteryx acutifolia*) estão apresentadas entre as plantas que provocam fibrose cardíaca, pois, apesar de conterem MFA como princípio tóxico, raramente provocam doença com evolução superaguda. Além disso, provocam aborto e sinais clínicos e lesões relacionadas ao sistema nervoso central que não são descritas nas plantas que provocam mortes súbitas associadas ao exercício.

Amorimia amazonica ocorre nas florestas de Igapó da região amazônica nos estados do Acre, Amazonas e Rondônia (Schons et al. 2011, Duarte et al. 2013, Mamede 2015). Nos estados de Rondônia e Mato Grosso é responsável por surtos de mortes súbitas associadas ao exercício em bovinos e ovinos no Vale do Anari. As intoxicações ocorrem durante todo o ano, porém são mais frequentes no início do período chuvoso quando há pouca disponibilidade de forragens e *A. amazonica* está brotando (Schons et al. 2011).

Amorimia exotropicalis ocorre em locais sombreados na mata atlântica do Sudeste (São Paulo) e Sul (Paraná, Rio Grande do Sul e Santa Catarina). O primeiro surto de intoxicação em bovinos foi descrito no Estado de Santa Catarina (Gava et al. 1998) e mais recentemente nas regiões metropolitanas de Porto Alegre, Serra Gaúcha e microrregião de Vacaria, Rio Grande do Sul (Pavarini et al. 2011, Bandinelli et al. 2014). As intoxicações ocorrem durante todo o ano, porém, com maior concentração de casos entre os meses de maio e agosto, período em que há escassez de alimentos no Sul do Brasil. Desta forma, os bovinos podem invadir áreas de matas ou capões à procura de alimento. Bovinos também podem se intoxicar quando adentram nas matas à procura de abrigo das chuvas e ventos frios que também se concentram nessa época (Pavarini et al. 2011).

Amorimia pubiflora tem ocorrência registrada no cerrado da região Centro-Oeste (Goiás, Mato Grosso do Sul e Mato Grosso) e na mata atlântica da região Sudeste (Minas Gerais e São Paulo). Porém, surtos de intoxicação em bovinos só foram registrados em Mato Grosso e Mato Grosso do Sul. Nas regiões de sua ocorrência, *A. pubiflora* é uma das plantas tóxicas mais importantes, chegando a ser um fator limitante para expansão pecuária devido à ocorrência de mortes súbitas, com registros de mortalidade próximos a 50% (Becker et al. 2013). Em Mato Grosso do Sul, *A. pubiflora* foi responsável por vários surtos de mortes súbitas em diferentes meses do ano, mas os casos predominaram no período chuvoso com morbidade de até 3,5% e a taxa de letalidade de 100% (Lemos et al. 2011). Em Mato Grosso, as mortes de bovinos ocorrem mesmo com disponibilidade de forragem, no entanto é frequentemente relatado que as mortes se concentram no final do período da seca e início do período chuvoso (Becker et al. 2013).

Amorimia rigida têm sua ocorrência registrada na Bahia, Espírito Santo, Minas Gerais e Rio de Janeiro; seu habitat são as áreas de caatinga e da mata atlântica (Mamede 2015) e, segundo Tokarnia et al. (1985) ocorre nos lugares mais baixos das pastagens, pés-de-serra e beiras de rios. É possível que *A. rigida* ocorra em outros estados do Nordeste, porém, nos surtos mais recentes de intoxicações relatados nessa região, a espécie responsável foi *A. septentrionalis* (Vasconcelos et al. 2008b, Albuquerque et al. 2014). Intoxicações por *A. rigida* ocorrem principalmente na espécie bovina (Tokarnia et al. 1961, 1994, Medeiros et al. 2002, Da Silva et al. 2006, Vasconcelos et al. 2008b). Em caprinos e ovinos são menos frequentes (Oliveira et al. 1978, Pacífico da Silva et al. 2008, Lago et al. 2009). A intoxicação por *A. rigida* ocorre principalmente no início do período chuvoso quando está em brotação e as outras plantas ainda não cresceram. A planta também pode brotar após queimadas, período este também considerado como o de maior número de casos de intoxicações (Borboleta 2010, Tokarnia et al. 2012).

Amorimia septentrionalis ocorre sobre afloramentos rochosos da caatinga nos estados de Alagoas, Ceará, Paraíba, Pernambuco e Rio Grande do Norte (Mamede 2015). As intoxicações têm sido descritas principalmente no estado da Paraíba e em Pernambuco. É uma das principais plantas tóxicas para bovinos da região do Médio Capibaribe (Albuquerque et al. 2014). A doença ocorre principalmente no início do período chuvoso, quando a planta brota antes que outras forrageiras ou após o final desse período, quando algumas forrageiras secam e *A. septentrionalis* permanece verde (Vasconcelos et al. 2008b).

Niedenzuella stannea tem ocorrência confirmada nas regiões Centro-Oeste (Mato Grosso e Mato Grosso do Sul) e Norte (Acre, Amazonas, Amapá, Pará, Rondônia, Tocantins) e ocorre tanto na floresta amazônica quanto no pantanal. Até o momento, só existem históricos de intoxicações em bovinos na região do Araguaia, Mato Grosso. Os surtos ocorrem principalmente durante a estação seca, entre junho e agosto, quando a planta está em brotação. A toxicidade da planta foi demonstrada em bovinos e ovinos pela administração de folhas jovens (Caldeira et al. 2016, Arruda et al. 2017). A evolução da intoxicação é aguda ou hiperaguda, dependendo da quantidade de planta ingerida. Experimentalmente em bovinos, doses de 15g/kg produziram sinais clínicos seguidos de recuperação. A menor dose que provocou a morte de bovinos foi 20g/kg (Arruda et al. 2017).

A concentração de MFA em *A. amazonica*, *A. exotropa*, *A. pubiflora*, *A. rigida* e *A. septentrionalis* foram determinadas em amostras de herbário, com concentrações nas folhas de 0,0007%, 0,02%, 0,06%, 0,002% e 0,002% respectivamente. Porém, nessas espécies sabe-se que existe variação da quantidade de MFA tanto nas folhas quanto nas flores, caules e sementes (Lee et al. 2012). Experimentalmente, sinais clínicos de intoxicação foram observados com doses únicas entre 3,0 e 6,0g/Kg das folhas de *A. amazonica*. Doses únicas entre 7,5-10g/kg de folhas frescas de *A. exotropa* causaram intoxicação e morte de bovinos (Gava et al. 1998) e doses entre 5-20g/kg das folhas de *A. pubiflora* também foram capazes de causar sinais clínicos de intoxicação em bovinos. Devido à significativa variação da toxidez de *A. rigida* para bovinos, não se determinou a dose letal para essa espécie (Tokarnia et al. 2012). Em coelhos, a dose letal foi de 4g/kg das folhas dessecadas e 0,25g/kg dos frutos dessecados (Tokarnia et al. 1987). Na reprodução experimental da intoxicação por *A. septentrionalis* em caprinos e ovinos, doses únicas de 10 e 20g/kg foram letais. Já animais que receberam a dose de 5g/kg apresentaram sinais discretos e se recuperaram da intoxicação (Vasconcelos et al. 2008b).

As concentrações de MFA foram altamente variáveis entre as diferentes partes de *N. stannea*. As concentrações foram maiores nas sementes (0,06%), seguidas de frutos (0,0008 a 0,02%), flores (0,0003 a 0,006%) e folhas (0,0003%). Experimentalmente em bovinos, doses de 15g/kg provocaram apenas sinais clínicos com consequente recuperação dos animais. Doses entre 20-30g/kg provocaram sinais clínicos e morte (Arruda et al. 2017).

Plantas dos gêneros *Tanaecium* e *Fridericia*

Dentre as Bignoniaceae, são importantes as intoxicações por *Tanaecium bilabiatum* (anteriormente denominada *Arrabidea bilabiata*) e *Fridericia elegans* (anteriormente denominada *Pseudocalymma elegans*) (Lima et al. 2016, Santos-Barbosa et al. 2017). *T. bilabiatum* tem ampla ocorrência registrada no país e pode ser encontrada na floresta amazônica, caatinga, cerrado, mata atlântica, pampa e pantanal (Lohmann & Taylor 2014). Na Bacia Amazônica, essa planta é responsável por numerosas mortes de bovinos que ocorrem em extensas regiões de várzea e, segundo Tokarnia et al. (2012), depois de *P. marcgravii*, é a principal planta tóxica da região Amazônica para bovinos.

No estado de Roraima, surtos de intoxicações em bovinos com quadro clínico de mortes súbitas são atribuídos à *Fridericia japurensis* (anteriormente denominada *Arrabidea japurensis*)

(Tokarnia & Döbereiner 1981). No entanto, recentemente descobriu-se que a identificação de *F. japurensis* a partir de amostras de plantas coletadas em fazendas dessa região estava incorreta. Também se verificou que não existe MFA em *F. japurensis*, tanto em amostras coletadas em fazendas com casos confirmados de mortes súbitas, quanto em amostras de herbário. Na verdade, a planta responsável por surtos de mortes súbitas de bovinos no Estado de Roraima é também *T. bilabiatum* (Lima et al. 2016).

Fridericia elegans tem seu registro confirmado apenas no Rio de Janeiro, onde cresce no bioma Mata atlântica, especificamente nas costas dos morros de florestas caducifolia e ombrifolia (Lohmann 2015). Sabe-se de sua ocorrência nos municípios de São Miguel Pereira, Pacarambi, Saquarema, Rio Bonito e Campo Grande (Tokarnia et al. 2012). Sob condições naturais, a intoxicação por esta planta tem sido observada em bovinos (Helayer et al. 2009) e há histórico de intoxicação em equinos. Experimentalmente podem ser intoxicados bovinos, equinos, coelhos, caprinos e ovinos (Tokarnia et al. 1993, Consorte et al. 1994, Helayer et al. 2009, Tokarnia et al. 2012).

A concentração de MFA nas folhas de *T. bilabiatum* variou significativamente de acordo com os locais de coleta, sendo determinada entre 0,0001% e 0,039% (Lima et al. 2016) e experimentalmente em coelhos, a menor dose que causou morte foi de 0,5g/kg com a brotação coletada na época da seca. Já com as folhas maduras, a menor dose que causou a morte dos coelhos foi de 4,0g/kg (Jabour et al. 2006). Para bovinos, 1,25 g/kg das folhas frescas causaram sinais graves de intoxicação, enquanto 2,5g/kg provocaram a morte (Döbereiner et al. 1983). A concentração de MFA em *F. elegans* não foi determinada. A administração, por via oral, de doses entre 0,5 e 1g/kg da brotação da planta causou sinais clínicos de intoxicação e morte de bovinos, enquanto a dose de 0,25g/kg foi capaz de causar apenas sinais clínicos, mas não levou à morte (Helayer et al. 2009).

Sinais clínicos, lesões macro e microscópicas associadas às intoxicações por plantas que contém monofluoroacetato de sódio (MFA)

O MFA é altamente tóxico para todas as espécies de mamíferos, incluindo humanos. No entanto, os efeitos tóxicos são muito variáveis em função da espécie intoxicada, da sensibilidade individual e dose ingerida, McIlroy 1981, Tokarnia et al. 2012). Porém, em ruminantes o quadro clínico consiste principalmente em intoxicações com evolução hiperaguda. O início dos sinais clínicos se dá poucas horas após a ingestão da dose tóxica e o exercício físico ou movimentação pode precipitar ou causar os sinais clínicos (entre 4-30 horas) (Tokarnia et al. 2012). Os sinais clínicos da intoxicação em bovinos, búfalos, caprinos e ovinos consistem em anorexia, apatia, letargia, micções frequentes, decúbito esternal prolongado, pulso venoso positivo, taquicardia, taquipneia, dispneia, instabilidade, tremores musculares, quedas e, durante a fase agônica, apresentam decúbito lateral, movimentos de pedalagem, opistótono, vocalizações e morte. Também podem estar presentes sinais clínicos decorrentes do decúbito prolongado, tais como diminuição dos movimentos ruminais, algumas vezes atonia, leve timpanismo e fezes ressecadas (Helayer et al. 2009). Esses sinais clínicos podem variar nas intoxicações, tendo em vista que a quantidade de MFA é significativamente variável nas espécies descritas neste trabalho.

Os achados de necropsia são ausentes na maioria dos casos de intoxicação por plantas que contêm MFA em ruminantes. Porém, lesões inespecíficas tais como hemorragias petequiais no epicárdio, endocárdio e músculos papilares podem ser observadas e são geralmente decorrentes da fase agônica de morte. Outros achados consistem em hidropericárdio, edema e congestão pulmonar, palidez dos rins, congestão de grandes vasos e da mucosa do intestino delgado. Os achados histológicos são escassos, quando presentes, são condizentes com alterações degenerativas ou circulatórias, tais como degeneração hidrópico-vacuolar das células epiteliais renais, principalmente dos túbulos contorcidos distais com evidente picnose nuclear. Na intoxicação por *P. aeneofusca* descreveram-se lesões inespecíficas no coração, tais como áreas difusas de hemorragia, edema das células de fibras de Purkinje e necrose coagulativa de fibras miocárdicas, com fibras em cariólise ou picnose, aumento da eosinofilia citoplasmática e perda das estriações transversais. Nos miocardiócitos podem ser observados vacúolos intranucleares discretos com marginalização da cromatina e nos espaços intersticiais pode haver edema discreto, depósitos de fibrina e infiltração de células mononucleares (Brito et al. 2016, Arruda et al. 2017). Possivelmente essas lesões também podem ser encontradas em outras intoxicações por plantas que contêm MFA.

Na intoxicação por *Amorimia* spp. em ruminantes, o quadro clínico e as lesões macro e microscópicas também são típicas de insuficiência cardíaca aguda. Entretanto, adicionalmente, podem incluir coágulos no interior do ventrículo esquerdo, congestão hepática e do trato gastrointestinal (Tokarnia et al. 1961, 1994, Paraguassu 1983, Pacífico da Silva et al. 2008, Vasconcelos et al. 2008b, Pavarini et al. 2011). Como as concentrações de MFA são menores em *Amorimia* spp., a letalidade é relativamente mais baixa do que a letalidade de *Palicourea* spp. (Medeiros et al. 2002). Em alguns casos, como nas intoxicações por *A. exotropicalis*, *A. amazonica* e *A. septentrionalis*, a evolução pode ser subaguda e, dessa forma, o coração pode exibir aspecto globular com áreas esbranquiçadas no miocárdio, além de áreas focais vermelhas entremeadas por áreas brancacentas na musculatura papilar esquerda (Soares et al. 2011, Bandinelli et al. 2014, Brito et al. 2016). Sendo assim, pode haver necrose de coagulação com infiltrado inflamatório composto por macrófagos, linfócitos, neutrófilos degenerados, além de tecido conjuntivo (fibrose) e debris celulares (Bandinelli et al. 2014, Brito et al. 2016).

Diagnóstico, tratamento e medidas preventivas ou de controle

Para o diagnóstico é fundamental o conhecimento das plantas que contêm MFA que ocorrem em cada região. A presença dessas plantas associadas ao histórico de que os ruminantes morrem ou adoecem ao serem movimentados sugerem o diagnóstico de intoxicação. A lesão microscópica dos rins, quando presente, é de grande valor diagnóstico. A presença de fibrose cardíaca também é de valor diagnóstico para os casos de intoxicação subaguda por *Amorimia* spp. (Tokarnia et al. 2012). Recentemente foi demonstrado que o MFA pode ser detectado no soro sanguíneo de animais que foram intoxicados por plantas que contêm esse composto, contudo, esse método ainda não está disponível na rotina médico-veterinária (Santos-Barbosa et al. 2017).

Não existe tratamento para as intoxicações por plantas que contêm MFA. O controle das intoxicações é difícil, especialmente em fazendas muito extensas. Nesses casos, a utilização de cercas ou a remoção manual das plantas não são medidas eficazes. A utilização de herbicidas é dispendiosa e só é eficaz em pequenas áreas, as quais também podem ser cercadas (Riet-Correa & Medeiros 2001).

A utilização de doses entre 2,0 e 3,0g/kg de acetamida pode ser eficaz para a prevenção da intoxicação, uma vez que esse composto apresenta efeito protetor contra o MFA. Em um estudo realizado no Brasil, o tratamento prévio com acetamida evitou o aparecimento de sinais clínicos e o óbito de ovinos e caprinos intoxicados por *F. elegans* (Helayer et al. 2011). No entanto, a eficácia da acetamida depende de diversos fatores, como a toxidez da planta em questão, tempo decorrido entre a intoxicação e o fornecimento do antídoto e doses de acetamida administradas (Egyed & Schultz 1986).

Em bovinos foi induzida experimentalmente aversão alimentar condicionada em condições de campo, administrando-se cloreto de lítio após a ingestão de *P. aeneofusca*. Nessa espécie, o efeito aversivo perdurou por 12 meses, mostrando-se um método eficaz (Brito et al. 2016). Em ovinos (Pacífico da Silva & Soto-Blanco 2010) e caprinos (Barbosa et al. 2008) a mesma técnica foi utilizada para prevenir a intoxicação por *A. septentrionalis* com resultados satisfatórios em condições experimentais. Também foi comprovado que a administração de doses não tóxicas repetidas de folhas de *A. septentrionalis* induz resistência à intoxicação por essa planta e que essa resistência pode ser transmitida de animais resistentes para animais susceptíveis pela transfaunação de líquido ruminal (Duarte 2012). A mesma técnica foi utilizada com sucesso contra a intoxicação por *A. pubiflora* (Becker et al. 2016).

Em outro estudo, a inoculação intraruminal de bactérias degradadoras de MFA foi recentemente utilizada com sucesso para a prevenção da intoxicação por *A. septentrionalis* em que a administração intraruminal contínua de *Ralstonia* sp. e *Burkholderia* sp. proporcionou proteção completa em caprinos (Da Silva et al. 2016). Entretanto, esses métodos não estão disponíveis comercialmente. Em fazendas onde a intoxicação é frequente um método eficaz pode ser deixar os animais sem movimentação, em áreas em que não existem as plantas, por um período de 7 a 15 dias (Tokarnia et al. 2012).

Plantas que provocam fibrose cardíaca

Nesse grupo existem três espécies de plantas tóxicas: *Niedenzuella multiglandulosa*, anteriormente denominada *Tetrapterys multiglandulosa* e *Niedenzuella acutifolia*, anteriormente denominada *Tetrapterys acutifolia* (ambas da família Malpighiaceae) (Tokarnia et al. 1989, Riet-Correa et al. 2001, Anderson 2006, Carvalho et al. 2006, Caldas et al. 2011) e *Ateleia glazioviana* (da família Fabaceae) (Gava et al. 2001, Gava et al. 2003, Rissi et al. 2007). Por produzirem intoxicações bastante semelhantes em relação aos quadros clínicos e patológicos, serão apresentadas em conjunto. De uma forma geral, as intoxicações por esse grupo de plantas apresentam evolução subaguda à crônica e cursam com alterações degenerativas e fibrose cardíaca.

Niedenzuella multiglandulosa tem ocorrência registrada nos estados da Bahia, Goiás, Mato Grosso do Sul, Minas Gerais, Espírito Santo, Rio de Janeiro, São Paulo e Paraná. *N. acutifolia* tem ocorrência descrita no Acre, Amazonas, Mato Grosso,

Goias, Tocantins, Maranhão, Pernambuco, Bahia, Minas Gerais, Espírito Santo, Rio de Janeiro, São Paulo, Paraná e Santa Catarina, podendo ocorrer no cerrado, mata atlântica e floresta amazônica (Mamede 2015). Os casos de intoxicação por *N. multiglandulosa* foram registrados no Rio de Janeiro, São Paulo e Mato Grosso do Sul. Os casos de intoxicação por *N. acutifolia* foram constatados em diversos municípios dos estados do Rio de Janeiro, São Paulo, Minas Gerais e Espírito Santo. As intoxicações ocorrem durante todo o ano e a morbidade varia de 6 a 28%, com letalidade próxima a 100% (Tokarnia et al. 1989, Riet-Correa et al. 2001).

As intoxicações naturais ocorrem somente em bovinos e, diferentemente das intoxicações por *N. stannea*, as intoxicações por *N. multiglandulosa* e *N. acutifolia* têm evolução subaguda à crônica (Carvalho et al. 2006). A doença foi reproduzida experimentalmente em bovinos por ingestão dos brotos frescos nas doses de 5g/kg durante 60 dias, 10g/kg durante 13 a 41 dias e 20g/kg durante 10 dias. Em um experimento com bovinos, doses únicas de 100 g/kg não provocaram morte súbita. Constataram-se apenas sinais clínicos discretos (Tokarnia et al. 1989). Experimentalmente a intoxicação também foi reproduzida em ovinos (Riet-Correa et al. 2005, Cardinal et al. 2010).

Ateleia glazioveana, árvore com cerca de 5-15m de altura e 20-30cm de diâmetro, ocorre na Mata Atlântica, nas florestas estacionais semidecíduais e em florestas ombrófilas, principalmente nos Estados do Paraná, Rio Grande do Sul e Santa Catarina. Mas também possui ocorrência registrada nos Estados do Espírito Santo, Rio de Janeiro, São Paulo, Mato Grosso do Sul e Rio Grande do Norte (Mansano et al. 2015). Sob condições naturais, surtos de intoxicações foram descritos principalmente em bovinos no Oeste de Santa Catarina e Noroeste, Centro-Norte e Planalto Médio do Rio Grande do Sul (Gava et al. 2001, Rissi et al. 2007). Intoxicações em ovinos também podem ocorrer (Gava et al. 2003).

As intoxicações em bovinos geralmente estão associadas ao período de escassez de alimentos, principalmente quando ocorre seca no outono ou em invernos mais rigorosos. A maior maturação das folhas que ocorre no outono e a maior produção de sementes são fatores importantes para a ocorrência da doença, pois nesses casos a planta apresenta maior toxicidade (Gava et al. 2001). A intoxicação por *A. glazioveana* foi reproduzida experimentalmente em bovinos que consumiram entre 40 e 50g/kg das folhas verdes uma única vez. Lesões cardíacas crônicas foram reproduzidas experimentalmente em bovinos, com doses fracionadas de 2,5, 5,0 e 7,5g/kg por longo período e com dose inicial de 1g/kg, acrescida de 1g/kg/dia até atingir 15g/kg, num total de 120g/kg (Gava et al. 2001). Em ovinos, doses fracionadas totalizando 60 ou 80g/kg até 125g/kg das folhas de *A. glazioveana* causaram lesões cardíacas (Stigger et al. 2001, Raffi et al. 2006, Almeida et al. 2008).

O princípio tóxico de *A. glazioveana* é desconhecido. Porém, as lesões cardíacas observadas nessa intoxicação são semelhantes às observadas nas intoxicações por plantas da família Rubiaceae do Sul da África, que contêm como toxina uma substância do grupo das poliaminas denominada pavetamina, (García y Santos et al. 2004, Riet-Correa et al. 2005). Mais recentemente demonstrou-se que uma isoflavona extraída das folhas de *A. glazioveana*, denominada glaziovina A apresenta efeito citotóxico por inibir a polimerização de microtúbulos (Hayakawa et al. 2016). Todavia ainda não foram

realizados experimentos para determinar se essa substância é responsável pelas lesões cardíacas presentes em bovinos intoxicados por *A. glazioveana*.

Niedenzuella multiglandulosa e *N. acutifolia* apresentam MFA como princípio ativo. Porém, as concentrações dessa toxina não foram publicadas, pois a detecção foi realizada em espécimes de herbário (Santos-Barbosa et al. 2017). Tendo em vista que as intoxicações apresentam evolução subaguda a crônica, é possível que a quantidade de MFA nessas espécies seja menor do que em *Palicourea* spp. ou que haja interação com outras substâncias tóxicas, possivelmente toxinas do grupo das poliaminas, similar ao que se sugere como princípio tóxico da *A. glazioveana* (García y Santos et al. 2004, Riet-Correa et al. 2005).

Sinais clínicos, lesões macro e microscópicas associadas às intoxicações por plantas que provocam fibrose cardíaca

Diferentemente das outras intoxicações por plantas que contém MFA, as intoxicações por *N. multiglandulosa* e *N. acutifolia* cursam sinais clínicos relacionados à insuficiência cardíaca congestiva. Além disso, causam sinais clínicos e lesões (edema intramielínico) relacionados ao sistema nervoso e são causa frequente de aborto e mortalidade neonatal com presença de lesões cardíacas e no sistema nervoso de fetos e neonatos (Riet-Correa et al. 2005, Carvalho et al. 2006).

Os principais sinais clínicos, porém, consistem em edemas subcutâneos nos locais de declive como edema de barbela e edema esternal ("peito inchado"), ingurgitamento e pulso venoso positivo da jugular, arritmia cardíaca, dispneia, letargia, anorexia, fraqueza, dificuldade de locomoção, tremores musculares e fezes ressequidas (Carvalho et al. 2006, Tokarnia et al. 2012). Nesses casos são observadas lesões cardíacas que consistem em áreas claras que podem ser vistas no epicárdio, manchas e feixes esbranquiçados, muito nítidos, ocupando áreas extensas do miocárdio, que às vezes está endurecido. Há alterações secundárias como edemas e derrames serosos em cavidades. O fígado apresenta, em quase todos os casos, alterações que consistem em aumento do padrão lobular e às vezes maior firmeza que o normal. Os principais achados histológicos restringem-se ao coração e fígado, sendo observados cardiomiócitos com aumento de volume e número de núcleos, picnose, citoplasma tumefeito e eosinofílico, áreas multifocais de fibrose, às vezes, circundada por extensas áreas focais de necrose massiva no coração e, no fígado, observa-se congestão, tumefação, vacuolização e lise de hepatócitos, fibrose periportal e centrolobular (Carvalho et al. 2009, Caldas et al. 2011, Tokarnia et al. 2012).

Bovinos intoxicados por *A. glazioveana* também podem apresentar três diferentes manifestações, com sinais cardíacos, neurológicos ou reprodutivos (García y Santos et al. 2004, Raffi et al. 2006). Esses sinais podem ocorrer separadamente ou em conjunto dentro de um mesmo surto (Gava et al. 2001, Gava & Barros 2001). Os sinais clínicos mais comuns, para bovinos e ovinos intoxicados naturalmente ou experimentalmente incluem apatia, depressão, letargia, cegueira, andar lento e cambaleante, salivação, fezes secas, emagrecimento progressivo, decúbito frequente, podendo ocorrer mandíbula apoiada ao chão, ingurgitamento da jugular e leve edema na região esternal, taquicardia e taquipneia, relutância em mover-se, cabeça baixa, instabilidade dos membros pélvicos, movimentos de pedalagem e morte espontânea devido ao

esforço (Gava et al. 2001, Stigger et al. 2001). O quadro clínico-patológico manifestado pelos bovinos intoxicados por *A. glazioveana* é semelhante ao produzido pela intoxicação por *N. multiglandulosa* e *N. acutifolia*. Essa planta, quando ingerida pelos bovinos em grande quantidade e por um curto período não causa lesões cardíacas significativas, mas, se ingerida em doses fracionadas por períodos mais longos, produz lesões cardíacas associadas à insuficiência cardíaca crônica com edemas de declive (Tokarnia et al. 1989, Gava et al. 2001, Carvalho et al. 2006). Alterações macro e microscópicas causadas pela intoxicação por *A. glazioveana* variam de acordo com a manifestação clínica (cardíaca, neurológica ou reprodutiva). Lesões macroscópicas incluem áreas esbranquiçadas no miocárdio e o fígado com aspecto de noz-moscada. As alterações histológicas mais citadas são tumefação e necrose de miofibras cardíacas, fibrose intersticial no miocárdio, e degeneração esponjosa no encéfalo (Gava et al. 2001, Stigger et al. 2001, Raffi et al. 2006).

Diagnóstico, tratamento e medidas preventivas ou de controle

O diagnóstico das intoxicações por plantas que provocam fibrose cardíaca deve ser baseado nos dados epidemiológicos, em que há presença das plantas e histórico de seu consumo associados à presença do quadro clínico bastante característico de insuficiência cardíaca, com evidente edema de barbela e da região esternal e ingurgitamento de jugulares em bovinos adultos. Em bovinos jovens esses sinais clínicos são menos característicos.

No diagnóstico diferencial deve se levar em consideração outras doenças cardíacas de bovinos como a pericardite traumática e as endocardites (Gava et al. 2001), que podem ser confundidas clinicamente com a intoxicação crônica por plantas que provocam fibrose cardíaca. Apesar disso, esses casos não ocorrem sob a forma de surtos, tendo lesões de necropsia características e que permitem o diagnóstico definitivo. Lesões cardíacas semelhantes também podem ser observadas nas intoxicações por antibióticos ionóforos e deficiência de selênio e também, apesar de serem raras, nas intoxicações pelas sementes de *Senna occidentalis* e *Senna obtusifolia* (Nogueira et al. 2009, Carmo et al. 2011, Tokarnia et al. 2012, Carvalho et al. 2014). Nessas condições a musculatura esquelética também é afetada, o que não ocorre nas intoxicações por *A. glazioveana*, *N. multiglandulosa* e *N. acutifolia*. Outra enfermidade que ocorre em bovinos adultos na região da Serra Geral de Santa Catarina, chamada de “doença do peito inchado”, deve ser levada em consideração por apresentar quadro clínico similar às intoxicações por *A. glazioveana*, *N. multiglandulosa* e *N. acutifolia*. Porém, a lesão característica é uma intensa fibrose intersticial do miocárdio, não ocorrendo lesões degenerativo-necróticas.

Não se conhece tratamento eficaz para as intoxicações por plantas que provocam fibrose cardíaca. A profilaxia consiste na erradicação das plantas das áreas de pastagens. No caso de *A. glazioveana* a erradicação pode ser difícil porque o corte das árvores favorece a brotação, facilitando o acesso aos bovinos.

Plantas que contêm glicosídeos cardiotoxícos

Nesse grupo existem duas espécies de plantas tóxicas: *Nerium oleander* (Apocynaceae) (Leániz et al. 2013) e *Kalanchoe blossfeldiana* (Crassulaceae). Ambas as espécies são ornamentais

e pouco importantes para animais de fazenda, tendo em vista que os surtos de intoxicação são menos frequentes e ocorrem por erros de manejo, geralmente quando as plantas são podadas e deixadas nas áreas de pastagem ou quando são, equivocadamente, oferecidas aos animais (Riet-Correa & Méndez 2007).

Nerium oleander é uma planta arbustiva encontrada em todo o Brasil e que pode atingir 4 metros de altura (Zibbu & Batra 2010, Koch et al. 2015). Surtos naturais de intoxicação foram diagnosticados apenas em bovinos nos estados da Paraíba, Rio Grande do Norte e Rio Grande do Sul (Soto-Blanco et al. 2006, Pedroso et al. 2009, Assis et al. 2010). A toxicidade de *N. oleander* se deve à elevada quantidade de cardenólídeos, sobretudo oleandrina, presente em todas as partes da planta, como folhas, ramos, flores, raízes e seiva, frescas ou secas (Zibbu & Batra 2010). Os cardenólídeos inibem a enzima Na⁺/K⁺ ATPase da membrana dos cardiomiócitos, promovendo redução do potássio e aumento do sódio intracelular, resultando no acúmulo de cálcio. Esses distúrbios eletrolíticos afetam a condutividade e contratilidade do coração (Soto-Blanco et al. 2006). Estudos anteriores demonstraram que a média da concentração de oleandrina nas folhas de *N. oleander* é elevada, geralmente superior a 4,5mg g⁻¹ (Soto-Blanco et al. 2006, Pedroza et al. 2015). Experimentalmente, em bovinos, as doses de 0,5 e 1,0g/kg de folhas de *N. oleander* desencadearam sinais clínicos severos e morte (Pedroso et al. 2009). De acordo com Soto-Blanco et al. (2006), a dose letal para esta espécie seria de 0,005% do peso corporal do animal de folhas secas. Em ovinos, a dose letal foi estimada entre 0,5 e 1g/kg de peso corporal de folhas verdes (Armién et al. 1994).

Kalanchoe blossfeldiana é uma espécie de suculenta com hábito perene e que mede aproximadamente 45cm de altura. As folhas são de cor verde escura, opostas e têm aspecto elíptico e espatulado. Suas flores têm longa duração e as cores variam de branco a amarelo e tons de vermelho. Florescem no fim do inverno e início da primavera (Costa 2011). No Brasil só há um relato de intoxicação em bovinos no agreste de Pernambuco (Ribeiro et al. 2016). *K. blossfeldiana* contém como princípio tóxico bufadienólidos, que também são potentes glicosídeos cardiotoxícos presentes em todas as partes da planta. Para bovinos, a dose letal das flores e folhas de *Kalanchoe* spp. foi estimada entre 7g/kg e 40g/kg, respectivamente (Ribeiro et al. 2016).

Sinais clínicos, lesões macro e microscópicas associadas às intoxicações por plantas que contêm glicosídeos cardiotoxícos

Os sinais clínicos da intoxicação por *N. oleander* são observados entre 1 e 24 horas após a ingestão das folhas (Baskin et al. 2007) e consistem principalmente em andar cambaleante, polidipsia, desidratação, sialorreia, micção frequente, ranger de dentes, tremores musculares generalizados, aumento da frequência respiratória, dificuldade de locomoção, regurgitação de conteúdo ruminal, relutância em caminhar, queda brusca do animal ao chão, decúbito lateral, movimentos de pedalagem, vocalização, intensa taquicardia, mugidos, vômito, diarreia (às vezes sanguinolenta), ataxia, extremidades frias, dispneia, paralisia, coma e morte (Assis et al. 2010, Pedroso et al. 2009, Baskin et al. 2007). Há também efeitos diuréticos que estão ligados diretamente aos efeitos dos glicosídeos nos túbulos renais, especialmente nos estágios iniciais da intoxicação,

resultando em elevação do fluxo sanguíneo renal e aumento da filtração glomerular e da diurese (Adams 1995). Em alguns casos também se pode notar hidrotórax, hidropericárdio e ascite.

As lesões macroscópicas da intoxicação por *N. oleander* são inespecíficas (Leániz et al. 2013) e consistem em congestão de mucosas (ocular, bucal e vulvar) e principalmente hemorragias. No coração essas hemorragias podem ser do tipo petequeial até sufusões que podem ser notadas no epicárdio, endocárdio e por vezes formam coágulos no átrio e ventrículo esquerdo. No miocárdio e septo interventricular pode haver ainda áreas levemente pálidas que correspondem à necrose. Os pulmões frequentemente encontram-se congestionados e edemaciados. Hemorragias podem ser notadas também na pleura, tecidos subcutâneos, músculos intercostais, omento e serosa do rúmen. À superfície de corte, o fígado está frequentemente vermelho-escuro e os rins podem estar de coloração amarelo-pálida com petéquias na região medular (Pedroso et al. 2009, Assis et al. 2010, Di Paolo et al. 2010).

Ao exame microscópico nota-se achados em diferentes estruturas, como o miocárdio, com hemorragias subendoteliais locais e difusas, infiltrado de células mononucleares no endocárdio, nos músculos papilares dos ventrículos direito e esquerdo. Nas fibras musculares cardíacas pode haver picnose, aumento da eosinofilia, áreas extensas e multifocais de degeneração e necrose hialina e vacuolização e hemorragia subendocárdica (Pedroso et al. 2009, Di Paolo et al. 2010). No fígado pode haver áreas focais de degeneração e necrose de hepatócitos, com hemorragia, congestão difusa acentuada, células inflamatórias no parênquima e necrose individual de hepatócitos e, no baço, infiltrado linfocitário na polpa branca, com macrófagos contendo hemossiderina (Pedroso et al. 2009, Assis et al. 2010, Di Paolo et al. 2010). O tecido renal pode apresentar congestão severa e extensa necrose nas células epiteliais dos túbulos distais e proximais, além de hemorragia e frequente pigmento de hemossiderina no citoplasma das células epiteliais dos túbulos renais (Aslani et al. 2007, Di Paolo et al. 2010).

Os sinais clínicos da intoxicação por *K. blossfeldiana* surgem poucas horas após a ingestão da planta e a evolução do quadro clínico, dependendo da quantidade de folhas ingeridas, dura em média de 4 a 5 dias. Os principais sinais clínicos incluem anorexia, inquietação, mucosas conjuntivais e vasos episclerais congestionados, desidratação, muflor nasal ressecado, taquipneia, taquicardia, atonia ruminal, diarreia hemorrágica, prostração e decúbito lateral permanente seguido de morte (Ribeiro et al. 2016). À necropsia notam-se hemorragias petequiais e equimoses nas aurículas, epicárdio e músculos papilares. O fígado pode estar aumentado de volume, congestionado e com a vesícula biliar distendida. O intestino delgado pode ter áreas de congestão severa e de hemorragias petequiais nas serosas e na mucosa pode haver hemorragia, por vezes contendo coágulos. As lesões microscópicas consistem em áreas extensas ou multifocais de degeneração e necrose de fibras musculares cardíacas. Na aurícula as principais lesões consistem em edema intersticial, infiltrado inflamatório, hemorragia e necrose de coagulação. Áreas focais de degeneração e necrose de hepatócitos também são constantemente observadas. Na submucosa do intestino delgado pode haver edema, presença de infiltrado inflamatório mononuclear e macrófagos contendo hemossiderina; já na mucosa são

frequentes as áreas de hemorragia, diminuição da altura das vilosidades e necrose do epitélio, ocasionalmente associada à presença de infiltrado inflamatório de polimorfonucleares (Ribeiro et al. 2016).

Diagnóstico, tratamento e medidas preventivas ou de controle

O diagnóstico de intoxicação por *N. oleander* e *K. blossfeldiana* deve ser baseado no histórico de consumo das plantas pelos animais, na epidemiologia, sinais clínicos, lesões macroscópicas e achados histológicos compatíveis com intoxicações por plantas que contêm glicosídeos cardiotoxícos. No diagnóstico diferencial devem ser levadas em consideração as intoxicações por antibióticos ionóforos e as por plantas que contêm MFA (Tokarnia et al. 2012). Não existe antídoto para a intoxicação por *N. oleander* e *K. blossfeldiana* em bovinos. O tratamento deve ser sintomático e de suporte (Smith 2004).

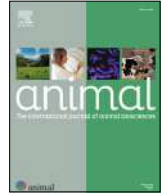
REFERÊNCIAS

- Adams H.R. 1995. Digitalis and vasodilator drugs, p.455-463. In: Adams H.R. (Ed.), Veterinary Pharmacology and Therapeutics. 7th ed. Iowa State University Press, Ames.
- Albuquerque S.S., Brito L.B., Tavares R.M., Rocha B.P., Andrade M.L. & Mendonça F.S. 2013. Mortes súbitas em caprinos associadas à intoxicação por *Palicourea aeneofusca* (Rubiaceae) no Agreste de Pernambuco. Arch. Vet. Sci. 18(3):364-366.
- Albuquerque S.S.C., Rocha B.P., Almeida V.M., Oliveira J.S., Riet-Correa F., Lee S.T., Evêncio Neto J. & Mendonça F.S. 2014. Cardiac fibrosis associated to the poisoning by *Amorimia septentrionalis* in cattle. Pesq. Vet. Bras. 34(5):433-437. <<http://dx.doi.org/10.1590/S0100-736X2014000500008>>
- Almeida M.B., Priebe A.P.S., Riet-Correa B., Riet-Correa G., Fiss L., Raffi M.B. & Schild A.L. 2008. Evolução e Reversibilidade das Lesões Neurológicas e Cardíacas em Ovinos Intoxicados Experimentalmente por *Ateleia glazioviana* e *Tetrapterys multiglandulosa*. Pesq. Vet. Bras. 28(3):129-134. <<http://dx.doi.org/10.1590/S0100-736X2008000300001>>
- Anderson W.R. 2006. Eight segregates from the neotropical genus *Mascagnia* (Malpighiaceae). Novon, J. Bot. Nomenclature 16(2):168-204. <[http://dx.doi.org/10.3417/1055-3177\(2006\)16\[168:ESFTNG\]2.0.CO;2](http://dx.doi.org/10.3417/1055-3177(2006)16[168:ESFTNG]2.0.CO;2)>
- Armien A.G., Peixoto P.V., Barbosa J.D. & Tokarnia C.H. 1994. Intoxicação experimental por *Nerium oleander* (Apocinaeae) em ovinos. Pesq. Vet. Bras. 14:85-93.
- Arruda F.P.D., Caldeira F.H.B., Ducatti K.R., Bezerra K.S., Marcolongo-Pereira C., Lee S.T., Cook D., Riet-Correa F. & Colodel E.M. 2017. Experimental poisoning by *Niedenzuella stannea* in cattle and corresponding detection of monofluoroacetate. Ciência Rural 47(3):1-6. <<http://dx.doi.org/10.1590/0103-8478cr20160761>>
- Aslani M.R., Maleki M., Mohri M., Sharifi K., Najjar-Nezhad V. & Afshari E. 2007. Castor bean (*Ricinus communis*) toxicosis in a sheep flock. Toxicon 49(3):400-406. <<http://dx.doi.org/10.1016/j.toxicon.2006.10.010>> <PMid:17157890>
- Assis T.S., Medeiros R.M.T., Riet-Correa F., Galiza G.J.N., Dantas A.F.M. & Oliveira D.M. 2010. Intoxicações por plantas diagnosticadas em ruminantes e equinos e estimativa das perdas econômicas na Paraíba. Pesq. Vet. Bras. 30(1):13-20. <<http://dx.doi.org/10.1590/S0100-736X2010000100003>>
- Bandinelli M.B., Bassuino D.M., Fredo G., Mari C., Driemeier D., Sonne L. & Pavarini S.P. 2014. Identificação e distribuição de lesões cardíacas em bovinos intoxicados por *Amorimia exotropa*. Pesq. Vet. Bras. 34(9):837-844. <<http://dx.doi.org/10.1590/S0100-736X2014000900006>>
- Barbosa R.R., Pacífico da Silva I. & Soto-Blanco B. 2008. Development of conditioned taste aversion to *Mascagnia rigida* in goats. Pesq. Vet. Bras. 28(12):571-574. <<http://dx.doi.org/10.1590/S0100-736X2008001200001>>

- Baskin S.I., Czerwinski S.E., Anderson J.B. & Sebastian M.M. 2007. Cardiovascular toxicity, p.193-205. In: Gupta R.C. (Ed.), *Veterinary Toxicology: basic and clinical principles*. Elsevier, New York, NY. <<http://dx.doi.org/10.1016/B978-012370467-2/501110-3>>
- Becker M., Caldeira F.H.B., Carneiro F.M., Oliveira L.P.D., Tokarnia C.H., Riet-Correa F., Lee S.T. & Colodel E.M. 2013. The importance of poisoning by *Amorimia pubiflora* (Malpighiaceae) in cattle in Mato Grosso: experimental reproduction of the poisoning in sheep and cattle. *Pesq. Vet. Bras.* 33(9):1049-1056. <<http://dx.doi.org/10.1590/S0100-736X2013000900001>>
- Becker M., Carneiro F.M., Oliveira L.P.D., Silva M.I.V.D., Riet-Correa F., Lee S.T., Pescador C.A., Nakazato L. & Colodel E.M. 2016. Induction and transfer of resistance to poisoning by *Amorimia pubiflora* in sheep with non-toxic dose of the plant and ruminal content. *Ciência Rural* 46(4):674-680. <<http://dx.doi.org/10.1590/0103-8478cr20141484>>
- Borboleta L.R. 2010. Intoxicação experimental com extratos de *Mascagnia rigida* (A. Juss.) Griseb. (Malpighiaceae) em coelhos (*Oryctolagus cuniculus*): estudos clínico, laboratorial e anatomopatológico. Dissertação de Mestrado em Ciência Animal, Curso de Pós-graduação em Ciência Animal, Universidade Federal de Minas Gerais, Belo Horizonte. 142p.
- Brito L.B.D., Albuquerque R.F., Rocha B.P., Albuquerque S.S., Lee S.T., Medeiros R.M.T., Riet-Correa F. & Mendonça F.D.S. 2016. Spontaneous and experimental poisoning of cattle by *Palicourea aeneofusca* in the region of Pernambuco and induction of conditioned food aversion. *Ciência Rural* 46(1):138-143. <<http://dx.doi.org/10.1590/0103-8478cr20150079>>
- Caldas S.A., Peixoto T.C., Nogueira V.A., França T.N., Tokarnia C.H. & Peixoto P.V. 2011. Aborto em bovinos devido à intoxicação por *Tetrapteryx acutifolia* (Malpighiaceae). *Pesq. Vet. Bras.* 31(9):737-746. <<http://dx.doi.org/10.1590/S0100-736X2011000900003>>
- Caldeira F.B., Dias G.B., Arruda F.P., Lourenço F.M., Bezerra K.S., Riet-Correa F. & Colodel E.M. 2016. Sudden death associated with *Niedenzuella stannea* (Malpighiaceae) in cattle in the State of Mato Grosso, Brazil: importance and epidemiological aspects. *Pesq. Vet. Bras.* 36:147-149.
- Camargo W.A. 1962. Uma nova "erva-de-rato" tóxica para bovinos, *Palicourea barbiflora*: comparação com a *Palicourea marcgravii* var. *pubescens* e com *Psychotria officinalis*, Rubiaceae. *Arqs Inst. Biológico, São Paulo*, 29:1-11.
- Cardinal S.G., Aniz A.C., Santos B.S., Carvalho N.M. & Lemos R.A.A. 2010. Lesões perinatais em cordeiros induzidas pela administração de *Tetrapteryx multiglandulosa* (Malpighiaceae) a ovelhas em diferentes estágios de gestação. *Pesq. Vet. Bras.* 30(1):73-78. <<http://dx.doi.org/10.1590/S0100-736X2010000100012>>
- Carmo P.M.S., Irigoyen L.F., Lucena R.B., Figuera R.A., Kommers G.D. & Barros C.S.L. 2011. Spontaneous coffee senna poisoning in cattle: report on 16 outbreaks. *Pesq. Vet. Bras.* 31(2):139-146. <<http://dx.doi.org/10.1590/S0100-736X2011000200008>>
- Carvalho A.Q., Carvalho N.M., Vieira G.P., Santos A.C., Franco G.L., Pott A., Barros C.S.L. & Lemos R.A.A. 2014. Intoxicação espontânea por *Senna obtusifolia* em bovinos no Pantanal Sul-Mato-Grossense. *Pesq. Vet. Bras.* 34(2):147-152. <<http://dx.doi.org/10.1590/S0100-736X2014000200009>>
- Carvalho G.D., Nunes L.C., Bragança H.B.N. & Porfírio L.C. 2009. Principais plantas tóxicas causadoras de morte súbita em bovinos no estado do Espírito Santo, Brasil. *Arch. Zootec.* 58:87-98.
- Carvalho F.K.L., Cook D., Lee S.T., Taylor C.M., Soares Oliveira J.B. & Riet-Correa F. 2016. Determination of toxicity in rabbits and corresponding detection of monofluoroacetate in four *Palicourea* (Rubiaceae) species from the Amazonas state, Brazil. *Toxicon* 109:42-44. <<http://dx.doi.org/10.1016/j.toxicon.2015.11.009>> <PMid:26603601>
- Carvalho N.M., Alonso L.A., Cunha T.G., Ravedutti J., Barros C.S.L. & Lemos R.A.A. 2006. Intoxicação de Bovinos por *Tetrapteryx multiglandulosa* (Malpighiaceae) em Mato Grosso do Sul. *Pesq. Vet. Bras.* 26(3):139-146. <<http://dx.doi.org/10.1590/S0100-736X2006000300002>>
- Consorte L.B., Peixoto P.V. & Tokarnia C.H. 1994. Intoxicação experimental por *Pseudocalymma elegans* (Bignoniaceae) em ovinos. *Pesq. Vet. Bras.* 14(4):123-133.
- Cook D., Lee S.T., Taylor C.M., Bassüner B., Riet-Correa F., Pfister J.A. & Gardner D.R. 2014. Detection of toxic monofluoroacetate in *Palicourea* species. *Toxicon* 80(15):9-16. <<http://dx.doi.org/10.1016/j.toxicon.2013.12.003>> <PMid:24440601>
- Costa T.N. 2011. Alterações hematológicas e bioquímicas séricas nas intoxicações de cães, gatos e ruminantes por plantas. Dissertação de Mestrado, Universidade Federal de Goiás, Goiânia. 30p.
- Da Silva L.C., Pessoa D.A., Lopes J.R., de Albuquerque L.G., da Silva L.S., Garino Junior F. & Riet-Correa F. 2016. Protection against *Amorimia septentrionalis* poisoning in goats by the continuous administration of sodium monofluoroacetate-degrading bacteria. *Toxicon* 111(1):65-68. <<http://dx.doi.org/10.1016/j.toxicon.2015.12.016>> <PMid:26747472>
- Davis C.C. & Anderson W.R. 2010. A complete generic phylogeny of Malpighiaceae inferred from nucleotide sequence data and morphology. *Amer. J. Bot.* 97(12):2031-2048. <<http://dx.doi.org/10.3732/ajb.1000146>> <PMid:21616850>
- Di Paolo L.A., Ancinas M.D., Tassara F., Peralta L.M. & Hoyo L. 2010. Intoxicación natural con *Nerium oleander* en llamas (*Lama glama*) en un establecimiento de la provincia de Buenos Aires. *Vet. Arg.* 27(263):2-11.
- Döbereiner J., Tokarnia C.H. & Silva M.F. 1983. Intoxicação por *Arrabidaea bilabiata* em bovinos na Região Amazônica do Brasil. *Pesq. Vet. Bras.* 3(1):17-24.
- Duarte A.L.L. 2012. Intoxicações por *Amorimia* spp. e *Callaeum psilophyllum* em ruminantes. Tese de Doutorado em Medicina Veterinária, Programa de Pós-Graduação em Medicina Veterinária, Universidade Federal de Campina Grande, PB. 68p.
- Duarte A.L., Medeiros R.M.T. & Riet-Corrêa F. 2013. Intoxicação por *Amorimia* spp. em ruminantes. *Ciência Rural* 43(7):1294-1301. <<http://dx.doi.org/10.1590/S0103-84782013005000081>>
- Egyed M.N. & Schultz R.A. 1986. The efficacy of acetamide for the treatment of experimental *Dichapetalum cymosum* (gifblaar) poisoning in sheep. *Onderstepoort J. Vet. Res.* 53(4):231-234. <PMid:3796950>
- García y Santos M.C., Schild A.L., Barros S.S., Riet-Correa F., Elias F. & Ramos A.T. 2004. Lesões perinatais em bovinos na intoxicação experimental por *Ateleia glazioviana* (Leg. Papilionoideae). *Pesq. Vet. Bras.* 24(8):178-184. <<http://dx.doi.org/10.1590/S0100-736X2004000400002>>
- Gava A. & Barros C.S.L. 2001. Field Observations of *Ateleia glazioviana* Poisoning in Cattle in Southern Brazil. *Vet. Hum. Toxicol.* 43(1):37-41. <PMid:11205077>
- Gava A., Barros C.S.L., Pilati C., Barros S.S. & Mori A.M. 2001. Intoxicação por *Ateleia glazioviana* (Leg. Papilionoideae) em bovinos. *Pesq. Vet. Bras.* 21(2):49-59. <<http://dx.doi.org/10.1590/S0100-736X2001000200003>>
- Gava D., Reis R.N., Rocha T.S., Pasquale E. & Gava A. 2003. Intoxicação natural por *Ateleia glazioviana* (Leg. Papilionoideae) em ovinos. XI Encontro Nacional de Patologia Veterinária, Botucatu, SP. 60p.
- Gava A., Cristani J., Branco J.V., Neves D.S., Mondadori A.J. & Sousa R.S. 1998. Morte súbita em bovinos causada pela ingestão de *Mascagnia* sp. (Malpighiaceae), no Estado de Santa Catarina. *Pesq. Vet. Bras.* 18(1):16-20. <<http://dx.doi.org/10.1590/S0100-736X1998000100003>>
- Hayakawa I., Shioda S., Chinen T., Hatanaka T., Ebisu H., Sakakura A., Usui T. & Kigoshi H. 2016. Discovery of O6 -benzyl glaziovianin A, a potent cytotoxic substance and a potent inhibitor of a,b-tubulin polymerization. *Bioorganic Med. Chem.* 24(21):5639-5645. <<http://dx.doi.org/10.1016/j.bmc.2016.09.026>> <PMid:27665177>
- Helayel M.A., França T.N., Seixas J.N., Nogueira V.A., Caldas S.A. & Peixoto P.V. 2009. Morte súbita em bovinos causada pela ingestão de *Pseudocalymma elegans* (Bignoniaceae) no município de Rio Bonito, RJ. *Pesq. Vet. Bras.* 29(7):498-508. <<http://dx.doi.org/10.1590/S0100-736X2009000700003>>

- Helayel M.A., Caldas S.A., Peixoto T.C., França T.N., Tokarnia C.H., Döbereiner J., Nogueira V.A. & Peixoto P.V. 2011. Antagonism of acetamid in experiments with sheep, goats and rabbits indicates that monofluoroacetate is the toxic principle of *Pseudocalymma elegans* Bignoniaceae. *Pesq. Vet. Bras.* 31(10):867-874. <<http://dx.doi.org/10.1590/S0100-736X2011001000006>>
- Jabour F.F., Seixas J.N., Tokarnia C.H. & Brito M.F. 2006. Variation of the toxicity of *Arrabidaea bilabiata* (Bignoniaceae) in rabbits. *Pesq. Vet. Bras.* 26(3):171-176. <<http://dx.doi.org/10.1590/S0100-736X2006000300008>>
- Koch I., Rapini A., Simões A.O., Kinoshita L.S., Spina A.P. & Castello A.C.D. 2015. Apocynaceae in Lista de Espécies da Flora do Brasil. Jardim Botânico do Rio de Janeiro. Disponível em <<http://floradobrasil.jbrj.gov.br/jabot/floradobrasil/FB33737>> Acesso em 12 jul. 2017.
- Krebs H.C., Kemmerling W. & Habermehl G. 1994. Qualitative and quantitative determination of fluoroacetic acid in *Arrabidaea bilabiata* and *Palicourea marcgravii* by ¹⁹F-NMR spectroscopy. *Toxicon* 32(8):909-913. <[http://dx.doi.org/10.1016/0041-0101\(94\)90369-7](http://dx.doi.org/10.1016/0041-0101(94)90369-7)> <PMid:7985195>
- Lago E.P., Melo M.M., Araújo R.B., Nascimento E.F., Silva E.F. & Melo M.B. 2009. Perfis eletrocardiográfico e ecodoppler cardiográfico de ovinos após ingestão da suspensão aquosa de *Mascagnia rigida* Griseb. (Malpighiaceae). *Arq. Bras. Med. Vet. Zootec.* 61(4):853-862. <<http://dx.doi.org/10.1590/S0102-09352009000400012>>
- Leániz J.A.B., Utaravičius E.L. & Aguirrezabala S.A. 2013. Estudio de la toxicidad de *Nerium oleander* en ovinos. Tesis de Grado, Universidad de La República. 61p.
- Lee S.T., Cook D., Riet-Correa F., Pfister J.A., Anderson W.R., Lima F.G. & Gardner D. 2012. Detection of monofluoroacetate in *Palicourea* and *Amorimia* species. *Toxicon* 60(5):791-796. <<http://dx.doi.org/10.1016/j.toxicon.2012.05.029>> <PMid:22699106>
- Lemos R.A.A., Guimarães E.B., Carvalho N.M., Nogueira A.P.A., Santos B.S., Souza R.I.C., Cardinal S.G. & Kassab H.O. 2011. Plant poisonings in Mato Grosso do Sul, p.68-72. In: Riet-Correa F., Pfister J., Schild A.L. & Wierenga T. (Eds), Poisoning by Plants, Mycotoxins, and Related Toxins. CAB International, Wallingford, UK. <<http://dx.doi.org/10.1079/9781845938338.0068>>
- Lima E.F., Medeiros R.M., Cook D., Lee S.T., Kaehler M., Santos-Barbosa J.M. & Riet-Correa F. 2016. Studies in regard to the classification and putative toxicity of *Fridericia japurensis* (*Arrabidaea japurensis*) in Brazil. *Toxicon* 115(1):22-27. <<http://dx.doi.org/10.1016/j.toxicon.2016.03.001>> <PMid:26945838>
- Lohmann L.G. 2015. Bignoniaceae in Lista de Espécies da Flora do Brasil. Jardim Botânico do Rio de Janeiro. Disponível em <<http://floradobrasil.jbrj.gov.br/jabot/floradobrasil/FB113368>> Acesso em 12 jul. 2017.
- Lohmann L.G. & Taylor C.M. 2014. A new generic classification of tribe Bignoniaceae (Bignoniaceae) 1. *Ann. Missouri Bot. Gard.* 99(3):348-489. <<http://dx.doi.org/10.3417/2003187>>
- Mamede M.C.H. 2015. *Amorimia* in Lista de Espécies da Flora do Brasil. Jardim Botânico do Rio de Janeiro. Disponível em <<http://floradobrasil.jbrj.gov.br/jabot/floradobrasil/FB101437>> Acesso em 7 jan. 2017.
- Mansano V.F., Pinto R.B. & Pennington T. 2015. *Ateleia* in Lista de Espécies da Flora do Brasil. Jardim Botânico do Rio de Janeiro. Disponível em <<http://floradobrasil.jbrj.gov.br/jabot/floradobrasil/FB82648>> Acesso em 7 jan. 2017.
- McIlroy J.C. 1981. The sensitivity of Australian animals to 1080 poison. I. Intra-specific variation and factors affecting acute toxicity. II. Marsupial and eutherian carnivores. *Aust. Wildl. Res.* 8(2):369-383. <<http://dx.doi.org/10.1071/WR9810369>>
- Medeiros R.M.T., Geraldo Neto S.A., Barbosa R.C., Lima E.F. & Riet-Correa F. 2002. Sudden bovine death from *Mascagnia rigida* in northeastern Brazil. *Vet. Hum. Toxicol.* 44(5):286-288. <PMid:12361113>
- Nogueira V.A., França T.N. & Peixoto P.V. 2009. Intoxicação por antibióticos ionóforos em animais. *Pesq. Vet. Bras.* 29(3):191-197. <<http://dx.doi.org/10.1590/S0100-736X2009000300001>>
- Oliveira A.C., Oliveira G.C., Paraguassu A.A. & Freire L.M.G.M. 1978. Intoxicação por um "tingui" (*Mascagnia rigida* Griseb.) em caprinos na Bahia. *Anais XVI Congr. Bras. Med. Vet.*, Salvador, 1:172.
- Oliveira-Neto T.S., Riet-Correa F., Lee S.T., Cook D., Barbosa F.M.S., Silva-Neto J.F., Simões S.V.D. & Lucena R.B. 2017. Poisoning in goats by the monofluoroacetate-containing plant *Palicourea aeneofusca* (Rubiaceae). *Toxicon* 135(1):12-16. <<http://dx.doi.org/10.1016/j.toxicon.2017.05.025>> <PMid:28576552>
- Pacífico da Silva I. & Soto-Blanco B. 2010. Conditioning taste aversion to *Mascagniarigida* (Malpighiaceae) in sheep. *Res. Vet. Sci.* 88(2):239-241. <<http://dx.doi.org/10.1016/j.rvsc.2009.08.012>> <PMid:19836034>
- Pacífico da Silva I., Lira R.A., Barbosa R.R., Batista J.S. & Soto-Blanco B. 2008. Intoxicação natural pelas folhas de *Mascagnia rigida* (Malpighiaceae) em ovinos. *Arqs Inst. Biológico, São Paulo*, 75(2):229-233.
- Paraguassu A.A. 1983. Intoxicação experimental por *Mascagnia rigida* Griseb (Malpighiaceae) em caprinos no Nordeste do Brasil. Dissertação de Mestrado em Medicina Veterinária, Curso de Pós-Graduação em Ciências Veterinárias, Universidade Federal Rural do Rio de Janeiro, RJ. 65p.
- Pavarini S.P., Soares M.P., Bandarra P.M., Gomes D.C., Bandinelli M.B., Cruz C.E. & Driemeier D. 2011. Mortes súbitas em bovinos causadas por *Amorimia exotropicalis* (Malpighiaceae) no Rio Grande do Sul. *Pesq. Vet. Bras.* 31(4):291-296. <<http://dx.doi.org/10.1590/S0100-736X2011000400004>>
- Pedroso P.M.O., Bandarra P.M., Bezerra Júnior P.S., Raymundo D.L., Borba M.R., Leal J.S. & Driemeier D. 2009. Intoxicação natural e experimental por *Nerium oleander* (Apocynaceae) em bovinos no Rio Grande do Sul. *Pesq. Vet. Bras.* 29(5):404-408. <<http://dx.doi.org/10.1590/S0100-736X2009000500008>>
- Pedroza H.P. 2015. *Psychotria hoffmannseggiana*: uma nova espécie de planta tóxica para bovinos. Dissertação de Mestrado, Escola de Veterinária, Universidade Federal de Minas Gerais, Belo Horizonte, MG. 41p.
- Pedroza H.P., Ferreira M.G., Carvalho J.G., Melo K.D.A., Keller K.M., Melo M.M. & Soto-Blanco B. 2015. Concentrações de oleandrina nas folhas de *Nerium oleander* de diferentes cores da floração. *Ciência Rural* 45(5):864-866. <<http://dx.doi.org/10.1590/0103-8478cr20140885>>
- Peixoto T.C., Oliveira L.I., Caldas S.A., Catunda Junior F.E.A., Carvalho M.G., França T.N. & Peixoto P.V. 2011. Efeito protetor da acetamida sobre as intoxicações experimentais em ratos por monofluoroacetato de sódio e por algumas plantas brasileiras que causam morte súbita. *Pesq. Vet. Bras.* 31(11):938-952. <<http://dx.doi.org/10.1590/S0100-736X2011001100002>>
- Raffi M.B., Rech R.R., Sallis E.S.V., Rodrigues A. & Barros C.S.L. 2006. Chronic cardiomyopathy and encephalic spongy changes in sheep experimentally fed *Ateleia glazioviana*. *Ciência Rural* 36(6):1860-1866. <<http://dx.doi.org/10.1590/S0103-84782006000600030>>
- Ribeiro D.P., Silva Filho G.B., Chaves H.A.S., Lemos B.O., Aguiar Filho C.R., Brito L.B., Almeida V.A. & Mendonça F.S. 2016. Intoxicação espontânea por *Kalanchoe blossfeldiana* em bovinos. *Pesq. Vet. Bras.* 36(Supl. 2):90-91.
- Riet-Correa F. & Medeiros R.M. 2001. Intoxicações por plantas em ruminantes no Brasil e no Uruguai: importância econômica, controle e riscos para a saúde pública. *Pesq. Vet. Bras.* 21(1):38-42. <<http://dx.doi.org/10.1590/S0100-736X2001000100008>>
- Riet-Correa F. & Méndez M.C. 2007. Plantas tóxicas e micotóxicas, p.191-193. In: Riet-Correa F., Schild A.L., Lemos R.A. & Borges J.R.J. (Eds), Doenças de Ruminantes e Equinos. Vol.2. 3ª ed. Pallotti, Santa Maria.
- Riet-Correa F., Schild A.L., Mendez M.C. & Lemos R.A.A. 2001. Doenças de Ruminantes e Equinos. Vol.2. Editora Varela, São Paulo, SP, p.279-283.
- Riet-Correa G., Terra F.F., Schild A.L., Riet-Correa F. & Barros S.S. 2005. Intoxicação experimental por *Tetrapteryx multiglandulosa* (Malpighiaceae) em ovinos. *Pesq. Vet. Bras.* 25(2):91-96. <<http://dx.doi.org/10.1590/S0100-736X2005000200005>>
- Rissi D.R., Rech R.R., Pierezan F., Gabriel A.L., Trost M.E., Brum J.S., Kommers G.D. & Barros C.S.L. 2007. Intoxicações por plantas e micotoxinas associadas

- a plantas em bovinos no Rio Grande do Sul: 461 casos. *Pesq. Vet. Bras.* 27(7):261-268. <<http://dx.doi.org/10.1590/S0100-736X2007000700002>>
- Santos-Barbosa J.M., Lee S.T., Cook D., Gardner D.R., Viana L.H. & Ré N. 2017. A gas chromatography–mass spectrometry method for the detection and quantitation of monofluoroacetate in plants toxic to livestock. *J. Agricult. Food Chem.* 65(7):1428-1433. <<http://dx.doi.org/10.1021/acs.jafc.7b00294>> <PMid:28132508>
- Schons S. 2011. Plantas tóxicas para ruminantes e equídeos na região central de Rondônia. Tese de Doutorado em Patologia, Universidade Federal de Pelotas, Pelotas. 78p.
- Schons S.V., Mello T.L., Riet-Correa F. & Schild A.L. 2011. Poisoning by *Amorimia* (*Mascagnia*) septium in sheep in northern Brazil. *Toxicon* 57:781-786.
- Silva D.M., Riet-Correa F., Medeiros R.M.T. & Oliveira O.F. 2006. Plantas tóxicas para ruminantes e equídeos no Seridó Ocidental e Oriental do Rio Grande do Norte. *Pesq. Vet. Bras.* 26(4):223-236. <<http://dx.doi.org/10.1590/S0100-736X2006000400007>>
- Smith G. 2004. Toxicology brief: *Kalanchoe* species poisoning in pets. *Vet. Med.* 11(1):933-936.
- Soares M.P., Pavarini S.P., Adrien M.L., Quevedo P.S., Schild A.L., Peixoto P.V., Cruz C.E.F. & Driemeier D. 2011. *Amorimia* exotropa poisoning as a presumptive cause of myocardial fibrosis in cattle. *J. Vet. Diagn. Invest.* 23(6):1223-1229. <<http://dx.doi.org/10.1177/1040638711425586>> <PMid:22362807>
- Soto-Blanco B., Fontenele-Neto J.D., Silva D.M., Reis P.F.C.C. & Nóbrega J.E. 2006. Acute cattle intoxication from *Nerium oleander* pods. *Trop. Anim. Health Prod.* 38(6):351-354. <<http://dx.doi.org/10.1007/s11250-006-4400-x>> <PMid:17243471>
- Stigger A.L., Barros C.S.L., Langohr I.M. & Barros S.S. 2001. Intoxicação experimental por *Ateleia glazioviana* (Leg.Papilionoideae) em ovinos. *Pesq. Vet. Bras.* 21(3):98-108. <<http://dx.doi.org/10.1590/S0100-736X2001000300002>>
- Taylor C.M. 1996. Overview of the Psychotriaceae (Rubiaceae) in the Neotropics. *Opera Bot. Belg.* 7:261-270.
- Taylor C.M. 2007. *Psychotria*, p.389-412. In: Jung-Mendaçolli S. (Ed.), *Rubiaceae: flora fanerogâmica do estado de São Paulo*. Instituto de Botânica, São Paulo.
- Taylor C.M. 2015a. Rubiacearum americanarum magna hama pars XXXIII: the new group *Palicourea* sect. *Didymocarpae* with four new species and two new subspecies (Palicoureaeae). *Novon, J. Bot. Nomenclature* 23(4):452-478. <<http://dx.doi.org/10.3417/2012003>>
- Taylor C.M. 2015b. Rubiacearum americanarum magna hama pars XXXIV: The new group *Palicourea* sect. *Tricephalium* with eight new species and a new subspecies. *Novon, J. Bot. Nomenclature* 24(1):55-95. <<http://dx.doi.org/10.3417/2015001>>
- Taylor C.M. & Gereau R.E. 2013. The genus *Carapichea* (Rubiaceae: Psychotriaceae). *Ann. Missouri Bot. Gard.* 99(1):100-127. <<http://dx.doi.org/10.3417/2011064>>
- Taylor C.M., Lorence D.H. & Gereau R.E. 2010. Rubiacearum americanarum magna hama pars XXV: the nocturnally flowering *Psychotria domingensis-Coussarea hondensis* group plus three other Mesoamerican *Psychotria* species transfer to *Palicourea*. *Novon, J. Bot. Nomenclature* 20(4):481-492. <<http://dx.doi.org/10.3417/2009124>>
- Tokarnia C.H. & Döbereiner J. 1981. Intoxicação por *Arrabidaea japurensis* (Bignoniaceae) em bovinos em Roraima. *Pesq. Vet. Bras.* 1(1):7-17.
- Tokarnia C.H., Canella C.F.C. & Döbereiner J. 1961. Intoxicação por um “tingui” (*Mascagnia rigida* Griseb.) em bovinos no Nordeste do Brasil. *Arqs Inst. Biol. Anim.* 4:203-215.
- Tokarnia C.H., Döbereiner J. & Peixoto P.V. 1985. Intoxicação por *Mascagnia* aff. *rigida* (Malpighiaceae) em bovinos no Norte do Espírito Santo. *Pesq. Vet. Bras.* 5(3):77-91.
- Tokarnia C.H., Döbereiner J. & Canella C.F.C. 1987. Intoxicação experimental por *Mascagnia rigida* (Malpighiaceae) em coelhos. *Pesq. Vet. Bras.* 7(1):11-16.
- Tokarnia C.H., Peixoto P.V. & Döbereiner J. 1993. Intoxicação experimental por *Pseudocalymma elegans* (Bignoniaceae) em caprinos. *Pesq. Agropec. Bras.* 13(1/2):35-39.
- Tokarnia C.H., Döbereiner J. & Peixoto P.V. 1994. Aspectos clínico-patológicos complementares da intoxicação por algumas plantas tóxicas brasileiras. *Pesq. Vet. Bras.* 14(4):111-122.
- Tokarnia C.H., Döbereiner J., Couceiro J.E.M. & Cordeiro Silva A.C. 1983. Intoxicação por *Palicourea aeneofusca* (Rubiaceae), A causa de mortes súbitas em bovinos na Zona da Mata Pernambucana. *Pesq. Vet. Bras.* 3(3):75-79.
- Tokarnia C.H., Peixoto P.V., Döbereiner J., Consorte I.B. & Gava A. 1989. *Tetrapteryx* spp. (Malpighiaceae): a causa de mortandades em bovinos caracterizadas por alterações cardíacas. *Pesq. Vet. Bras.* 9:23-44.
- Tokarnia C.H., Brito M.F., Barbosa J.D., Peixoto P.V. & Döbereiner J. 2012. Plantas que afetam o funcionamento do coração, p.27-94. In: *Ibid.* (Eds), *Plantas Tóxicas do Brasil para Animais de Produção*. 2ª ed. Helianthus, Rio de Janeiro.
- Vasconcelos J.S., Riet-Correa F., Dantas A.F., Medeiros R.M.T. & Dantas A.J.A. 2008a. Mortes súbitas em bovinos causadas por *Palicourea aeneofusca* (Rubiaceae) e *Mascagnia rigida* (Malpighiaceae) na Zona da Mata Paraibana. *Pesq. Vet. Bras.* 28(10):457-460. <<http://dx.doi.org/10.1590/S0100-736X2008001000003>>
- Vasconcelos J.S., Riet-Correa F., Dantas A.F.M., Medeiros R.M., Galiza G.J.N., Oliveira D.M. & Pessoa A.F. 2008b. Intoxicação por *Mascagnia rigida* (Malpighiaceae) em ovinos e caprinos. *Pesq. Vet. Bras.* 28(10):521-526. <<http://dx.doi.org/10.1590/S0100-736X2008001000013>>
- Zibbu G. & Batra A. 2010. A review on chemistry and pharmacological activity of *Nerium oleander* L. *J. Chem. Phar. Res.* 2(6):351-358.



Review: Current status of corpus luteum assessment by Doppler ultrasonography to diagnose non-pregnancy and select embryo recipients in cattle



Guilherme Pugliesi^{a,*}, Amanda Guimarães da Silva^a, Joao Henrique Moreira Viana^b, Luiz Gustavo Bruno Siqueira^c

^a Department of Animal Reproduction, School of Veterinary Medicine and Animal Science, University of São Paulo, Pirassununga, SP 13635-900, Brazil

^b Embrapa Recursos Genéticos e Biotecnologia, Brasília, DF 70770-190, Brazil

^c Embrapa Gado de Leite, Juiz de Fora, MG 36038-330, Brazil

ARTICLE INFO

Article history:

Received 5 October 2022

Revised 13 February 2023

Accepted 20 February 2023

Keywords:

Embryo

Imaging technologies

Luteal function

Pregnancy

Progesterone

ABSTRACT

A number of potentials uses of Doppler ultrasonography have been explored in the last decades, both as research tools in reproductive physiology investigations and for the reproductive management of farm animals. The objective of this review was to address some of the recent strategies developed in fixed-time reproductive programs and resynchronization of ovulation in cattle, based on the evaluation of corpus luteum function by color-Doppler ultrasound imaging. Recent studies in dairy and beef cattle pointed out to a high accuracy when Doppler ultrasonography is used to assess the functionality of the corpus luteum and identify non-pregnant females at 20–24 days after breeding. Therefore, super-early resynchronization programs starting in the second week after timed-artificial insemination or embryo transfer have been developed and are being implemented in commercial assisted reproduction programs; thus, anticipating conception with proven semen or genetically superior embryos. In addition, assessment of corpus luteum blood perfusion can be used for identifying high fertility embryo recipients in fixed-time embryo transfer programs.

© 2023 The Authors. Published by Elsevier B.V. on behalf of The Animal Consortium. This is an open access article under the CC BY license (<http://creativecommons.org/licenses/by/4.0/>).

Implications

Current alternatives to evaluate corpus luteum function by color-Doppler ultrasound imaging pointed to new tools that could improve reproductive performance and profitability of dairy and beef cattle operations. Defined methods to determine luteal blood perfusion allowed the estimation of luteal function at different phases of the estrous cycle and early pregnancy and its association with circulating progesterone profile. This review provides an overview of the technical and physiological concepts underlying the use of Doppler ultrasonography for the assessment of corpus luteum blood perfusion and highlights the applications in the reproductive management in order to build applied uses in cattle.

Introduction

The basic principle of the Doppler ultrasound is the Doppler effect, a shift in the frequency of the sound wave reflected by an

object moving toward or away from the probe. In medical ultrasound, this shift is observed in the echo from blood cells and is, thus, used to depict blood flow within a tissue or organ (Ginther, 2007). The Doppler ultrasound provides important information about the functional status of a tissue or organ, leading to its adoption in many areas of human and veterinary medicine. In cattle reproduction, Doppler ultrasound has been used for over two decades for the study of vascular perfusion in the ovaries, uterus and vagina, as well as fetuses and placenta (reviewed by Herzog & Bollwein, 2007; Matsui & Miyamoto, 2009; Bollwein et al., 2016).

In spite of the undeniable gains for diagnostic quality and accuracy, devices equipped with Doppler mode and respective licenses are usually significantly more expensive than their conventional, B-mode-only counterparts. This price difference hampered a broader adoption of the technology by field practitioners in the past. A turning point was the demonstration that Doppler ultrasound could be used as a practical tool for the reproductive management of herds, particularly for the early diagnosis of non-pregnancy based on corpus luteum (CL) blood perfusion (CLBP) (Siqueira et al., 2013; Pugliesi et al., 2014). The early detection of non-pregnant cattle is critical for the development of strategies

* Corresponding author.

E-mail address: gpugliesi@usp.br (G. Pugliesi).

to reduce the number of days open and calving intervals, thus improving reproductive performance of cattle herds (Gnemmi et al., 2022). The development of practical applications of Doppler ultrasound in reproductive management ultimately led to a substantial increase in the interest on the technology, as seen by the number of scientific papers published in this subject over the past 10 years by crossing related key words in databases such as PubMed (<https://pubmed.ncbi.nlm.nih.gov/>).

The aim of this review is to present the technical and physiological concepts underlying the use of color-Doppler ultrasonography for the assessment of CLBP, and subsequent applications in the reproductive management of dairy and beef herds.

Corpus luteum assessment by Doppler ultrasonography

The Doppler signal can be displayed at the ultrasound device screen as spectral graphs or color-flow images. The spectral mode presents the Doppler signal as a time \times velocity graphic, depicting changes in blood flow associated with the cardiac cycle (Ginther, 2007). Blood velocities and the pulsatility and resistance indexes can be obtained from the spectral graph. However, such measurements are calculated for an individual artery and, thus are more useful if a single, large vessel, accounts for most of a tissue's or organ's blood supply (e.g., the uterine artery; Herzog & Bollwein, 2007). Moreover, immobility is required to obtain a good spectral graph, particularly for small vessels, making the exam time-consuming and frequently not feasible in large animals. Therefore, most studies on CLBP in cattle were performed based on the analysis of the colored area displayed in the color-flow Doppler image.

The color-flow mode generates real-time and easy-to-interpret images of the blood perfusion, which depicts the vascularization of the CL. The use of color-Doppler data for research or as a diagnostic tool, however, usually requires a comparative analysis considering changes over time, or individual differences among animals, or even relative to cutoff values. Therefore, after visual assessment, CLBP still needs to be quantified. In this regard, one must consider that the CL is surrounded by complex plexuses of tortuous capillaries and small vessels (Macchiarelli et al., 1998), making the correct estimation of its vascularization a major challenge. Different approaches have been proposed to evaluate CLBP, taking into account not only accuracy but also the magnitude of expected differences, the possibility of real-time decisions, and feasibility under field conditions.

The most straightforward way to characterize CLBP is the subjective scoring by the evaluator of the amount of colored area within the Doppler image (Siqueira et al., 2013; Guimarães et al., 2015) (Fig. 1). This approach has the advantage to account for the whole scanning of the tissue, because the score is given based on a mental 3D reconstruction of the organ. Moreover, it allows

real-time diagnosis and rapid decision-making, which is frequently required for a practical use of the technology. As for any other subjective scoring system, it relies on the evaluator's experience and consistency tend to increase over time. The agreement rate between evaluators with similar knowledge of the technology is very high though, and the correlation with objective evaluations is high (Siqueira et al., 2013).

Although the technician can perceive small differences in blood perfusion, the scoring system limits our capacity to discriminate them. In this regard, the accuracy of the diagnosis depends on the expected difference among categories. For instance, CLBP dramatically changes between pregnant and non-pregnant cattle from day 16 after AI onwards (Siqueira et al., 2019), and a subjective score can be effectively used to predict non-pregnant status (Siqueira et al., 2013; Pugliesi et al., 2014). On the other hand, association studies such as those to determine the relationship between CLBP and progesterone (P4) production may require the discrimination of minor changes in CLBP (Herzog et al., 2010; Pugliesi et al., 2019b).

The colored area or the number of colored pixels (RGB value \neq 0) within an image could be objectively measured using internal calipers of the ultrasound device or assisted by an image analysis software (Herzog et al., 2010; Siqueira et al., 2019) (Fig. 2). The results are presented as a continuous variable, expressed as absolute (e.g., mm²) or relative (% of tissue) values. The use of relative indexes is interesting because it takes into account the total volume of tissue supported by a certain amount of blood supply and thus provides a better idea of its physiological status. In fact, Siqueira et al. (2019) obtained a slightly higher area under curve for CLBP adjusted by CL size than for CLBP alone (0.81 vs 0.78, respectively) in the Receiving Operator Curve analysis used to determine the relationships between each CL endpoint and pregnancy status.

Images generated with either color-flow or power Doppler can be used to measure blood perfusion. Depending on the device settings, however, the colored signal in images generated with power Doppler may have blurry edges, compared with those from color Doppler (Fig. 2A and B), thus making it difficult to delimitate a specific-colored area. On the other hand, flow intensity information provided by power Doppler would be more useful than flow direction, typically assessed by color Doppler. Nevertheless, differences in mean pixel color are more complex to analyze and are currently not taken into account in most studies.

For research purposes, the calculation of blood perfusion area can overcome the intrinsic limitations related to score subjectivity and to the lack of statistical power associated with analysis of discrete variables. This approach, however, requires the selection of a representative image frame, which end up creating a certain degree of subjectivity as well. Frequently, this selected image is

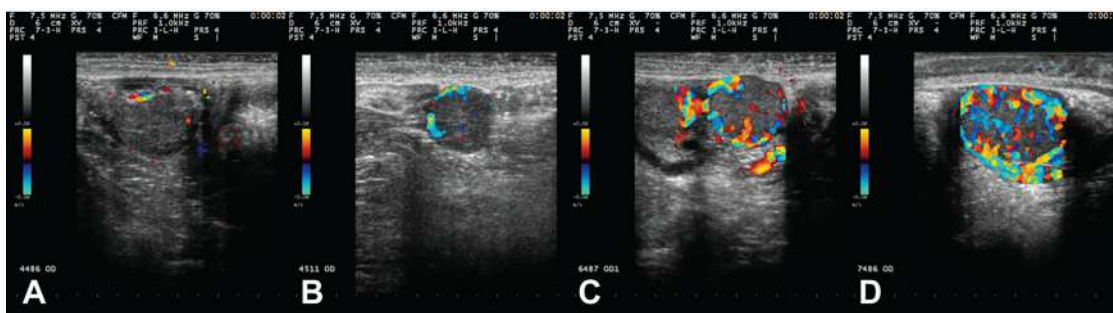


Fig. 1. (A–D) Color-Doppler images of bovine corpora lutea showing different degrees of CLBP (increasing from A to D). Panel A also represents non-pregnant females diagnosed based on the CLBP to detect luteolysis (CL with \leq 25% of blood perfusion and without color signals in the center of the luteal tissue). Panels B, C and D also indicate, respectively, low, medium and high CLBP. Abbreviations: CLBP = corpus luteum blood perfusion; CL = corpus luteum.

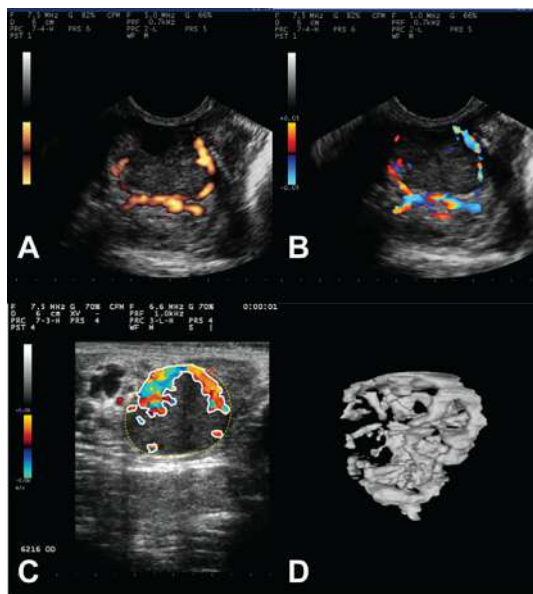


Fig. 2. (A–D) Different approaches to evaluate Doppler images of bovine corpora lutea. (A, B) subjective evaluation of images generated with power- (A) or color-flow (B) Doppler; (C) objective quantification of the colored area within a CL assessed by color-flow imaging. Colored pixels are delimited by a white line and the entire CL area by a yellow-dotted line; (D) Three-dimensional reconstruction of CLBP. Abbreviations: CLBP = corpus luteum blood perfusion; CL = corpus luteum.

arbitrarily defined as the cross-section frame of the central area of the CL at its maximum diameter or the frame with the greater amount of Doppler signal (Viana et al., 2013). Nevertheless, due to the uneven distribution of vascularization around follicles and CL, even minor differences in probe position or angle may cause bias in measurements, as observed for ovarian follicles (Arashiro et al., 2013).

Objective measurement of the color-Doppler signal usually requires postacquisition image processing and analysis. Fortunately, the current trend in biomedical imaging is that computer-assisted image analysis tools will become progressively available as embedded technology in ultrasound devices, allowing real-time diagnosis. In general, single-image analysis does not demand a great computer processing capacity and many software for image analysis, including some license-free or open-source, are widely available.

Volumetry is currently used in internal medicine imaging to measure structures of irregular shape and could be an alternative to assess CLBP. The vascularization of the CL is typically branched and tortuous, and the three- or four-dimensional (3D/4D) reconstruction is likely to provide the best representation of the vascular architecture of the tissue (Viana et al., 2013). In fact, this approach takes into account multiple frames representing the whole organ, while providing an objective measurement of the Doppler signal (Scully et al., 2014). The limitations for the use of volumetry for CLBP evaluation are mostly technological. Ultrasound built-in 3D/4D measurement tools require substantial data processing capacity. In addition, postprocessing image analysis using recorded videoclips is labor-intensive and demand-specific 3D reconstruction software (Viana et al., 2013; Scully et al., 2014). Most 3D/4D ultrasound devices currently available are either too expensive and unsuitable for use in the field or lack processing capacity to avoid image delay and associated distortion due to organ movement during scanning. Nevertheless, technological advances may turn volumetry into an important tool for the study of CL hemodynamics in the future.

Luteal blood perfusion during the estrous cycle and early pregnancy

The CL is a transitory endocrine gland that secretes primarily P4, which is essential for pregnancy establishment in ruminants and other farm animals (Mann and Lamming, 1995). Development of the CL after ovulation is often divided into three main phases: early luteal phase or luteogenesis; mid-luteal or static phase; regression or luteolysis (Niswender et al., 2000). The maternal recognition of pregnancy is associated to the maintenance of a fully functional CL, secreting adequate amounts of P4 to support early embryonic development (Lonergan, 2011).

Due to its transitory nature, the CL must develop physically and functioning very rapidly just so an eventual gestation can be established or, in case of conception failure, a new estrous cycle begins. These particular features of the CL are mainly governed by intense angiogenesis (Acosta and Miyamoto, 2004) for appropriate development of luteal cells during luteogenesis (early luteal phase), and nutrients and steroid precursors delivery to support P4 secretion into the bloodstream (mid-luteal phase). Because of this highly angiogenic and vascular nature of the CL (Fraser and Wulff, 2003), the use of Doppler ultrasonography has become a reliable and useful tool to indirectly assess CL function by imaging blood perfusion into the gland (Bollwein et al., 2016).

In this scenario, color-Doppler flow imaging has long been successfully used to quantify blood flow to the ovaries of ruminants during a regular estrous cycle (Honnens et al., 2008; Herzog et al., 2010). Blood perfusion in the ovary bearing a CL dramatically increases from estrus to mid-cycle (diestrus) in ewes (Niswender et al., 1975), cattle (Herzog et al., 2010) and other species (Miyazaki et al., 1998) followed by a decrease at the end of the estrous cycle (Siqueira et al., 2019). Besides the regular pattern of increase-plateau-decrease blood perfusion during CL development in the estrous cycle, studies have also demonstrated a progressive increase in CLBP in pregnant females (Herzog et al., 2011; Siqueira et al., 2019) perhaps as a consequence of the presence of the conceptus and the secretion of luteotropic factors.

If conception fails, luteolysis takes place and is driven by uterus-borne luteolysins, primarily prostaglandin $F_{2\alpha}$ (Niswender et al., 2000). Some authors have divided luteolysis into two main events: functional luteolysis (loss of function) and structural luteolysis (luteal tissue physical regression). First, the drop in CLBP (Siqueira et al., 2019) almost immediately suppresses P4 production and secretion. Then, luteal cells go into apoptosis, followed by necrosis and tissue remodeling (Pate, 1994). These two major events of the luteolysis process occur at different timepoints, i.e., there is a temporal difference between loss of function (reduction in circulating P4) and CL physical regression (reduction in size) (Siqueira et al., 2009a; 2019). Therefore, CLBP is highly correlated with plasma P4 concentrations, whereas correlations between area of luteal tissue and plasma P4 were not as high during static and regression phases (Herzog et al., 2010). Likewise, circulating P4 is correlated to blood flow to the ovary bearing a CL in cattle (Herzog et al., 2010).

There is strong evidence to support the idea that higher CLBP is positively correlated with an increased odd of successful pregnancy establishment. In a study on vascular and morphological features of the bovine CL, Siqueira et al. (2019) reported a progressive and consistently greater CLBP from day 16 to day 20 after timed-artificial insemination (TAI) in pregnant compared with non-pregnant females. Area of luteal tissue, however, only differed between pregnant and non-pregnant on day 20, at the very end of a normal estrous cycle length. Likewise, other CL characteristics such as circulating P4 and CL echotexture were not good predictors of the odds of getting pregnant. A progressive increase in CLBP

(Herzog et al., 2011) and uterine blood flow in the first weeks of pregnancy (Honnens et al., 2008) have also been previously reported and the latter might be indirectly involved in the increased blood perfusion of the CL-bearing ovary.

Interrelationships among circulating progesterone, luteal tissue area, echotexture, and blood perfusion

The CL development and capacity to produce and secrete P4 rely on the amount of steroidogenic luteal cells (small and large) and the vascular support to provide nutrients and precursors for steroid secretion. Therefore, luteal tissue area not surprisingly has a high, positive correlation with plasma P4, mainly during early diestrus (Niswender et al., 2000; Siqueira et al., 2009a; Scully et al., 2014). During this phase, luteogenesis and CL development are responsible for a gradual increase in P4 secretion and concentration in plasma. At mid-diestrus, CL size (luteal area) achieves its maximum values, followed by a peak in circulating P4 a few days later (Siqueira et al., 2009a).

Extensive angiogenesis and the distribution of luteal cells within the CL are sonographic visualized as a hypoechoic image pattern and changes in this pattern might reflect distinct luteal phases and function (Tom et al., 1998). In this regard, previous studies have investigated the correlations between plasma P4 and quantitative CL echotexture (defined as the patterning of echogenicity). Results were, however, rather inconsistent (Siqueira et al., 2009a; 2019). In general, it seems that pixel brightness (mean pixel value) within CL tissue has limited value for inferences about CL function (plasma P4 secretion). In contrast, the variation in pixel brightness within the luteal tissue, i.e., pixel heterogeneity, appears to be a good indicator of luteal function and has a fair-to-high correlation with plasma P4 during luteolysis (Siqueira et al., 2009a). In other words, an ultrasonic image of a heterogeneous luteal tissue is often observed in early luteal phase (metestrus) and after onset of luteolysis, reflecting the ongoing organization (metestrus) or disorganization (luteolysis) of the CL itself (luteal cells, connective tissue, and blood vessels). An ultrasound image with low pixel heterogeneity values, however, is observed during diestrus, concomitantly with a high-circulating P4 scenario, evidence of a homogeneous luteal tissue mostly covered by small and large luteal steroid-secreting cells (Niswender et al., 2000).

Use for early detection of pregnancy status

Ultrasound-based pregnancy diagnosis is usually performed by B-mode and only recommended after 28–30 days of pregnancy (Pieterse et al., 1990), as at this period, the accuracy in conceptus visualization reaches 100% (Nation et al., 2003). Yet, the detection of spontaneous CL regression by ultrasound in non-pregnant cows could allow an earlier assessment of gestational status (Pugliesi et al., 2013; Pugliesi et al., 2014; Scully et al., 2014; 2015; Siqueira et al., 2019).

Evaluation of CL size has been used with high accuracy to identify non-pregnant cattle between after day 20 of gestation (Kastelic et al., 1991), but plasma/serum P4 concentrations have a greater correlation with CLBP than CL size during the luteolytic period in ruminants (Herzog et al., 2010; Balaro et al., 2017; Rocha et al., 2019). This indicates that a decrease in CLBP occurs prior to structural luteolysis and has been observed as early as day 16 after TAI in dairy cows and heifers (Siqueira et al., 2019). Also, a considerable rate of false negative results is observed when using only CL area for detection of luteolysis in non-pregnant beef cows, as some animals have a small but functional CL for pregnancy maintenance (Pugliesi et al., 2018).

To our knowledge, the first attempt to diagnosis pregnancy by luteolysis detection using Doppler imaging was reported by Utt et al. (2009) in beef recipient cows; however, the method used to determine CLBP was time-consuming and resulted in low accuracy (Table 1). Thus, more in-depth studies during spontaneous luteolysis characterized the CLBP changes between pregnant and non-pregnant cows (Matsui and Miyamoto, 2009; Pugliesi et al., 2014). The results allowed the definition of CLBP during luteolysis and served as a basis in pioneered investigations in dairy (Siqueira et al., 2013) and beef (Pugliesi et al., 2014) for the conception of applied criteria to identify a functional or non-functional CL at early pregnancy. In dairy females, a high accuracy and negative predictive value (NPV) was obtained by Siqueira et al. (2013) at 20 days post-TAI using only CLBP. In beef cows, 91% accuracy and 100% NPV were obtained to determine pregnancy status on day 20 post-TAI (Pugliesi et al., 2014). Although different definitions were used to identify a non-functional CL in these studies, the criteria are similar to detect non-pregnant females and the early diagnoses were compared with the gold standard method on day 30 of pregnancy. Both methods use a subjective and real-time evaluation (Fig. 1) that is simpler and more practical than using pixels counting to determine colored area and classify the CL as functional or not (Pugliesi et al., 2018).

Because these methods do not allow visualization of the embryo, one can state that color-Doppler ultrasound technique allows the detection of luteolysis for early indirect identification/diagnosis of non-pregnant females. Other studies (Table 1) were performed in different breeds and parity classes and confirmed a high accuracy and null or extremely low rate of false negative results using the proposed cut-offs in dairy and beef cattle. Altogether, these outcomes support that determination of CLBP is an accurate diagnosis method for detection of pregnancy status, as there is a low likelihood of incorrectly detecting a pregnant female as non-pregnant, resulting in high NPV when applied after 19 days of pregnancy.

Nonetheless, proportion of false-positive (FP) results (cows diagnosed as pregnant by Doppler, but actually not confirmed as pregnant by the gold standard diagnosis) is the main factor differing among the studies (Table 1). The FP results may occur due to different reasons that result in the presence of an active CL on the day of CLBP-based diagnosis. Late ovulation in timed-programs and variations in time of physiological luteolysis among breeds and parity order are possible explanations, but the greatest part to blame for FP is apparently related to the rate of early embryonic loss between the Doppler and the confirmatory diagnosis. More recently, different studies in Nelore (Dalmaso de Melo et al., 2020), *Bos taurus* beef (Holton et al., 2022a; 2022b) and Holstein (Madoz et al., 2022) females have indicated by evaluating the expression of interferon-stimulated genes in circulating immune cells and/or pregnancy-associated proteins, that at least one third of the FP results are occurring due to early embryonic loss between days 19/20 and 30–34 of pregnancy. Collectively, these results indicate that most FP results are probably a result of prolonged luteal phase rather than embryonic mortality beyond maternal recognition of pregnancy. This is supported by the rate of 10–15% of Nelore heifers and cows synchronized for TAI, but not inseminated, that did not undergo luteolysis up to 22 days after arbitrary estrus (Ataíde et al., 2021).

In addition, it is noteworthy that no significant differences in CLBP on days 20 and 22 were observed between females diagnosed as true positive and FP (Holton et al., 2022a), but CLBP and plasma P4 concentrations on day 20 were lesser in females with indicative of embryonic mortality between days 20 and 25 of pregnancy (Dalmaso de Melo et al., 2020). Also, we performed a recent analysis (unpublished; Fig. 3) which indicates that the proportion of CLBP at day 20 is negatively associated with the rate of FP results.

Table 1

Studies comparing the use of Doppler ultrasonography to detect luteal function for diagnosis of pregnancy status between day 17 and day 22 and the B-mode ultrasonography for detection of embryo after day 28 of pregnancy in beef and dairy cows and heifers.

Authors	Type/breed	Parity order	Type of service	Moment of gestation, d	Animals, n	Conception rate, %	Accuracy, %	False positive, % (total)	False negative, % (total)	PPV, %	NPV, %
Utt et al., 2009	Beef (Crossbreed)	Cows	TET	17	50	46	60	30.6	9.4	54.4	73.3
				19		68.8	24.6	61.4	82.9		
				21		71.4	21	64.8	81.5		
Siqueira et al., 2013	Dairy (Holstein-Gir)	Parous cows	TAI	20	317	46.1	74.6	24.6	0.7	64.8	97.7
		Heifers		209	47.4	76.6	22.7	0.6	67.2	98	
Pugliesi et al., 2014	Beef (Nelore)	Parous cows	TAI	20	111	37.8	91	9	0	80.8	100
Guimarães et al., 2015	Beef (Nelore)	Parous cows	TET	21	163	43.6	88.3	11.7	0	78.9	100
Scully et al., 2014 ¹	Dairy (<i>Bos taurus</i>)	Parous cows	AI after estrus	18	80	52.8	68.1	20.9	11.1	66.6	70.3
				19	80	56.8	82.4	13.5	4.1	79.5	88
				20	90	42.2	77.7	17.3	4.9	70.8	87.8
				21	94	45.2	87.1	11.8	1.1	78.8	97.5
				22	246	49.6	94.7	5.3	0	90.4	100
Pugliesi et al., 2018	Beef (Nelore)	Parous cows	TAI	22	231	41.6	90	10	0	80.5	100
		Heifers		221	35.5	83.8	16.2	0	68.8	100	
Ataíde et al., 2018	Beef (Nelore)	Parous cows	TET	22	221	35.5	83.8	16.2	0	68.8	100
Andrade et al., 2019	Beef (Nelore)	Heifers	TAI	21	113	–	87.8	12.2	0	77.3	100
Dalmaso de Melo et al., 2020	Beef (Nelore)	Parous cows	TAI	20	144	58	93	7	0	89	100
		Heifers		100	52	88.3	11.7	0	81.8	100	
Wellert et al., 2020	Beef (Angus-cross)	Parous cows	TAI	21	84	–	–	–	0	89.4	100
		Heifers		25	–	–	–	0	75	100	
Dubuc et al., 2020	Dairy (Holstein)	Parous cows	AI	21	1 632	22	62.1	37.5	0.4	52	98.1
Holton et al., 2022a	Beef (<i>Bos taurus</i>)	Parous cows	TAI	20	208	52.9	87	13	0	80	100
				22	209	52.6	92	8	0	85	100
Holton et al., 2022b	Beef (<i>Bos taurus</i>)	Heifers	TAI	20	183	–	90	10	0	86	100
				22	–	–	92	8	0	90	100
Madoz et al., 2022	Dairy (Holstein)	Parous cows	TAI	19/20	131	37.4	74.8	24.5	0.7	60	98.2
Ferraz et al., 2022	Dairy (Holstein)	Parous cows	TAI	21	140	28.6	53	46.3	0.7	38	98
		Heifers		32	31.3	66	34	0	48	100	

Abbreviations: PPV = positive predictive value; NPV = negative predictive value; TET = timed-embryo transfer; TAI = timed-artificial insemination; AI = artificial insemination.

¹ This study also considered the uterine echotexture and corpus luteum size as additional criteria to the luteal blood perfusion for diagnosis of non-pregnant animals.

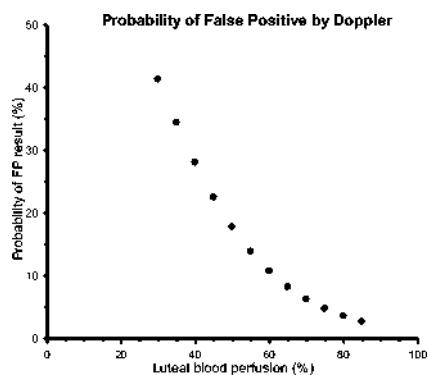


Fig. 3. Probability of false-positive result (females identified with a functional CL on day 20 post-TAI by Doppler ultrasonography, but non-pregnant on day 30) according to the CLBP at the Doppler evaluation in beef cattle ($n = 159$). Probability of FP = $\exp(-0.0591x + 1.4201)/1 + \exp(-0.0591x + 1.4201)$; $P = 0.008$. Abbreviations: CLBP = corpus luteum blood perfusion; CL = corpus luteum; FP = false positive; TAI = timed-artificial insemination.

So, the probability to have a FP result is greater than 25% in females with $\leq 40\%$ of CLBP, and less than 5% in females with $\geq 75\%$ of CLBP at time of pregnancy diagnosis.

By comparing the results related to accuracy in the different studies (Table 1), it is possible to observe a greater FP rate and lesser positive predictive value and accuracy in dairy compared with beef cattle, in which pregnancy losses are normally lower, but other factors may be also involved as moment of ovulation after TAI and time of luteolysis (Reese et al., 2020). On the other hand, an influence of parity (nulliparous vs multiparous) on FP rate seems to occur only in beef animals. In dairy, FP rates did not differ between lactating cows and heifers (Siqueira et al., 2013; Ferraz et al., 2022) whereas in beef, studies (Dalmaso de Melo et al., 2020; Holton et al., 2022a) reported increased FP rate and reduced accuracy in heifers compared with suckled cows. At least in *Bos indicus* beef animals, this difference is probably caused by a postponed spontaneous luteolysis in Nelore heifers than in suckled cows (Ataide et al., 2021).

Although there are well-known intrinsic differences in ovarian physiology between *B. indicus* and *B. taurus* females (Sartori et al., 2016), the accuracies of pregnancy diagnosis by Doppler on days 20 and 22 post-TAI in *Bos taurus* beef cattle (87 and 92%, respectively; Holton et al., 2022a), were similar to those observed in *B. indicus* (Dalmaso de Melo et al., 2020). Finally, it is important to note that the accuracy increases over time after service (Pugliesi et al., 2014; Scully et al., 2015; Siqueira et al., 2019), mainly because a greater proportion of non-pregnant cows are detected around luteolysis. In this regard, Holton et al. (2022a) reported a 40% reduction in FP rate when the diagnosis was performed on day 22 compared with day 20 post-TAI in beef cows. In general,

studies have indicated that non-pregnancy diagnosis based on CLBP is a feasible and accurate method only when performed after day 20 of pregnancy in cattle.

In small ruminants, the subjective CLBP assessment using color-Doppler ultrasonography to distinguish pregnant and non-pregnant animals also resulted in high accuracy ($>85\%$) and 100% of NPV (Arashiro et al., 2018; Cosentino et al., 2018). In goats, Cosentino et al. (2018) demonstrated that pregnancy diagnosis could be accurately performed beginning 21 days postbreeding. In ewes, the luteolytic period is earlier than goats and cows, and subjective CLBP assessment was considered a highly efficient method as early as 17 days after breeding (Arashiro et al., 2018).

In most studies, inferences about CL functional status and prediction of non-pregnancy were based on the quantification of the colored area within the CL Doppler image. In this regard, differences in settings of the ultrasound device that changes the amount of signal displayed as colored pixels can potentially affect accuracy of a given exam by increasing the proportion of FP or FN. During B-mode ultrasonography, most settings (transducer frequency, overall gain, gray-scale curve) can be intuitively adjusted by an experienced examiner to obtain a clear image. Moreover, although echotexture attributes such as mean pixel value or pixel heterogeneity can be used to evaluate the CL (Siqueira et al., 2009a), in routine gynecologic exams, most inferences on CL function are based only on its presence or size (area or diameter). Thus, small differences in B-mode image settings are less likely to interfere on the interpretation of scanning.

On the other hand, changes in color-Doppler settings might have a deeper impact on exam accuracy. The pulse repetition frequency (PRF) is of particular importance, as it defines the capacity of the device to display the Doppler signal. The higher the PRF, the lesser the signal displayed as colored areas in the image (Fig. 4). Yet, the use of a very low PRF (and thus set to a high sensitivity scenario) may increase the chance of occurring flash artifacts due to minor movements during scanning, such as those caused by breathing (Fig. 5).

In a recent study (unpublished data), we scanned cows 20 days after TAI and recorded three images of each CL using PRF values of 0.7, 1.0, and 1.5 KHz, respectively. The stored images were later used to predict non-pregnant status by a second evaluator who was blinded of the differences in PRF and the fact that more than one image referred to the same cow. Results were compared to those of pregnancy diagnosis at day 30, as previously described (Siqueira et al., 2013). As expected, reducing PRF from 1.0 to 0.7 KHz (and thus increasing the colored area in the image) decreased PPV and specificity (79.2 and 72.2% vs 67.9 and 50.0%, respectively), whereas increasing PRF from 1.0 to 1.4 KHz decreased NPV and sensitivity (100 and 100% vs 81.3 and 84.2%, respectively). These results demonstrate that minor differences on Doppler settings may lead to image misinterpretation and, thus, the accuracy of non-pregnancy diagnosis based on color-Doppler evaluation of

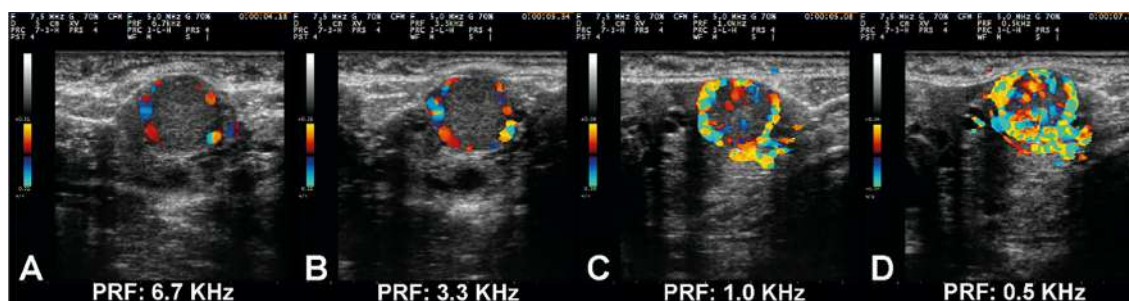


Fig. 4. (A–D) Color-Doppler images of the same bovine CL generated using decreasing PRF values. (A) PRF set at 6.7 KHz, (B) PRF set at 3.3 KHz, (C) PRF set at 1.0 KHz, (D) PRF set at 0.5 KHz. Abbreviations: CL = corpus luteum; PRF = pulse repetition frequency.

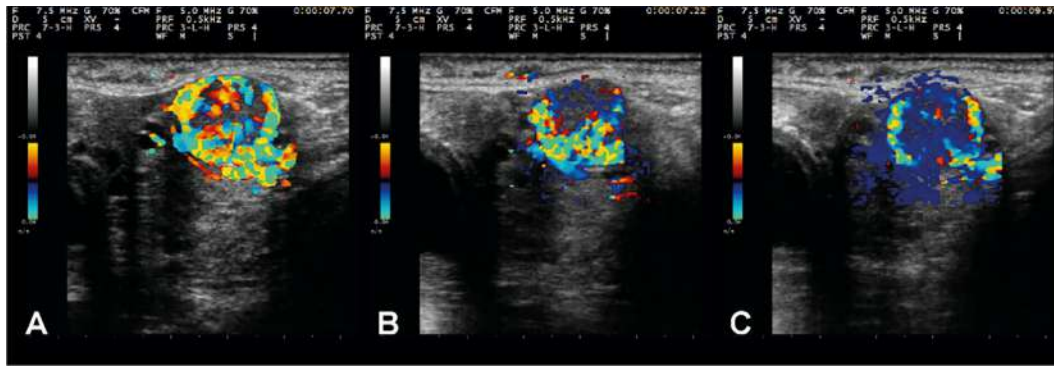


Fig. 5. (A–C) Effect of movement during acquisition of an image of a bovine CL using color-Doppler set to low (0.5 KHz) PRF value. (A) Image without flash artifacts, (B) Image with minor artifacts, (C) Image with major artifacts. Abbreviations: CL = corpus luteum; PRF = pulse repetition frequency.

CLBP requires the use of consistent standard settings throughout exams.

Application in fixed-time programs in cattle

Resynchronization protocols provide a chance for a second round of TAI or timed-embryo transfer (TET) and may increase the reproductive efficiency of beef and dairy cattle (Baruselli et al., 2017). Due to the high efficiency of detecting non-pregnant females earlier by using Doppler imaging, new resynchronization protocols for the anticipation of the second TAI or TET were developed (Pugliesi et al., 2018). Therefore, it is possible to perform two TAIs or TETs within 22–24 days compared with 40 or 32 days when using the conventional or early resynchronization protocols, respectively (Fig. 6). For this, the so-called super-early resynchronization protocols must begin in all females between 12 and 18 days after TAI or estrus, regardless of gestational status. Alternatively, CLBP evaluation can be performed to resynchronize only females without an active CL. In this regard, (Guimarães et al., 2015) performed the detection of non-pregnant recipients by

Doppler on day 21 after previous estrus (14 days after TET) and obtained 79.3% of non-pregnant animals resynchronized earlier than the conventional management.

The onset of the super-early resynchronization protocol may vary according to the time of Doppler exam and duration of the protocol, but it usually precedes the period of maternal recognition of pregnancy (days 12–17 after estrus). Thus, the association of drugs used for these protocols must not jeopardize the ongoing pregnancy. Considering that estradiol is involved in CL regression (Araujo et al., 2009), administration of exogenous estradiol esters in the second week of pregnancy is controversial. Initial studies comparing the use of estradiol to resynchronize bovine females from the second week postbreeding had varying results according to parity, type (dairy or beef), breed, dose, and time of treatment (El-Zarkouny and Stevenson, 2004; Colazo et al., 2006; Machado et al., 2008). In the first study to evaluate the association of super-early resynchronization and Doppler diagnosis, a negative effect on pregnancy rate was observed in cows receiving 1.5 mg estradiol benzoate (EB) on day 13 post-TAI (Vieira et al., 2014). On the other hand, negative effects on pregnancy rates were not

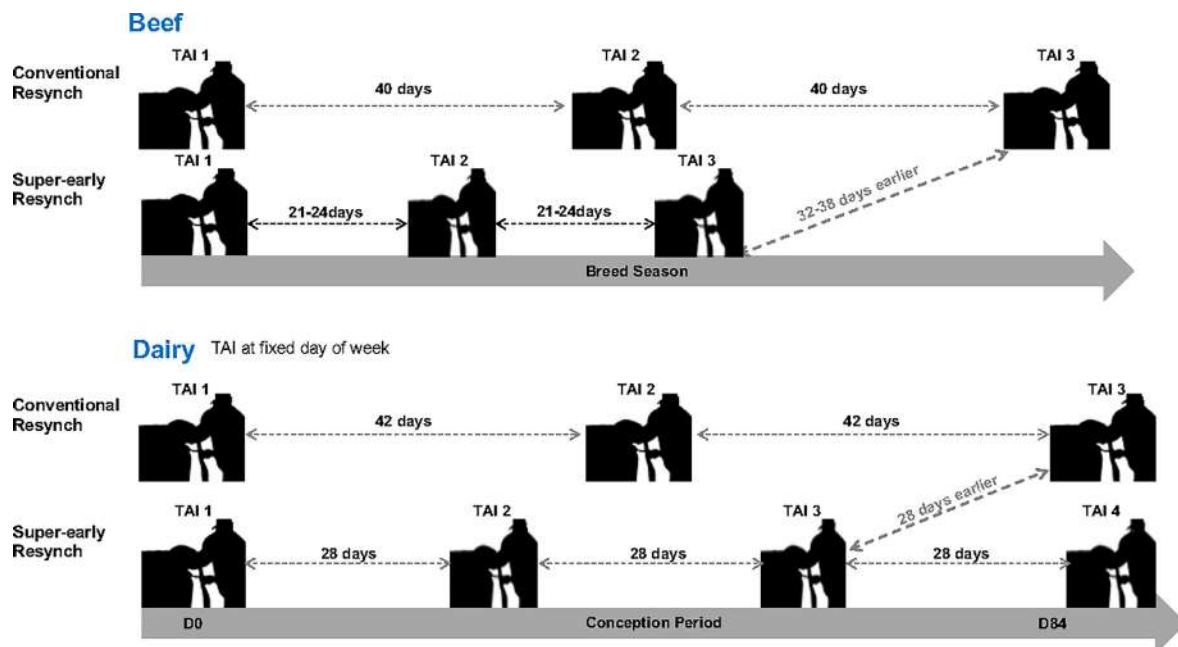


Fig. 6. Schematic illustration of the super-early resynchronization strategy compared to the conventional resynchronization in TAI programs in beef and dairy cattle. In dairy, the TAI is usually performed on the same day of week. Super-early resynchronization may start 12–15 days after TAI in beef and 17–19 days after TAI in dairy, resulting in an interval between TAIs of 21–24 days in beef and 28 days in dairy cattle. Conventional resynchronization is performed after pregnancy diagnosis on days 28–32 of pregnancy, resulting in an interval of 40–42 days in beef and dairy herds. Abbreviations: TAI = timed-artificial insemination; Resynch = resynchronization.

observed when EB treatment (1 mg) was administered 13 days after first TAI in beef cows (Stevenson et al., 2003) or lactating dairy cattle (El-Zarkouny and Stevenson, 2004). Therefore, our group and others have been dedicated to develop different strategies for super-early resynchronization protocols without using EB or limiting its use to a maximal dose of 1 mg.

In beef cattle, initial studies were carried out in heifers to evaluate the use of 1 mg EB (Motta et al., 2020) and to compare with the administration of injectable P4 (Vieira et al., 2021) in the resynchronization protocols initiated 14 days after TAI. In both studies, the Doppler diagnosis for evaluation of CLBP was performed on Day 22 and heifers diagnosed as non-pregnant were re-inseminated on Day 24 after first TAI. Although Motta et al. (2020) reported that the additional treatment with estradiol or EB associated with a P4 device anticipated luteolysis in non-pregnant heifers, no difference was observed in pregnancy rates from first TAI among experimental groups. This indicated that there is no harmful effect on the pre-existing pregnancy when using 1 mg EB or estradiol in *Bos indicus* and crossbred heifers. In fact, the additional treatment with 1 mg EB 14 days post-TAI resulted in greater pregnancy rates (Motta et al., 2020; Vieira et al., 2021). Vieira et al. (2021) compared pregnancy rates in beef heifers resynchronized 14 days after the first TAI using a P4 intravaginal device associated with either long-acting P4 or 1 mg EB, and observed that the EB treatment resulted in greater resynchronization pregnancy rates than injectable P4 treatment.

In agreement with what has been observed for beef heifers, Palhão et al. (2020) reported that the use of 1 mg EB to resynchronize suckled beef cows on Day 13 post-TAI did not compromise pregnancy rate to first TAI. However, Silva et al. (2022) compared the use of 1 or 2 mg EB 14 days after TAI and reported a reduction in pregnancy rate at first TAI in *Bos indicus* beef cows resynchronized with 2 mg EB. Furthermore, cows receiving 2 mg EB had a two-fold greater risk of early pregnancy loss compared with cows that received 1 mg EB. Together, these studies indicate that the use of 1 mg EB associated with a P4 device is safe and efficient for super-early resynchronization of beef heifers and suckled beef cows.

Because of the controversial results of the first studies using estradiol or EB, alternatives were also concomitant investigated. Thus, considering that high plasma P4 concentrations have a potential inhibiting effect on the growth of luteinizing hormone- and follicle-stimulating hormone-dependent follicles in cattle (Cavaliere, 2018), the effects of short-acting or long-acting injectable P4 at different doses have been evaluated for super-early resynchronization in heifers and cows (Pugliesi et al., 2019a; Ataíde et al., 2021). Studies comparing the use or not of the additional treatment with injectable P4 at doses greater than 75 mg indicated a positive effect on conception rates of resynchronized beef cows and heifers (Pugliesi et al., 2019a; Ataíde et al., 2021). In Pugliesi et al. (2019a), the interval between the first and second TAI was only 22 days and resulted in a 75% pregnancy rate after two TAIs. In Ataíde et al. (2018), Nelore beef females were submitted to two consecutive resynchronizations, allowing three TAIs in 48 days, and the cumulative pregnancy rate reached 83.3%. Thus, the treatment with injectable P4 in its different presentations for super-early resynchronization offers the potential to increase pregnancy outcomes.

In *Bos indicus* beef cattle, where postpartum anestrus is a great issue, super-early resynchronization may have a greater impact on reproductive performance compared to *Bos taurus* beef breeds. The implementation of super-early resynchronization protocols has the potential to increase the number of cows becoming pregnant within the first month of the breeding season, as it allows for two services (TAI or TET) at 21- to 24-day intervals. In this regard, Ojeda-Rojas et al. (2021) compared using a simulation model dif-

ferent types of resynchronization strategies in *Bos indicus* beef cattle and reported that the scenario of two TAIs within a 24-day interval represents the reproductive program with the best technical performance. Moreover, three TAIs at a 24-day interval lead to a greater number of births early in the calving season and heavier calves at weaning, when compared with only natural mating or other resynchronization strategies (Ojeda-Rojas et al., 2021). Considering that this result was based on a model rather than an actual controlled study, further studies for investigation of impact of super-early resynchronization on the calving distribution are encouraged. In a preliminary study using controlled data (unpublished) obtained from two consecutive breeding seasons with the same group of Nelore females, we have also observed an earlier calving after using three TAIs at a 24-day interval. A 43% increase in births at the first month of calving season (218 vs 152 births) and 9% increase in total number of calves born (394 vs 361 calves) were observed after the super-early resynchronization was adopted compared to previous season using only TAI and cleanup bulls. In addition, a retrospective analysis in order to evaluate calving distribution indicated that calves born in the first three weeks of birth season were ~22 kg heavier than those born in the last three weeks.

In dairy cattle, investigations on super-early resynchronization protocols have been scarcer when compared with beef cattle. One of the factors that contributes for the reduced number of studies in dairy and the application of these protocols is the fit of a Doppler diagnosis into the schedule of weekly reproductive management visits by the veterinarian in dairy operations (Fig. 6). Another factor to be considered for the development of resynchronization protocols for dairy cattle was the greater proportion of FP results reported in all studies, mainly for lactating dairy cows (Siqueira et al., 2013). Nevertheless, a recent study by our group (Neto et al., 2022) reported that starting resynchronization 17 days after TAI increases pregnancy rate within the first 84 days after the end of the voluntary waiting period compared, with the traditional resynchronization starting 31 days after TAI in dairy cows. Also, the use of 1 mg EB associated with a P4 device at the onset of the protocol did not impact pregnancy from first TAI and reduces by half the proportion of FP results (cows with functional CL at 24 days after previous TAI). The association of a low EB dose given at a later timepoint relative to the period of maternal recognition of pregnancy, as performed by Neto et al. (2022) and Freitas et al. (2022) on 17–19 days after TAI, may have an even lower risk to harm a pre-existing pregnancy due to greater conceptus' signaling to maintain the CL active at this period. In countries where estradiol drugs are not allowed, the super-early resynchronization can be performed using only the P4 device or the P4 device associated to injectable P4 (if allowed), but conception rates are approximately 12% less when EB or injectable P4 is not used to synchronize follicular wave emergence.

Use of Doppler for recipient selection

A correct selection of eligible recipients is one of the leading objectives for an embryo transfer program in cattle. Among the several characteristics of the reproductive tract, the presence of an evident, active CL is considered one of the most important factors to determine whether a healthy recipient should be used to reach a high likelihood of pregnancy (Phillips and Jahnke, 2016). Usually, luteal size is assessed by palpation or by gray-scale ultrasonography per rectum and a larger CL is preferable over a smaller CL. Picking recipients founded only on CL size may result in transfer of embryos to recipients with a non-adequate uterine environment associated to less functional CL (Pinaffi et al., 2015).

Indeed, a pioneered study in cattle (Pinaffi et al., 2015) classifying recipient cows as having low ($\leq 40\%$) or high ($>40\%$) CLBP at the time of embryo transfer (day 7) indicated a significant greater pregnancy rate in those with high CLBP compared with low CLBP (48% vs 0%). In agreement, CLBP on the day of embryo transfer was greater in pregnant than non-pregnant Holstein recipients (Kanazawa et al., 2016). But, the CLBP was determined in this later report based on the area of CLBP and the time-averaged maximum velocity at the base of the spiral artery, which have low applicability in large-scale operations since they are time-consuming.

In this regard, we have studied (Pugliesi et al., 2019b) the association between CL characteristics assessed by ultrasonography at the time of embryo transfer and pregnancy rate in beef recipients, using real-time evaluations to determine CLBP. In this study, we used the two most practical approaches to subjectively evaluate CLBP (i.e., estimation of the proportion of tissue with colored signals [0–100%] and a scoring system (depicted in Fig. 1)). Thus, beef recipients ($n = 444$) were retrospectively divided into three subgroups according to CL area and three subgroups based on CLBP [low ($\leq 40\%$), medium (45–50%) or high ($\geq 55\%$)]. Results indicated that CLBP determined by color-Doppler ultrasonography was the most important factor evaluated at embryo transfer that affected pregnancy outcome. Our results demonstrated a positive and linear association between the proportion of CLBP and pregnancy outcomes in synchronized beef recipients. Latter studies (Aragon et al., 2018; Munhoz et al., 2018; Silva et al., 2018) have also evaluated CLBP using different real-time criteria. Although not significant, pregnancy rates per embryo transfer in recipients classified as presenting high/excellent CLBP were approximately 1.26–2.33-fold greater compared with those females with low/bad CLBP in Holstein cows (42 vs 18%; Aragon et al., 2018), Holstein-Gir cows and heifers (51.8 vs 33%; Munhoz et al., 2018) and Angus heifers (60.6 vs 48.1%; Silva et al., 2018).

Consistent with the results in cattle, our group (Morelli et al., 2022) recently detected that CLBP in recipient mares was the only luteal sonographic characteristic that affected pregnancy establishment after transfer of *in vivo* equine embryos (low CLBP: 65.5% [38/58] vs high CLBP: 88.4% [38/43]). This also reflected a progressive increase in the pregnancy rate associated with increased CLBP. In addition, in buffalo, pregnancy rates were 2.5-fold greater in recipients with high CLBP ($\geq 50\%$) than those with low CLBP ($<50\%$) at the time of embryo transfer (Silva et al., 2018). This indicated that CLBP could be used as a main criterion to select highly receptive recipients for different large animal species.

Considering that the number of recipients at the time of embryo transfer in fixed-time programs in cattle is limited and usually lesser than the number of embryos, one strategy for using Doppler in recipient selection is rejecting females with a non-functional yet palpable CL. This represented 9.5% of the females bearing a CL at time of embryo transfer (Pugliesi et al., 2019b). In addition, if an excessive number of recipients were available, CLBP evaluation could be used to prioritize the transfer of embryos only into recipients with medium or high CLBP ($>40\%$). Consequently, embryos would not be transferred to females with a non- or sub-functional CL identified by Doppler imaging (Pugliesi et al., 2019b). Alternatively, embryos of high generic merit could be rather transferred in recipients ranked by high CLBP.

Although all the studies have been pointing to the same positive effect of CLBP on pregnancy rates in recipients, the mechanisms associated with this effect to favor pregnancy establishment are still not fully understood. The hypothesis that high CLBP could be associated with embryotropic effects of circulating P4 during embryo development seems not to be supported by results of recent studies, because correlations with circulating P4 are weak for CLBP and moderate or strong for luteal size at early diestrus (Rocha et al., 2019). In addition, Siqueira et al. (2009a and

2009b) and Chagas e Silva et al. (2002) observed that circulating P4 concentrations on the day of embryo transfer are of limited practical use for recipient selection in dairy and beef cattle. Alternatively, an increased CLBP could be associated with a greater resistance of the CL to undergo regression or with a greater vascularization to the reproductive tract. These alternative hypotheses, however, still remain to be investigated in further studies for a better understanding of the mechanisms involved in the positive effects of CLBP on pregnancy establishment in cattle.

Final considerations

Along the last decades, the cumulative knowledge about CLBP determined by color-Doppler ultrasonography indicated that this luteal characteristic is a practical and real-time tool to evaluate CL function. Based on the high correlations between circulating P4 vs CLBP compared with P4 vs CL size, the evaluation of CLBP during the phase of luteal regression has been used to anticipate the detection of non-pregnant cattle in TAI and TET programs. Several studies have used a subjective and real-time evaluation of CLBP in beef and dairy cattle. This method has shown a high accuracy and low or near to zero false negative results and, consequently, very high NPV. In beef females, when the diagnosis is performed 20–22 days post-TAI, the accuracy compared with the gold standard diagnosis on the 30th day of gestation exceeded 90%.

Although CLBP assessment can detect non-pregnant females, CL function is not a specific biomarker of pregnancy; therefore, a considerable percentage of false-positive results (12–30%) may occur, mainly in dairy cows and heifers. The detection of non-pregnancy by evaluation of CLBP earlier than the conventional methods (visualization of embryo and heartbeat) allowed for the development of new strategies of resynchronization of ovulation in a super-early manner, resulting in the possibility of two services (TAI or TET) within a 22- to 24-day interval. It is worth mentioning that such methods to evaluate CLBP and their practical applications boosted the commercial use of Doppler ultrasound for early detection of non-pregnant bovine females in an unprecedented and pioneering way in South America, mainly in Brazil. Finally, a greater CLBP at the day of embryo transfer in prospective pregnant females and other findings indicating that CLBP may be a better indicator of luteal activity in studies in cattle and horses suggest that evaluation of CLBP at embryo transfer is a more valuable information to estimate the probability of pregnancy success than systemic P4 concentrations in embryo recipients. It is noteworthy, however, that in order to obtain these great advances, training and understanding of the imaging principles and equipment is required, because the device's settings must be properly regulated and the operator very well prepared to carry out the assessments correctly.

Ethics approval

The authors did not use any live animal to conduct this review.

Data and model availability statement

Data or models were not deposited in an official repository. No new datasets were created.

Author ORCIDs

Guilherme Pugliesi: <https://orcid.org/0000-0001-5739-0677>.

Amanda Guimarães Silva: <https://orcid.org/0000-0003-0918-4208>.

Joao H. M. Viana: <https://orcid.org/0000-0002-3742-2368>.

Luiz Gustavo B. Siqueira: <https://orcid.org/0000-0002-2800-5829>.

Author contributions

Guilherme Pugliesi: conceptualization, writing original draft, review and editing.

Amanda Guimarães Silva: writing original draft, review and editing.

Joao H. M. Viana: conceptualization, writing original draft and editing.

Luiz Gustavo B. Siqueira: conceptualization, writing original draft and editing.

Declaration of interest

The authors have declared that no conflict of interest exists.

Acknowledgements

None.

Financial support statement

This work is supported by the funding agencies: São Paulo Research Foundation (FAPESP), the National Council of Technological and Scientific Development (CNPq) Project 422372/2018-8, and the Coordination for the Improvement of Higher Education Personnel – Brazil (CAPES).

Transparency Declaration

This article is part of a supplement entitled Keynote lectures from the 11th International Ruminant Reproduction Symposium supported by the British Society of Animal Science.

References

- Acosta, T.J., Miyamoto, A., 2004. Vascular control of ovarian function: Ovulation, corpus luteum formation and regression. *Animal Reproduction Science* 82–83, 127–140. <https://doi.org/10.1016/j.anireprosci.2004.04.022>.
- Andrade, J.P.N., Andrade, F.S., Guerson, Y.B., Domingues, R.R., Gomez-León, V.E., Cunha, T.O., Jacob, J.C.F., Sales, J.N., Martins, J.P.N., Mello, M.R.B., 2019. Early pregnancy diagnosis at 21 days post artificial insemination using corpus luteum vascular perfusion compared to corpus luteum diameter and/or echogenicity in Nelore heifers. *Animal Reproduction Science* 209. <https://doi.org/10.1016/j.anireprosci.2019.106144>.
- Aragón, F.A.L.F., Rezende, R.G., Soriano, S., Sica, A.F., Abreu, L., Mingoti, R., Elliff, F.M., Zanatta, G., Baruselli, P.S., 2018. Factors that affect the conception rate to FTET of Holstein recipients evaluated by Color Doppler ultrasound. *Animal Reproduction (Abstract)* 15, 351.
- Arashiro, E.K.N., Palhao, M.P., Santos, J.R.L., Fontes, R.C., Siqueira, L.G.B., Henry, M., Viana, J.H.M., 2013. Three-dimensional modeling of color Doppler images: a new approach to study follicular vascularization in cattle. *Animal Reproduction* 10, 662–669.
- Arashiro, E.K.N., Ungerfeld, R., Clariget, R.P., Pinto, P.H.N., Balaro, M.F.A., Bragança, G. M., Ribeiro, L.S., da Fonseca, J.F., Brandão, F.Z., 2018. Early pregnancy diagnosis in ewes by subjective assessment of luteal vascularisation using colour Doppler ultrasonography. *Theriogenology* 106, 247–252. <https://doi.org/10.1016/j.theriogenology.2017.10.029>.
- Araujo, R.R., Ginther, O.J., Ferreira, J.C., Palhao, M.M., Beg, M.A., Wiltbank, M.C., 2009. Role of follicular estradiol-17beta in timing of luteolysis in heifers. *Biology of Reproduction* 81, 426–437. <https://doi.org/10.1095/biolreprod.108.073825>.
- Ataide, G.A., Pellegrino, C.A.G., Claro Jr, I., Meneghetti, M., Grázia, J.G., Góis, A.C.N., Gonçalves, F., Torres, F., Vasconcelos, J.L.M., Pugliesi, G., 2018. Eficácia da Ultrassonografia Doppler para detecção de não prenhez em vacas de corte receptoras. In: Proceedings of the 32nd Annual Meeting of the Brazilian Embryo Technology Society (SBTE), August 16th to 18th, 2018, Florianópolis, SC, Brazil, pp. 177–178.
- Ataide, G.A., Kloster, A., Moraes, É.G., Motta, I.G., Junior, I.C., Vasconcelos, L.M., Assis, P., Paula, G.D., Pugliesi, G., 2021. Early resynchronization of follicular wave emergence among Nelore cattle using injectable and intravaginal progesterone for three timed artificial inseminations. *Animal Reproduction Science* 229. <https://doi.org/10.1016/j.anireprosci.2021.106759> 106759.
- Balaro, M.F.A., Santos, A.S., Moura, L.F.G.M., Fonseca, J.F., Brandão, F.Z., 2017. Luteal dynamic and functionality assessment in dairy goats by luteal blood flow, luteal biometry, and hormonal assay. *Theriogenology* 95, 118–126. <https://doi.org/10.1016/j.theriogenology.2017.02.021>.
- Baruselli, P.S., Ferreira, R.M., Colli, M.H.A., Elliff, F.M., Sá Filho, M.F., Vieira, L., Freitas, B.G., 2017. Timed artificial insemination: Current challenges and recent advances in reproductive efficiency in beef and dairy herds in Brazil. *Animal Reproduction* 14, 558–571. <https://doi.org/10.21451/1984-3143-AR999>.
- Bollwein, H., Heppelmann, M., Lüttgenau, J., 2016. Ultrasonographic Doppler Use for Female Reproduction Management. *Veterinary Clinics of North America - Food Animal Practice* 32, 149–164. <https://doi.org/10.1016/j.cvfa.2015.09.005>.
- Cavaliere, J., 2018. Effect of treatment of Bos indicus heifers with progesterone 0, 3 and 6 days after follicular aspiration on follicular dynamics and the timing of oestrus and ovulation. *Animal Reproduction Science* 193, 9–18. <https://doi.org/10.1016/j.anireprosci.2018.03.026>.
- Chagas e Silva, J., Lopes da Costa, L., Robalo Silva, J., 2002. Plasma progesterone profiles and factors affecting embryo-fetal mortality following embryo transfer in dairy cattle. *Theriogenology* 58, 51–59. [https://doi.org/10.1016/S0093-691X\(02\)00906-8](https://doi.org/10.1016/S0093-691X(02)00906-8).
- Colazo, M.G., Kastelic, J.P., Mainar-Jaime, R.C., Gavaga, Q.A., Whittaker, P.R., Small, J. A., Martinez, M.F., Wilde, R.E., Veira, D.M., Mapletoft, R.J., 2006. Resynchronization of previously timed-inseminated beef heifers with progestins. *Theriogenology* 65, 557–572. <https://doi.org/10.1016/j.theriogenology.2005.06.001>.
- Cosentino, I.O., Balaro, M.F.A., Leal, F.S.C., da Silva Carvalho, A.B., Cortat de Souza, P.R., Arashiro, E.K.N., Brandão, F.Z., 2018. Accuracy of assessment of luteal morphology and luteal blood flow for prediction of early pregnancy in goats. *Theriogenology* 121, 104–111. <https://doi.org/10.1016/j.theriogenology.2018.08.007>.
- Dalmaso de Melo, G., Mello, B.P., Ferreira, C.A., Souto Godoy Filho, C.A., Rocha, C.C., Silva, A.G., Reese, S.T., Madureira, E.H., Pohler, K.G., Pugliesi, G., 2020. Applied use of interferon-tau stimulated genes expression in polymorphonuclear cells to detect pregnancy compared to other early predictors in beef cattle. *Theriogenology* 152, 94–105. <https://doi.org/10.1016/j.theriogenology.2020.04.001>.
- Dubuc, J., Houle, J., Rousseau, M., Roy, J.P., Buczinski, S., 2020. Short communication: Accuracy of corpus luteum color flow Doppler ultrasonography to diagnose nonpregnancy in dairy cows on day 21 after insemination. *Journal of Dairy Science* 103, 2019–2023. <https://doi.org/10.3168/jds.2019-17234>.
- El-Zarkouny, S.Z., Stevenson, J.S., 2004. Resynchronizing estrus with progesterone or progesterone plus estrogen in cows of unknown pregnancy status. *Journal of Dairy Science* 87, 3306–3321. [https://doi.org/10.3168/jds.S0022-0302\(04\)73467-0](https://doi.org/10.3168/jds.S0022-0302(04)73467-0).
- Ferraz, P.A., Poit, D.A.S., Neto, A.L., Luiz, F., Azrak, A.J., Carneiro, A.L., Pardo, F.J.D., Pohler, K.G., Baruselli, P.S., Pugliesi, G., 2022. Determination of pregnancy loss at different moments of early gestation in dairy cattle subjected to TAI. *Animal Reproduction (Abstract)* 19, 22136.
- Fraser, H.M., Wulff, C., 2003. Angiogenesis in the corpus luteum. *Reproductive Biology and Endocrinology* 1, 1–8. <https://doi.org/10.1186/1477-7827-1-88>.
- Freitas, B.G., Machado, R., Lima, B., Catuzzi, C., Carolina, A., Motta, I.G., 2022. Efficiency of injectable P4 or EB at the beginning of resynchronization protocol (19 days after TAI) in lactating dairy cow. *Animal Reproduction (Abstract)* 19, 22063.
- Ginther, O.J. (Ed.), 2007. *Ultrasonic Imaging and Animal Reproduction: Color-Doppler Ultrasonography*. Equiservices Publishing, Cross Plains, WI, USA.
- Gnemmi, G.M., Maraboli, C.V.A., Gnemmi, B., Saleri, R., De Rensis, F., 2022. Use and adequacy of non-pregnancy diagnosis in cow. Which future? *Reproduction in Domestic Animals* 57, 45–52. <https://doi.org/10.1111/rda.14206>.
- Guimarães, C.R.B., Oliveira, M.E., Rossi, J.R., Fernandes, C.A.C., Viana, J.H.M., Palhao, M.P., 2015. Corpus luteum blood flow evaluation on Day 21 to improve the management of embryo recipient herds. *Theriogenology* 84, 237–241. <https://doi.org/10.1016/j.theriogenology.2015.03.005>.
- Herzog, K., Bollwein, H., 2007. Application of Doppler ultrasonography in cattle reproduction. *Reproduction in Domestic Animals* 42, 51–58. <https://doi.org/10.1111/j.1439-0531.2007.00903.x>.
- Herzog, K., Brockhan-Lüdemann, M., Kaske, M., Beindorff, N., Paul, V., Niemann, H., Bollwein, H., 2010. Luteal blood flow is a more appropriate indicator for luteal function during the bovine estrous cycle than luteal size. *Theriogenology* 73, 691–697. <https://doi.org/10.1016/j.theriogenology.2009.11.016>.
- Herzog, K., Voss, C., Kastelic, J.P., Beindorff, N., Paul, V., Niemann, H., Bollwein, H., 2011. Luteal blood flow increases during the first three weeks of pregnancy in lactating dairy cows. *Theriogenology* 75, 549–554. <https://doi.org/10.1016/j.theriogenology.2010.09.024>.
- Holton, M.P., Dalmaso, G., Dias, N.W., Pancini, S., Lamb, G.C., Pohler, K.G., et al., 2022a. Early pregnancy diagnosis in Bos taurus beef replacement heifers using color Doppler ultrasonography. *Journal of Animal Science* 100, 12. <https://doi.org/10.1093/jas/skac028.023>.
- Holton, M.P., Oosthuizen, N., de Melo, G.D., Davis, D.B., Stewart Jr, R.L., Pohler, K.G., Lamb, G.C., Fontes, P.L.P., 2022b. Luteal color doppler ultrasonography and pregnancy-associated glycoproteins as early pregnancy diagnostic tools and predictors of pregnancy loss in Bos taurus postpartum beef cows. *Journal of Animal Science* 100, 1–9. <https://doi.org/10.1093/jas/skac018>.
- Honnens, A., Voss, C., Herzog, K., Niemann, H., Rath, D., Bollwein, H., 2008. Uterine blood flow during the first 3 weeks of pregnancy in dairy cows. *Theriogenology* 70, 1048–1056. <https://doi.org/10.1016/j.theriogenology.2008.06.022>.

- Kanazawa, T., Seki, M., Ishiyama, K., Kubo, T., Kaneda, Y., Sakaguchi, M., Izaike, Y., Takahashi, T., 2016. Pregnancy prediction on the day of embryo transfer (Day 7) and Day 14 by measuring luteal blood flow in dairy cows. *Theriogenology* 86, 1436–1444. <https://doi.org/10.1016/j.theriogenology.2016.05.001>.
- Kastelic, J.P., Bergfelt, D.R., Ginther, O.J., 1991. Ultrasonic detection of the conceptus and characterization of intrauterine fluid on Days 10 to 22 in heifers. *Theriogenology* 35, 569–581. [https://doi.org/10.1016/0093-691X\(91\)90453-K](https://doi.org/10.1016/0093-691X(91)90453-K).
- Lonergan, P., 2011. Influence of progesterone on oocyte quality and embryo development in cows. *Theriogenology* 76, 1594–1601. <https://doi.org/10.1016/j.theriogenology.2011.06.012>.
- Macchiarelli, G., Nottola, S.A., Picucci, K., Stallone, T., Motta, P.M., 1998. The microvasculature of the corpus luteum in pregnant rabbit. A scanning electron microscopy study of corrosion casts. *Italian Journal of Anatomy and Embryology* 103, 191–202. <http://europepmc.org/abstract/MED/11315950>.
- Machado, R., Bergamaschi, M.A.C.M., Barbosa, R.T., Madureira, E.H., Alencar, M.M., Binelli, M., 2008. Taxas de serviço, concepção e prenhez de vacas nelore tratadas com gonadotrofina coriônica humana e 17beta-estradiol após a inseminação artificial em tempo fixo. *Brazilian Journal of Veterinary Research and Animal Science* 45, 221. <https://doi.org/10.11606/issn.1678-4456.bjvras.2008.266700>.
- Madoz, L.V., Lorenti, S.N., Rearte, R., Quintero-Rodríguez, L., Migliorisi, A.L., Jaureguiberry, M., Gabler, C., Drillich, M., de la Sota, R.L., 2022. Detection of nonpregnant cows and potential embryo losses by color Doppler ultrasound and interferon-stimulated gene expression in grazing dairy cows. *Journal of Dairy Science* 105, 6973–6984. <https://doi.org/10.3168/jds.2021-21171>.
- Mann, G.E., Lammung, G.E., 1995. Progesterone inhibition of the development of the luteolytic signal in cows. *Journal of Reproduction and Fertility* 104, 1–5.
- Matsui, M., Miyamoto, A., 2009. Evaluation of ovarian blood flow by colour Doppler ultrasound: Practical use for reproductive management in the cow. *The Veterinary Journal* 181, 232–240. <https://doi.org/10.1016/j.tvjl.2008.02.027>.
- Miyazaki, T., Tanaka, M., Miyakoshi, K., Minegishi, K., Kasai, K., Yoshimura, Y., 1998. Power and colour Doppler ultrasonography for the evaluation of the vasculature of the human corpus luteum. *Human Reproduction* 13, 2836–2841. <https://doi.org/10.1093/humrep/13.10.2836>.
- Morelli, K.G., Lourenço, G.G., Marangon, V.R., Oshiro, T.S.I., Silva, I.V.R., Schmidke, A., Resende, F.D., Pugliesi, G., 2022. Does Doppler ultrasonography for recipient selection improve the pregnancy success in equine embryo transfer programs? *Animal Reproduction (Abstract)* 19, 22081.
- Motta, I.G., Rocha, C.C., Bisinotto, D.Z., Melo, G.D., Ataíde Júnior, G.A., Silva, A.G., Gonzaga, V.H.G., Santos, J.A., Freitas, B.G., Lemes, K.M., Madureira, E.H., Pugliesi, G., 2020. Increased pregnancy rate in beef heifers resynchronized with estradiol at 14 days after TAI. *Theriogenology* 147, 62–70. <https://doi.org/10.1016/j.theriogenology.2020.02.009>.
- Munhoz, A.K., Pereira, M.H.C., Vasconcelos, J.L.M., 2018. Conception rate according to corpus luteum vascularization in embryo recipients cows and heifers. *Animal Reproduction (Abstract)* 15, 342.
- Nation, D.P., Malmø, J., Davis, G.M., Macmillan, K.L., 2003. Ultrasonography at 28 to 35 days after insemination. *Australian Veterinary Journal* 81, 63–65.
- Neto, A.L., Bisinotto, D.Z., Poit, D.A.S., Ferraz, P.A., Silva, F.M., Ferreira, W.D.A., Azrak, A.J., Pugliesi, G., 2022. Impacts on pregnancy outcomes of anticipating resynchronization of ovulation by early detection of non-pregnant dairy cows. *Animal Reproduction (Abstract)* 19, 22053.
- Niswender, G.D., Nett, T.M., Diekman, M.A.A., Fort, C., State, P., 1975. Flow of blood to the ovaries of ewes throughout estrous cycle. *Biology of Reproduction* 13, 381–388.
- Niswender, G.D., Juengel, J.L., Silva, P.J., Rollyson, M.K., McIntush, E.W., 2000. Mechanisms controlling the function and life span of the corpus luteum. *Physiological Reviews* 80, 1–29. <https://doi.org/10.1152/physrev.2000.80.1.1>.
- Ojeda-Rojas, O.A., Gonella-Díaz, A.M., Bustos-Coral, D., Sartorello, G.L., Reijers, T.S. S.S., Pugliesi, G., Zerlotti Mercadante, M.E., de Lima, C.G., Gameiro, A.H., 2021. An agent-based simulation model to compare different reproductive strategies in cow-calf operations: Technical performance. *Theriogenology* 160, 102–115. <https://doi.org/10.1016/j.theriogenology.2020.10.035>.
- Palhão, M.P., Ribeiro, A.C., Martins, A.B., Guimarães, C.R.B., Alvarez, R.D., Seber, M.F., Fernandes, C.A.C., Neves, J.P., Viana, J.H.M., 2020. Early resynchronization of non-pregnant beef cows based in corpus luteum blood flow evaluation 21 days after Timed-AI. *Theriogenology* 146, 26–30. <https://doi.org/10.1016/j.theriogenology.2020.01.064>.
- Pate, J.L., 1994. Cellular components involved in luteolysis. *Journal of Animal Science* 72, 1884–1890. <https://doi.org/10.2527/1994.7271884x>.
- Phillips, P.E., Jahnke, M.M., 2016. Embryo transfer (techniques, donors, and recipients). *The veterinary clinics of north america. Food Animal Practice* 32, 365–385. <https://doi.org/10.1016/j.cvfa.2016.01.008>.
- Pieterse, M.C., Taverne, M.A., Kruij, T.A., Willemsse, A.H., 1990. Detection of corpora lutea and follicles in cows: a comparison of transvaginal ultrasonography and rectal palpation. *The Veterinary Record* 126, 552–554. <http://europepmc.org/abstract/MED/2368295>.
- Pinaffi, F.L.V., Santos, É.S., da Silva, M.G., Maturana Filho, M., Madureira, E.H., Silva, L.A., Pinaffi, F.L.V., Santos, É.S., da Silva, M.G., Maturana Filho, M., Madureira, E.H., Silva, L.A., 2015. Follicle and corpus luteum size and vascularity as predictors of fertility at the time of artificial insemination and embryo transfer in beef cattle. *Pesquisa Veterinária Brasileira* 35, 470–476. <https://doi.org/10.1590/S0100-736X2015000500015>.
- Pugliesi, G., Pinaffi, F.L.V., Beg, M.A., Ginther, O.J., 2013. Use of corpus luteum area as a predictor of ongoing functional luteolysis in dairy heifers. *Reproduction, Fertility and Development* 25, 235. <https://doi.org/10.1071/RDv25n1Ab173>.
- Pugliesi, G., Miagawa, B.T., Paiva, Y.N., França, M.R., Silva, L.A., Binelli, M., 2014. Conceptus-induced changes in the gene expression of blood immune cells and the ultrasound-accessed luteal function in beef cattle: How early can we detect pregnancy? *Biology of Reproduction* 91, 1–12. <https://doi.org/10.1095/biolreprod.114.121525>.
- Pugliesi, G., de Melo, G.D., Ataíde, G.A., Pellegrino, C.A.G., Silva, J.B., Rocha, C.C., Motta, I.G., Vasconcelos, J.L.M., Binelli, M., 2018. Use of Doppler ultrasonography in embryo transfer programs: Feasibility and field results. *Animal Reproduction* 15, 239–246. <https://doi.org/10.21451/1984-3143-AR2018-0059>.
- Pugliesi, G., Bisinotto, D.Z., Mello, B.P., Lahr, F.C., Ferreira, C.A., Melo, G.D., Bastos, M.R., Madureira, E.H., 2019a. A novel strategy for resynchronization of ovulation in Nelore cows using injectable progesterone (P4) and P4 releasing devices to perform two timed inseminations within 22 days. *Reproduction in Domestic Animals* 54, 1149–1154. <https://doi.org/10.1111/rda.13475>.
- Pugliesi, G., de Melo, G.D., Silva, J.B., Carvalhêdo, A.S., Lopes, E., de Siqueira Filho, E., Silva, L.A., Binelli, M., 2019b. Use of color-Doppler ultrasonography for selection of recipients in timed-embryo transfer programs in beef cattle. *Theriogenology* 135, 73–79. <https://doi.org/10.1016/j.theriogenology.2019.06.006>.
- Reese, S.T., Franco, G.A., Poole, R.K., Hood, R., Fernandez Montero, L., Oliveira Filho, R. V., Cooke, R.F., Pohler, K.G., 2020. Pregnancy loss in beef cattle: A meta-analysis. *Animal Reproduction Science* 212, . <https://doi.org/10.1016/j.anireprosci.2019.106251> 106251.
- Rocha, C.C., Martins, T., Cardoso, B.O., Silva, L.A., Binelli, M., Pugliesi, G., 2019. Ultrasonography-accessed luteal size endpoint that most closely associates with circulating progesterone during the estrous cycle and early pregnancy in beef cows. *Animal Reproduction Science* 201, 12–21. <https://doi.org/10.1016/j.anireprosci.2018.12.003>.
- Sartori, R., Gimenes, L.U., Monteiro, P.L.J., Melo, L.F., Baruselli, P.S., Bastos, M.R., 2016. Metabolic and endocrine differences between Bos taurus and Bos indicus females that impact the interaction of nutrition with reproduction. *Theriogenology* 86, 32–40. <https://doi.org/10.1016/j.theriogenology.2016.04.016>.
- Scully, S., Evans, A.C.O., Duffy, P., Crowe, M.A., 2014. Characterization of follicle and CL development in beef heifers using high resolution three-dimensional ultrasonography. *Theriogenology* 81, 407–418. <https://doi.org/10.1016/j.theriogenology.2013.10.012>.
- Scully, S., Evans, A.C.O., Carter, F., Duffy, P., Lonergan, P., Crowe, M.A., 2015. Ultrasound monitoring of blood flow and echotexture of the corpus luteum and uterus during early pregnancy of beef heifers. *Theriogenology* 83, 449–458. <https://doi.org/10.1016/j.theriogenology.2014.10.009>.
- Silva, A.G., Nishimura, T.K., Rocha, C.C., Motta, I.G., Laurindo Neto, A., Ferraz, P.A., Bruni, G.A., Orlandi, R.E., Massoneto, J.P.M., Pugliesi, G., 2022. Comparison of estradiol benzoate doses for resynchronization of ovulation at 14 days after timed-AI in suckled beef cows. *Theriogenology* 184, 41–50. <https://doi.org/10.1016/j.theriogenology.2022.02.025>.
- Silva, A., Veiga, P., Castro, T., Bartolomé, J., Wallace, S.P., 2018. Color-Doppler Mode Ultrasonography for selection of Angus embryo recipients. *Animal Reproduction (Abstract)* 15, 371.
- Silva, J.C.B., 2020. Sazonalidade reprodutiva em búfalas: efeitos na produção in vitro de embriões e nas taxas de concepção utilizando embriões criopreservados. In: *Proceedings of the XXXIII Annual Meeting of the Brazilian Embryo Technology Society (SBTE)*, August 15th to 18th, 2018, Ilha de Comandatuba, BA, Brazil, pp. 28.
- Siqueira, L.G.B., Torres, C.A.A., Amorim, L.S., Souza, E.D., Camargo, L.S.A., Fernandes, C.A.C., Viana, J.H.M., 2009a. Interrelationships among morphology, echotexture, and function of the bovine corpus luteum during the estrous cycle. *Animal Reproduction Science* 115, 18–28. <https://doi.org/10.1016/j.anireprosci.2008.11.009>.
- Siqueira, L.G.B., Torres, C.A.A., Souza, E.D., Monteiro, P.L.J., Arashiro, E.K.N., Camargo, L.S.A., Fernandes, C.A.C., Viana, J.H.M., 2009b. Pregnancy rates and corpus luteum-related factors affecting pregnancy establishment in bovine recipients synchronized for fixed-time embryo transfer. *Theriogenology* 72, 949–958. <https://doi.org/10.1016/j.THERIOGENOLOGY.2009.06.013>.
- Siqueira, L.G.B., Areas, V.S., Ghetti, A.M., Fonseca, J.F., Palhao, M.P., Fernandes, C.A.C., Viana, J.H.M., 2013. Color Doppler flow imaging for the early detection of nonpregnant cattle at 20 days after timed artificial insemination. *Journal of Dairy Science* 96, 6461–6472. <https://doi.org/10.3168/jds.2013-6814>.
- Siqueira, L.G.B., Arashiro, E.K., Ghetti, A.M., Souza, E.D., Feres, L.F., Pfeifer, L.F., Fonseca, J.F., Viana, J.H., 2019. Vascular and morphological features of the corpus luteum 12 to 20 days after timed artificial insemination in dairy cattle. *Journal of Dairy Science* 102, 5612–5622. <https://doi.org/10.3168/jds.2018-15853>.
- Stevenson, J.S., Johnson, S.K., Medina-Britos, M.A., Richardson-Adams, A.M., Lamb, G.C., 2003. Resynchronization of estrus in cattle of unknown pregnancy status using estrogen, progesterone, or both. *Journal of Animal Science* 81, 1681–1692. <https://doi.org/10.2527/2003.8171681x>.
- Tom, J.W., Pierson, R.A., Adams, G.P., 1998. Quantitative echotexture analysis of bovine corpora lutea. *Theriogenology* 49, 1345–1352. [https://doi.org/10.1016/S0093-691X\(98\)00081-8](https://doi.org/10.1016/S0093-691X(98)00081-8).
- Utt, M.D., Johnson, G.L., Beal, W.E., 2009. The evaluation of corpus luteum blood flow using color-flow Doppler ultrasound for early pregnancy diagnosis in bovine embryo recipients. *Theriogenology* 71, 707–715. <https://doi.org/10.1016/j.theriogenology.2008.09.032>.

- Viana, J.H.M., Arashiro, E.K.N., Siqueira, L.G.B., Ghetti, A.M., Areas, V.S., Guimarães, C.R.B., 2013. Doppler ultrasonography as a tool for ovarian management. *Animal Reproduction* 10, 215–222.
- Vieira, C.C., Pinto, H.F., Buss, V., Gonzalez de Freitas, B., Guerreiro, B.M., Leivas, F.G., Pugliesi, G., Mesquita, F.S., 2021. Resynchronization of follicular wave using long-acting injectable progesterone or estradiol benzoate at 14 days post-TAI in *Bos taurus* x *Bos indicus* beef heifers. *Theriogenology* 176, 194–199. <https://doi.org/10.1016/j.theriogenology.2021.09.017>.
- Vieira, L.M., Sá Filho, M.F., Pugliesi, G., Guerreiro, B.M., Cristaldo, M.A., Batista, E.O.S., Freitas, B.G., Carvalho, F.J., Guimaraes, L.H.C., Baruselli, P.S., 2014. Resynchronization in dairy cows 13 days after TAI followed by pregnancy diagnosis based on corpus luteum vascularization by color doppler. *Animal Reproduction (Abstract)* 11, 378.
- Wellert, S.R., Battista, S.E., Kieffer, J., Lurch, R.N., Garcia-Guerra, A., 2020. Comparison of different Doppler ultrasound settings for pregnancy diagnosis based on corpus luteum perfusion at 21 days after AI in beef cattle. *Reproduction, Fertility and Development* 32, 211. <https://doi.org/10.1071/RDv32n2Ab168>.

WHAT IS YOUR DIAGNOSIS?

What is your diagnosis? Hematology and blood smear of a dog

Sandra Lapsina¹ | Martina Stirn¹ | Marilisa Novacco | Claudia Cueni² |
Marina L Meli¹ | Regina Hofmann-Lehmann¹ | Barbara Riond¹

¹Clinical Laboratory, Department for Clinical Diagnostics and Services, Vetsuisse Faculty, University of Zurich, Zurich, Switzerland

²Clinic for Small Animal Internal Medicine, Vetsuisse Faculty, University of Zurich, Zurich, Switzerland

Correspondence

Barbara Riond, Clinical Laboratory, Department of Clinical Diagnostics and Services, Vetsuisse Faculty, University of Zurich, Winterthurerstrasse 260, 8057, Zurich, Switzerland.

Email: briond@vetclinics.uzh.ch

1 | CASE PRESENTATION

An 8-year-old spayed female smooth-haired Dachshund with a travel history to Italy was referred to the Clinic for Small Animal Internal Medicine at the Vetsuisse Faculty, University of Zurich, with severe anemia. Clinical examination revealed dehydration of 5%, heart rate of 160 beats/min with a bounding pulse of the same frequency, systolic heart murmur grade 2-3/6, respiratory rate of 36 breaths/minute, and rectal body temperature of 37.4°C. An abdominal ultrasound showed severe colopathy, generalized hepatopathy, hepatomegaly, moderate peritoneal effusion, gastropathy, a mildly thickened gallbladder wall, and single portal lymphadenomegaly. At presentation to our clinic, we performed a hematologic analysis on a Sysmex XN-1000 (Sysmex Corporation, Kobe, Japan). The CBC revealed severe regenerative anemia, severe thrombocytopenia, and an inflammatory leukogram with possible stress leukogram (Table 1).

TABLE 1 Hematologic and biochemical values upon presentation at the referral veterinary clinic on 04/12/21

Parameter	Result	Reference interval
HCT (%)	5	42–55
Hb (g/dl)	2.2	14.4–19.1
RBC (x10 ⁶ /μl)	0.5	6.1–8.1
MCH (pg)	42	23–26
MCHC (g/dl)	48	34–36
MCV (fl)	87	64–73
Reticulocytes (μL)	278 600	>115 000
WBC (x10 ³ /μl)	7.1	4.7–11.3
Corrected for nRBCs		
PLT (x10 ³ /μl)	23	130–394
Band neutrophils (x10 ³ /μl)	0.53	0.00–0.08
Segmented neutrophils (x10 ³ /μl)	4.28	2.50–7.44
Monocytes (x10 ³ /μl)	1.50	0.20–0.92
Lymphocytes (x10 ³ /μl)	0.82	1.15–3.40
nRBCs (/100 WBC)	63	
RBC morphology	2+ hypochromasia, 3+ anisocytosis, 2+ polychromasia, 2+ macrocytosis, 1+ microcytes	
Total protein (g/L)	42	46–71
Albumin (g/L)	27	29–37
Globulin (g/L)	15	19–37

Note: Abbreviations: Hb, hemoglobin; HCT, hematocrit; MCH, mean corpuscular hemoglobin; MCHC, mean corpuscular hemoglobin concentration; MCV, mean cell volume; nRBCs, nucleated red blood cells; PLT, platelets; RBC, red blood cells; WBC, white blood cells.

This is an open access article under the terms of the [Creative Commons Attribution-NonCommercial-NoDerivs](https://creativecommons.org/licenses/by-nc-nd/4.0/) License, which permits use and distribution in any medium, provided the original work is properly cited, the use is non-commercial and no modifications or adaptations are made.

© 2022 The Authors. *Veterinary Clinical Pathology* published by Wiley Periodicals LLC on behalf of American Society for Veterinary Clinical Pathology.

Hematologic interpretation: Severe regenerative anemia, severe thrombocytopenia, and mild regenerative left shift due to the presence of a hemotropic *Mycoplasma* spp.

The initial presentation to the referring veterinarian was 4 weeks earlier, where the dog underwent resection of a highly metastatic duodenal adenocarcinoma with lymphatic vessel invasion and splenectomy due to splenic nodular hyperplasia. The dog received two separate blood transfusions due to a hematocrit (HCT) of 13% and recurring anemia (see Table 2). No information was available about the first donor, whereas the second donor had tested negative for blood-borne pathogens.

On the Sysmex, the red blood cell (RBC) indices revealed moderately increased mean corpuscular hemoglobin (MCH) (42; RI 23–26 pg), moderately increased mean corpuscular hemoglobin concentration (MCHC) (48; RI 34–36 g/dL), and moderately increased mean corpuscular volume (MCV) (87; RI 64–73 fL). Hemolysis and lipemia were absent. Absolute reticulocyte numbers were moderately increased, indicating a regenerative response.

The peripheral blood smear showed marked anisocytosis, moderate polychromasia, moderate macrocytosis, and mild microcytosis (Figure 1). Moderately increased numbers of nucleated red blood cells (rubricytes and metarubricytes) were observed; no dysplastic changes were noted. Most of the erythrocytes were covered by coccoid organisms in chain formations measuring approximately <1 µm in diameter. The observed clinical and pathologic changes were consistent with severe regenerative anemia, and the coccoid organisms were suspected to be hemotropic *Mycoplasma* spp. (also known as hemoplasmas). A cytologic examination of the peritoneal effusion revealed a protein-rich transudate. Most of the erythrocytes in the peritoneal fluid were covered with similar coccoid organisms, often forming chains (Figure 2). Serum biochemistry testing measured total protein

and albumin concentrations and calculated globulin concentrations on a Cobas C 501 module (Roche Diagnostics, Rotkreuz, Switzerland).

2 | ADDITIONAL RESULTS

Species-specific TaqMan real-time PCR testing for canine hemoplasma infections included *Mycoplasma haemocanis* and “*Candidatus Mycoplasma haematoparvum*”, as previously described.¹ To perform

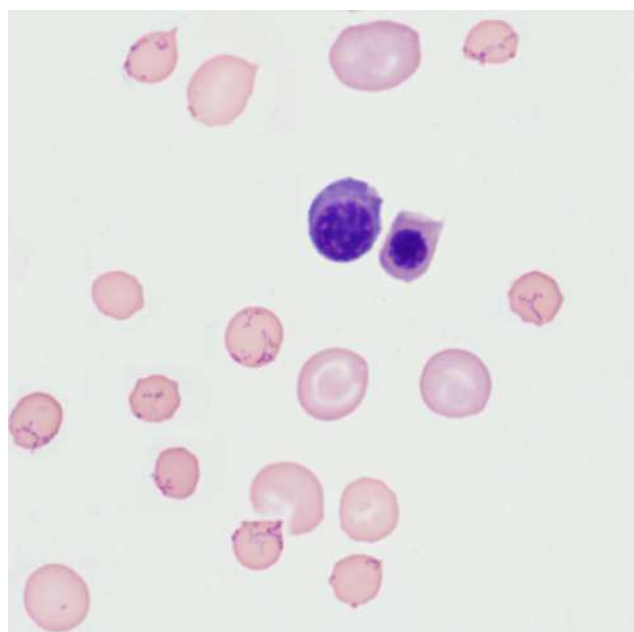


FIGURE 1 Photomicrograph of a peripheral blood smear of an 8-year-old Dachshund. Wright-Giemsa stain, 1000 x magnification

TABLE 2 Timetable of presentations to the referring veterinarian and referral clinic with HCT (%), PCR results, blood smear evaluation and clinical key information

Date	Place of appointment	Development of the case
03/16/2021	Referring veterinarian	HCT 13%, duodenal mass detected
03/18/2021	Referring veterinarian	HCT 13%, 1st blood transfusion (no information about donor); resection of the duodenal mass, as well as splenectomy
03/24/2021	Referring veterinarian	HCT 37%
04/09/2021	Referring veterinarian	Fatigue; HCT 11%
04/10/2021	Referring veterinarian	2nd blood transfusion (donor PCR negative for <i>Mycoplasma haemocanis</i>), afterwards HCT 18%
04/12/2021	Referral clinic	HCT 5%; <i>Mycoplasma</i> spp. detected microscopically, 1st PCR testing (positive; CT-value 15.1), start of the treatment, 3rd blood transfusion (not tested for <i>M. haemocanis</i>)
04/13/2021	Referral clinic	HCT 11%; 4th blood transfusion; 2nd PCR testing (positive; CT-value 33.9), no <i>Mycoplasma</i> spp. visible microscopically
04/14/2021	Referral clinic	HCT 22%; 3rd PCR testing (positive; CT-value 35.2)
04/15/2021	Referral clinic	HCT 28%
04/22/2021	Referral clinic	HCT 30%
05/03/2021	Referral clinic	HCT 33%

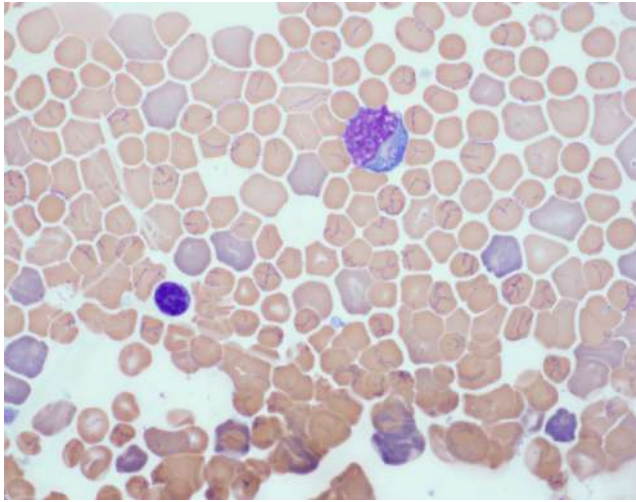


FIGURE 2 Photomicrograph of a cytocentrifuged preparation of peritoneal fluid of an 8-year-old Dachshund. Wright-Giemsa stain, 1000 x magnification

these tests, genomic DNA was extracted from 100 μ L of EDTA whole blood using the DNeasy Blood & Tissue Kit (Qiagen, Hombrechtikon, Switzerland) following manufacturer's instructions. DNA was eluted into 100 μ L buffer AE. During extraction, a negative control consisting of 200 μ L of phosphate-buffered saline was concurrently prepared to monitor for cross-contamination. Negative PCR controls and the extraction control were run with the sample. A standard curve (10-fold dilution of complete 16S ribosomal RNA gene of *M. haemocanis* cloned into pMK-RQ backbone) was used for the copy number determination. All real-time PCR assays were performed using an ABI PRISM 7500 Fast Sequence Detection System (Applied Biosystems, Rotkreuz, Switzerland). The extraction and negative PCR controls tested PCR negative. The sample resulted in a negative PCR for "*Candidatus Mycoplasma haematoparvum*" and positive for *M. haemocanis*. High blood loads were detected with a threshold cycle (CT) value of 15.1, corresponding to a load of 1.5×10^{10} bacterial copies per mL of blood, confirming the *M. haemocanis* infection. Therapy with doxycycline, enrofloxacin, and prednisolone was started the same day, and no *M. haemocanis* bacteria could be found on the peripheral blood smear the next day or anytime in the following 3 weeks. However, PCR for *M. haemocanis* was positive for two days after treatment with increasing CT values (33.9 and 35.2 for the second and the third day, respectively, corresponding to 3.8×10^4 and 1.6×10^4 bacterial copies per mL).

3 | DISCUSSION

Hemotropic mycoplasmas are small uncultivable wall-less bacteria that adhere to the erythrocytes of various mammalian species.¹ In dogs, two *Mycoplasma* spp. are documented: *M. haemocanis* and "*Candidatus Mycoplasma haematoparvum*".¹ The brown dog tick *Rhipicephalus sanguineus* is believed to play a role as both vector and reservoir for canine hemotropic mycoplasmas.² Blood-sucking

arthropods, including mange mites, are also suspected as possible vectors.³ Additionally, blood transfusion has been documented as a route of transmission, and also the possibility of direct transmission with infected blood during dogfights has been suggested.³ Canine hemoplasmosis shows worldwide distribution, but higher prevalence has been documented in parts of Europe with Mediterranean or sub-Mediterranean climates compared with Switzerland.^{1,3,4}

In dogs, both acute and chronic canine hemoplasmosis have been documented. In acute infection many bacteria, as well as rapidly developing anemia, can be observed. Affected animals are usually immunosuppressed or splenectomized.³

The dog in this report showed acute canine hemoplasmosis due to infection with *M. haemocanis* and detection of many bacteria within peripheral blood by both microscopic evaluation of the blood smear and PCR analysis. Aside from splenectomy, immunosuppression due to a history of duodenal adenocarcinoma also contributed to the typical picture of canine hemoplasmosis with an acute onset of severe anemia in this dog.

Cases of non-splenectomized dogs with acute canine hemoplasmosis have also been documented but usually are associated with a concurrent infection of babesiosis or ehrlichiosis, neoplasia or septicemia with another bacterium.

The clinical signs of acute canine hemoplasmosis include lethargy, anorexia, weight loss, pale mucous membranes, and fever. Packed cell volumes (PCVs) can be as low as 11%; anisocytosis, polychromasia, normoblastemia, occasional spherocytes, a positive Coombs test, and thrombocytopenia can be observed. In the present case, the dog showed an even lower PCV of 5% with a moderate number of nucleated red blood cells, moderate reticulocytosis, marked anisocytosis, moderate polychromasia, and severe thrombocytopenia. No spherocytes were noted.

In most cases, the dogs recover and remain chronically infected though in severe cases the outcome can be lethal.³ The chronic form has been reported in both splenectomized and non-splenectomized dogs and is usually asymptomatic, the bacteria on peripheral blood smears are observed only periodically and in low numbers.³

Conventional or quantitative real-time PCR is considered the gold standard to diagnose canine hemoplasmosis. Blood samples should be taken before the initiation of therapy. However, a negative PCR result does not exclude an acute infection in the dog; fluctuations of $>10^6$ logs in bacteremia have been reported for feline hemotropic mycoplasma,³ and therefore, re-testing is recommended in cases of clinical suspicion. It is also known that identifying hemotropic mycoplasma by light microscopy on Wright-Giemsa-stained peripheral blood smears has low sensitivity (0–37%) and moderate to high specificity (84–98%) due to often very low organism concentrations and their visual resemblance to stain precipitates, drying- artifacts ("water inclusions"), basophilic stippling, and small Howell-Jolly bodies.⁵ Furthermore, the bacteria tend to detach from the erythrocytes in EDTA anticoagulated whole blood within a few hours of storage. Therefore, the peripheral blood smears need to be fresh.³ Antibiotic therapy and low to moderate bacteremia can also provide false-negative results.

The present case is of interest in that the dog showed acute canine hemoplasmosis with signs of severe regenerative anemia and high

numbers of *M. haemocanis* bacteria on the blood smear detectable by light microscopy. Therefore, microscopic identification of infectious agents in the blood smear should be included routinely in CBC analyses in diagnostic and veterinary practice laboratories. However, extensive searching for organisms on blood smears of anemic animals is not recommended since PCR testing is the most sensitive technique and mandatory for confirmation and species determination.

The dog, in this case, was splenectomized 3.5 weeks before presentation to our referral and had received two blood transfusions prior to detection of *M. haemocanis*, one of which derived from an untested donor (1st transfusion), which represents a possible source of infection. Furthermore, the owners reported travel to Italy for the past several years, which might have resulted in contact with local dogs, ticks, or arthropods and infection with *M. haemocanis*. However, clear evidence is lacking for both assumptions. The excised duodenal adenocarcinoma with high metastatic rate is a contributing factor for the clinical development of the acute hemoplasmosis. The animal responded well to therapy with doxycycline, enrofloxacin, and prednisolone by showing HCT increase to 33% 3 weeks later, but PCR results stayed weakly positive at least for 2 more days. The HCT increased to 37% (42–55) on the last recorded test result. This patient was mostly a chronic carrier, and re-activation of the infection is possible with immunosuppression.

ACKNOWLEDGEMENTS

The article is funded by Universitat Zurich. [Correction added on 11 May 2023, after first online publication: CSAL funding statement has been added.]. Open Access Funding provided by Universitat Zurich.

ORCID

Sandra Lapsina  <https://orcid.org/0000-0001-8635-1327>

Marilisa Novacco  <https://orcid.org/0000-0001-6290-1291>

Marina L Meli  <https://orcid.org/0000-0002-3609-2416>

Regina Hofmann-Lehmann  <https://orcid.org/0000-0001-9750-4296>

Barbara Riond  <https://orcid.org/0000-0003-2848-2091>

REFERENCES



1. Wengi N, Willi B, Boretti FS, et al. Real-time PCR-based prevalence study, infection follow-up and molecular characterization of canine hemotropic mycoplasmas. *Vet Microbiol.* 2008;126(1–3):132–141.
2. Seneviratna P, Weerasinghe AS. Transmission of Haemobartonella canis by the dog tick, Rhipicephalus sanguineus. *Res Vet Sci.* 1973;14(1):112–114.
3. Willi B, Novacco M, Meli M, et al. Haemotropic mycoplasmas of cats and dogs: transmission, diagnosis, prevalence and importance in Europe. *Schweiz Arch Tierheilkd.* 2010;152(5):237–244.
4. Novacco M, Meli ML, Gentilini F, et al. Prevalence and geographical distribution of canine hemotropic mycoplasma infections in Mediterranean countries and analysis of risk factors for infection. *Vet Microbiol.* 2010;142(3–4):276–284.
5. Aquino LC, Kamani J, Haruna AM, et al. Analysis of risk factors and prevalence of haemoplasma infection in dogs. *Vet Parasitol.* 2016;221:111–117.

How to cite this article: Lapsina S, Stirn M, Novacco M, et al. What is your diagnosis? Blood smear of a dog. *Vet Clin Pathol.* 2023;52(Suppl. 2):93–96. doi: [10.1111/vcp.13109](https://doi.org/10.1111/vcp.13109)

CONSENSUS STATEMENT

Consensus Statements of the American College of Veterinary Internal Medicine (ACVIM) provide the veterinary community with up-to-date information on the pathophysiology, diagnosis, and treatment of clinically important animal diseases. The ACVIM Board of Regents oversees selection of relevant topics, identification of panel members with the expertise to draft the statements, and other aspects of assuring the integrity of the process. The statements are derived from evidence-based medicine whenever possible and the panel offers interpretive comments when such evidence is inadequate or contradictory. A draft is prepared by the panel, followed by solicitation of input by the ACVIM membership which may be incorporated into the statement. It is then submitted to the Journal of Veterinary Internal Medicine, where it is edited prior to publication. The authors are solely responsible for the content of the statements.

ACVIM consensus statement guidelines on diagnosing and distinguishing low-grade neoplastic from inflammatory lymphocytic chronic enteropathies in cats

Sina Marsilio^{1†}  | Valerie Freiche^{2†}  | Eric Johnson³ | Chiara Leo⁴ | Anton W. Langerak⁵ | Iain Peters⁶ | Mark R. Ackermann⁷

¹Department of Veterinary Medicine and Epidemiology, UC Davis School of Veterinary Medicine, Davis, California, USA

²Ecole Nationale Vétérinaire d'Alfort, CHUVA, Unité de Médecine Interne, Maisons-Alfort, France

³Department of Surgical & Radiological Sciences, UC Davis School of Veterinary Medicine, Davis, California, USA

⁴Anicura Istituto Veterinario Novara, Novara, Italy

⁵Erasmus MC, University Medical Center, Rotterdam, The Netherlands

⁶Veterinary Pathology Group (VPG), Exeter, UK

⁷Oregon Veterinary Diagnostic Laboratory, Oregon State University, Corvallis, Oregon, USA

Correspondence

Sina Marsilio, Department of Veterinary Medicine and Epidemiology, UC Davis School of Veterinary Medicine, 1275 Med Science Dr, Davis, CA 95616, USA.

Email: smarsilio@ucdavis.edu

Present address

Mark R. Ackermann, US Department of Agriculture, National Animal Disease Center, Ames, Iowa, USA.

Abstract

Background: Lymphoplasmacytic enteritis (LPE) and low-grade intestinal T cell lymphoma (LGITL) are common diseases in older cats, but their diagnosis and differentiation remain challenging.

Objectives: To summarize the current literature on etiopathogenesis and diagnosis of LPE and LGITL in cats and provide guidance on the differentiation between LPE and LGITL in cats. To provide statements established using evidence-based approaches or

Abbreviations: ACVIM, American College of Veterinary Internal Medicine; AL, alimentary lymphoma; ALT, alanine transaminase; AUS, abdominal ultrasound; CBC, complete blood count; CE, chronic enteropathy; CT, computed tomography; EATL, enteropathy-associated T-cell lymphoma; EPI, exocrine pancreatic insufficiency; FCEAI, feline chronic enteropathy activity index; FFPE, formalin-fixed and paraffin-embedded; FIP, feline infectious peritonitis; FIV, feline immunodeficiency virus; FeLV, feline leukemia virus; f-PLI, feline pancreatic lipase immunoreactivity; GRADE, Grading of Recommendations Assessment, Development and Evaluation; GI-TLPD, gastrointestinal T-cell lymphoproliferative disorder; H&E, hematoxylin and eosin; IBD, inflammatory bowel disease; IGH, immunoglobulin heavy chain; IHC, immunohistochemistry; JAK, Janus kinase; LDH, lactate dehydrogenase; LGITL, low-grade intestinal T-cell lymphoma; LPE, lymphoplasmacytic enteritis; MALT, mucosa-associated lymphoid tissue; MEITL, monomorphic epitheliotropic intestinal T-cell lymphoma; MMA, methylmalonic acid; MRI, magnetic resonance imaging; NK, natural killer; PARR, PCR for antigen receptor rearrangement; PCR, polymerase chain reaction; SCL, small cell lymphoma; STAT, signal transducer and activator of transcription; TCR, T-cell receptor; WHO, World Health Organization; WSAVA, World Small Animal Veterinary Association.

[†]Sina Marsilio and Valerie Freiche contributed equally to this study.

This is an open access article under the terms of the [Creative Commons Attribution-NonCommercial](https://creativecommons.org/licenses/by-nc/4.0/) License, which permits use, distribution and reproduction in any medium, provided the original work is properly cited and is not used for commercial purposes.

© 2023 The Authors. *Journal of Veterinary Internal Medicine* published by Wiley Periodicals LLC on behalf of American College of Veterinary Internal Medicine.

where such evidence is lacking, statements based on consensus of experts in the field.

Animals: None.

Methods: A panel of 6 experts in the field (2 internists, 1 radiologist, 1 anatomic pathologist, 1 clonality expert, 1 oncologist) with the support of a human medical immunologist, was formed to assess and summarize evidence in the peer-reviewed literature and complement it with consensus recommendations.

Results: Despite increasing interest on the topic for clinicians and pathologists, few prospective studies were available, and interpretation of the pertinent literature often was challenging because of the heterogeneity of the cases. Most recommendations by the panel were supported by a moderate or low level of evidence. Several understudied areas were identified, including cellular markers using immunohistochemistry, genomics, and transcriptomic studies.

Conclusions and Clinical Importance: To date, no single diagnostic criterion or known biomarker reliably differentiates inflammatory lesions from neoplastic lymphoproliferations in the intestinal tract of cats and a diagnosis currently is established by integrating all available clinical and diagnostic data. Histopathology remains the mainstay to better differentiate LPE from LGITL in cats with chronic enteropathy.

KEYWORDS

alimentary, cat, chronic diarrhea, endoscopy, gastrointestinal, histology, immunohistochemistry, inflammatory bowel disease, lymphoma, lymphoplasmacytic enteritis, lymphoproliferative disorders, T-cell

1 | INTRODUCTION

Chronic enteropathy (CE) is a common disorder in cats, especially in the older cat population and its prevalence has increased over the past 2 decades.¹ Differentiating chronic inflammatory enteropathy from intestinal low-grade lymphoma in cats can be difficult because physical examination findings, laboratory data, diagnostic imaging findings, and even histopathologic features frequently overlap.

The most recent revision of the World Health Organization (WHO) classification of lymphoid neoplasms in people includes a primary, indolent clonal T-cell proliferation of the gastrointestinal tract as a provisional entity named indolent T-cell lymphoproliferative disorder of the gastrointestinal tract (GI-TLPD).² This disorder shares many similarities with intestinal low-grade lymphoma in cats, including the challenge to differentiate it from inflammatory disorders and its frequent misdiagnosis as enteropathy-associated T-cell lymphoma (EATL), formerly known as EATL type I, or monomorphic epitheliotropic intestinal T-cell lymphoma (MEITL), formerly known as EATL type II.^{2,3} Lymphoproliferative disorders (LPDs) are characterized by an uncontrolled proliferation of lymphocytes and can be differentiated into lymphomas, leukemias, and monoclonal gammopathies.^{2,4,5} Although LPDs including intestinal low-grade lymphomas in cats are characterized by monoclonal or oligoclonal rearrangements of the lymphocyte receptors, clonality is not equivalent with malignancy and

clonality has been well described in reactive lesions in humans⁶⁻¹⁰ and companion animals.¹¹ In fact, the capacity for clonal expansion upon antigen-recognition is a hallmark of both B-lymphocytes and T-lymphocytes.¹²⁻¹⁶ Although all lymphomas are clonal, not all reactive lesions are polyclonal.¹⁷

Part of the veterinary community has argued that a comprehensive diagnostic evaluation of cats with CE may be unnecessary because it does not appear to change prognosis or treatment. However, data from more recent studies indicate that prognosis and treatment strategy may need adjustment based on the underlying diagnosis.^{18,19} An evaluation including intestinal biopsies does not only exclude other differential diagnoses including large cell lymphomas, infectious, eosinophilic, or mast cell disease but also could allow for a more accurate prognosis and treatment plan in the future.

The following report by the American College of Veterinary Internal Medicine (ACVIM) consensus statement panel on CE in cats proposes a classification of CE based on the state-of-the-art diagnostic methods and provides recommendations for the diagnostic approach and management of cats with CE.

The panel recognizes that even after applying all currently available diagnostic tests, ambiguous cases will remain and that some diagnostic approaches are unclear and even arbitrary. Nonetheless, there appear to be correlations among certain clinical, laboratory, histopathological, immunohistochemical, and clonality features that predict a

different disease outcome and may lead to different treatment approaches in the future.

2 | MATERIALS AND METHODS

A panel of 6 experts in the field (2 internists [S. Marsilio, V. Freiche], 1 radiologist [E. Johnson], 1 anatomic pathologist [M. R. Ackermann], 1 clonality expert [I. Peters], 1 oncologist [C. Leo]) was formed to assess and summarize evidence in the peer-reviewed literature and complement it with consensus recommendations. An immunologist and clonality expert in human medicine served as a panel consultant [A. W. Langerak].

During the first consensus meeting, different options for building consensus were considered and included the Delphi method, the nominal group technique, and the Grading of Recommendations Assessment, Development and Evaluation (GRADE) method. The members decided to employ a modified Delphi method that incorporates a combination of anonymous commenting on a series of statement drafts in addition to regular video conferences. Committee members used a 5-point Likert scale to rank each statement (Table 1). Consensus was defined as reached if ≥ 6 of 7 committee members indicated strong agreement (score = 5) or agreement (score = 4) with the statement. Three review rounds were permitted per statement until a final decision was adopted. For the section on clonality analysis, the panel consulted with an external immunologist between review rounds. A Qualtrics survey was distributed among the panel experts for final and anonymous voting on the statements according to the adopted Likert scale (Table 1).

PubMed, Google Scholar, and Web of Science were used along with the following search terms to identify relevant articles (in alphabetical order): “alimentary lymphoma,” “cat,” “clonality,” “clonal expansion,” “enteropathy,” “feline,” “histopathology,” “immunohistochemistry,” “inflammatory bowel disease,” “lymphoma,” “lymphoplasmacytic enteritis,” “lymphoproliferative disorders,” “PCR for antigen receptor rearrangement,” “radiology,” “small cell lymphoma,” “ultrasonography,” “ultrasound.” The group also added additional subtopic-relevant terminology. In addition, review articles were used to identify additional relevant articles not captured in the original searches. Articles were excluded if they were published only in abstract form, were not available in English, did not address relevant topics or only contained case reports or small case series.

TABLE 1 Likert scale.

Strongly disagree	Disagree	Undecided	Agree	Strongly agree
1	2	3	4	5

Note: The Likert Scale assumes that the strength/intensity of an attitude is linear, that is, on a continuum from strongly disagree to strongly agree, and that attitudes can be measured.

References documenting peer-reviewed published studies containing original data were reviewed by the panel and graded. A modified system of evidence (Table 2) was used to rate the level of evidence.^{20,21} For each statement for which consensus was reached, a level of evidence was determined based on review of the literature (Table 2).

3 | RESULTS

3.1 | Terminology

The terminology for CE in cats used in the literature varies. Terms commonly used to describe inflammatory lesions are inflammatory bowel disease (IBD), lymphoplasmacytic enteritis (LPE), and eosinophilic enteritis. Terms commonly found to describe neoplastic lesions are small cell lymphoma, low-grade lymphoma, alimentary lymphoma (AL), lymphosarcoma, enteropathy-associated T-cell lymphoma (EATL), monomorphic epitheliotropic intestinal T-cell lymphoma (MEITL), and low-grade intestinal T-cell lymphoma (LGITL). For the purpose of this consensus statement, the experts adopted the following terms:

- Chronic enteropathy for cats with chronic (at least 3 weeks' duration) signs of gastrointestinal disease where extragastrointestinal, metabolic, and infectious causes have been ruled out.
- Lymphoplasmacytic enteritis for inflammatory lesions in the gastrointestinal tract of cats with CE that are dominated by lymphocytic infiltration in the lamina propria.
- Low-grade intestinal T-cell lymphoma for lesions in the gastrointestinal tract of cats with CE characterized by a monomorphic infiltration of the lamina propria or epithelium or both of cats with small, mature, neoplastic (clonal) T lymphocytes.

TABLE 2 Evidence levels.^{20,21}

Evidence level	Key features
I	<ul style="list-style-type: none"> • Randomized controlled trials in cats • Prospective, nonrandomized controlled trials in cats, with adequate sample size and no major methodological flaws
II	<ul style="list-style-type: none"> • Experimental laboratory trials in cats • Prospective studies with inadequate sample size • Retrospective clinical studies with intervention and control groups
III	<ul style="list-style-type: none"> • Retrospective clinical studies and case series in cats without control groups
O	<ul style="list-style-type: none"> • Studies in other species
E	<ul style="list-style-type: none"> • Expert opinion

3.2 | Incidence

The true incidence of LPE or LGITL remains unknown. However, studies imply that the incidence of intestinal lymphoma may have increased since the advent of the FeLV vaccine¹ and that presently most AL cases do not exhibit circulating FeLV antigen.²²

Whether this situation is a true increase in incidence or a reflection of other factors such as an increased caseload (i.e., because of urbanization), improved healthcare for cats, and increased longevity has not been studied.

3.3 | Etiopathogenesis

3.3.1 | Infectious agents

Although a causative relationship between high-grade lymphomas such as mediastinal lymphoma and FeLV infection has been well documented, the association between low grade lymphomas such as LGITL and FeLV and FIV infections is poorly documented. The majority of cats with LGITL test serologically negative for both FeLV and FIV.^{1,23,24} However, some studies found FeLV genetic material in samples from cats with LGITL using immunohistochemistry (IHC) or polymerase chain reaction (PCR)^{25,26} and hence the role of regressive infections in lymphomagenesis is still unclear.²⁷ To our knowledge, no studies have investigated the role of retroviruses in cats with LPE.

Bacterial mucosal colonization has been investigated as a driver of neoplastic transformation in humans, dogs, and cats. Gastric colonization with *Helicobacter pylori* is strongly associated with gastric inflammation and development of gastric adenocarcinomas and mucosa-associated lymphoid tissue (MALT) lymphoma in humans.^{28,29} Although a statistically significant association of mucosa-invading and intravascular bacteria has been found in intestinal large cell lymphomas in cats, no association between LGITL and bacterial invasion has been reported.³⁰ Dysbiosis in humans and animal models of LPE has been found to promote inflammation and malignant transformation, especially the development of colorectal cancer.³¹ The role of dysbiosis in CE of cats is poorly understood. Previous studies reported intestinal dysbiosis in cats with LPE and LGITL, which parallels findings in humans.^{32,33} However, dysbiotic patterns were not significantly different between cats with LGITL and LPE.³²

3.3.2 | Chronic inflammation

Chronic inflammation is a well-known promoter of oncogenesis, and several arguments support the hypothesis that LPE and LGITL represent a continuum rather than 2 separate disease entities. Progression of LPE to LGITL previously has been suspected based on the frequent coexistence of inflammatory and neoplastic lesions in cats with LGITL, a previous history of LPE or both.³⁴⁻³⁶ In addition, concurrent inflammation in the same or other parts of the gastrointestinal tract has been documented in up to 60% of cats with LGITL.³⁵⁻³⁹ The duration

of clinical signs has been documented to be significantly longer in cats with LGITL compared with LPE.⁴⁰ Epitheliotropism can be found in both entities.^{18,34,41,42} In some cases of LGITL, an apical-to-basal gradient has been described, suggesting chronic endoluminal antigenic stimulation; no LGITL cases have been shown to emerge from the depth of the mucosa.¹⁸ Minimal and mostly gradual differences within the fecal microbiome and metabolome of cats with LGITL or LPE have been reported and there is high similarity with perturbations seen in humans with IBD.^{32,43} Recently dysregulations of the janus kinase (JAK)-signal transducer and activator of transcription (STAT) pathway with high expression of STAT5 were documented in cats with LGITL.^{3,19} The JAK-STAT pathway plays a critical regulatory role in lymphocyte development, differentiation, and proliferation, and its dysregulation has been shown to be a major oncogenic driver in several lymphoma subtypes in humans.⁴⁴

3.3.3 | Other factors

The role of exposure to environmental tobacco smoke in the pathogenesis of CE in cats has been evoked but remains controversial. One study found a significantly increased risk of development of lymphoma in cats exposed to environmental tobacco smoke. However, this study did not specify the type of lymphoma.⁴⁵ A second study did not find any association between hair nicotine concentration and the development of gastrointestinal lymphoma.⁴⁶

3.4 | Signalment and clinical presentation

Statement

There are currently no known pathognomonic signalment or clinical findings that can reliably distinguish between LPE and LGITL in cats, because both conditions overlap with a wide range of presentations, including no clinical signs at all

Evidence level

II/III

Panel vote

6 out of 6 members strongly agreed

Cats with LGITL^{38,47,48} have been reported to be older than cats with LPE⁴⁹⁻⁵² (median ages, 13 and 8, respectively). However, a significant age overlap exists with LPE ranging from 1.3 to 16 years vs LGITL ranging from 4 to 20 years. Interpretation of the pertinent literature is challenging because of inconsistent use of classification schemes. Recent studies imply that LGITL is very uncommon in cats under 8 years of age.⁴⁰ The role of breed is unclear. To date, no specific association has been found consistently between breed and LGITL in cats, although domestic shorthair and Siamese breeds are over-represented in some studies of AL.^{38,39,53} Some studies also have mentioned an overrepresentation of male neutered cats.^{39,40,54}

Duration of clinical signs before presentation is generally chronic in both cats with LPE and LGITL. However, a recent study found clinical signs to be present for longer in LGITL cats (median, 365 days; range, 62-1460 days) compared with LPE cats (median, 107 days; range, 7-1095 days; $P < .001$).⁴⁰ In contrast to dogs, the clinical phenotype of CE in cats is not dominated by diarrhea. Other common clinical signs include weight loss, lethargy, hyporexia, polyphagia, vomiting, and more rarely constipation.^{32,36-38,43,47,48,52,55-63} No study found significantly different clinical signs in cats with LPE or LGITL, and cats with LGITL can present with minimal or even no clinical signs.⁶⁴ The absence of diarrhea does not rule out severe intestinal disease including LGITL. Although weight loss is the most common clinical sign, it often is overlooked by clients or even veterinarians. Cats can have substantial sarcopenia, especially of epaxial muscles whereas an abdominal fat pad is preserved.

Findings on physical examination may include abdominal pain or discomfort and diffusely thickened bowel loops. Mesenteric lymphadenopathy may be found on abdominal palpation and large abdominal masses or lymph nodes more often reflect higher grade gastrointestinal lymphomas or other diseases including other neoplasms, infectious diseases (e.g., feline infectious peritonitis [FIP], fungal disease, mycobacteria), or gastrointestinal eosinophilic sclerosing fibroplasia of cats. The clinical presentation can vary widely depending on the individual cat and possible comorbidities, such as hyperthyroidism, chronic kidney disease, chronic pancreatitis, chronic cholangitis, urolithiasis, and hypertrophic cardiomyopathy. Also, cats with LPE or LGITL may have a normal physical examination findings.

3.5 | Anatomical location

Any part of the gastrointestinal tract can be affected by LPE or LGITL, but some locations are more frequently reported in LGITL: jejunum, ileum, duodenum, stomach, and colon, in descending order of occurrence.^{34,35,38} The stomach is more commonly involved in cats with large cell lymphomas,^{34,38,65,66} but is rarely affected by LGITL and has not been reported to be exclusively affected without involvement of the small intestinal tract. Although colonic involvement in cats with LPE is more common, it is rare in cats with LGITL.

3.6 | Laboratory data

Statement

Laboratory tests cannot differentiate between LPE and LGITL and currently there are no specific cancer markers for LGITL in cats. Low serum cobalamin concentrations are more frequent in cats with LGITL.

Evidence level

II

Panel recommendation

6 out of 6 members strongly agreed

Laboratory tests are always required to distinguish CE from other diseases causing chronic gastrointestinal signs and a typical diagnostic evaluation involves a CBC, serum biochemistry panel, urine and fecal analyses, and total thyroxine concentration. Cats with outdoor access or those in multi-cat households should be tested for FeLV and FIV, given the previously reported associations with intestinal lymphoma.^{1,61}

Interpretation of the literature regarding laboratory data and biomarkers was substantially compromised because not all studies reliably differentiated between LPE and LGITL or provided information on the fraction of cats with biochemical changes. Today, there is no single biomarker or biomarker panel that reliably diagnoses LPE or LGITL in cats. However, laboratory tests are needed to rule out metabolic, endocrine, and infectious diseases as well as exocrine pancreatic insufficiency, pancreatitis, or chronic cholangitis, the latter 2 often occur concurrently with a CE.^{52,55,58,67-74}

The current paradigm in veterinary medicine requires differentiating food-responsive enteropathies from CE using dietary trials. However, the differentiation of LPE and LGITL requires more advanced diagnostic techniques such as histopathology, immunohistochemistry and PCR for antigen receptor rearrangement (PARR). That said, even with the most advanced techniques, ambiguous cases still remain and the distinction between LPE and LGITL is not entirely clear today.

Hypoalbuminemia, although common, is usually mild and may be because of negative acute phase reactivity or enteral loss with reports ranging from 14% to 100% of cases.^{40,50,75,76} Severe protein-losing enteropathy and marked hypoalbuminemia are extremely rare in cats with CE. Total protein concentration is often normal or even increased because of concurrent hyperglobulinemia and an increased total protein concentration is part of the feline chronic enteropathy activity index (FCEAI).⁵² In addition, mild hypoglobulinemia and pan-hypoproteinemia also are described in both LPE (39%) and LGITL (55%).^{40,75} Increased liver enzyme activities have been reported in cats with LPE and LGITL.^{40,52,77} One study found increased ALT serum activity to be predictive of histopathological severity of LPE, and ALT activity was included as a parameter in the FCEAI.⁵² Another recent study found increased liver enzyme activity in only 14% of cats with LGITL and in 0% of cats with LPE, and ALT was significantly different between the groups.⁴⁰

Acute and chronic pancreatitis has been identified in humans with IBD.⁷⁸ Frequent reports also exist in cats with CE, based both on histopathological results and increased feline pancreatic lipase immunoreactivity (f-PLI) serum concentration.^{68,71,72,79} Although the prevalence of pancreatitis appears to be higher in cats with CE, histopathological lesions consistent with pancreatitis are also common in clinically healthy older cats, and their occurrence has been correlated with age.⁷⁹ Anecdotal evidence seems to be high, but few comprehensive studies are available, and the true association or even causative relationship between CE and pancreatitis in cats remains to be assessed.⁸⁰ Similar to dogs, the presence of increased f-PLI serum concentration or

ultrasonographic changes alone may not be truly representative of disease status, and it is currently unclear whether extrapancreatic disease can lead to increased serum f-PLI concentrations in cats as reported in dogs.⁸¹ Whether pancreatitis is truly linked to CE or an incidental comorbidity, it should be ruled out using a combination of clinical signs, serum f-PLI concentration, imaging findings and pancreatic histopathology.

Few retrospective studies have investigated signalment, clinical signs, and concurrent diseases in cats with exocrine pancreatic insufficiency (EPI).^{74,82} They highlight EPI as an important differential diagnosis of CE in cats. One study showed an association between CE and EPI in cats based on ultrasonographic findings, intestinal biopsy results or both.⁸² Therefore, feline trypsin-like immunoreactivity (f-TLI) should be assessed in cats with clinical signs of chronic gastrointestinal disease and EPI should be considered as a differential diagnosis as well as a potential comorbidity.

Cobalamin and folate are water soluble vitamins present in dietary proteins and folates are synthesized by intestinal bacteria. Cobalamin binds to intrinsic factor which, in cats, originates exclusively from pancreatic secretion.^{83,84} Although folate is absorbed in the proximal small intestinal tract, cobalamin mainly is absorbed in the distal small intestinal tract, especially the ileum.^{83,85} Therefore, decreased serum concentrations of either or both B vitamins may give clues to disease localization. Hypocobalaminemia frequently has been documented in cats with CE with a reported prevalence between 18% and 80%.^{40,47,67,73,75,86-93} In studies that compared serum cobalamin concentrations between cats with LPE and those with LGITL, the prevalence of hypocobalaminemia was reported to be significantly higher in cats with LGITL.^{40,67,88,89,94} An increase in serum methylmalonic acid (MMA) concentration indicates cellular cobalamin deficiency and hence has been investigated in correlation with serum cobalamin concentrations in cats.^{87,88,95,96} Serum cobalamin concentrations of <209 and 290 ng/L have been shown to have sensitivities of 51% and 74% and specificities of 96% and 80% for an increase of serum MMA indicating cellular cobalamin deficiency.^{88,95} However, given the safety profile of cobalamin supplementation, identification of the serum concentration with the highest sensitivity for increases in MMA would be desirable. Conversely, cats with clinically relevant gastrointestinal disease may have normal serum cobalamin concentrations, and the absence of hypocobalaminemia does not exclude any gastrointestinal disease.⁸⁹ Increased serum cobalamin concentrations have been associated with inflammatory, immune-mediated, hepatic, and neoplastic diseases in cats.^{97,98}

Both, hypofolatemia and hyperfolatemia have been reported in cats with CE.^{47,67,75,87} Increased folate concentrations have been associated with small intestinal bacterial overgrowth in people,^{99,100} but an association with dysbiosis in dogs and cats is not documented. One study reported serum folate concentrations of 15.5 µg/L to have a 80% sensitivity and 100% specificity for a diagnosis of LGITL in cats. However, hemolysis can cause

clinically relevant increases in serum folate concentrations and thus should be considered when interpreting results.^{89,101} Folate supplementation has been shown to be beneficial in people with IBD and hypofolatemia¹⁰² but no data has been published in cats.

Other biochemical abnormalities reported in cats with chronic gastrointestinal disease are iron deficiency anemia, hypophosphatemia, hypovitaminosis D, increased serum lactate dehydrogenase (LDH) activity.^{60,86,96,103} However, none of these markers has been shown to differentiate LPE from LGITL in cats. Feline thymidine kinase 1 recently has been suggested as a new specific biomarker in cats with lymphoma.^{104,105} However, studies have not specifically investigated its value for LGITL, but included multiple lymphoma subtypes or lacked an appropriate control group including inflammatory intestinal lesions.^{104,105}

3.7 | Diagnostic imaging

Statement

Abdominal ultrasonography is an important diagnostic tool in the diagnostic evaluation of cats with CE. It allows for cross-sectional evaluation, anatomical localization, characterization of bowel wall mural architecture, and mesenteric lymph nodes as well as evaluation of other abdominal organs. The sonographic abnormalities of CE have been well described, however, substantial crossover between the LGITL and LPE exists and clinically relevant pathology can be present in the bowel with a normal ultrasound appearance. Thus, currently no imaging technology reliably differentiates LPE from LGITL, and intestinal histopathology is required for establishing the diagnosis of CE.

Evidence level

II/III

Panel recommendation

5 out of 6 members strongly agreed, 1 member agreed

3.7.1 | Radiography

Limited data on the diagnostic utility of abdominal radiographs in cats and only few studies in dogs with clinical signs of CE are available.^{76,106-110} Two studies comparing planar radiographs to abdominal ultrasound examination (AUS) in cats found radiographs either nondiagnostic⁷⁶ or diagnostic in only 1.9% of cases.¹⁰⁷ In cats with clinical signs of abdominal disease, combined assessment of radiographs and AUS allowed for a final diagnosis of renal disease or abdominal masses in 23.8% of cases; none of the cats was diagnosed with diffuse gastrointestinal disease.¹⁰⁷ Although radiographs may be useful to exclude abdominal masses and obstructions,¹⁰⁶ they appear rarely to provide additional benefits to AUS.

3.7.2 | Abdominal ultrasound examination

Various studies have investigated the diagnostic utility of AUS for the diagnosis and differentiation of LPE from LGITL in cats,^{40,52,58,62,65,67,69,111} and evidence suggests that AUS is a critical step in the diagnostic evaluation of cats with clinical signs of chronic gastrointestinal disease. Besides the assessment of the intestinal tract, AUS allows for diagnostic evaluation of other organs, including the liver and biliary system, the pancreas, abdominal lymph nodes, the spleen, and the urinary tract. This feature is particularly important because multiple comorbidities often are identified in older cats and the term triaditis has been coined to describe the concurrent occurrence of LPE, pancreatitis, and cholangitis in cats.^{71,72,112} In addition, AUS is a useful tool for identifying abnormal intestinal segments and helps with planning subsequent diagnostic procedures such as full-thickness laparotomic vs endoscopic biopsies. It also can be used in AUS-assisted fine needle aspiration of enlarged lymph nodes, abdominal masses, or aspirates of the liver and spleen.

Diffuse thickening of the muscularis propria, submucosa, or mucosa layer in the small bowel is the most common ultrasonographic finding and has been observed in 50% to 95% of cats with CE.^{3,38,40,58,62,65,69,93,111} Again, the interpretation of the pertinent literature is challenging because the evaluated variables vary between total intestinal wall thickness and muscularis or mucosal layer, and not all studies specify the segment imaged by ultrasonography. Currently available data suggest that substantial overlap exists for ultrasonographic changes of the intestinal wall between cats with LPE and LGITL. Two studies showed that cats with LGITL had significantly increased thickness of the muscularis propria layer¹¹¹ or the mucosa,⁴⁰ compared with cats with LPE. A single prospective study showed that the jejunal mucosal wall layer was significantly thicker in cats with LGITL (median, 1.4 mm; range, 0.7-2.3 mm) compared with LPE (median, 1.0 mm; range, 0.4-2.8 mm).⁴⁰ Various studies have investigated the predictive value of ultrasonographic findings for the identification of histopathologic lesions with highly variable results.^{69,111,113} Although 2 studies found high predictive value of ultrasonographic changes for the presence of transmural disease¹¹¹ or

unspecified histopathologic small intestinal disease,⁶⁹ these findings were not confirmed by others.¹¹³ The latter study found that although ultrasonographic abnormalities in the mucosa were highly predictive of mucosal histologic lesions, the presence of thickened submucosa or muscularis layer did not correlate with histopathologic lesions in these segments.¹¹³ A major caveat of these approaches is that a substantial overlap exists between healthy cats and cats with CE and that both ultrasonographic and histopathologic changes also have been documented even in clinically healthy cats.^{64,65,111} Hence, the presence of either is not necessarily predictive of clinical disease. One study evaluated the muscularis-to-submucosa ratio and the muscularis-to-mucosa ratio in cats with LPE and LGITL compared with healthy cats (Figure 1). Although the muscularis-to-submucosa ratio was lower in healthy cats than in cats with LPE or LGITL, in some small intestinal segments, the muscularis-to-submucosa ratio was not significantly different between groups.⁶⁵ In this study, a muscularis-to-submucosa ratio >1 was indicative of an abnormal bowel segment, but no difference was found between LPE and LGITL.⁶⁵ Eosinophilic enteritis has been identified as an important differential diagnosis in cats with diffuse thickening of the muscularis layer.¹¹⁴ In a retrospective study, cats with eosinophilic enteritis had a significantly thicker muscularis layer than cats with lymphoplasmacytic enteritis.¹¹⁴

Several studies have investigated abdominal lymphadenopathy in cats with LPE and LGITL compared with healthy cats.^{40,65,111} Results of 2 studies found median or mean lymph node size to be significantly higher in cats with LGITL compared with healthy cats, but no difference between LPE and LGITL was found.^{65,111} One study found that jejunal lymph node size, echogenicity, and structure was significantly different in cats with LGITL compared with cats with LPE. Jejunal lymph nodes in cats with LGITL were significantly thicker (LGITL: median, 6.7 mm; range, 2.9-12 mm; LPE: median, 4.2 mm; range, 1.8-8.8 mm), significantly rounder and more hypoechoic compared with cats with LPE (Figure 2).⁴⁰ The same study showed that the presence of mild abdominal effusion tended to be associated with a final diagnosis of LGITL (45% in cats with LGITL vs 14% in cats with LPE).^{40,94} Specific lesions in liver and spleen that allow for differentiation of LPE from LGITL have not been reported in cats.

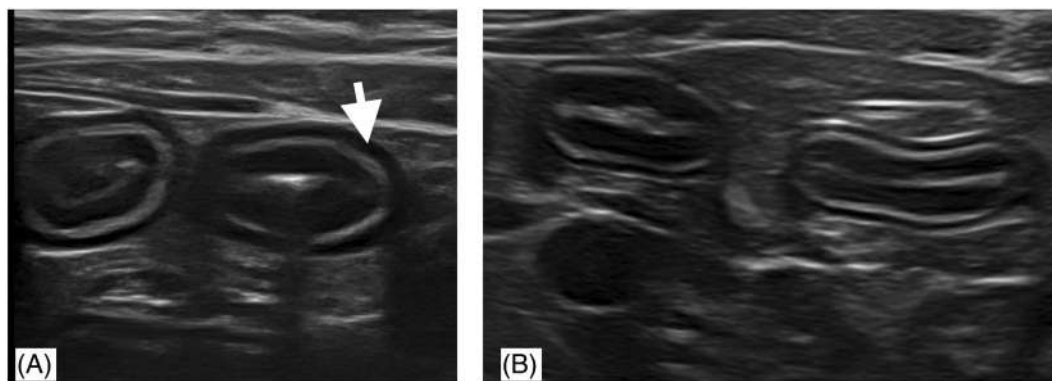


FIGURE 1 (A) Ultrasonographic aspect of the jejunum in cats finally diagnosed with a CE (LPE or LGITL): the muscularis layer is diffusely thickened (arrow). (B) Normal aspect of the jejunal wall.

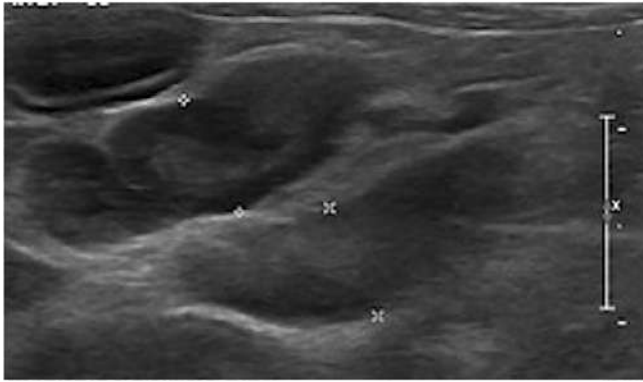


FIGURE 2 Ultrasonographic aspect of the jejunal lymph node in a LGITL case. The lymph node appears rounded and hypochoic.

Conversely, a study on ultrasonographic findings in 22 cats with hypcobalaminemia reported the absence of ultrasonographic changes in 54% of cats with LPE, in 15% in cats with LGITL, and in 12% with other intestinal neoplasia. One cat with unremarkable abdominal ultrasound examination was later diagnosed with histoplasmosis.⁹³ This observation indicates that the absence of ultrasonographic changes does not exclude the presence of clinically relevant gastrointestinal disease in cats.

Similar to other diagnostic tests, interpretation of relevant literature evaluating ultrasonography is difficult because of variable equipment (especially over time), interobserver variability, the nature of the study (prospective vs retrospective, study approach [i.e., from a radiology, internal medicine, or pathology point of view]), the number of cases, enrollment criteria of healthy or diseased cats, segmental or subclinical disease, the presence of concurrent diseases, different lymphomas, and previous treatments including antimicrobials, and immunosuppressants.

No studies currently are available on the merit of other imaging modalities such as computer tomography (CT) or magnetic resonance imaging (MRI) for the diagnosis or differentiation of cats with LPE or LGITL.

3.8 | Cytology

Statement

Although cytology is helpful to exclude important differential diagnoses in cats with CE, cytology cannot be used to differentiate LPE from LGITL.

Evidence level

III

Panel recommendation

5 out of 6 members strongly agreed, 1 member agreed

Cytology can be of benefit in the diagnostic evaluation of cats with clinical signs of CE and is often the first line of diagnosis in cats

with abdominal masses, lymphadenomegaly, or organomegaly. Fine needle aspirates can be helpful in excluding important differential diagnoses such as high-grade lymphomas, other round-cell neoplasia, or fungal disease.^{23,61,115-120}

However, because of the lack of architectural information and overlapping cellular morphology, cytologic examination of fine needle aspirates from the intestinal wall is not helpful for reaching a definitive diagnosis of either LPE or LGITL (Figure 3). Lymphoplasmacytic enteritis in cats is characterized by a mixed infiltrate of mature lymphocytes and plasma cells. The infiltration generally is located in the lamina propria and in some areas extending into the epithelium. Inflammatory lesions can occur with architectural changes such as crypt distortion and villus blunting.^{41,42} Well-differentiated, mature, small lymphocytes are the hallmark of LGITL in cats. Architectural alteration of the lamina propria and epithelium can vary from minimal compromise to complete effacement.^{18,37,61,63,121-124} Concurrent inflammatory changes are seen often.^{34,35,55,58,69,125} No value is added by performing a jejunal lymph node fine needle aspirate compared with histopathologic evaluation of the intestinal wall alone. A recent study investigated the use of needle rinse cell block technique for the diagnostic evaluation of gastrointestinal nodular lesions.¹²⁶ In this technique, a cell pellet is formed from fine needle aspirates, embedded in formalin and processed conventionally into a hematoxylin and eosin (H&E)-stained histology slide. However, although this technique appears to be an interesting ancillary tool for gastrointestinal nodular lesions, it does not add architectural context over that obtained using conventional cytology.

3.9 | Biopsies

Statement

The collection of intestinal tissue biopsy specimens is the current gold standard for the diagnosis of and differentiation between LPE vs LGITL in cats. No clearly demonstrated superiority in quality exists for biopsy specimens obtained by laparotomy (full thickness) vs endoscopic biopsy specimens, because poor technique can affect sample quality and hamper diagnostic evaluation for both methods. It has been shown that all inflammatory and neoplastic lesions are present in the lamina propria and hence, if mucosal samples of sufficient quality are procured endoscopically, a diagnosis is possible without obtaining full-thickness biopsy specimens. However, because of limited access to the jejunum by endoscopy, jejunal lesions cannot be reliably sampled although this small intestinal segment is frequently abnormal.

Evidence level

II

Panel recommendation

4 out of 6 members strongly agreed, 2 members agreed

The current gold standard for the diagnosis and differentiation of CE in cats requires collection and histopathologic examination of intestinal tissue biopsy specimens. However, the optimal sampling technique is still a matter of controversy.

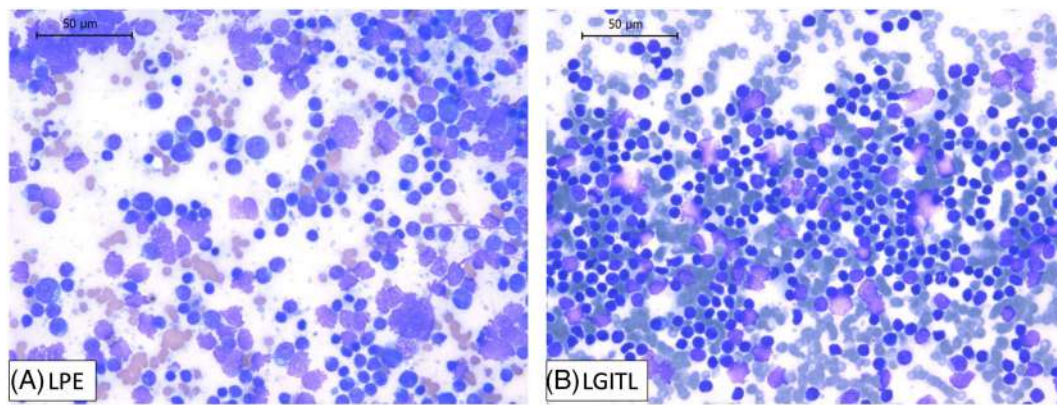


FIGURE 3 (A) Fine needle aspirate of an enlarged mesenteric lymph node from a cat later diagnosed with lymphoplasmacytic enteritis on small intestinal tissue biopsies. The aspirate mostly comprises small mature lymphocytes and reactive lymphocytes. One mitotic figure is visible ($\times 100$). (B) Fine needle aspirate of an enlarged mesenteric lymph node from a cat later diagnosed with small cell lymphoma on small intestinal tissue biopsies ($\times 100$). The aspirate mostly comprises small mature lymphocytes with few plasma cells in a blood-contaminated background. The number of small lymphocytes is not predictive of the final diagnosis and the sample is not diagnostic for small cell lymphoma.

Laparotomy is a widely available technique that can be performed in most small animal hospitals. It allows for sampling of full-thickness intestinal biopsy specimens and extraintestinal biopsy specimens. Furthermore, with laparotomy, jejunal samples can be collected, which can be important because the jejunum has been reported to be the most frequently affected intestinal segment in both diseases.^{34,37,38} In addition, extraintestinal samples can be of value in cats with comorbidities such as hepatic or pancreatic disease or in cases with localized or eccentric intestinal lesions based on prior ultrasonographic assessment. Biopsy specimens obtained by laparotomy allow for the assessment of the entire gastrointestinal wall, but lesions of LPE and LGITL generally originate in the mucosa and may expand transmurally from there.^{18,34} Transmural infiltration however has not yet been convincingly shown to be associated with shorter survival in cats with LGITL. One study comparing survival times in cats with mucosal and transmural infiltrates found cats with transmural T-cell lymphomas to have shorter survival times (median, 1.5 months) compared with cats with mucosal T-cell lymphomas (median, 29 months).³⁴ However, most transmural lymphomas were classified as large cell lymphomas including large granular lymphocyte lymphomas, the latter of which typically carry a grave prognosis with reported median survival times of 5 to 90 days.¹²⁷ Survival data on transmural LGITLs was only available for 4 cats with a range of survival between 3 days and 28 months. The limited number of samples (usually ≤ 5 biopsy specimens are collected) taken at laparotomy and the inability to see the mucosa while selecting a site for sample collection are major limitation of this technique. The low number of specimens results in a limited mucosal area available for analysis. Additional disadvantages include risks associated with surgery such as dehiscence, prolonged recovery time, wound healing complications, and the necessity to postpone treatment until wound healing is complete. Also, the diagnostic yield of the technique can be hampered when wedge-shaped biopsy specimens are obtained, which represents a common operator-related error. Wedge-shaped biopsy specimens have a large serosal area that funnels down

through the muscularis into the mucosa. These biopsy specimens often appear of sufficient size, but the assessable mucosal area is small, damaged, or even absent. Occasionally, the mucosa, submucosa or both detaches from the muscularis and is lost during processing (Figure 4).

By contrast, endoscopy is mostly available at referral centers and few animal hospitals. It allows for direct visual examination of the mucosal surface and is minimally invasive. Targeted biopsy specimens from mucosal sites with gross lesions can be collected, which can be advantageous when lesions are distributed in a multifocal pattern. Furthermore, if necessary, medical treatment can be started immediately after endoscopy pending histopathology results. With appropriate endoscopic equipment, the proximal jejunum can regularly be examined and biopsied, although lesions located in the mid to distal jejunum are outside the range of the endoscope. Limiting factors for endoscopic procedures include difficult pyloric intubation, loss of pyloric elasticity, and acquired pyloric narrowing in cats with CE.¹²⁸ Moreover, intubation of the ileum may present a challenge in some cases where the angulation of the ileo-colic junction does not allow for entry into the distal ileum. Operator-related errors include inadequate sample number or quality (e.g., superficial samples consisting only of crushed villi). One study reported that a minimum of 6 mucosal biopsy specimens of adequate quality from the duodenum of cats and 3 to 5 from the ileum are required for a reliable histopathological evaluation.¹²⁹ However, another study determined that 10 to 15 duodenal biopsy specimens were required to confirm mild inflammatory lesions with confidence of at least 90%.¹²⁹ Studies in dogs¹³⁰ and cats¹³¹ indicated that size of the forceps was correlated with the quality of the biopsy specimens and that larger capacity forceps provide superior sample quality. The presence of a spike in the center of the biopsy forceps was not found to have any effect on sample quality in dogs.¹³⁰ A study evaluating quality and adequacy of biopsy specimens collected using reusable or single-use forceps did not identify any difference in the quality of biopsy specimens in dogs.¹³²

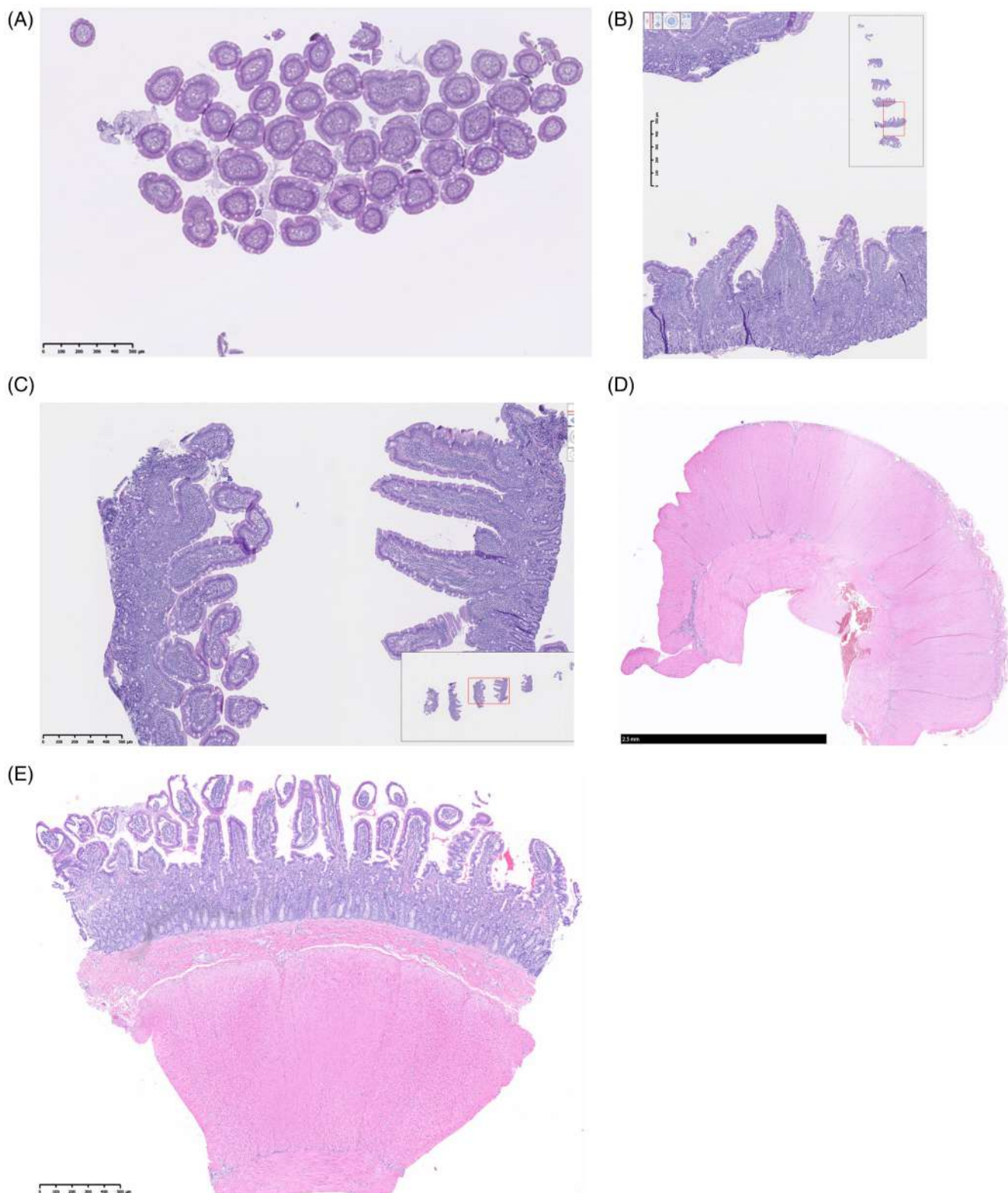


FIGURE 4 (Orientation) Hematoxylin and Eosin-stained endoscopically obtained biopsy specimens from cats with chronic enteropathies illustrating common errors associated with endoscopic (A-C) or surgical (D, E) biopsies. (A) Suboptimal sample orientation led to cutting this biopsy specimen tangentially, resulting in “villus slaw.” The biopsy specimen is uninterpretable. (B,C) Examples of optimally oriented biopsy specimens from the same slide. Villi and crypts are cut parallel to the lamina propria and the entire lamina propria is visible for optimal interpretation. The images are the $\times 5$ magnification of the red square in the slide map on the bottom right of images B and C. (D) Full-thickness duodenal biopsy specimen. While the biopsy is large and well-oriented the entire mucosa is missing making this specimen uninterpretable. (E) Full-thickness duodenal biopsy specimen. The biopsy specimen is well-oriented and fully accessible for histopathologic assessment. All biopsies on the slide are optimally oriented.

One prospective study directly compared endoscopically-obtained gastric and duodenal biopsy specimens with full-thickness biopsies obtained from the stomach, duodenum, jejunum, and ileum via laparotomy or laparoscopy in 22 cats with LPE or AL.⁶² The authors concluded that endoscopically-collected biopsy specimens were inadequate for accurate differentiation of LPE from LGITL and that surgically-acquired full-thickness biopsy specimens from the jejunum and ileum were necessary for accurate diagnosis. However, the study only required the collection of 6 endoscopic duodenal biopsy specimens, and not all duodenal specimens were deemed adequate by the pathologist. In at least 5 cats, the endoscope was not passed through the pylorus into the duodenum and biopsy specimens were collected blindly with ≥ 3 specimens collected.

A second retrospective study assessed the diagnostic value of full-thickness intestinal biopsy specimens utilizing a 4 mm punch biopsy and extraintestinal biopsy specimens from cats with chronic signs of gastrointestinal disease. The authors concluded that full-thickness biopsy specimens were helpful in the diagnosis. However, they did not directly compare full-thickness and endoscopic biopsy specimens or investigate the agreement between diagnoses when considering all available samples vs limiting diagnosis to the mucosa.¹³³

3.10 | Histopathology and immunohistochemistry

Statement

Histology is required for the diagnosis and differentiation of LPE from LGITL in cats. It requires proper sampling, processing, and interpretation of key lesions (which includes inflammatory infiltrates, neoplastic cells, and other intestinal wall changes).

Ambiguous cases often require ancillary tests such as immunohistochemistry and clonality tests.

Evidence level

II/O

Panel recommendation

6 out of 6 members strongly agreed

3.10.1 | Histology

Histopathologic examination of H&E-stained biopsy specimens remains the gold standard for the diagnosis and differentiation of CE in cats, and preparation of biopsy specimens (including orientation) is critical. Even adequately collected samples can lead to suboptimal or even inadequate H&E staining if specimens are misoriented (Figure 4). One study compared mounting intestinal biopsy specimens on cucumber slices or moisturized synthetic foam sponges to free flotation in formalin¹³⁴ and determined that mounted samples had significantly fewer artifacts and that pathologists had higher confidence in their histopathologic interpretation. Some histopathology laboratories orient free-floating samples before paraffin embedding. Like mounting, proper orientation of the sample during embedding can improve diagnostic

accuracy. Figure 5 and Video S1 explain the process of orientation before embedding the sample in paraffin.

Even with adequate sample numbers and quality and optimal processing, it can be difficult to arrive at a precise diagnosis. Such cases require additional diagnostic tests including immunohistochemistry and clonality tests as discussed in later sections.

Clinicians should attempt to build a strong communication connection with their pathologist to optimize sample quality and report interpretation for the best possible patient care.

Interobserver variability among pathologists can be a concern. One study investigating the agreement among 5 different pathologists assessed the degree of cellular infiltrates in the intestinal mucosa of dogs and cats and identified a very high rate of interobserver variability.¹³⁵ As a response, the World Small Animal Veterinary Association (WSAVA) histopathology standardization group was formed and published criteria for the histopathologic assessment of endoscopic samples from the gastrointestinal tract in dogs and cats in 2008. A standard form was developed including a grading scheme from 0 (normal) to 3 (severe), assessing architectural changes (epithelial injury, villus blunting, crypt distention, fibrosis, and lacteal dilatation) and the degree and quality of cellular infiltrates in the mucosa.^{41,42} However, interobserver variability remains an issue despite attempts to simplify the grading scheme.¹³⁶ In addition, the scope of the WSAVA standardization did not encompass the differentiation of LGITL from LPE in cats, and the standardization was designed and validated only for IBD. Since the WSAVA recommendations were published, a new histopathological assessment scheme for the assessment of intestinal biopsy samples from cats with CE has been proposed.¹⁸ The scheme is based on the 2016 revision of the World Health Organization (WHO) classification of lymphoid neoplasms in humans,² the WHO classification of lymphoma in dogs, immunohistochemical expression of CD3, upregulation of STAT 5, and Ki67 expression (see Section 3.10.2), and clonality analysis in cases with lymphoma. Different patterns of cellular distribution in LGITLs have been recognized by pathologists, ranging from massive infiltration of the lamina propria with complete effacement of the lamina propria and loss of architecture, and marked epitheliotropism, to more subtle forms including specific patterns such as gradients within the lamina propria or nests or plaques or both within the intraepithelial compartment (Figure 6). Based on findings in a variety of cases, lesions appear to originate in the apical part of the villi and expand through the lamina propria or even transmurally. In the newly proposed histopathology grading scheme created for cats, differentiating LPE from LGITL can be improved if epithelium and lamina propria are assessed separately and in a structured fashion.¹⁸

Regardless of the assessment scheme used, histopathologic examination of H&E-stained biopsy specimens can be insufficient to reach a final diagnosis, and immunohistochemistry can be a valuable tool in ambiguous cases. Ambiguous cases present both inflammatory and neoplastic features, such as epitheliotropism in a polymorphic background, inconsistent nest or plaque identification within single villi, and areas of monomorphic lymphocytes within the lamina propria in an otherwise polymorphic background.

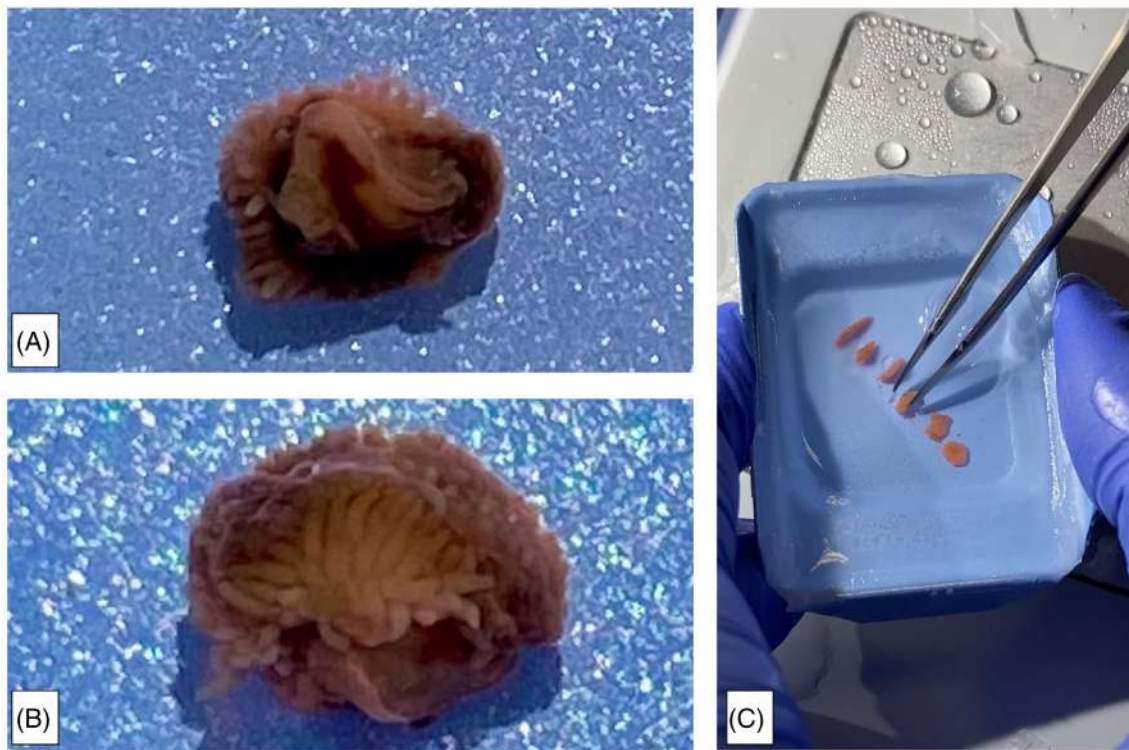


FIGURE 5 (Orientation): Histologic processing of endoscopically obtained formalin-fixed biopsy specimens by a histologist. (A) Jejunum biopsy specimen. The specimen is upside down with the villi facing downward. (B) Jejunum biopsy after reorientation, Villi are visible, pointing upward. (C) The histologist is orienting biopsy specimens in a position that allows for cutting the specimen parallel to the lamina propria. In this image the four specimens on top have been reoriented, whereas the two bottom specimens are still in a tangential position. Courtesy of Kelly Mallet, Texas A&M Gastrointestinal Laboratory, College Station, TX.

Chronic inflammation potentially can increase the risk of developing LGITL, and concurrent LPE has been described in up to 60% of cases with LGITL.^{34,36-39} Thus, it has been hypothesized that LPE may precede or promote gastrointestinal neoplasia.^{38,61,63,121-123}

In addition, some cats diagnosed with LGITL have been observed to develop large cell lymphoma over time.¹³⁷ It is currently unknown whether these neoplasms represent true disease progression or are separate entities because the co-existence of lymphomas originating from distinct clones has been documented.³⁴ At this point, no single diagnostic test is available to reliably differentiate LPE from LGITL. The combination of clinical data (e.g., age, duration of clinical signs), imaging, laboratory data, histopathology, immunohistochemistry, and clonality assays appear to be the best approach to reach a final diagnosis. However, grading schemes and diagnostic tests are expected to evolve over time and eventually improve the accuracy of diagnostic testing and, most importantly, treatment options for affected cats. More biomarkers also are being developed and tested for sensitivity and specificity.

3.10.2 | Special stains and immunohistochemistry

Immunohistochemistry can be readily performed as a complementary technique to standard histology on formalin-fixed and paraffin-

embedded (FFPE) biopsy specimens (see Table 3). For ambiguous cases, it is an essential ancillary diagnostic tool. Immunohistochemistry utilizes specific antibodies to recognize and bind antigenic determinants (epitopes), enabling microscopic detection of biomarkers for differentiation and proliferation.^{34,36,51,121,138-141} Cellular infiltrates seen on H&E-stained sections can be interrogated for their differentiation by applying antibody markers thereby investigating whether an infiltrate appears monomorphic or mixed. Monomorphic infiltrates imply the presence of cellular clones whereas a mixed infiltrate implies the presence of antigenic stimulation during inflammation. However, this technique does not allow for absolute differentiation. Concurrent inflammation frequently is identified in adjacent or the same intestinal location in cats with LGITL.³⁵⁻³⁹ On the other hand, chronic antigenic stimulation has been described to lead to monoclonal lymphocyte proliferations.⁹ Commonly used antibodies for cellular phenotyping include cluster of differentiation (CD)3 to detect T-lymphocytes,^{34,36,51,56,121,139,141,142} CD20, CD79a, B lymphocyte antigen 36 (BLA.36), and paired box gene 5 (Pax5) for B-lymphocytes,^{34,36,51,138,140,143} macrophage marker antibody 387 (MAC387) for macrophages,^{18,144-146} and granzyme B to detect natural killer (NK) cells. Finally, the proliferative cell fraction can be assessed using Ki67 expression,^{147,148} a nuclear protein with maximal expression during M phase that is absent after mitosis is completed.¹⁴⁷ Most intestinal lymphomas in cats appear to be CD3 positive small cell

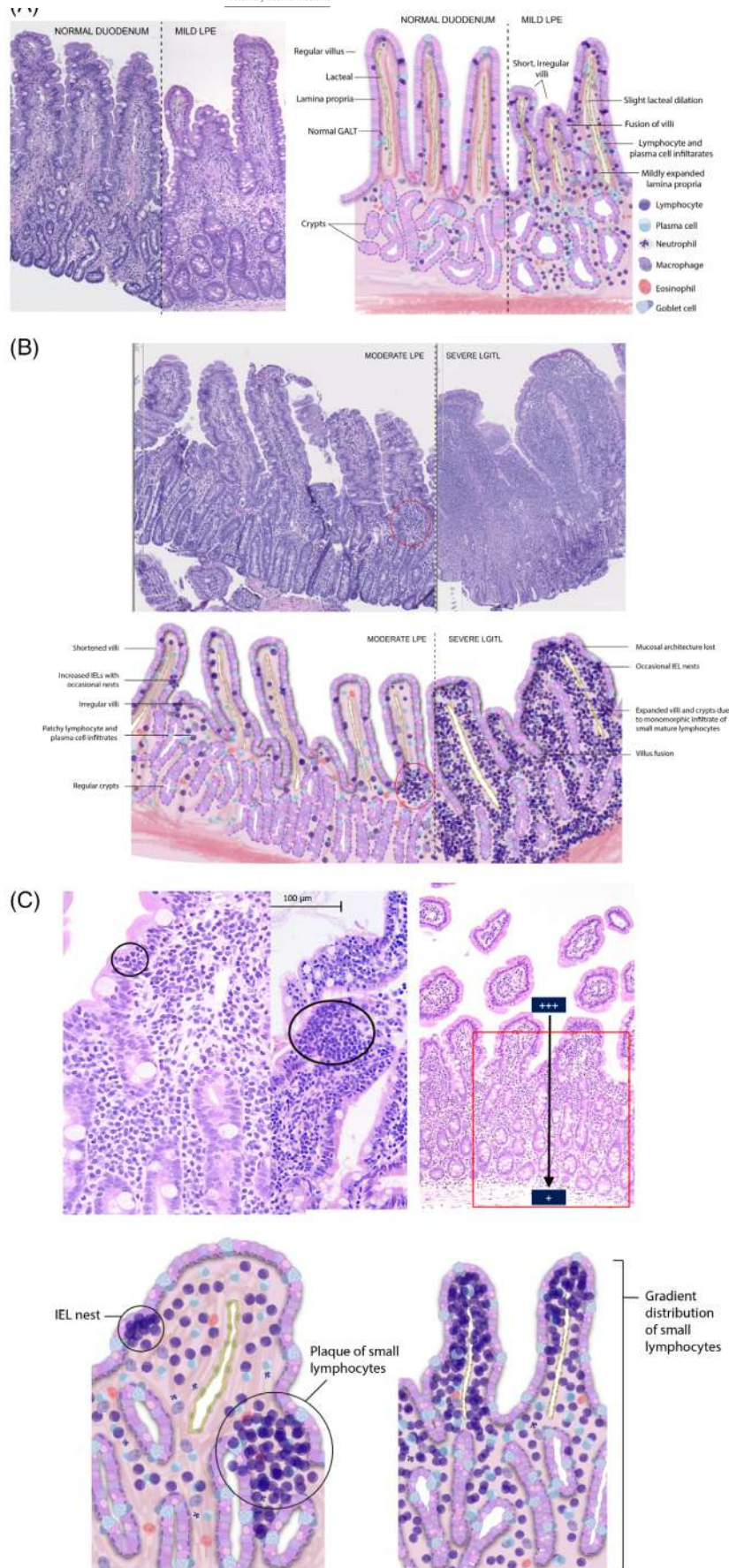


FIGURE 6 Legend on next page.

lymphomas that reportedly represent from 63% to 74% of all intestinal lymphomas (Figure 7).^{34,36} Other types of lymphoma include large cell T-cell lymphomas, B-cell lymphomas, NK cell lymphomas, and large granular lymphocyte lymphomas. However, interpretation of the pertinent literature is obscured because of highly variable inclusion criteria such as different anatomic sites, mucosal vs transmural lymphomas, different subtypes, FeLV+ vs FeLV- cats, and interobserver variability.^{54,63,140,149-152}

Since the advent of whole genome sequencing of the canine and more recently the feline genome, the field of comparative pathology has made considerable efforts to establish small animals as models for spontaneously occurring diseases in humans.¹⁵³ Canine and feline companions share many disease characteristics, including environment, biological behavior, histological appearance, genetic tumor mutations, and response to treatment with their owners. The EATL-type tumors are rare peripheral T-cell lymphomas arising from intraepithelial intestinal cytotoxic T-cell lymphocytes. Two disease variants are recognized by the current WHO classification in people, namely enteropathy-associated T-cell lymphoma (EATL)-Type I and EATL-Type II (recently renamed monomorphic epitheliotropic intestinal T-cell lymphoma [MEITL] or monomorphic CD56⁺ intestinal T-cell lymphoma).² Although EATL-Type I is associated with celiac disease, EATL-Type II (MEITL) is less common and infrequently associated with celiac disease. Because of its morphologic features, including size of lymphocytes and epitheliotropism, previous studies suggested LGITL as a relevant model of MEITL.^{19,34,154} However, despite LGITL having histologic similarities with MEITL, the clinical course of these 2 diseases and their immunophenotyping differ markedly. The MEITL neoplasms in humans co-express CD3 and CD56 (a natural killer cell marker), have high mitotic index with high expression rate of Ki-67, do not feature concurrent inflammatory lesions, and have an aggressive clinical course with a median survival time of only 7 months.^{2,57,155-157} In contrast, LGITLs in cats are generally slowly progressing, indolent neoplasms, with a low mitotic index and a low expression of Ki-67 (Figure 8), frequently featuring concurrent inflammatory lesions, and are characterized by CD3⁺/CD56⁻ cells.^{18,142} Moreover, 2 recent studies described a high expression of signal transducer and activator of transcription (STAT)5 in LGITL cases.^{3,41} In this context, STAT5 phosphorylation

suggests that the JAK/STAT signaling pathway could play a key role in LGITL (Figure 9).

The most recent WHO classification of lymphoid neoplasms in people was the first to include a new class of indolent gastrointestinal T-cell lymphoma in humans, gastrointestinal T-cell lymphoproliferative disorder (GI-TLPD).^{2,158} This subtype of intestinal lymphoma has a slow clinical course with a median follow-up time of >5 years (median survival time not reached).^{155,158-164} The disorder is characterized by small lymphocytes within the mucosa with variable epitheliotropism, high expression of CD3 (100%), variable expression of STAT5 (0%-44%), low expression of Ki 67 and STAT3, and absent expression of CD56.¹⁵⁵ Dysregulation of the JAK/STAT pathway has been well described in several lymphoma subtypes.^{44,165} The LGITL in cats bear striking similarities to GI-TLPDs in humans with respect to receptor expression profiles, mitotic indices, and clinical course and thus LGITL in cats recently has been validated as a relevant model for GI-TLPD in humans.^{18,57,142} Although LGITL in cats and GI-TLPD share many features including biological behavior, histopathologic characteristics, and immunophenotype (CD3⁺, STAT5⁺, CD56⁻) further research to determine whether the cell types are truly identical is required.⁵⁷

TABLE 3 Common immunohistochemical markers used in diagnostic samples from cats with lymphoplasmacytic enteritis and low-grade intestinal T-cell lymphoma (LGITL).

Cellular population or function	Antibody
T-cells	CD3
B-cells	CD 20, CD79a, BLA36, Pax5
NK-cells	Granzyme B, CD56
Macrophages	MAC387 (recognizes L1 protein, Calprotectin)
M-phase (cellular mitosis)	Ki-67
Upregulation of signal transduction as oncogenic markers	STAT3, STAT5
Cytotoxic T cells	TIA1
Calcium-binding protein expressed in neutrophils among other cells	S100/Calgranulin

FIGURE 6 Examples of histologic appearance of intestinal biopsy specimens from cats diagnosed with feline lymphoplasmacytic enteritis (LPE) or low-grade intestinal T-cell lymphoma (LGITL). (A) Hematoxylin and eosin (H&E) stained biopsy specimen of a normal feline intestine and mild LPE and their schematic views. There is a normal resident population of lymphocytes, plasma cells, macrophages, neutrophils, and eosinophils within the lamina propria. A small number of resident intraepithelial lymphocytes is present. Schematic view of a case of mild LPE (right). There is an increased population of lymphocytes and plasma cells present in the lamina propria. The number of IELs can be slightly increased. Architectural changes such as villus blunting, crypt distention, fibrosis, and epithelial injury may be present. (B) H&E-stained duodenal biopsy specimen from a cat with moderate LPE and marked LGITL and their schematic view. Left: Moderate numbers of lymphocytes and plasma cells are present in the lamina propria. An increased number of IEL as well as villus blunting can be observed. Right: H&E-stained biopsy specimen of a feline duodenum with unambiguous LGITL. A monomorphic population of small mature lymphocytes diffusely infiltrates and expands the lamina propria. Architectural changes such as severe villus blunting, fusion of villi, and crypt distention and distortion are frequently present. The villus-to-crypt transition is blurred and a clear distinction is often lost. (C) H&E-stained jejunal biopsies specimens histologic features in LGITL cases and their schematic view: nests, plaques, and gradient.

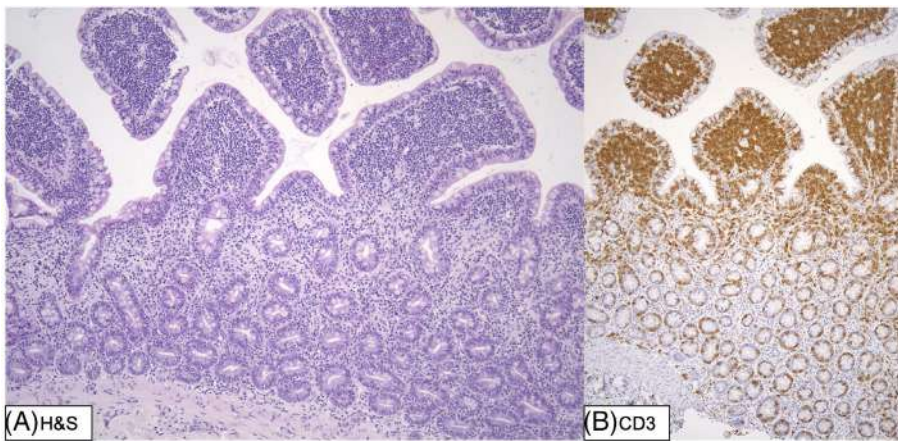


FIGURE 7 (A) H&E-stained jejunal biopsy specimen of a cat with LGITL. A monomorphic population of small mature lymphocytes with a gradient distribution most dense in the villus tips with a gradual decline toward the crypt area. (B) Anti-CD3 antibody staining of a jejunal biopsy specimen from a cat with LGITL with a gradient distribution as shown in A.

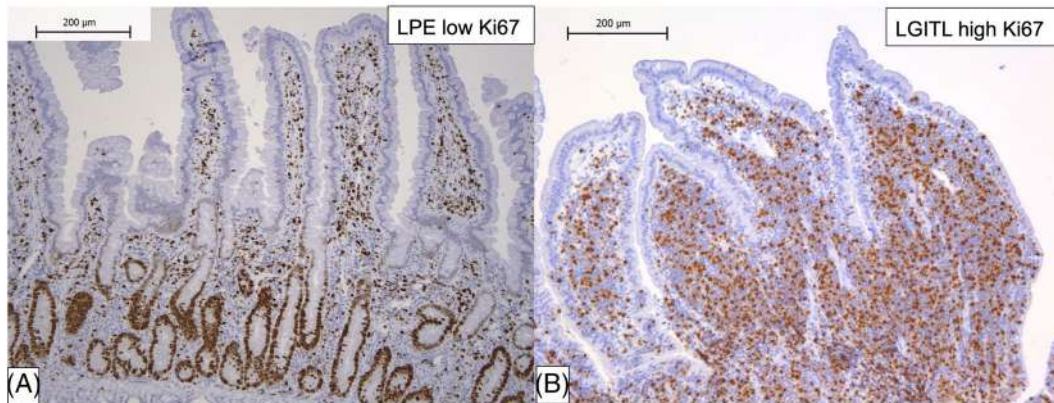


FIGURE 8 Comparative expression of Ki 67 in a LPE case (A) and a LGITL case (B).

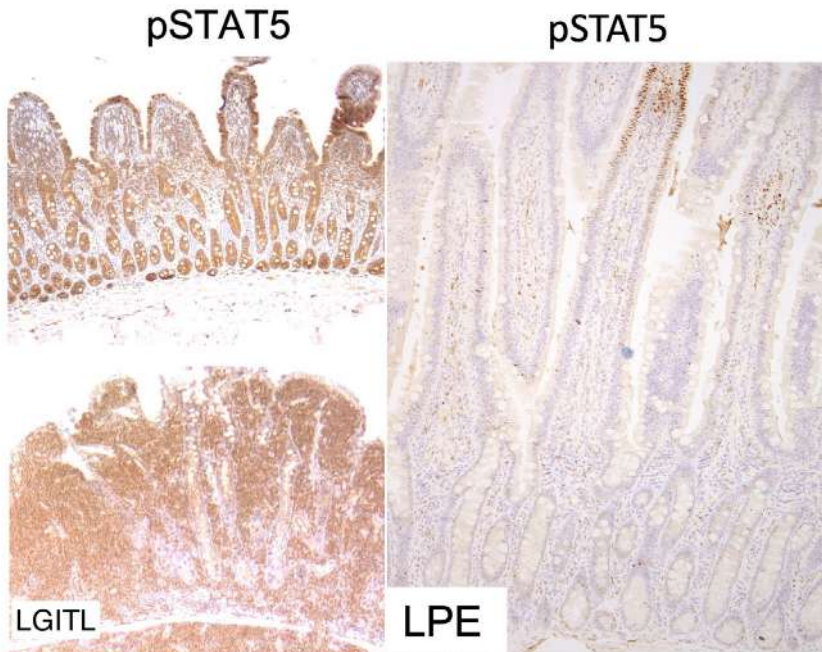


FIGURE 9 Comparative expression of STAT5 in a LGITL case (left) and a LPE case (right).

Recent studies investigated additional diagnostic and prognostic markers including TIA1 cytotoxic granule-associated RNA binding protein and S100/Calgranulin. The presence of intraepithelial TIA1⁺

cytotoxic lymphocytes was associated with poor prognosis in cats with LGITL¹⁶⁶; S100/Calgranulin was not discriminant between LGITL and LPE.⁹⁴

3.11 | Clonality analysis

Statement

Clonality can be an important part of the diagnostic evaluation of cats with CE. However, clonality must be interpreted in conjunction with clinical, histopathological, and immunohistochemical results and cannot be used as a sole means to reclassify cases.

Evidence level

II/O

Panel recommendation

6 out of 6 members strongly agreed

To differentiate neoplastic lymphoid proliferations from reactive lesions, tests assessing clonality increasingly have been used in veterinary pathology in conjunction with other diagnostic techniques, but only a few have been validated.^{34,35,167-179} Clonality assessment can be performed using different techniques including flow cytometry, Southern blot analysis and PCR. Polymerase chain reaction for receptor antigen rearrangement is currently the only technique that can be applied to FFPE tissue samples and thus it is the most commonly performed technique on biopsy specimens from cats with CE.^{35,167,169,180} The test is based on amplification of the CDR3 region of the T-cell receptor (TCR) for T-cells and immunoglobulin heavy chain genes for B-cells during repeat PCR cycles.^{11,17,35,37,174,175,180,181} A previous study was the first to report this diagnostic tool for intestinal T-cell lymphoma in cats.³⁵ A priori neoplastic lesions such as LGITLs are thought to consist of the proliferation of a single or few cell populations resulting in a clonal PCR product (monoclonal or oligoclonal), whereas reactive lesions are expected to consist of heterogenous lymphocyte populations leading to a polyclonal PCR product.^{34,35} However, deviations from this rule are occasionally described, which, beside technical challenges, limit the value of PARR as the final determining diagnostic technique as it has commonly been promoted in veterinary medicine.^{56,167,182}

Several technical challenges exist, including poor DNA quality, low amounts of target DNA (i.e., low numbers of T-cells, in patchy disease), and limited primer coverage. Formalin-fixation has been shown to cause cross-links and fragmenting of nucleic acid resulting in decreased fragment size in purified DNA.¹⁸³ The impact of fixation on an individual sample is difficult to predict but is likely related to the duration of fixation, temperature, and whether adequately buffered formalin is used.¹⁸³ In addition, the relatively small amount of tissue present in paraffin shavings used for DNA extraction further limits the potential DNA yield.¹⁷ Standardized protocols in human medicine include a control PCR amplifying multiple differently-sized gene fragments to help identify problems related to sample quality¹⁷ and previous studies in cats included a germline DNA PCR amplification control.^{34,35} Small DNA fragments will result in a loss of larger PCR products, affecting the size profile obtained from the PCR reactions, and thus complicating result interpretation. Poor quality DNA, especially if low numbers of lymphocytes are present, can result in apparent clonal rearrangement patterns that are not reproducible among

reaction repeats (pseudo-clonality) and therefore reaction duplicates should be run.^{17,181,183} Formalin fixation issues can be overcome by contemporaneous collection of biopsy specimens that are stored frozen for subsequent clonality analysis, which has been shown to improve sensitivity.¹⁸⁴ T-cells are present within both the lamina propria and the epithelial layer of the mucosa of the intestine of cats and considered part of the normal resident gut-associated lymphoid tissue.^{139,145,185} Clonality analysis will amplify the T-cell receptor gene DNA from all T-cells present within a sample, regardless of whether they are considered clinically relevant (i.e., suspicious for LGITL) or not. In emerging LGITLs or patchy disease, the DNA from T-cells of interest may only comprise a small proportion of the total T-cell DNA. The proportion of clonal T-cells required for a clonal result is reported to be as low as 5% to 10%,³⁵ but this likely varies among different samples based upon gene usage in the clonal vs polyclonal population. Conversely, low numbers of lymphocytes have been reported to result in coincidental dominant peaks causing overinterpretation of results.¹⁸¹

Besides technical challenges, predicaments concerning the misinterpretation and overinterpretation of clonality assays are common. Clonality assays occasionally are used as a determinant for the cellular phenotype (i.e., whether a population of cells is of T-cell or B-cell lineage). However, cross-lineage rearrangements, where T-cells rearrange B-cell receptor genes and vice versa, have been reported in lymphomas of humans,⁶⁻⁸ dogs,¹⁸⁶ and cats.¹¹ One study showed 8 of 92 cases of LGITLs in cats to have clonal rearrangement of that of B-cells whereas IHC determined these populations to in fact be of T-cell lineage.¹¹ Therefore, PARR complements rather than replaces the use of IHC because it cannot determine lymphocyte phenotype.

Some authors have reclassified cases based on clonality results alone and 1 study implied that clonality was associated with shorter survival times.^{36,182}

First, a subset of cats with clonal rearrangements did show long-term survival of >500 days in this study.¹⁸² Second, although the authors did not report the age of cats for the 2 separate groups, cats with LGITL tend to be older than cats with IBD and hence shorter survival times are to be expected in that population.^{38,47,48} Third, shorter survival times could be a related to longer standing or more severe intestinal inflammation leading to benign clonal expansion rather than representing true malignancy. Most importantly, the group of cats with clonal results did include cats that were already diagnosed by histopathology with LGITL and hence a shorter survival time is not unexpected. It would be of value to see whether cats that were reclassified on the basis of clonality results alone also show shorter survival times compared with cats with polyclonal results. In human medicine, only 5% to 15% of cases are considered to benefit from additional molecular clonality diagnostic testing and hence the recent trend to use molecular clonality as the single determining factor in the decision on malignancy vs benign lesions is unjustified and far from common practice in human medicine.^{17,187} Much data indicates that clonality is not synonymous with malignancy and it has been shown that any strong chronic antigenic stimulation can promote selective proliferation of lymphocyte clones. Benign clonal expansions have

been documented in humans,¹⁸⁸⁻¹⁹³ dogs,¹⁹⁴⁻¹⁹⁶ and cats with infectious diseases¹⁹⁷ (e.g., ehrlichiosis, leishmaniasis, feline immunodeficiency virus), chronic inflammatory intestinal disorders, neoplasia, and drug administration. In addition, it has been reported that inflammatory and low-grade neoplastic lymphoid lesions can coexist in the same cat.^{34,65}

Previous studies have focused primarily on the sensitivity of clonality. The reported sensitivity of PARR on FFPE tissue in cats is reported to be between 89% and 91%.^{34,35,167} Insufficient primer coverage of all possible rearrangements may have previously limited sensitivity.¹⁶⁷ Recently, a new multiplex assay was developed for T-cell lymphomas in cats targeting the T-cell receptor beta, delta, and gamma loci and the new assay was reported to have 95.5% sensitivity.¹⁶⁷ However, clonality assays are designed to differentiate inflammatory from neoplastic lesions, and hence specificity is of much greater concern. Although studies reported a specificity of up to 100% for PARR analysis in T-cell neoplasia of cats, these studies mostly included biopsy specimens from healthy young cats and cats with nonlymphoproliferative disorders or nongastrointestinal tissue as controls.^{35,167} However, assessment of a specificity relevant for clinical practice (i.e., differentiation of LPE from LGITL in cats) would require systematic comparison of intestinal biopsy specimens from cats with LPE to those from cats with LGITL. Studies in humans and cats have shown the TCR gamma PARR assay to have specificities as low as 54%¹⁰ and 33%,^{18,64} respectively, for the differentiation of inflammatory from neoplastic lesions. The specificity of the new multiplex clonality assay targeting the TCR gamma, delta, and beta loci has not yet been investigated comparatively in a clinical study.

After recognition of the above-mentioned limitations of clonality assays in human medicine, the EuroClonality (BIOMED-2) consortium was founded in 2003.^{17,181,198} The group aimed to standardize the preanalytical¹⁷ (e.g., sample requirements), analytical¹⁷ (eg, standardized primer sets), and postanalytical¹⁸¹ (e.g., assay interpretation) steps of the assay and provided stringent guidelines accordingly. Unfortunately, no standardization for the performance and interpretation of clonality assays currently is available in the veterinary community.¹⁹⁸

In light of these limitations, clinicians should refrain from reclassification of cases based on clonality results alone. Instead, clinical, morphological, and immunophenotypical data should be integrated with clonality analysis to decrease the chance of a misdiagnosis, as practiced in human medicine.^{17,34,36,57,144,180,181}

4 | CONCLUSION

To date, no single diagnostic criterion or known biomarker is available that reliably differentiates inflammatory lesions from neoplastic lymphoproliferations in the intestinal tract of cats, and both frequently coexist in the same individual. To further investigate the relationship between LPE and LGITL, studies using immunohistochemical and genetic research tools are needed. Cancer genomics refers to the

study of tumor genomes using various profiling strategies including whole genome DNA sequencing and characterization of the transcriptome (ie, the RNA transcripts of DNA). A wide range of emerging “omics” and multiview clustering algorithms now provide unprecedented opportunities to further classify cancers into subtypes, improve the survival prediction and therapeutic outcome of these subtypes, and understand key pathophysiological processes through different molecular layers.¹⁹⁹⁻²⁰¹ These and other techniques currently are contributing to rapid advancements in the field of oncology. In addition to novel research techniques, longitudinal studies including long-term follow-up of cats with chronic enteropathy are needed; until then, ambiguous cases will remain. However, defining the differences between inflammatory and neoplastic lesions may have impact at both the individual and the population level. Further definition of the disorder may lead to a better understanding of etiopathogenesis and predisposing factors, new targets for diagnosis and treatment, and improve patient outcome. Finally, LGITL in cats has been shown to be a suitable model for of GI-LPDs in humans under the One Health concept. This consensus statement summarizes the state-of-the-art knowledge about CE in cats for the veterinary community within and beyond the ACVIM.

ACKNOWLEDGMENT

No funding was received for this study. Sina Marsilio, Valerie Freiche, are co-chairs. Eric G. Johnson, Chiara Leo, Iain Peters, and Mark M. Ackermann are panel members. Anton W. Langerak is an advisory task force member. We thank Kate Patterson at MediPics and Prose in Fairlight, New South Wales, Australia for creating Figure 3B. We also thank Dr. Frederic P. Gaschen and Dr. Michael D. Willard for their valuable comments and suggestions that helped produce this consensus statement and Dr. Gaschen for his thorough and constructive review of the manuscript.

CONFLICT OF INTEREST DECLARATION

Dr. S. Marsilio is a paid consultant for Dutch Pet, Inc., an online veterinary pet telehealth service and a paid speaker for Idexx Laboratories, Westbrook, ME.

Dr. V. Freiche is a paid speaker for Royal Canin, Aimargues, France, Dômes Pharma Vétérinaire, Lempdes, France, and Nestlé Purina, St Louis, MO.

Dr. E Johnson has nothing to disclose.

Dr. C. Leo is a paid consultant for Mars Anicura Inc., a paid teleconsultant for Vet-CT, an online veterinary pet telehealth service based in the UK and a paid speaker for UNISVET, an Italy-based continuing education company.

Dr. A.W. Langerak is the director of the Laboratory Medical Immunology (LMI) (ISO 15189 certified) at the Erasmus MC, University Medical Center, Rotterdam, The Netherlands. The LMI provides patient services including clonality testing on a fee-for-service basis. Dr. A.-W. Langerak receives funding for research support from Roche-Genentech, South San Francisco, CA, Janssen, Beerse, Belgium, and Gilead, Foster City, CA. Dr. A.W. Langerak is a paid speaker for Janssen, Beerse, Belgium, Gilead, Foster City, CA, and AbbVie, North

Chicago, IL. Dr. A.W. Langerak is also a founding member of the Euro-Clonality/BIMED-2 group, a non-profit organization providing analytical guidelines for the performance of clonality assays in human medicine.

Dr. I. Peters is an employee at the Veterinary Pathology Group (VPG), Exeter, Devon, UK which provides clonality testing and other laboratory services on a fee-for-service basis. None of these organizations influenced the outcome of this consensus statement.

Dr. M. Ackermann has nothing to disclose.

OFF-LABEL ANTIMICROBIAL DECLARATION

Authors declare no off label use of antimicrobials.

INSTITUTIONAL ANIMAL CARE AND USE COMMITTEE (IACUC) OR OTHER APPROVAL DECLARATION

Authors declare no IACUC or other approval was needed.

HUMAN ETHICS APPROVAL DECLARATION

Authors declare human ethics approval was not needed for this study.

ORCID

Sina Marsilio  <https://orcid.org/0000-0002-0693-0669>

Valerie Freiche  <https://orcid.org/0000-0003-2041-078X>

REFERENCES

- Louwerens M, London CA, Pedersen NC, Lyons LA. Feline lymphoma in the post-feline leukemia virus era. *J Vet Intern Med.* 2005; 19:329-335.
- Swerdlow SH, Campo E, Pileri SA, et al. The 2016 revision of the World Health Organization classification of lymphoid neoplasms. *Blood.* 2016;127:2375-2390.
- Freiche V, Cordonnier N, Paulin MV, et al. Feline low-grade intestinal T cell lymphoma: a unique natural model of human indolent T cell lymphoproliferative disorder of the gastrointestinal tract. *Lab Invest.* 2021;101:794-804.
- Vaillant AAJ, Stang CM. *Lymphoproliferative Disorders.* Treasure Island, FL: StatPearls Publishing; 2021.
- Moticka EJ. *A Historical Perspective on Evidence-Based Immunology.* Amsterdam, Netherlands: Elsevier; 2015.
- Langerak A, Szczepański T, van der Burg M, et al. Heteroduplex PCR analysis of rearranged T cell receptor genes for clonality assessment in suspect T cell proliferations. *Leukemia.* 1997;11:2192-2199.
- Szczepański T, Beishuizen A, Pongers-Willems MJ, et al. Cross-lineage T cell receptor gene rearrangements occur in more than ninety percent of childhood precursor-B acute lymphoblastic leukemias: alternative PCR targets for detection of minimal residual disease. *Leukemia.* 1999;13:196-205.
- Szczepański T, Langerak AW, van Dongen JJ, et al. Lymphoma with multi-gene rearrangement on the level of immunoglobulin heavy chain, light chain, and T-cell receptor β chain. *Am J Hematol.* 1998;59:99-100.
- Kakiuchi N, Ogawa S. Clonal expansion in non-cancer tissues. *Nat Rev Cancer.* 2021;21:239-256.
- Kokovic I, Novakovic BJ, Cerkovnik P, et al. Clonality analysis of lymphoid proliferations using the BIOMED-2 clonality assays: a single institution experience. *Radiol Oncol.* 2014;48:155-162.
- Andrews C, Operacz M, Maes R, Kiupel M. Cross lineage rearrangement in feline enteropathy-associated T-cell lymphoma. *Vet Pathol.* 2016;53:559-562.
- Burnet FM. A modification of Jerne's theory of antibody production using the concept of clonal selection. *Aust J Sci.* 1957;20:67-69.
- Burnet SFM. *The Clonal Selection Theory of Acquired Immunity.* Nashville, TN: Vanderbilt University Press Nashville; 1959.
- Dutton RW, Mishell RI. Cell populations and cell proliferation in the in vitro response of normal mouse spleen to heterologous erythrocytes: analysis by the hot pulse technique. *J Exp Med.* 1967;126:443-454.
- Buchholz VR, Flossdorf M, Hensel I, et al. Disparate individual fates compose robust CD8+ T cell immunity. *Science.* 2013;340:630-635.
- Gerlach C, Rohr JC, Perié L, et al. Heterogeneous differentiation patterns of individual CD8+ T cells. *Science.* 2013;340:635-639.
- van Dongen JJ, Langerak AW, Bruggemann M, et al. Design and standardization of PCR primers and protocols for detection of clonal immunoglobulin and T-cell receptor gene recombinations in suspect lymphoproliferations: report of the BIOMED-2 concerted action BMH4-CT98-3936. *Leukemia.* 2003;17:2257-2317.
- Freiche V, Paulin MV, Cordonnier N, et al. Histopathologic, phenotypic, and molecular criteria to discriminate low-grade intestinal T-cell lymphoma in cats from lymphoplasmacytic enteritis. *J Vet Intern Med.* 2021;35(6):2673-2684.
- Kieslinger M, Swoboda A, Kramer N, et al. A recurrent STAT5BN642H driver mutation in feline alimentary T cell lymphoma. *Cancers (Basel).* 2021;13:5238.
- Burns PB, Rohrich RJ, Chung KC. The levels of evidence and their role in evidence-based medicine. *Plast Reconstr Surg.* 2011;128:305-310.
- Hill N, Frappier-Davignon L, Morrison B. The periodic health examination. *Can Med Assoc J.* 1979;121:1193-1254.
- Sato H, Fujino Y, Chino J, et al. Prognostic analyses on anatomical and morphological classification of feline lymphoma. *J Vet Med Sci.* 2014;76:807-811.
- Zwahlen C, Lucroy M, Kraegel S, Madewell BR. Results of chemotherapy for cats with alimentary malignant lymphoma: 21 cases (1993-1997). *J Am Vet Med Assoc.* 1998;213:1144-1149.
- Meichner K, Kruse DB, Hirschberger J, Hartmann K. Changes in prevalence of progressive feline leukaemia virus infection in cats with lymphoma in Germany. *Vet Rec.* 2012;171:348.
- Weiss ATA, Klopffleisch R, Gruber AD. Prevalence of feline leukaemia provirus DNA in feline lymphomas. *J Feline Med Surg.* 2010;12:929-935.
- Jackson M, Haines D, Meric S, Misra V. Feline leukemia virus detection by immunohistochemistry and polymerase chain reaction in formalin-fixed, paraffin-embedded tumor tissue from cats with lymphosarcoma. *Can J Vet Res.* 1993;57:269-276.
- Stützer B, Simon K, Lutz H, et al. Incidence of persistent viraemia and latent feline leukaemia virus infection in cats with lymphoma. *J Feline Med Surg.* 2011;13:81-87.
- Farinha P, Gascoyne RD. Helicobacter pylori and MALT lymphoma. *Gastroenterology.* 2005;128:1579-1605.
- Wang F, Meng W, Wang B, Qiao L. Helicobacter pylori-induced gastric inflammation and gastric cancer. *Cancer Lett.* 2014;345:196-202.
- Hoehne SN, McDonough SP, Rishniw M, et al. Identification of mucosa-invading and intravascular bacteria in feline small intestinal lymphoma. *Vet Pathol.* 2017;54:234-241.
- Zou S, Fang L, Lee M-H. Dysbiosis of gut microbiota in promoting the development of colorectal cancer. *Gastroenterol Rep.* 2018;6:1-12.
- Marsilio S, Pilla R, Sarawichitr B, et al. Characterization of the fecal microbiome in cats with inflammatory bowel disease or alimentary small cell lymphoma. *Sci Rep.* 2019;9:19208.
- Sung CH, Marsilio S, Chow B, et al. Dysbiosis index to evaluate the fecal microbiota in healthy cats and cats with chronic enteropathies. *J Feline Med Surg.* 2022;24:e1-e12.

34. Moore PF, Rodriguez-Bertos A, Kass PH. Feline gastrointestinal lymphoma: mucosal architecture, immunophenotype, and molecular clonality. *Vet Pathol.* 2012;49:658-668.
35. Moore PF, Woo JC, Vernau W, Kosten S, Graham PS. Characterization of feline T cell receptor gamma (TCRG) variable region genes for the molecular diagnosis of feline intestinal T cell lymphoma. *Vet Immunol Immunopathol.* 2005;106:167-178.
36. Kiupel M, Smedley RC, Pfent C, et al. Diagnostic algorithm to differentiate lymphoma from inflammation in feline small intestinal biopsy samples. *Vet Pathol.* 2011;48:212-222.
37. Briscoe KA, Krockenberger M, Beatty JA, et al. Histopathological and immunohistochemical evaluation of 53 cases of feline lymphoplasmacytic enteritis and low-grade alimentary lymphoma. *J Comp Pathol.* 2011;145:187-198.
38. Lingard AE, Briscoe K, Beatty JA, et al. Low-grade alimentary lymphoma: clinicopathological findings and response to treatment in 17 cases. *J Feline Med Surg.* 2009;11:692-700.
39. Carreras JK, Goldschmidt M, Lamb M, McLear R, Drobatz KJ, Sørensen KU. Feline epitheliotropic intestinal malignant lymphoma: 10 cases (1997-2000). *J Vet Intern Med.* 2003;17:326-331.
40. Freiche V, Fages J, Paulin MV, et al. Clinical, laboratory and ultrasonographic findings differentiating low-grade intestinal T-cell lymphoma from lymphoplasmacytic enteritis in cats. *J Vet Intern Med.* 2021;35(6):2685-2696.
41. Day MJ, Bilzer T, Mansell J, et al. Histopathological standards for the diagnosis of gastrointestinal inflammation in endoscopic biopsy samples from the dog and cat: a report from the World Small Animal Veterinary Association Gastrointestinal Standardization Group. *J Comp Pathol.* 2008;138(Suppl 1):S1-S43.
42. Washabau RJ, Day MJ, Willard MD, et al. Endoscopic, biopsy, and histopathologic guidelines for the evaluation of gastrointestinal inflammation in companion animals. *J Vet Intern Med.* 2010;24:10-26.
43. Marsilio S, Chow B, Hill SL, et al. Untargeted metabolomic analysis in cats with naturally occurring inflammatory bowel disease and alimentary small cell lymphoma. *Sci Rep.* 2021;11:9198.
44. Waldmann TA, Chen J. Disorders of the JAK/STAT pathway in T cell lymphoma pathogenesis: implications for immunotherapy. *Annu Rev Immunol.* 2017;35:533-550.
45. Bertone ER, Snyder LA, Moore AS. Environmental tobacco smoke and risk of malignant lymphoma in pet cats. *Am J Epidemiol.* 2002;156:268-273.
46. Smith V, Knottenbelt C, Watson D, et al. Hair nicotine concentration of cats with gastrointestinal lymphoma and unaffected control cases. *Vet Rec.* 2020;186:414.
47. Kiselow MA, Rassnick KM, McDonough SP, et al. Outcome of cats with low-grade lymphocytic lymphoma: 41 cases (1995-2005). *J Am Vet Med Assoc.* 2008;232:405-410.
48. Stein TJ, Pellin M, Steinberg H, Chun R. Treatment of feline gastrointestinal small-cell lymphoma with chlorambucil and glucocorticoids. *J Am Anim Hosp Assoc.* 2010;46:413-417.
49. Marsilio S, Pilla R, Sarawichitr B, et al. Characterization of the fecal microbiome in cats with inflammatory bowel disease or alimentary small cell lymphoma. *Sci Rep.* 2019;9:19208.
50. Janeczko S, Atwater D, Bogel E, et al. The relationship of mucosal bacteria to duodenal histopathology, cytokine mRNA, and clinical disease activity in cats with inflammatory bowel disease. *Vet Microbiol.* 2008;128:178-193.
51. Waly NE, Stokes CR, Gruffydd-Jones TJ, Day MJ. Immune cell populations in the duodenal mucosa of cats with inflammatory bowel disease. *J Vet Intern Med.* 2004;18:816-825.
52. Jergens AE, Crandell JM, Evans R, Ackermann M, Miles KG, Wang C. A clinical index for disease activity in cats with chronic enteropathy. *J Vet Intern Med.* 2010;24:1027-1033.
53. Risetto K, Villamil JA, Selting KA, Tyler J, Henry CJ. Recent trends in feline intestinal neoplasia: an epidemiologic study of 1,129 cases in the veterinary medical database from 1964 to 2004. *J Am Anim Hosp Assoc.* 2011;47:28-36.
54. Gabor L, Malik R, Canfield P. Clinical and anatomical features of lymphosarcoma in 118 cats. *Aust Vet J.* 1998;76:725-732.
55. Jergens AE, Moore FM, Haynes JS, Miles KG. Idiopathic inflammatory bowel disease in dogs and cats: 84 cases (1987-1990). *J Am Vet Med Assoc.* 1992;201:1603-1608.
56. Chow B, Hill SL, Richter KP, et al. Comprehensive comparison of upper and lower endoscopic small intestinal biopsy in cats with chronic enteropathy. *J Vet Intern Med.* 2021;35:190-198.
57. Freiche V, Cordonnier N, Paulin MV, et al. Feline Low-Grade Intestinal T Cell Lymphoma: A Unique Natural Model of Human Indolent T Cell Lymphoproliferative Disorder of the Gastrointestinal Tract. *Lab Invest.* 2021;101(6):794-804.
58. Norsworthy GD, Estep JS, Hollinger C, et al. Prevalence and underlying causes of histologic abnormalities in cats suspected to have chronic small bowel disease: 300 cases (2008-2013). *J Am Vet Med Assoc.* 2015;247:629-635.
59. Carrasco V, Rodriguez-Bertos A, Rodriguez-Franco F, et al. Distinguishing intestinal lymphoma from inflammatory bowel disease in canine duodenal endoscopic biopsy samples. *Vet Pathol.* 2015;52:668-675.
60. Lalor S, Schwartz AM, Titmarsh H, et al. Cats with inflammatory bowel disease and intestinal small cell lymphoma have low serum concentrations of 25-hydroxyvitamin D. *J Vet Intern Med.* 2014;28:351-355.
61. Mahony OM, Moore AS, Cotter SM, Engler SJ, Brown D, Penninck DG. Alimentary lymphoma in cats: 28 cases (1988-1993). *J Am Vet Med Assoc.* 1995;207:1593-1598.
62. Evans SE, Bonczynski JJ, Broussard JD, Han E, Baer KE. Comparison of endoscopic and full-thickness biopsy specimens for diagnosis of inflammatory bowel disease and alimentary tract lymphoma in cats. *J Am Vet Med Assoc.* 2006;229:1447-1450.
63. Fondacaro JV, Richter KP, Carpenter JL, et al. Feline gastrointestinal lymphoma: 67 cases (1988-1996). *Eur J Comp Gastroenterol.* 1999;4:5-11.
64. Marsilio S, Ackermann MR, Lidbury JA, Suchodolski JS, Steiner JM. Results of histopathology, immunohistochemistry, and molecular clonality testing of small intestinal biopsy specimens from clinically healthy client-owned cats. *J Vet Intern Med.* 2019;33:551-558.
65. Daniaux LA, Laurensen MP, Marks SL, et al. Ultrasonographic thickening of the muscularis propria in feline small intestinal small cell T-cell lymphoma and inflammatory bowel disease. *J Feline Med Surg.* 2014;16:89-98.
66. Bernardin F, Martinez Rivera L, Ragety G, Gomes E, Hernandez J. Spontaneous gastrointestinal perforation in cats: a retrospective study of 13 cases. *J Feline Med Surg.* 2015;17:873-879.
67. Gianella P, Pietra M, Crisi P, et al. Evaluation of clinicopathological features in cats with chronic gastrointestinal signs. *Pol J Vet Sci.* 2017;20(2):403-410.
68. Forman MA, Steiner JM, Armstrong PJ, et al. ACVIM consensus statement on pancreatitis in cats. *J Vet Intern Med.* 2021;35:703-723.
69. Norsworthy GD, Scot Estep J, Kiupel M, Olson JC, Gassler LN. Diagnosis of chronic small bowel disease in cats: 100 cases (2008-2012). *J Am Vet Med Assoc.* 2013;243:1455-1461.
70. Center SA, Randolph JF, Warner KL, Flanders JA, Harvey HJ. Clinical features, concurrent disorders, and survival time in cats with suppurative cholangitis-cholangiohepatitis syndrome. *J Am Vet Med Assoc.* 2022;260:212-227.
71. Weiss D, Gagne J, Armstrong P. Relationship between inflammatory hepatic disease and inflammatory bowel disease, pancreatitis, and nephritis in cats. *J Am Vet Med Assoc.* 1996;209:1114-1116.

72. Fragkou F, Adamama-Moraitou K, Poutahidis T, et al. Prevalence and clinicopathological features of triaditis in a prospective case series of symptomatic and asymptomatic cats. *J Vet Intern Med.* 2016;30:1031-1045.
73. Geesaman BM, Whitehouse WH, Viviano KR. Serum cobalamin and methylmalonic acid concentrations in hyperthyroid cats before and after radioiodine treatment. *J Vet Intern Med.* 2016;30:560-565.
74. Xenoulis PG, Zoran DL, Fosgate GT, Suchodolski JS, Steiner JM. Feline exocrine pancreatic insufficiency: a retrospective study of 150 cases. *J Vet Intern Med.* 2016;30:1790-1797.
75. Burke KF, Broussard JD, Ruau CG, Suchodolski JS, Williams DA, Steiner JM. Evaluation of fecal α 1-proteinase inhibitor concentrations in cats with idiopathic inflammatory bowel disease and cats with gastrointestinal neoplasia. *Vet J.* 2013;196:189-196.
76. Baez JL, Hendrick MJ, Walker LM, Washabau RJ. Radiographic, ultrasonographic, and endoscopic findings in cats with inflammatory bowel disease of the stomach and small intestine: 33 cases (1990-1997). *J Am Vet Med Assoc.* 1999;215:349-354.
77. Bailey S, Benigni L, Eastwood J, et al. Comparisons between cats with normal and increased fPLI concentrations in cats diagnosed with inflammatory bowel disease. *J Small Anim Pract.* 2010;51:484-489.
78. Ramos LR, Sachar DB, DiMaio CJ, et al. Inflammatory bowel disease and pancreatitis: a review. *J Crohns Colitis.* 2016;10:95-104.
79. De Cock HE, Forman M, Farver TB, et al. Prevalence and histopathologic characteristics of pancreatitis in cats. *Vet Pathol.* 2007;44:39-49.
80. Simpson K. Pancreatitis and triaditis in cats: causes and treatment. *J Small Anim Pract.* 2015;56:40-49.
81. Oppliger S, Hartnack S, Reusch CE, Kook PH. Agreement of serum feline pancreas-specific lipase and colorimetric lipase assays with pancreatic ultrasonographic findings in cats with suspicion of pancreatitis: 161 cases (2008-2012). *J Am Vet Med Assoc.* 2014;244:1060-1065.
82. Auger M, Fazio C, Steiner JM, et al. Abdominal ultrasound and clinicopathologic findings in 22 cats with exocrine pancreatic insufficiency. *J Vet Intern Med.* 2021;35:2652-2661.
83. Fyfe J. Feline intrinsic factor (IF) is pancreatic in origin and mediates ileal cobalamin (CBL) absorption. *J Vet Intern Med.* 1993;7:133.
84. Fyfe JC. The functional cobalamin (vitamin B12)-intrinsic factor receptor is a novel complex of cubilin and amnionless. *Blood.* 2004;103:1573-1579.
85. Batt R, Morgan J. Role of serum folate and vitamin B12 concentrations in the differentiation of small intestinal abnormalities in the dog. *Res Vet Sci.* 1982;32:17-22.
86. Reed N, Gunn-Moore D, Simpson K. Cobalamin, folate and inorganic phosphate abnormalities in ill cats. *J Feline Med Surg.* 2007;9:278-288.
87. Ruau CG, Steiner JM, Williams DA. Early biochemical and clinical responses to cobalamin supplementation in cats with signs of gastrointestinal disease and severe hypcobalaminemia. *J Vet Intern Med.* 2005;19:155-160.
88. Worhunsky P, Toulza O, Rishniw M, et al. The relationship of serum cobalamin to methylmalonic acid concentrations and clinical variables in cats. *J Vet Intern Med.* 2013;27:1056-1063.
89. Simpson KW, Fyfe J, Cornetta A, et al. Subnormal concentrations of serum cobalamin (vitamin B12) in cats with gastrointestinal disease. *J Vet Intern Med.* 2001;15:26-32.
90. Maunder CL, Day MJ, Hibbert A, Steiner JM, Suchodolski JS, Hall EJ. Serum cobalamin concentrations in cats with gastrointestinal signs: correlation with histopathological findings and duration of clinical signs. *J Feline Med Surg.* 2012;14:686-693.
91. Puig J, Cattin I, Seth M. Concurrent diseases in hyperthyroid cats undergoing assessment prior to radioiodine treatment. *J Feline Med Surg.* 2015;17:537-542.
92. Kook P, Lutz S, Sewell A, et al. Evaluation of serum cobalamin concentration in cats with clinical signs of gastrointestinal disease. *Schweiz Arch Tierheilkd.* 2012;154:479-486.
93. Jugan MC, August JR. Serum cobalamin concentrations and small intestinal ultrasound changes in 75 cats with clinical signs of gastrointestinal disease: a retrospective study. *J Feline Med Surg.* 2017;19:48-56.
94. Riggers DS, Gurtner C, Protschka M, et al. Intestinal S100/calgranulin expression in cats with chronic inflammatory enteropathy and intestinal lymphoma. *Animals.* 2022;12:2044.
95. Ruau CG, Steiner JM, Williams DA. Relationships between low serum cobalamin concentrations and methylmalonic acidemia in cats. *J Vet Intern Med.* 2009;23:472-475.
96. Hunt A, Jugan MC. Anemia, iron deficiency, and cobalamin deficiency in cats with chronic gastrointestinal disease. *J Vet Intern Med.* 2021;35:172-178.
97. Trehy MR, German AJ, Silvestrini P, Serrano G, Batchelor DJ. Hypercobalaminaemia is associated with hepatic and neoplastic disease in cats: a cross sectional study. *BMC Vet Res.* 2014;10:175.
98. Kather S, Grützner N, Kook PH, Dengler F, Heilmann RM. Review of cobalamin status and disorders of cobalamin metabolism in dogs. *J Vet Intern Med.* 2020;34:13-28.
99. Camilo E, Zimmerman J, Mason JB, et al. Folate synthesized by bacteria in the human upper small intestine is assimilated by the host. *Gastroenterology.* 1996;110:991-998.
100. Russell RM, Krasinski SD, Samloff IM, Jacob RA, Hartz SC, Brovender SR. Folic acid malabsorption in atrophic gastritis: possible compensation by bacterial folate synthesis. *Gastroenterology.* 1986;91:1476-1482.
101. Minović I, Dikkeschei LD, Vos MJ, Kootstra-Ros JE. Interpretation of folate results in hemolytic plasma samples: a practical approach. *Ann Lab Med.* 2021;41:485-488.
102. Habibi F, Habibi ME, Gharavinia A, et al. Quality of life in inflammatory bowel disease patients: a cross-sectional study. *J Res Med Sci.* 2017;22:104.
103. Terragni R, Morselli-Labate AM, Vignoli M, Bottero E, Brunetti B, Saunders JH. Is serum total LDH evaluation able to differentiate between alimentary lymphoma and inflammatory bowel disease in a real world clinical setting? *PLoS One.* 2016;11:e0151641.
104. Taylor SS, Dodkin S, Papasouliotis K, et al. Serum thymidine kinase activity in clinically healthy and diseased cats: a potential biomarker for lymphoma. *J Feline Med Surg.* 2013;15:142-147.
105. Wang L, Sharif H, Saellström S, Rönnerberg H, Eriksson S. Feline thymidine kinase 1: molecular characterization and evaluation of its serum form as a diagnostic biomarker. *BMC Vet Res.* 2021;17:1-10.
106. Kosovskiy J, Matthiesen D, Patnaik A. Small intestinal adenocarcinoma in cats: 32 cases (1978-1985). *J Am Vet Med Assoc.* 1988;192:233-235.
107. Won WW, Sharma A, Wu W. Retrospective comparison of abdominal ultrasonography and radiography in the investigation of feline abdominal disease. *Can Vet J.* 2015;56:1065-1068.
108. Kapatkin A, Mullen H, Matthiesen D, Patnaik AK. Leiomyosarcoma in dogs: 44 cases (1983-1988). *J Am Vet Med Assoc.* 1992;201:1077-1079.
109. Crawshaw J, Berg J, Sardinas J, et al. Prognosis for dogs with non-lymphomatous, small intestinal tumors treated by surgical excision. *J Am Anim Hosp Assoc.* 1998;34:451-456.
110. Couto CG, Rutgers HC, Sherding RG, Rojko J. Gastrointestinal lymphoma in 20 dogs: a retrospective study. *J Vet Intern Med.* 1989;3:73-78.
111. Zwingenberger AL, Marks SL, Baker TW, Moore PF. Ultrasonographic evaluation of the muscularis propria in cats with diffuse small intestinal lymphoma or inflammatory bowel disease. *J Vet Intern Med.* 2010;24:289-292.

112. Clark JEC, Haddad JL, Brown DC, Morgan MJ, Van Winkle TJ, Rondeau MP. Feline cholangitis: a necropsy study of 44 cats (1986-2008). *J Feline Med Surg.* 2011;13:570-576.
113. Guttin T, Walsh A, Durham AC, Reetz JA, Brown DC, Rondeau MP. Ability of ultrasonography to predict the presence and location of histologic lesions in the small intestine of cats. *J Vet Intern Med.* 2019;33:1278-1285.
114. Tucker S, Penninck DG, Keating JH, Webster CRL. Clinicopathological and ultrasonographic features of cats with eosinophilic enteritis. *J Feline Med Surg.* 2014;16:950-956.
115. Finotello R, Vasconi ME, Sabattini S, et al. Feline large granular lymphocyte lymphoma: An Italian Society of Veterinary Oncology (SIONCOV) retrospective study. *Vet Comp Oncol.* 2018;16:159-166.
116. Cook AK, Cunningham LY, Cowell AK, Wheat LJ. Clinical evaluation of urine histoplasma capsulatum antigen measurement in cats with suspected disseminated histoplasmosis. *J Feline Med Surg.* 2012;14:512-515.
117. Roccabianca P, Vernau W, Caniatti M, Moore PF. Feline large granular lymphocyte (LGL) lymphoma with secondary leukemia: primary intestinal origin with predominance of a CD3/CD8a phenotypic. *Vet Pathol.* 2006;43:15-28.
118. Franks PT, Harvey JW, Mays MC, Senior DF, Bowen DJ, Hall BJ. Feline large granular lymphoma. *Vet Pathol.* 1986;23:200-202.
119. Krick EL, Little L, Patel R, et al. Description of clinical and pathological findings, treatment and outcome of feline large granular lymphocyte lymphoma (1996-2004). *Vet Comp Oncol.* 2008;6:102-110.
120. Wellman M, Hammer A, DiBartola S, Carothers MA, Kociba GJ, Rojko JL. Lymphoma involving large granular lymphocytes in cats: 11 cases (1982-1991). *J Am Vet Med Assoc.* 1992;201:1265-1269.
121. Waly NE, Gruffydd-Jones TJ, Stokes CR, et al. Immunohistochemical diagnosis of alimentary lymphomas and severe intestinal inflammation in cats. *J Comp Pathol.* 2005;133:253-260.
122. Castro-Lopez J, Teles M, Fierro C, et al. Pilot study: duodenal MDR1 and COX2 gene expression in cats with inflammatory bowel disease and low-grade alimentary lymphoma. *J Feline Med Surg.* 2018;20:759-766.
123. Hart JR, Shaker E, Patnaik AK, et al. Lymphocytic-plasmacytic enterocolitis in cats - 60 cases (1988-1990). *J Am Anim Hosp Assoc.* 1994;30:505-514.
124. Roccabianca P, Woo JC, Moore PF. Characterization of the diffuse mucosal associated lymphoid tissue of feline small intestine. *Vet Immunol Immunopathol.* 2000;75:27-42.
125. Dennis JS, Kruger JM, Mullaney TP. Lymphocytic/plasmacytic gastroenteritis in cats: 14 cases (1985-1990). *J Am Vet Med Assoc.* 1992;200:1712-1718.
126. Marrinhas C, Oliveira LF, Sampaio F, et al. Needle rinse cell blocks as an ancillary technique: diagnostic and clinical utility in gastrointestinal neoplasia. *Vet Clin Pathol.* 2022;50(Suppl 1):47-54.
127. Elliott J, Finotello R. A dexamethasone, melphalan, actinomycin-D and cytarabine chemotherapy protocol as a rescue treatment for feline lymphoma. *Vet Comp Oncol.* 2018;16:E144-E151.
128. Freiche V, Da Riz F, Bencheikroun G, et al. Endoscopic assessment of presumed acquired pyloric narrowing in cats: a retrospective study of 27 cases. *Res Vet Sci.* 2021;136:408-415.
129. Willard MD, Mansell J, Fosgate GT, et al. Effect of sample quality on the sensitivity of endoscopic biopsy for detecting gastric and duodenal lesions in dogs and cats. *J Vet Intern Med.* 2008;22:1084-1089.
130. Goutal-Landry C, Mansell J, Ryan K, et al. Effect of endoscopic forceps on quality of duodenal mucosal biopsy in healthy dogs. *J Vet Intern Med.* 2013;27:456-461.
131. Bottero E, Mussi E, Pieramati C, De Lorenzi D, Silvestri S, Lepri E. Comparison of 2 differently sized endoscopic biopsy forceps in the evaluation of intestinal disease in cats. *J Vet Intern Med.* 2019;33:523-530.
132. Cartwright J, Hill T, Smith S, et al. Evaluating quality and adequacy of gastrointestinal samples collected using reusable or disposable forceps. *J Vet Intern Med.* 2016;30:1002-1007.
133. Kleinschmidt S, Harder J, Nolte I, Marsilio S, Hewicker-Trautwein M. Chronic inflammatory and non-inflammatory diseases of the gastrointestinal tract in cats: diagnostic advantages of full-thickness intestinal and extraintestinal biopsies. *J Feline Med Surg.* 2010;12:97-103.
134. Ruiz GC, Reyes-Gomez E, Hall EJ, Freiche V. Comparison of 3 handling techniques for endoscopically obtained gastric and duodenal biopsy specimens: a prospective study in dogs and cats. *J Vet Intern Med.* 2016;30:1014-1021.
135. Willard MD, Jergens AE, Duncan RB, et al. Interobserver variation among histopathologic evaluations of intestinal tissues from dogs and cats. *J Am Vet Med Assoc.* 2002;220:1177-1182.
136. Jergens AE, Evans RB, Ackermann M, et al. Design of a simplified histopathologic model for gastrointestinal inflammation in dogs. *Vet Pathol.* 2014;51:946-950.
137. Wright KZ, Hohenhaus AE, Verrilli AM, Vaughan-Wasser S. Feline large-cell lymphoma following previous treatment for small-cell gastrointestinal lymphoma: incidence, clinical signs, clinicopathologic data, treatment of a secondary malignancy, response and survival. *J Feline Med Surg.* 2019;21:353-362.
138. Vezzali E, Parodi AL, Marcato PS, Bettini G. Histopathologic classification of 171 cases of canine and feline non-Hodgkin lymphoma according to the WHO. *Vet Comp Oncol.* 2010;8:38-49.
139. Waly N, Gruffydd-Jones TJ, Stokes CR, Day MJ. The distribution of leucocyte subsets in the small intestine of healthy cats. *J Comp Pathol.* 2001;124:172-182.
140. Pohlman LM, Higginbotham ML, Welles EG, Johnson CM. Immunophenotypic and histologic classification of 50 cases of feline gastrointestinal lymphoma. *Vet Pathol.* 2009;46:259-268.
141. Patterson-Kane J, Kugler BP, Francis K. The possible prognostic significance of immunophenotype in feline alimentary lymphoma: a pilot study. *J Comp Pathol.* 2004;130:220-222.
142. Wolfesberger B, Fuchs-Baumgartinger A, Greß V, et al. World Health Organisation classification of lymphoid tumours in veterinary and human medicine: a comparative evaluation of gastrointestinal lymphomas in 61 cats. *J Comp Pathol.* 2018;159:1-10.
143. Felisberto R, Matos J, Alves M, Cabeçadas J, Henriques J. Evaluation of Pax5 expression and comparison with BLA.36 and CD79 α cy in feline non-Hodgkin lymphoma. *Vet Comp Oncol.* 2017;15:1257-1268.
144. Paulin MV, Couronne L, Beguin J, et al. Feline low-grade alimentary lymphoma: an emerging entity and a potential animal model for human disease. *BMC Vet Res.* 2018;14:306.
145. Marsilio S, Kleinschmidt S, Harder J, Nolte I, Hewicker-Trautwein M. Numbers and distribution of immune cells in the tunica mucosa of the small and large intestine of full-thickness biopsies from healthy pet cats. *Anat Histol Embryol.* 2011;40:61-67.
146. Marsilio S, Kleinschmidt S, Nolte I, Hewicker-Trautwein M. Immunohistochemical and morphometric analysis of intestinal full-thickness biopsy samples from cats with lymphoplasmacytic inflammatory bowel disease. *J Comp Pathol.* 2014;150:416-423.
147. Gerdes J, Lemke H, Baisch H, Wacker HH, Schwab U, Stein H. Cell cycle analysis of a cell proliferation-associated human nuclear antigen defined by the monoclonal antibody Ki-67. *J Immunol.* 1984;133:1710-1715.
148. Bryant R, Banks P, O'Malley D. Ki67 staining pattern as a diagnostic tool in the evaluation of lymphoproliferative disorders. *Histopathology.* 2006;48:505-515.
149. Vail DM, Moore AS, Ogilvie GK, Volk LM. Feline lymphoma (145 cases): proliferation indices, cluster of differentiation 3 immunoreactivity, and their association with prognosis in 90 cats. *J Vet Intern Med.* 1998;12:349-354.

150. Sato M, Veir JK, Legare M, Lappin MR. A retrospective study on the safety and efficacy of leflunomide in dogs. *J Vet Intern Med.* 2017; 31:1502-1507.
151. Chino J, Fujino Y, Kobayashi T, et al. Cytomorphological and immunological classification of feline lymphomas: clinicopathological features of 76 cases. *J Vet Med Sci.* 2013;75:701-707.
152. Jackson ML, Wood SL, Misra V, Haines DM. Immunohistochemical identification of B and T lymphocytes in formalin-fixed, paraffin-embedded feline lymphosarcomas: relation to feline leukemia virus status, tumor site, and patient age. *Can J Vet Res.* 1996;60:199-204.
153. Cannon CM. Cats, cancer and comparative oncology. *Vet Sci.* 2015; 2:111-126.
154. Allenspach KA, Mochel JP, Du Y, et al. Correlating gastrointestinal histopathologic changes to clinical disease activity in dogs with idiopathic inflammatory bowel disease. *Vet Pathol.* 2019;56:435-443.
155. Matnani R, Ganapathi KA, Lewis SK, Green PH, Alobeid B, Bhagat G. Indolent T- and NK-cell lymphoproliferative disorders of the gastrointestinal tract: a review and update. *Hematol Oncol.* 2017;35:3-16.
156. Tan SY, Chuang SS, Tang T, et al. Type II EATL (epitheliotropic intestinal T-cell lymphoma): a neoplasm of intra-epithelial T-cells with predominant CD8alphaalpha phenotype. *Leukemia.* 2013;27:1688-1696.
157. Ondrejka S, Jagadeesh D. Enteropathy-associated T-cell lymphoma. *Curr Hematol Malig Rep.* 2016;11:504-513.
158. Sanguedolce F, Zanelli M, Zizzo M, et al. Indolent T-cell lymphoproliferative disorders of the gastrointestinal tract (iTLPD-GI): a review. *Cancers (Basel).* 2021;13(11):2790.
159. Kucuk C, Wei L, You H. Indolent T-cell lymphoproliferative disease of the GI tract: insights for better diagnosis, prognosis, and appropriate therapy. *Front Oncol.* 2020;10:1276.
160. Zanelli M, Zizzo M, Sanguedolce F, et al. Indolent T-cell lymphoproliferative disorder of the gastrointestinal tract: a tricky diagnosis of a gastric case. *BMC Gastroenterol.* 2020;20:336.
161. Perry AM, Warnke RA, Hu Q, et al. Indolent T-cell lymphoproliferative disease of the gastrointestinal tract. *Blood.* 2013;122:3599-3606.
162. Soderquist CR, Bhagat G. Indolent T- and NK-cell lymphoproliferative disorders of the gastrointestinal tract: current understanding and outstanding questions. *Hemato.* 2022;3:219-231.
163. van Vliet C, Spagnolo DV. T- and NK-cell lymphoproliferative disorders of the gastrointestinal tract: review and update. *Pathology.* 2020;52:128-141.
164. Kohri M, Tsukasaki K, Akuzawa Y, et al. Peripheral T-cell lymphoma with gastrointestinal involvement and indolent T-lymphoproliferative disorders of the gastrointestinal tract. *Leuk Res.* 2020;91:106336.
165. Yu H, Lee H, Herrmann A, Buettner R, Jove R. Revisiting STAT3 signalling in cancer: new and unexpected biological functions. *Nat Rev Cancer.* 2014;14:736-746.
166. Ii T, Chambers JK, Nakashima K, Goto-Koshino Y, Mizuno T, Uchida K. Intraepithelial cytotoxic lymphocytes are associated with a poor prognosis in feline intestinal T-cell lymphoma. *Vet Pathol.* 2022;59:931-939.
167. Radtanakatkanon A, Moore PF, Keller SM, Vernau W. Novel clonality assays for T cell lymphoma in cats targeting the T cell receptor beta, T cell receptor delta, and T cell receptor gamma loci. *J Vet Intern Med.* 2021;35:2865-2875.
168. Henrich M, Hecht W, Weiss AT, Reinacher M. A new subgroup of immunoglobulin heavy chain variable region genes for the assessment of clonality in feline B-cell lymphomas. *Vet Immunol Immunopathol.* 2009;130:59-69.
169. Radtanakatkanon A, Keller SM, Darzentas N, et al. Topology and expressed repertoire of the *Felis catus* T cell receptor loci. *BMC Genomics.* 2020;21:1-13.
170. Mochizuki H, Nakamura K, Sato H, et al. GeneScan analysis to detect clonality of T-cell receptor γ gene rearrangement in feline lymphoid neoplasms. *Vet Immunol Immunopathol.* 2012;145: 402-409.
171. Mochizuki H, Nakamura K, Sato H, et al. Multiplex PCR and Genescan analysis to detect immunoglobulin heavy chain gene rearrangement in feline B-cell neoplasms. *Vet Immunol Immunopathol.* 2011; 143:38-45.
172. Weiss ATA, Hecht W, Reinacher M. Feline T-cell receptor γ V- and J-region sequences retrieved from the trace archive and from transcriptome analysis of cats. *Vet Med Int.* 2010;2010:953272.
173. Weiss ATA, Klopffleisch R, Gruber A. T-cell receptor γ chain variable and joining region genes of subgroup 1 are clonally rearranged in feline B- and T-cell lymphoma. *J Comp Pathol.* 2011;144:123-134.
174. Werner J, Woo J, Vernau W, et al. Characterization of feline immunoglobulin heavy chain variable region genes for the molecular diagnosis of B-cell neoplasia. *Vet Pathol.* 2005;42:596-607.
175. Hammer SE, Groiss S, Fuchs-Baumgartinger A, et al. Characterization of a PCR-based lymphocyte clonality assay as a complementary tool for the diagnosis of feline lymphoma. *Vet Comp Oncol.* 2016;15: 1354-1369.
176. Gress V, Wolfesberger B, Fuchs-Baumgartinger A, et al. Characterization of the T-cell receptor gamma chain gene rearrangements as an adjunct tool in the diagnosis of T-cell lymphomas in the gastrointestinal tract of cats. *Res Vet Sci.* 2016;107:261-266.
177. Weiss ATA, von Deetzen M-C, Hecht W, Reinacher M, Gruber AD. Molecular characterization of the feline T-cell receptor γ alternate reading frame protein (TARP) ortholog. *J Vet Sci.* 2012;13:345-353.
178. Cho K-W, Youn H-Y, Okuda M, et al. Cloning and mapping of cat (*Felis catus*) immunoglobulin and T-cell receptor genes. *Immunogenetics.* 1998;47:226-233.
179. Weiss ATA, Hecht W, Henrich M, Reinacher M. Characterization of C-, J- and V-region-genes of the feline T-cell receptor γ . *Vet Immunol Immunopathol.* 2008;124:63-74.
180. Keller SM, Vernau W, Moore PF. Clonality testing in veterinary medicine: a review with diagnostic guidelines. *Vet Pathol.* 2016;53: 711-725.
181. Langerak AW, Groenen PJ, Bruggemann M, et al. EuroClonality/BIOMED-2 guidelines for interpretation and reporting of Ig/TCR clonality testing in suspected lymphoproliferations. *Leukemia.* 2012;26:2159-2171.
182. Sabattini S, Bottero E, Turba ME, Vicchi F, Bo S, Bettini G. Differentiating feline inflammatory bowel disease from alimentary lymphoma in duodenal endoscopic biopsies. *J Small Anim Pract.* 2016;57: 396-401.
183. Lenze D, Müller H-H, Hummel M. Considerations for the use of formalin-fixed and paraffin-embedded tissue specimens for clonality analysis. *J Hematop.* 2012;5:27-34.
184. Arber DA, Brazier RM, Bagg A, Bijwaard KE. Evaluation of T cell receptor testing in lymphoid neoplasms: results of a multicenter study of 29 extracted DNA and paraffin-embedded samples. *J Mol Diagn.* 2001;3:133-140.
185. Buettner M, Lochner M. Development and function of secondary and tertiary lymphoid organs in the small intestine and the colon. *Front Immunol.* 2016;7:342.
186. Valli V, Vernau W, De Lorimier L-P, et al. Canine indolent nodular lymphoma. *Vet Pathol.* 2006;43:241-256.
187. van Krieken J, Langerak A, Macintyre E, et al. Improved reliability of lymphoma diagnostics via PCR-based clonality testing:—report of the BIOMED-2 concerted action BHM4-CT98-3936. *Leukemia.* 2007;21:201-206.
188. Magro CM, Crowson AN, Kovatich AJ, Burns F. Drug-induced reversible lymphoid dyscrasia: a clonal lymphomatoid dermatitis of memory and activated T cells. *Hum Pathol.* 2003;34:119-129.

189. Alaibac M, Daga A, Harms G, et al. Molecular analysis of the gamma delta T-cell receptor repertoire in normal human skin and in oriental cutaneous leishmaniasis. *Exp Dermatol*. 1993;2:106-112.
190. Marko D, Perry AM, Ponnampalam A, Nasr MR. Cytopenias and clonal expansion of gamma/delta T-cells in a patient with anaplasmosis: a potential diagnostic pitfall. *J Clin Exp Hematop*. 2017;56:160-164.
191. Celli R, Hui P, Bogardus S, et al. Clinical Insignificance of monoclonal T-cell populations and duodenal intraepithelial T-Cell phenotypes in celiac and Nonceliac Patients. *The American Journal of Surgical Pathology*. 2019;43(2):151-160.
192. Singleton TP, Yin B, Teferra A, Mao JZ. Spectrum of clonal large granular lymphocytes (LGLs) of $\alpha\beta$ T cells: T-cell clones of undetermined significance, T-cell LGL leukemias, and T-cell immunoclonal. *Am J Clin Pathol*. 2015;144:137-144.
193. Doorenspleet M, Westera L, Peters C, et al. Profoundly expanded T-cell clones in the inflamed and uninfamed intestine of patients with Crohn's disease. *J Crohns Colitis*. 2017;11:831-839.
194. Burkhard MJ, Meyer DJ, Rosychuk RA, O'Neil SP, Schultheiss PC. Monoclonal gammopathy in a dog with chronic pyoderma. *J Vet Intern Med*. 1995;9:357-360.
195. Diehl KJ, Lappin MR, Jones RL, Cayatte S. Monoclonal gammopathy in a dog with plasmacytic gastroenterocolitis. *J Am Vet Med Assoc*. 1992;201:1233-1236.
196. Font A, Closa JM, Mascort J. Monoclonal gammopathy in a dog with visceral leishmaniasis. *J Vet Intern Med*. 1994;8:233-235.
197. Miller MM, Thompson EM, Suter SE, Fogle JE. CD8+ clonality is associated with prolonged acute plasma viremia and altered mRNA cytokine profiles during the course of feline immunodeficiency virus infection. *Vet Immunol Immunopathol*. 2013;152:200-208.
198. Langerak AW. Toward standardization of clonality testing in veterinary medicine. *Vet Pathol*. 2016;53:705-706.
199. Vucic EA, Thu KL, Robison K, et al. Translating cancer 'omics' to improved outcomes. *Genome Res*. 2012;22:188-195.
200. Heo YJ, Hwa C, Lee G-H, Park JM, An JY. Integrative multi-omics approaches in cancer research: from biological networks to clinical subtypes. *Mol Cells*. 2021;44:433-443.
201. O'Malley DP, Goldstein NS, Banks PM. The recognition and classification of lymphoproliferative disorders of the gut. *Hum Pathol*. 2014;45:899-916.

SUPPORTING INFORMATION

Additional supporting information can be found online in the Supporting Information section at the end of this article.

How to cite this article: Marsilio S, Freiche V, Johnson E, et al. ACVIM consensus statement guidelines on diagnosing and distinguishing low-grade neoplastic from inflammatory lymphocytic chronic enteropathies in cats. *J Vet Intern Med*. 2023;37(3):794-816. doi:[10.1111/jvim.16690](https://doi.org/10.1111/jvim.16690)



Primary retropharyngeal leiomyosarcoma in a young cat

Janusz Jaworski¹, Aaron Harper¹,
Hayley Crosby-Durrani² and Jon Hall¹

Journal of Feline Medicine and Surgery Open Reports
1–6

© The Author(s) 2023

Article reuse guidelines:

sagepub.com/journals-permissions

DOI: 10.1177/20551169231164612

journals.sagepub.com/home/jfmsopenreports

This paper was handled and processed by the European Editorial Office (ISFM) for publication in *JFMS Open Reports*



Abstract

Case summary An Oriental Shorthair cat, aged 1 year and 6 months, developed progressive stridor and a palpable right ventral cervical mass. Fine-needle aspiration of the mass was inconclusive, while thoracic radiography and CT showed no evidence of metastasis. There was initial improvement in stridor with oral doxycycline and prednisolone treatment, but it recurred 4 weeks later and excisional biopsy was performed. Histopathology with immunohistochemistry diagnosed leiomyosarcoma with incomplete surgical margins. Adjunctive radiation therapy was declined. Repeated physical examination and CT 7 months postoperatively documented no evidence of mass recurrence.

Relevance and novel information This is the first reported case of retropharyngeal leiomyosarcoma in a young cat with no evidence of local reoccurrence 7 months following an excisional biopsy.

Keywords: Leiomyosarcoma; computed tomography; retropharyngeal; stridor; surgery

Accepted: 2 March 2023

Introduction

Leiomyosarcomas are uncommon, malignant tumours arising from smooth muscle cells¹ and have been reported in the duodenum,² iliocaecocolon,³ large intestine,¹ urinary bladder,⁴ stomach,⁵ oesophagus,⁶ spleen,¹ uterus,⁷ pancreas,⁸ liver,⁹ kidney,¹⁰ vulva,¹¹ eye,¹² cutaneous smooth muscle,^{13,14} and dermal interphalangeal region¹⁵ and heart.¹⁶ They are frequently non-encapsulated and invasive tumours.¹ Histological features vary from densely packed, relatively homogeneous spindle cells with the appearance of smooth muscle to more pleomorphic ovoid or round cells.¹ Surgery is the recommended treatment of choice and the prognosis depends on the anatomical location of the tumour and the presence of metastasis.^{2–16}

To the authors' knowledge, this report describes a novel diagnosis of retropharyngeal leiomyosarcoma in a young cat with a good outcome following marginal surgical excision. This tumour should be considered as a differential diagnosis for a retropharyngeal mass in the cat.

Case description

A neutered male Oriental Shorthair cat, aged 1 year and 6 months, was seen by the primary care practice (PCP)

with stridor that had progressively worsened over the course of 3 weeks. Clinical examination was unremarkable. Haematology and serum biochemistry were within normal limits. The patient was sedated and examination of the oral cavity revealed a large retropharyngeal mass (Figure 1). A fine-needle aspirate of the mass was obtained and thoracic radiographs showed a caudodorsal bronchial lung pattern (Figure 2), prompting bronchoalveolar lavage (BAL) to be performed under general anaesthesia.

The BAL results were consistent with mixed eosinophilic inflammation with suspected allergic disease. Fine-needle aspiration (FNA) results were inconclusive.

¹Wear Referrals Veterinary Specialists, Bradbury, Stockton-on-Tees, UK

²Department of Veterinary Anatomy, Physiology and Pathology, University of Liverpool, Neston, Wirral, UK

Corresponding author:

Janusz Jaworski DVM, CertAVP, BSAVA PG CertSAS, GPCert(DI), MRCVS, Wear Referrals Veterinary Specialists, Bradbury, Stockton-on-Tees TS21 2ES, UK
Email: j.jaworski88@gmail.com



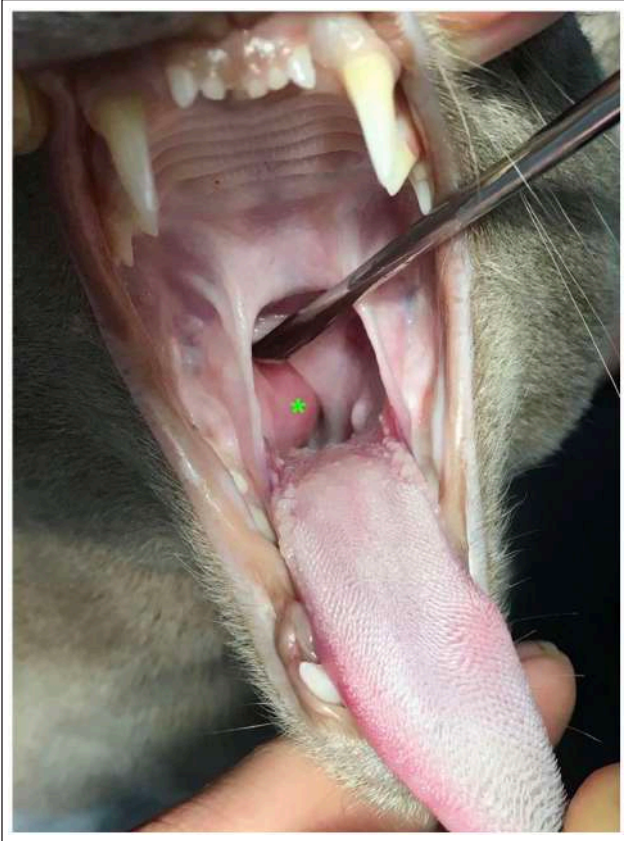


Figure 1 Intraoral image with dorsal elevation of the soft palate demonstrating a submucosal retropharyngeal mass (green star)

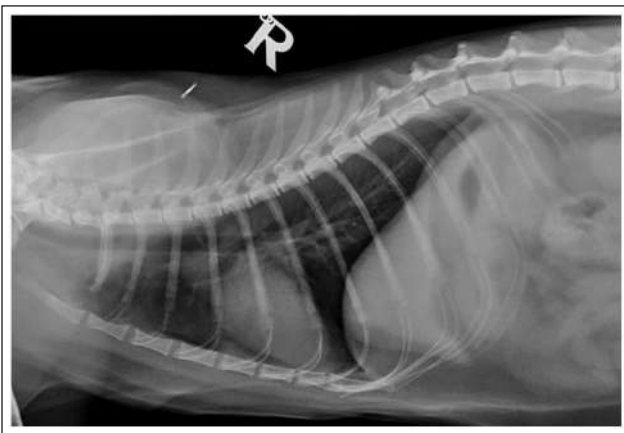


Figure 2 Right lateral thoracic radiograph demonstrating a caudodorsal interstitial lung pattern

The cat received a subcutaneous injection of dexamethasone (0.2 mg/kg [Colvasone; Norbrook]).

CT of the head and thorax were performed by the PCP and interpreted by a diagnostic imaging specialist. CT revealed a discrete right retropharyngeal/tonsillar mass with no local infiltration into the surrounding tis-

sues, ipsilateral medial retropharyngeal lymphadenopathy and unspecific pulmonary changes (Figure 3).

The cat was referred to Wear Referrals, Stockton-on-Tees, UK, and an approximately 1 × 2 cm firm soft tissue mass was palpated on the right lateral neck immediately ventral to the right tympanic bulla and cranioventral to the wing of the atlas, displacing the larynx to the left. The owner reported that the clinical signs were stable. The cat had moderate stridor but no other abnormalities on clinical examination. Owing to the cat's young age, lack of conclusive evidence of neoplasia and the possibility of an inflammatory diagnosis, the cat was prescribed doxycycline (10 mg/kg PO q24h [Ronaxan; Merial]) and prednisolone (1 mg/kg PO q24h [Prednicare; Animalcare]) for 4 weeks. The cat was re-examined 4 weeks later and the stridor had improved, although the mass was unchanged in size. Medications were continued for a further 5 weeks. On re-examination, the stridor had recurred and excisional biopsy was recommended.

The cat was premedicated with medetomidine (5 µg/kg IV [Dorbene; Zoetis]) and butorphanol (0.3 mg/kg IV [Torbugesic; Zoetis]). Cefuroxime (20 mg/kg IV [Zinacef; GSK]) was administered 30 mins prior to surgery. General anaesthesia was induced using alfaxalone (4 mg/kg IV [Alfaxan; Jurox]). Intubation was achieved using a 3.5 mm endotracheal tube, and anaesthesia was maintained with isoflurane (IsoFlo; Zoetis) in 100% oxygen. Analgesia was provided with fentanyl (0.2 µg/kg/min IV [Fentadon; Dechra]) as a constant rate infusion.

The patient was positioned in dorsal recumbency, with the neck extended and supported by a sandbag. A ventral midline cervical incision was created, and a combination of blunt and sharp dissection through subcutaneous tissue and sphincter coli muscle was performed to identify the mass ventral to the right tympanic bulla. The mass was marginally dissected from the local neurovascular structures (branches from the lingual vein, the hypoglossal nerve), muscles (digastricus, styloglossus and hypoglossus) and other adjacent anatomy (the lateral surface of the larynx and ventral surface of the right tympanic bulla) using a combination of delicate, blunt and sharp dissection and bipolar electrocautery. Lavage and routine closure were performed. The mass was submitted for histopathology.

Intravenous fentanyl was discontinued immediately postoperatively, and the cat received buprenorphine (0.02 mg/kg IV q6h [Buprecare; Animalcare]). The cat was discharged 18 h postoperatively with prednisolone (0.6 mg/kg PO q24h [Prednicare; Animalcare]) for 4 weeks with a tapering dose and buprenorphine (0.02 mg/kg sublingually q8h [Buprecare; Animalcare]) for 3 days. The patient was reviewed 4 weeks following the surgery. The owner reported that the stridor had fully resolved.

Histology described an infiltrative but partially encapsulated malignant tumour of mesenchymal origin.

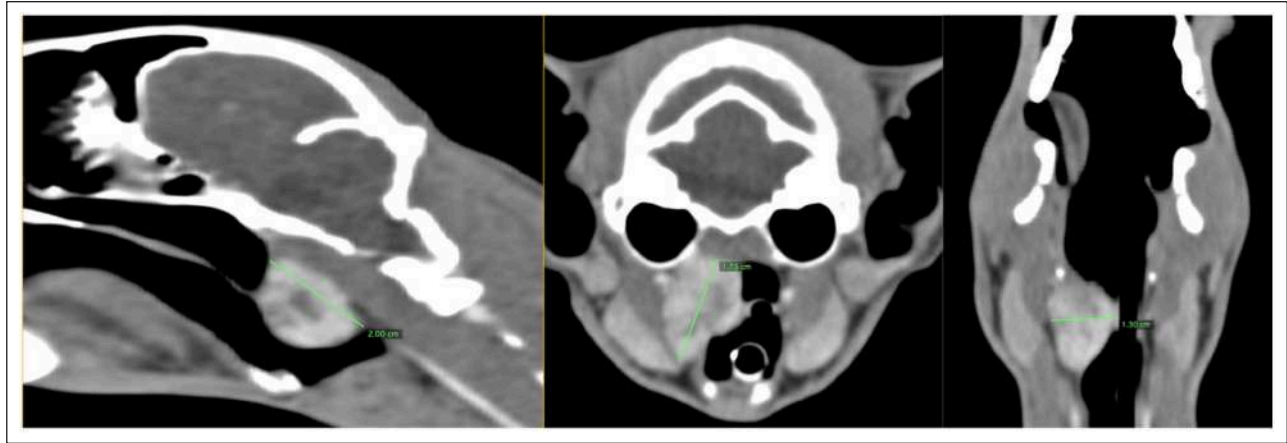


Figure 3 Contrast-enhanced CT multiplanar reconstruction using soft tissue windowing, demonstrating right-sided retropharyngeal mass (green marker)

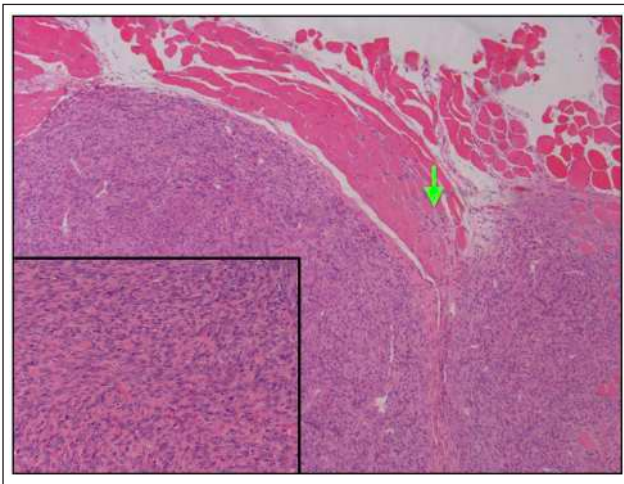


Figure 4 Low-power microscopic view ($\times 40$) of leiomyosarcoma infiltrating adjacent skeletal muscle (green arrow; haematoxylin and eosin stain). The inset represents a high-powered view ($\times 200$) of mesenchymal neoplastic cells

Neoplastic cells were spindloid with indistinct cell borders, abundant eosinophilic cytoplasm and elongated ovoid nuclei, arranged in bundles and whorls within fibrovascular stroma. Chromatin was finely stippled to coarsely clumped with 1–3 small nucleoli per cell. Neoplastic cells exhibited moderate to marked anisocytosis and anisokaryosis with a mitotic count of 1 per 10 high-power fields at $\times 200$ magnification and an area of 2.37 mm^2 (Figure 4). Immunohistochemistry revealed diffuse strong staining of the neoplastic cells with antivimentin (1:500 dilution [Monoclonal Mouse Anti-Human Vimentin Clone; Dako]), antidesmin (1:100 dilution [Monoclonal Mouse Anti-Human Desmin Clone; Dako]) and anti-alpha smooth muscle actin (1:100 dilution [Monoclonal Mouse Anti-Human Smooth Muscle Actin Clone; Dako]) antibodies at $\times 200$ magnification (Figures 5

and 6), consistent with a leiomyosarcoma. The neoplastic cells showed negative immunohistochemistry labeling for myoglobin (1:100 dilution [Monoclonal Mouse Anti-Human Myoglobin Clone; Dako]) (Figure 7).

While gross cytoreduction had been achieved to maximise diagnostic value and therapeutic benefit for the cat, histologically clear margins were not complete. Adjunctive radiation therapy of the primary tumour location was discussed, but the owners declined this option.

The cat was re-examined 7 months following surgery. The owner reported no recurrence of stridor and the cat was normal on examination. Repeat contrast-enhanced CT 16-slice helical scans (Somatom Emotion; Siemens) of the head and thorax was performed. CT revealed no evidence of primary mass recurrence (Figure 8), static right retropharyngeal mild lymphadenopathy and a poorly defined, mildly contrast-enhancing soft tissue opacity within the cranial mediastinum (possible mildly enlarged mediastinal lymph node). Further investigation was declined.

Discussion

This report describes the first case of retropharyngeal leiomyosarcoma in a young cat and should be considered as a differential diagnosis for a mass in this location.

The main presenting clinical sign was stridor, likely due to the partial obstruction of the upper respiratory tract and displacement of the larynx, and the mass could be readily identified by palpation and direct visualisation.

As far as we are aware, the youngest cats diagnosed with leiomyosarcoma were one cat aged 3 years and 9 months, which was diagnosed with oesophageal angioleiomyosarcoma,⁶ followed by a 4-year-old cat with documented primary bladder leiomyosarcoma.⁴ While most of the reported cases feature middle-aged to

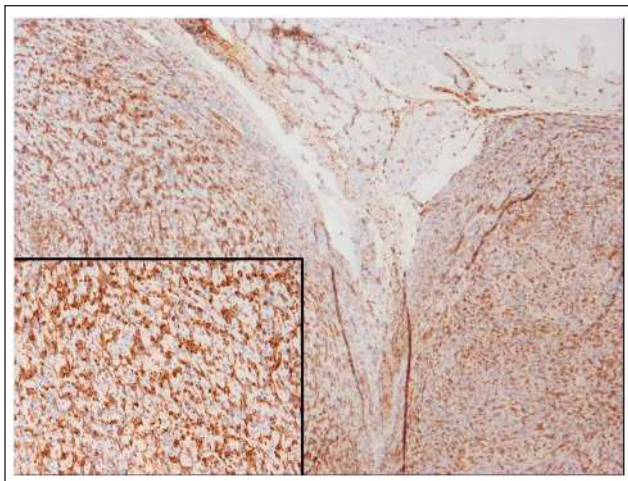


Figure 5 Low-power microscopic view ($\times 40$) of the vimentin immunohistochemistry of leiomyosarcoma. The inset is a high-power view of the neoplastic cells ($\times 200$). The brown colour indicates positive labelling of the neoplastic cells

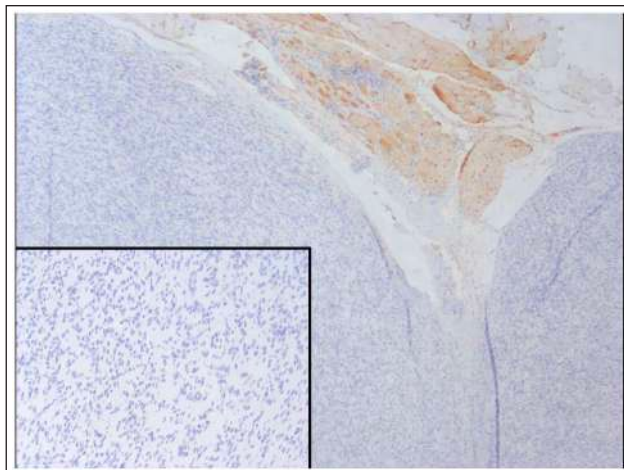


Figure 7 Low-power microscopic view ($\times 40$) of the myoglobin immunohistochemistry. The inset is a high-power view of neoplastic cells ($\times 200$). The neoplastic cells show negative immunohistochemistry labelling for myoglobin

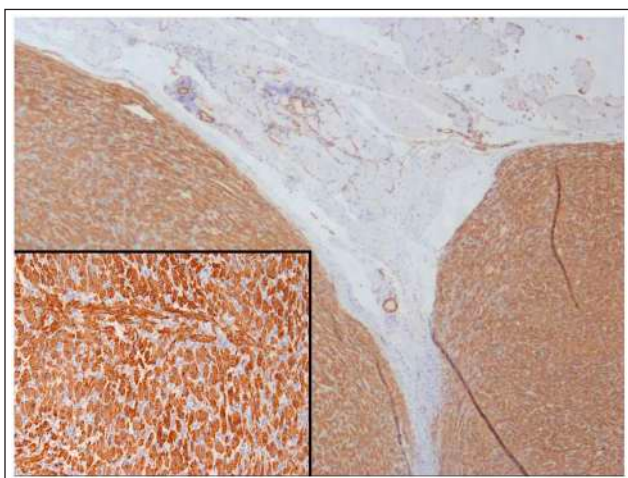


Figure 6 Low-power microscopic view ($\times 40$) of the alpha smooth muscle actin immunohistochemistry. The inset is a high-power view of the neoplastic cells ($\times 200$). The brown colour indicates strong and specific positive labelling of the neoplastic cells

older cats,^{1,3,11,15} the cat in this report was 1 year and 6 months old, which represents an uncommon, early presentation for this type of tumour.

The initial lack of a definitive diagnosis by FNA, the young age of the cat and the findings of eosinophilic pulmonary disease influenced the initial decision to provide a therapeutic trial with oral antibiotics and steroids. The initial improvement in clinical signs may be due to reduced peritumoral inflammation. The failure of the mass to respond to treatment then prompted the decision for a more invasive procedure. Excisional biopsy was elected over Tru-cut or incisional biopsy as

the clinical signs of stridor were likely due to the mass effect on the trachea and therefore a planned marginal excision would provide therapeutic benefit.

Immunohistochemistry was necessary because the histopathological features of the mass were similar to rhabdomyosarcoma and fibrosarcoma. The location of the mass, particularly in a young cat, also meant that other differential diagnoses would be more likely than leiomyosarcoma. Leiomyosarcomas that develop in the haired skin and subcutaneous tissues are thought to arise from smooth muscle associated with the vasculature or arrector pili muscles.¹ The oesophagus of the cat appeared radiologically normal and would only be expected to contain smooth muscle in the intrathoracic portion. It is possible that this tumour may have arisen from vascular smooth muscle in this area. An additional differential diagnosis considered in this case was laryngeal tumour¹⁷ or cyst.¹⁸ Oral examination and CT ruled out a laryngeal origin of this mass.

Postoperatively, the cat was prescribed prednisolone to decrease postoperative inflammation and respiratory tract obstruction following the extensive dissection in the area, and because eosinophilic lung disease had previously been noted on BAL (with an initial improvement in clinical signs when treated with prednisolone and oral antibiotics). It is unclear whether the treatment with prednisolone had any effect on the outcome, although corticosteroids are not generally considered to have anti-neoplastic action on mesenchymal tumours. Adjunctive radiation therapy has not been extensively reported for incompletely excised feline leiomyosarcomas, although it would be considered a beneficial therapy for residual microscopic disease. However, radiotherapy was declined by the owners.

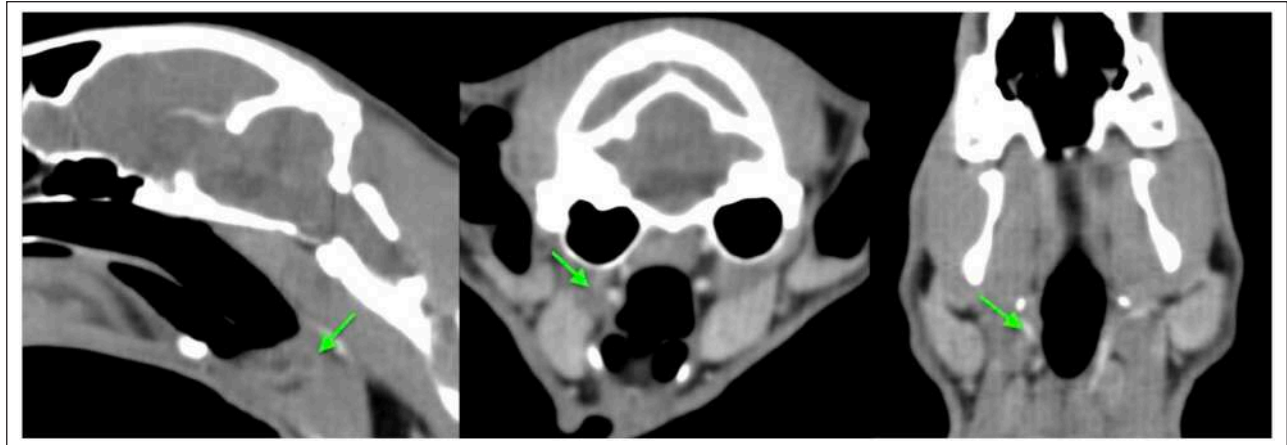


Figure 8 Contrast-enhanced CT multiplanar reconstruction using soft tissue windowing demonstrating lack of tumour reoccurrence 7 months following the surgery. Green arrows show previous location of the mass

Long-term follow-up data for cats treated for leiomyosarcoma are largely lacking. The reported prognosis following the surgical removal of the tumour varies from 1 month⁷ to 48 months.⁴ Numerous case reports documented the short-term prognosis and no tumour reoccurrence 5,⁸ 6^{6,12,15} and 10 months⁵ postoperatively, respectively. At the time of writing, the cat had shown no signs of tumour recurrence; the presence of mild unilateral retropharyngeal lymphadenopathy and cranial mediastinal lymphadenopathy could indicate metastatic disease, although leiomyosarcoma do not typically metastasise via the lymphatic route. Other causes of the imaging findings (eg, reactive hyperplasia or normal anatomical variance) were considered more likely. Continued surveillance of the cat and, ultimately, post-mortem examination are required for complete information.

Conclusions

Leiomyosarcoma should be a differential diagnosis for cats presenting with a retropharyngeal mass. A good medium-term outcome can be achieved with marginal excision.



Conflict of interest The authors declared no potential conflicts of interest with respect to the research, authorship, and/or publication of this article.

Funding The authors received no financial support for the research, authorship, and/or publication of this article.

Ethical approval The work described in this manuscript involved the use of non-experimental (owned or unowned) animals. Established internationally recognised high standards ('best practice') of veterinary clinical care for the individual patient were always followed and/or this work involved the use of cadavers. Ethical approval from a committee was therefore not specifically required for publication in *JFMS Open*

Reports. Although not required, where ethical approval was still obtained, it is stated in the manuscript.

Informed consent Informed consent (verbal or written) was obtained from the owner or legal custodian of all animal(s) described in this work (experimental or non-experimental animals, including cadavers) for all procedure(s) undertaken (prospective or retrospective studies). No animals or people are identifiable within this publication, and therefore additional informed consent for publication was not required.

ORCID iD Hayley Crosby-Durrani  <https://orcid.org/0000-0001-9297-0001>
Jon Hall  <https://orcid.org/0000-0001-9801-4264>

References

- Cooper BJ and Valentine BA. **Tumors of muscle**. In: Meuten DJ (ed). *Tumors in domestic animals*. 5th ed. Iowa: Wiley, 2017, pp 425–466.
- Henker LC, Dal Pont TP, Dos Santos IR, et al. **Duodenal leiomyosarcoma in a cat: cytologic, pathologic, and immunohistochemical findings**. *Vet Clin Pathol* 2022; 51: 507–510.
- Barrand KR and Scudamore CL. **Intestinal leiomyosarcoma in a cat**. *J Small Anim Pract* 1999; 40: 216–219.
- Buzatto AB, Elias F, Franzoni MS, et al. **Long-term survival of a cat with primary leiomyosarcoma of the urinary bladder**. *Vet Sci* 2019; 6. DOI: 10.3390/vetsci6030060.
- Hart K, Brooks Brownlie H, Ogden D, et al. **A case of gastric leiomyosarcoma in a domestic shorthair cat**. *JFMS Open Rep* 2018; 4. DOI: 10.1177/2055116918818912.
- Teo LH, Cahalan SD, Benigni L, et al. **Oesophageal angioleiomyosarcoma in a cat**. *J Feline Med Surg* 2014; 16: 846–852.
- Cooper TK, Ronnett BM, Ruben DS, et al. **Uterine myxoid leiomyosarcoma with widespread metastases in a cat**. *Vet Pathol* 2006; 43: 552–556.
- Bobis Villagrà D, Almeida M, Cox A, et al. **Pancreatic leiomyosarcoma in a domestic shorthair cat**. *JFMS Open Rep* 2022; 7. DOI: 10.1177/20551169221098328.

- 9 Patnaik AK. **A morphologic and immunocytochemical study of hepatic neoplasms in cats.** *Vet Pathol* 1992; 29: 405–415.
- 10 Evans D and Fowlkes N. **Renal leiomyosarcoma in a cat.** *J Vet Diagn Invest* 2016; 28: 315–318.
- 11 Firat I, Haktanir-Yatkin D, Sontas BH, et al. **Vulvar leiomyosarcoma in a cat.** *J Feline Med Surg* 2007; 9: 435–438.
- 12 Labelle P and Holmberg BJ. **Ocular myxoid leiomyosarcoma in a cat.** *Vet Ophthalmol* 2010; 13: 58–62.
- 13 Liu SM and Mikaelian I. **Cutaneous smooth muscle tumors in dogs and cats.** *Vet Pathol* 2003; 40: 685–692.
- 14 Finnie JW, Leong ASY and Milios J. **Multiple piloileiomyomas in cats.** *J Comp Pathol* 1995; 113: 201–204.
- 15 Jacobsen MC and Valentine BA. **Dermal intravascular leiomyosarcoma in a cat.** *Vet Pathol* 2000; 37: 100–103.
- 16 Schreeg ME, Evans BJ, Allen J, et al. **Cardiac leiomyosarcoma in a cat presenting for bilateral renal neoplasia.** *J Comp Pathol* 2019; 168: 19–24.
- 17 Carlisle CH, Biery DN and Thrall DE. **Tracheal and laryngeal tumors in the dog and cat: literature review and 13 additional patients.** *Vet Radiol Ultrasound* 2005; 32: 229–235.
- 18 Manson KC, Graham JL and Rozanski EA. **Diagnosis and management of laryngeal cyst in domestic shorthair cat.** *JFMS Open Rep* 2022; 8: DOI: 10.1177/20551169221104545.

Human Biofield Therapy and the Growth of Mouse Lung Carcinoma

Integrative Cancer Therapies
Volume 18: 1–12
© The Author(s) 2019
Article reuse guidelines:
sagepub.com/journals-permissions
DOI: 10.1177/1534735419840797
journals.sagepub.com/home/ict



Peiyang Yang, PhD¹, Yan Jiang, PhD¹, Patrea R. Rhea, BS¹, Tara Coway, BS¹, Dongmei Chen, MD¹, Mihai Gagea, PhD¹, Sean L. Harribance², and Lorenzo Cohen, PhD¹

Abstract

Biofield therapies have gained popularity and are being explored as possible treatments for cancer. In some cases, devices have been developed that mimic the electromagnetic fields that are emitted from people delivering biofield therapies. However, there is limited research examining if humans could potentially inhibit the proliferation of cancer cells and suppress tumor growth through modification of inflammation and the immune system. We found that human NSCLC A549 lung cancer cells exposed to Sean L. Harribance, a purported healer, showed reduced viability and downregulation of pAkt. We further observed that the experimental exposure slowed growth of mouse Lewis lung carcinoma evidenced by significantly smaller tumor volume in the experimental mice ($274.3 \pm 188.9 \text{ mm}^3$) than that of control mice ($740.5 \pm 460.2 \text{ mm}^3$; $P < .05$). Exposure to the experimental condition markedly reduced tumoral expression of pS6, a cytosolic marker of cell proliferation, by 45% compared with that of the control group. Results of reversed phase proteomic array suggested that the experimental exposure downregulated the PD-L1 expression in the tumor tissues. Similarly, the serum levels of cytokines, especially MCP-1, were significantly reduced in the experimental group ($P < .05$). Furthermore, TILs profiling showed that CD8⁺/CD4⁺ immune cell population was increased by almost 2-fold in the experimental condition whereas the number of intratumoral CD25⁺/CD4⁺ (T-reg cells) and CD68⁺ macrophages were 84% and 33%, respectively, lower than that of the control group. Together, these findings suggest that exposure to purported biofields from a human is capable of suppressing tumor growth, which might be in part mediated through modification of the tumor microenvironment, immune function, and anti-inflammatory activity in our mouse lung tumor model.

Keywords

biofield, Lewis lung carcinoma, PD-L1, immune modulation

Submitted October 16, 2018; revised February 25, 2019; accepted March 7, 2019

Introduction

Biofield therapies have gained popularity and are being explored as possible treatments for cancer. Clinical trials that have examined the effects of so-called biofield treatments such as Healing Touch, External Qigong, and Therapeutic Touch have demonstrated improvements in subjective outcomes such as pain and anxiety as well as immunological outcomes.^{1,2} However, other studies have not found support for the clinical effects of biofield treatments.³ Although this research is generally supportive, there are multiple methodological challenges in conducting clinical trials in this area. What is less known is whether these biofields can be emitted into other organisms to create biological changes. Preclinical studies using cultured cells and animal models are less subject to experimental bias and have supported that these “biofield therapies” do in fact modify cellular function and tumor growth.⁴

Multiple studies by Yan and colleagues demonstrated that external qigong inhibited activation of Akt, extracellular signal-regulated kinase 1/2, and nuclear factor- κ B; induced cell-cycle arrest and apoptosis; and modulated gene expression profiles in colorectal, prostate, and small-cell lung cancer cell lines.^{5–8} Similarly, a study by Gronowicz et al⁴ demonstrated that Therapeutic Touch modulated DNA synthesis and human osteoblast mineralization in culture and inhibited metastasis and modulated immune responses

¹The University of Texas MD Anderson Cancer Center, Houston, TX, USA

²Sean Harribance Institute for Parapsychology, Inc., Sugarland, TX, USA

Corresponding Author:

Peiyang Yang, Department of Palliative, Rehabilitation, and Integrative Medicine, The University of Texas MD Anderson Cancer Center, 1400 Pressler Street, Houston, TX 77030, USA.

Email: pyang@mdanderson.org



in BALB/c mice injected with the 66c14 breast cancer cells. This study sought to test the proposition that exposure to Sean L. Harribance (SLH), a purported healer,⁹⁻¹² could modulate cancer cell growth *in vitro* using human and mouse non-small cell lung cancer (NSCLC) cells and *in vivo* using a syngeneic mouse lung carcinoma model. The current study also aimed to identify the plausible biological mechanisms if any oncogenic changes were detected after the animals were exposed to SLH. We proposed the following null hypothesis for this study: Exposure to SLH would be unable to inhibit the growth of lung tumor cells *in vitro* and *in vivo* or affect other local or systemic oncogenic targets.

Methods

All experiments were performed in accordance with the relevant guidelines and regulations by The University of Texas MD Anderson Cancer Center. All assays and measurements were conducted by research staff blinded to group assignment.

Cell Line

Human NSCLC A549 cells and mouse Lewis lung carcinoma (LLC) cells were purchased from the ATCC (Manassas, VA) and maintained in a humidified atmosphere containing 5% CO₂ at 37°C. The cells were cultured in Dulbecco's modified Eagle's medium (DMEM; Sigma, St Louis, MO) supplemented with 10% fetal bovine serum (FBS).

Mice

All animal experiments were approved by The University of Texas MD Anderson Cancer Center Institutional Animal Care and Use Committee. Male C57/BL6 mice were purchased from Harlan Laboratories (Livermore, CA), fed lab chow diet (Harlan Laboratories) and water *ad libitum*, and housed at the MD Anderson animal facility. The mice were acclimatized for 3 days prior to initiation of the study. LLC cells (1×10^6) were injected into the right flanks of the mice at 6 to 8 weeks of age. When the resulting tumors were palpable, the mice were randomly assigned to a control or experimental group. The mice were killed with CO₂ overdose after 5 to 6 experimental/control sessions or after their tumor sizes reached the allowable size limit (≤ 1.5 cm in diameter) of the guidelines of the MD Anderson Institutional Animal Care and Use Committee. Tumor volume was measured every other day and calculated accordingly.¹³ At the end of the study, tumors were rapidly collected from the mice, weighed, and flash-frozen in liquid nitrogen or fixed in formalin for further analysis. Terminal blood was collected via cardiac puncture, and serum was prepared and stored at -80°C for cytokine analysis.

Experimental Exposure

SLH produced the experimental condition (Ex exposure). SLH has psychic abilities and more recently has been considered a healer. He has been documented to accurately infer the memories and experiences of people^{9,11,12} and his accuracy has been correlated with specific neurological anomalies within his right prefrontal cortex as measured by QEEG and single-photon emission computerized tomography. What has been called the "Harribance Configuration" is a brief gamma (30-40 Hz) pattern over the right temporofrontal regions. Spectral analyses showed a major power enhancement of around 20 Hz over the right frontocentral and temporal lobe.¹¹ Low-resolution electromagnetic tomography (sLORETA) revealed increased activation was also localized within the right temporal lobe and extended into the adjacent insula. SLH has been studied by numerous laboratories for over 20 years in various conditions.⁹⁻¹¹

Control Exposure

Lorenzo Cohen (LC) served for the control condition. The objective was to exactly mimic SLH's movements when working with the cell and animal experiments. This would control for exposure to a human and movement. He also ensured the integrity of what was going on in the room during all experimental procedures. LC is a research psychologist who has conducted extensive research in psycho-oncology and studied mind-body practices such as yoga, meditation, tai chi, and qigong (both external and internal qigong practices). Although a yoga practitioner himself, during the exposure sessions when he was observing and mimicking SLH's movements he did not focus any thought toward the cells/animals and simply replicated SLH's movements.

For *in vitro* studies, A549 cells (1×10^5) were plated overnight followed by one time only exposure either to Ex (SHL) or control (LC) conditions for 30 minutes at room temperature. For the *in vivo* studies, mice were exposed to either Ex or control conditions for 30 minutes every 2 to 3 days for 5 to 6 exposure sessions (approximately 2-3 weeks) or after the tumor size reached the allowable size limit. For both the *in vitro* and *in vivo* studies, SLH and LC were in the same room approximately 15 feet apart. We note that this distance is a bit close and that the purported electromagnetic fields (EMFs) or other emissions from SLH might influence the cells and animals in the control conditions. Yet this effect would ultimately support the null hypothesis by decreasing any group differences. For all experiments and all sessions, about half the time SLH either held both hands over the plated cells/experimental cages housing the mice or moved his right arm over the plates/cages. The other half of the time the plates/cages were kept on a shelf so that SLH could place his forehead near them as it was previously

shown that the EMF activity was especially high around his right prefrontal cortex.¹⁴ LC watched SLH the whole time and mimicked all of his movements.

Cells exposed to Ex and control conditions were housed in separate incubators. Similarly, the mice in the different groups were kept in separated racks in the housing facility.

Cell Viability

The effect of the Ex and control exposure on the growth of A549 and LLC cells was assessed by the PrestoBlue or MTT assay. A549 and LLC cells were seeded at a density of 10 000 per well in 96-well plates in DMEM medium and incubated for 24 hours. Following incubation, cells were exposed to the Ex or control conditions for 30 minutes at room temperature. They were then transferred back to incubator and incubated for additional 3 hours. The cell viability was measured right after the exposure conditions (approximately 30 minutes) or 3 hours using either PrestoBlue or MTT reagent according to the manufacturer's instructions. For cell viability measurement with PrestoBlue, briefly, 20 μ L of the PrestoBlue reagent was added to each well containing 200 μ L media. After 30 minutes of incubation at 37°C, the fluorescence was read at a wavelength of 590 (Ex/Em: 560/590 nm) using a V-Max Micro-plate Reader by Molecular Devices, Inc (Sunnyvale, CA). For the cell viability measured with the MTT assay, 100 μ L MTT (1 mg/mL) was added to each well and plates were incubated at 37°C for 2 hours. The stained cells were then dissolved in DMSO (dimethyl sulfoxide) and the absorbance of the solution was determined at 570 nm by a V-Max Micro-plate Reader (Molecular Devices, Inc). Experiments were repeated at least 2 times.

Mitochondrial Staining

Cells were plated in chamber slides at a concentration of 4×10^4 per well 24 hours prior to exposure. After Ex and control exposure, live cells were stained with MitoTracker Mitochondrion-Selective Probe (M7512 MitoTracker Red CMXRos, Thermofisher/Invitrogen) at a concentration of 500 nM diluted in phosphate-buffered saline (PBS) for 30 minutes. Stained cells were washed with PBS and fixed in 10% formalin for 30 minutes. Stained cells were then mounted with ProLong Gold Antifade and visualized on the same day using fluorescent microscopy at Excitation 567 nm and Emission at 599 nm.

Immunoblotting

Cytosolic extracts were prepared from A549 cells or tumor tissues exposed to Ex or control conditions. Briefly, cells were washed in PBS and then resuspended in 50 μ L of lysis buffer (20 mM HEPES [*N*-2-hydroxyethylpiperazine-*N'*-2-ethanesulfonic acid], pH 7.5, 10 mM KCl, 1.5 mM MgCl₂,

1 mM EDTA [ethylenediaminetetraacetic acid], and 1 mM dithiothreitol [DTT]). After sonication on ice for 3 minutes with a sonicator 3000 (Misonex Inc, Farmingdale, NY), the protein concentrations were determined by the Bradford assay. Immunoblot assays were performed as per standard procedure. Briefly, equal amounts (15 μ g) of protein were subjected to sodium dodecyl sulfate-polyacrylamide gel electrophoresis (SDS-PAGE) followed by transfer to PVDF membranes. Membranes were probed with the antibodies of pAkt (No. 9271, Cell Signaling, Danvers, MA), pERK (No. 9102S, Cell Signaling), PD-L1 (No. MAB90781, R&D System), and β -actin (No. A5441, Sigma, St Louis, MO). Secondary antibodies were chosen depending on the detection method. For the detection of protein using LICOR Odyssey scanner (LI-COR Biosciences, Lincoln, NE), membrane was incubated in IRDye Secondary antibody (1:20 000, No. 925-32211, LI-COR) at room temperature for 1 hour followed by 3 washes with TBS-T. Membrane was then imaged using LI-COR Odyssey scanner and bands were quantified with Image Studio Lite software. Alternatively, secondary antibodies consisting of horseradish peroxidase (HRP)-conjugated goat anti-mouse IgG and anti-rabbit IgG (1:500 vol/vol) were purchased from Santa Cruz (Santa Cruz, CA). The membranes were visualized using SuperSignal substrate (Pierce ECL Plus, Thermo Fisher Scientific). β -actin was detected for normalization of results.

Immunohistochemistry

Formalin-fixed, paraffin-embedded tissue sections were placed on slides and subjected to immunohistochemical staining for anti-Ki67, cleaved caspase-3, CD68, and pS6 antibodies.

Reverse-Phase Proteomic Array

Frozen tumor lysates were subjected to reverse-phase proteomic array (RPPA) analysis by the Functional Proteomics Reverse Phase Protein Array Core at MD Anderson. Briefly, tumors were pulverized in liquid nitrogen and then suspended in ice-cold lysis buffer (1% Triton X-100, 50 mM HEPES, pH 7.4, 150 mM sodium chloride, 1.5 mM magnesium chloride, 1 mM EDTA, 100 mM sodium fluoride, 10 mM sodium pyrophosphate, and 1 mM sodium orthovanadate, 10% glycerol) supplemented with proteinase inhibitors (Roche Applied Science, Madison, WI). The tumors were then diluted and subjected to RPPA analysis as described previously.¹⁵

Inflammation and Immune Profiling

Serum chemokine and cytokine levels were measured using customized Multiplex Assay Kits (Meso Scale Discovery,

Rockville, MD). Tumor and spleen immune cell profiling was performed using a published method.¹⁶ Briefly, spleen and tumor tissues were collected and placed in plain 1× HBSS. For isolation of lymphocytes from spleens and tumors, protocols described by Dorta et al were used.¹⁶ In each sample, 1×10^6 cells were used for staining for immune cell surface markers. Cells were then incubated at 4°C for 1 hour with antibodies against mouse CD4 (BioLegend, San Diego, CA), CD3 (BD Biosciences, San Jose, CA), CD8 (BioLegend), CD19 (BD Biosciences), and CD25 (BioLegend). Subsequently, the cells were washed twice with PBS containing 2% FBS and then fixed and permeabilized with FoxP3 Fix/Perm Kit (ThermoFisher Scientific, Waltham, MA). Then cells were washed twice with wash buffer and incubated with intracellular markers: Foxp3 (eBioscience, San Diego, CA), IFN- γ (BioLegend) for 1 hour at 4°C. Antibodies were diluted according to the manufacturers' recommendations. All the samples were collected on a BD LSRFORTESSA X-20 (BD Biosciences) and analyzed using FlowJo software (FlowJo v.10, Ashland, OR).

Statistical Analysis

The Prism software program (GraphPad Software, San Diego, CA) was used to perform statistical tests (*t* test or analysis of variance). *P* values less than .05 were considered statistically significant. All data are presented as means \pm standard error of the mean.

Results

Experimental Exposure Reduced the Viability of Human and Mouse NSCLC Cells by Reduction of PI3K/Akt Pathway

To investigate the effects of the experimental exposure on cell growth in NSCLC, both human and mouse NSCLC cells were exposed to the Ex and control conditions. As shown in Figure 1A, the Ex exposure moderately, yet significantly, reduced cell viability in human NSCLC A549 cells by 15% to 20% ($P < .05$) when the cell viability was measured soon after the completion of exposure (30 minutes) or 3 hours later. A comparable level of inhibitory effect on the growth of mouse NSCLC was also achieved when mouse LLC cells were exposed to the Ex condition compared with that of control (Figure 1B). To confirm the effects of Ex exposure on the growth of A549 cells, the cells were subjected to mitotracker staining, which is regularly used to stain the mitochondria of the cells. There were fewer cells in the Ex exposure condition and fewer mitotracker-positive cells (Figure 1C-c and d) relative to the controls (Figure 1C-a and b). Given past studies showed that bio-field therapy can inhibit the proliferation of breast cancer cells through down regulation of PI3K/Akt and ERK

pathways⁵ and to determine the molecular mechanisms associated with the Ex exposure-induced cell growth inhibition on A549 cells, we examined the expression of proteins associated with these 2 major oncogenic pathways, PI3K/Akt and ERK pathways, in A549 cells. As shown in Figure 1D, expression of phosphorylated Akt was suppressed in the A549 cells in a time-dependent manner in the Ex condition compared to that of the control condition. In contrast, there was only a trend showing increased expression of pERK measured soon after Ex exposure, but no changes or group differences in the abundance of phosphorylated ERK in A549 cells 3 hours after exposure.

Experimental Exposure Suppressed the Growth of LLC Tumor

To further investigate whether the growth inhibitory effect of Ex exposure in vitro lung cancer cells can be recapitulated in the in vivo setting, we conducted 3 experiments to examine the Ex exposure on tumor growth in the LLC mouse model. In 2 of the experiments, the Ex and control exposure was started either when a tumor had just become palpable or when its initial volume was no more than 20 mm³ (experiments 1 and 2). In both of these experiments, we found that the mean tumor volume was marginally smaller ($n = 5$ per group; Figure 2A) or significantly smaller ($n = 9$ per group; Figure 2B) in the Ex exposure condition than in the control condition. Also, after pooling results from experiments 1 and 2, the average tumor volume (Figure 2C) and tumor weight (Figure 2D; $n = 14$) were significantly smaller in the pooled Ex exposure conditions than in the control conditions ($P < .05$). In contrast, in the third experiment, in which the exposure to the 2 different conditions started after the initial tumor volume was 80 to 100 mm³, the effect on the tumor size was minimal (Figure 2E; $n = 4$ per group).

Experimental Exposure Inhibited the Proliferation of LLC Tumor

Histological examination of tumor sections revealed that the tumors in the mice in the Ex exposure condition had an average of 15% fewer Ki67-positive cells than did those in the control condition (Figure 3A-C); however, the differences did not reach statistical significance. In line with this, the tumors derived from the Ex exposure condition had marginally increased cleaved caspase-3-positive cells than did the control condition tumors (Figure 3D-F). Assessment of the phosphorylation of ribosomal protein S6 (pS6), a downstream target of mTOR/PI3K and a cytoplasmic cell proliferation marker,¹⁷ revealed the Ex exposure reduced pS6 expression by an average of 50% (Figure 3G-I; $P = .06$). Interestingly, the pathologist who was blinded to group assignment noted that 33% of the mice in the control group

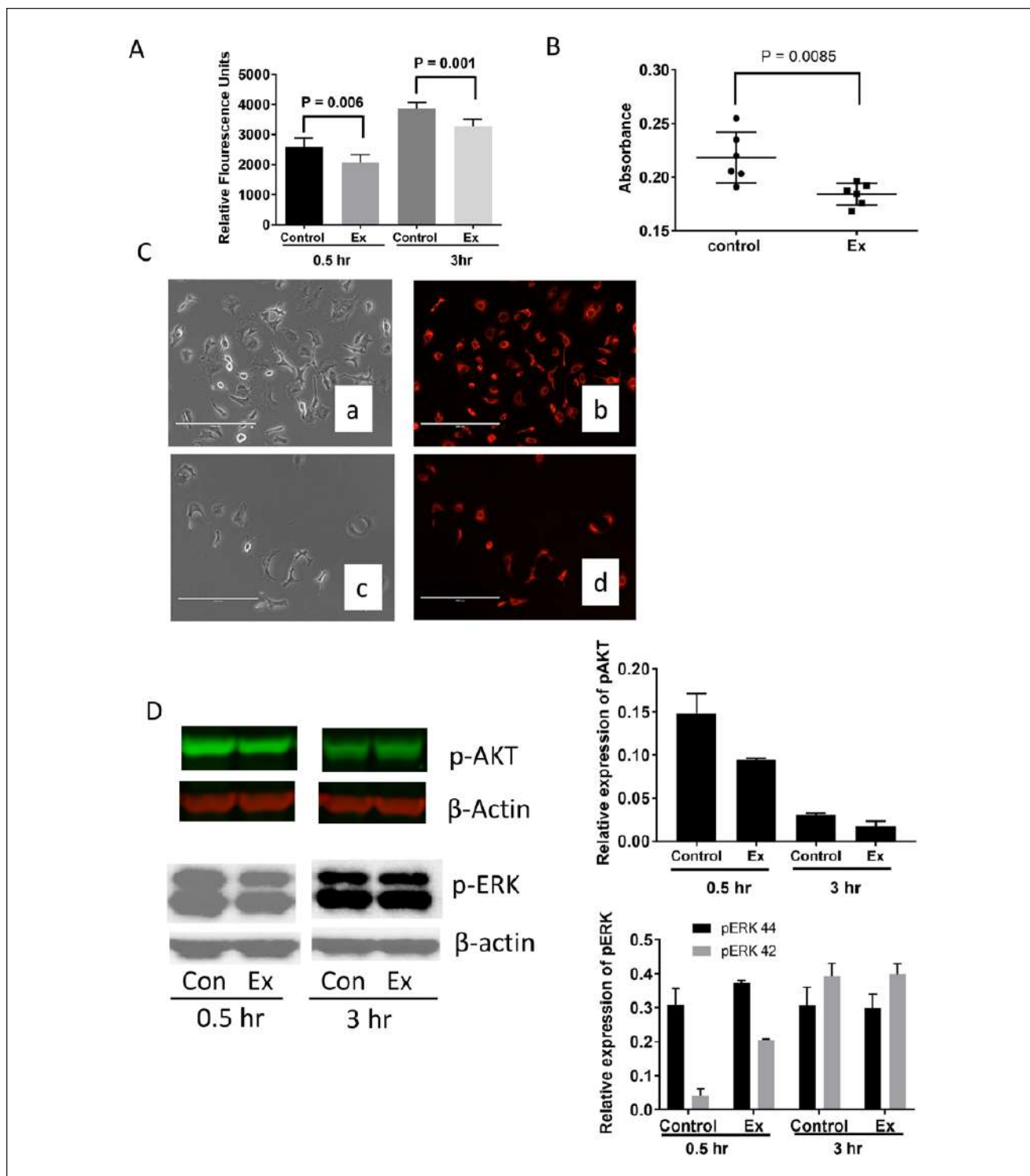


Figure 1. The effect of the experimental exposure (Ex) on the growth of human and mouse lung cancer cells. (A) The viability of human NSCLC A549 cells (Ex or control) measured 30 minutes and 3 hours after the exposures (3 hours). The Ex exposure led to a significant reduction of cell viability in this particular cell line. Cell viability was detected by PrestoBlue staining. (B) The viability of mouse Lewis Lung Carcinoma (LLC) cells 3 hours after the cells were exposed to Ex or control conditions measured by MTT assay. (C) The staining of mitotracker dye in A549 cells in control (a and b) and Ex (c and d) conditions. (D) Expression of pAkt and pERK in A549 cells at the end of the exposure (0.5 hour) or 3 hours after the Ex or control (Con) exposure. Data are presented as means \pm standard error from 2 replicated experiments.

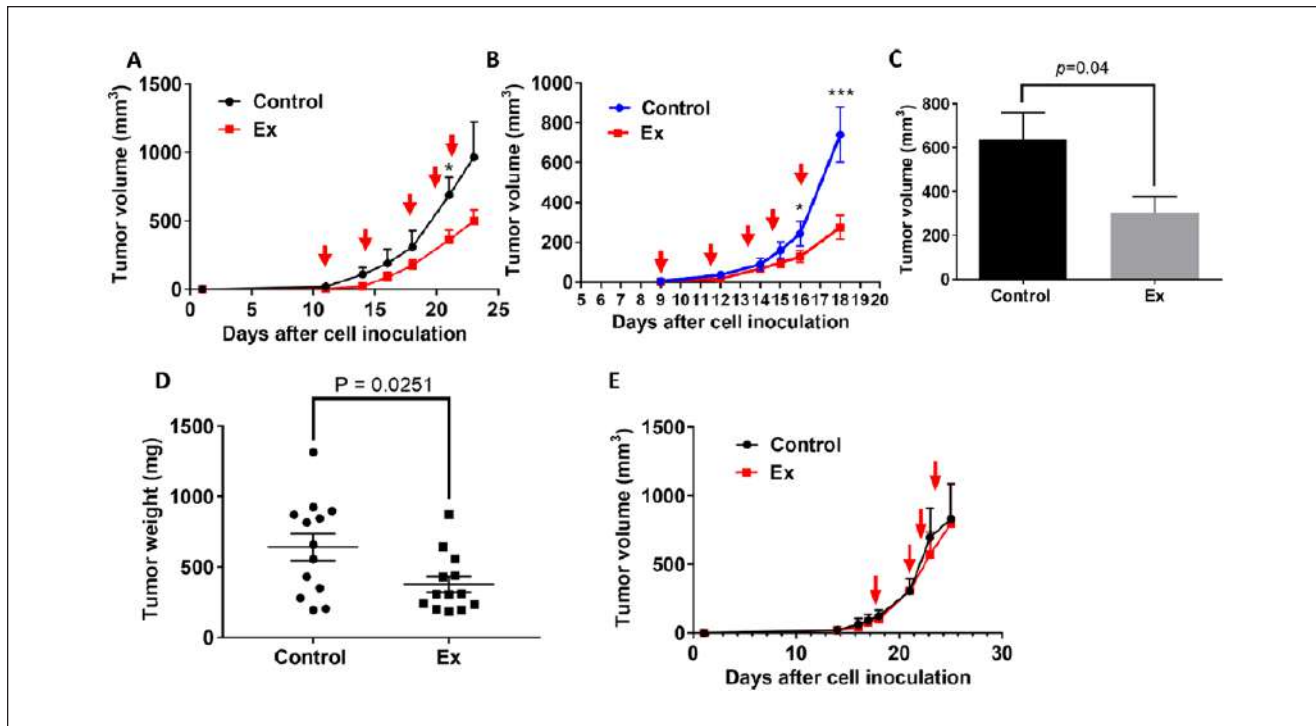


Figure 2. The effect of the experimental exposure (Ex) on tumor growth in a mouse LLC model. (A) The tumor growth curves for Ex ($n = 5$) and control ($n = 4$) mice with LLC in which the exposures were initiated when tumors were barely palpable (experiment #1). (B) The tumor growth curves for Ex ($n = 9$) and control ($n = 9$) mice in which exposures were initiated when tumor volumes were 4 to 6 mm³ (experiment #2). The red arrows indicate when the mice received the experimental and control exposure. (C) The final tumor volumes in the Ex and control exposure mice from experiment #2. (D) The mean tumor weights in Ex and control exposure groups from the pooled data from experiments 1 and 2 ($n = 13-14$ /group). (E) The tumor growth curves for Ex ($n = 4$) and control ($n = 4$) mice in which the exposures were initiated when tumor volume reached about 80 to 100 mm³ (experiment #3). The red arrow indicates when the mice received the experimental and control exposure. * $P < .05$, *** $P < .005$, for Ex exposure mice compared with controls. Data are presented as means \pm standard error.

had tumor infiltration of the surrounding tissues, whereas none of the mice in the experimental group had similar phenotypical infiltration (data not shown).

Experimental Exposure Altered Tumor Immunity and Inhibited Expression of PD-L1

A number of plausible mechanisms could account for the possible antitumor effects of the experimental exposure such as changing influx of Ca⁺ channels^{18,19} and disturbance of energy metabolism via alteration of mitochondrial potential.²⁰ However, those studies mainly focused specifically on changes in the tumor cells instead of interrogating the systemic effects of biofield therapies on the whole animal or on the stromal tissue surrounding tumors. To understand if the experimental exposure might reduce tumor growth by directly affecting tumor cells or changing the tumor microenvironment, we performed proteomic analysis of LLC samples using RPPA to identify any changes in the expression of proteins that regulate cell growth or cell signaling transduction or tumor cell immunity. While a

number of signaling pathways were altered in the tumors from mice of the Ex exposure condition relative to the control condition (Supplementary Figure S1, available online), the protein with the most noticeable change in expression among the 300 proteins examined was the checkpoint protein PD-L1. The relative level of expression of PD-L1 protein in the Ex exposure tumors was reduced by 78% compared with that of the control tumors (Figure 4A). Although the difference did not reach statistical significance, the reduction of PD-L1 protein expression in the Ex exposure tumors were further confirmed using Western blotting (Figure 4B and C). We also observed a 71% reduction in 3-phosphoinositide-dependent protein kinase-1 (PDK1) in the tumor tissue from the Ex group compared with that of control (Figure S1A).

Experimental Exposure Reduced Inflammation in LLC Tumor-Bearing Mice

Examination of serum cytokine levels revealed that expression of several inflammatory cytokines, such as interleukin

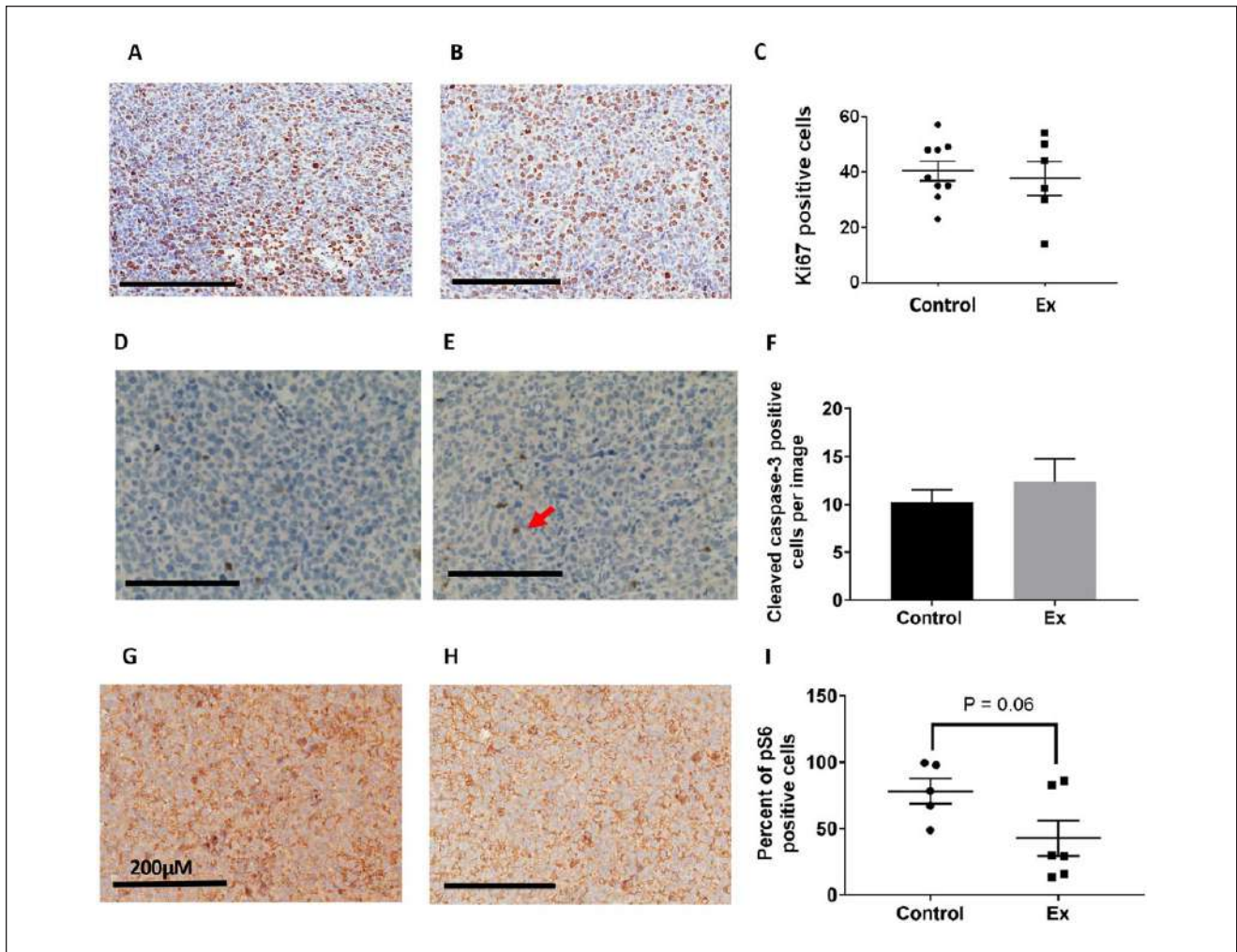


Figure 3. Immunohistochemical staining of LLC sections for proliferation and apoptotic markers. Stains of tumor sections obtained from (A) control and (B) experimental exposure (Ex) mice for the cell proliferation marker Ki67. (C) Quantification of Ki67-positive cells in the tumor sections. Stains of tumor sections obtained from (D) control and (E) Ex mice for cleaved caspase-3. The red arrow indicates apoptotic cells. (F) Quantification of cleaved caspase-3-positive cells in the tumor sections. Stains of tumor section obtained from (G) control and (H) Ex mice for pS6 protein. (I) Quantification of pS6 positive cells in the tumor sections.

6 (IL-6), monocyte chemoattractant protein 1 (MCP-1), mouse keratinocyte-derived chemokine, and tumor necrosis factor- α , were downregulated in the Ex exposure mice but not in the control mice. In particular, the reduction of MCP-1 expression was statistically significant in the Ex exposure mice ($P = .047$; Figure 4D).

To further examine whether the antitumor activity of the Ex exposure was associated with reduced inflammation and/or alteration of immune function, we examined the immune cell profiles in the tumors and spleens and the proportion of different immune cells and tumor-infiltrating cells. These analyses revealed that the tumors of the Ex exposure mice had lower numbers of regulatory T cells (approximately 84% lower; Figure 5A) and a 2-fold increase in CD8⁺ cytotoxic T-cells relative to the control mice

(Figure 5B). Given that MCP-1 is predominantly secreted by monocytes and macrophages,²¹ especially tumor-infiltrating macrophages, we measured the expression of CD68 in the tumor tissue. The number of CD68⁺ macrophages was notably higher in the control tumors than in the Ex exposure tumors ($P = .08$; Figure 5C-E).

Discussion

Although biofield therapies delivered via a device or human have proven capable of slowing the growth of cancer cells in vitro, few, if any, demonstrated that this kind of therapy can slow down the growth of tumors in animal models. Here, we showed that exposure to the experimental condition versus a control condition was capable of reducing the

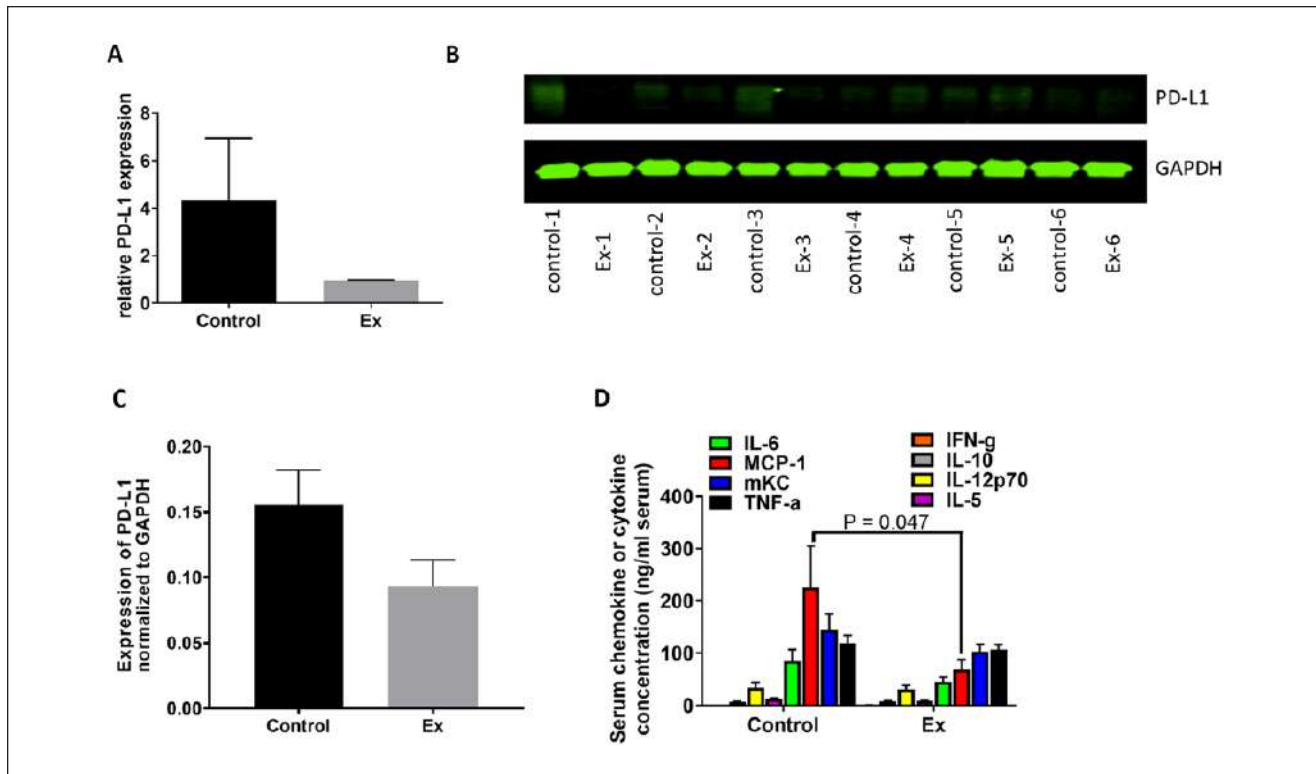


Figure 4. PD-L1 expression in LLCs and serum chemokine and cytokine levels. (A) PD-L1 expression in tumor samples measured by RPPA. (B) Western blot of PD-L1 expression in the tumors from study mice. (C) Quantitative data for the Western blot results. (D) The serum levels of cytokines and chemokines in the control and Ex exposure mice. MCP-1, monocyte chemoattractant protein-1; mKC, mouse keratinocyte-derived chemokine; TNF- α , tumor necrosis factor α ; IFN- γ , interferon- γ .

viability of both human A549 and mouse LLC cells as well as slowing down the growth of LLC mouse syngeneic tumors. We noted down regulation of pAkt and pS6 protein expression, suggesting the possible antitumor effect of this kind of biofield treatment was mediated through reduced proliferation and downregulation of PI3K/mTOR signaling. This is consistent with previous studies demonstrating that biofield therapies reduced the growth of colon cancer cell growth through modulation of PI3K pathway.⁵ Additionally, the pathologist who was blinded to group assignment did not note any tumor infiltration of the surrounding tissues for mice in the experimental exposure group, whereas one third of the controls had tumor infiltration of the surrounding tissues. This suggests that the experimental exposure reduced the local invasiveness of primary tumors. This is consistent with a previous study showing that Therapeutic Touch exposure led to less metastatic potential of lymph nodes in a breast cancer animal model.³ Although previous studies have shown biofield therapies modulate the immune system,^{4,22} we showed for the first time the potential mechanisms of the antitumor activity of the experimental exposure were at least partially mediated through modification of immune function and anti-inflammatory activity in our mouse lung tumor model. The one experiment where we

found no differences between the experimental and control was for the in vivo study where the exposures were started once the tumor volume was 80 to 100 mm³, disallowing rejection of the null hypothesis for this condition. However, overall our findings suggest rejection of the null hypothesis, as there were significant differences between the experimental and control conditions in both in vivo and in vitro models and in the exploration of the purported biological mediators.

Various mechanisms of action have been proposed for the effects of biofield therapies on the growth of tumor cells. For example, external Qigong was capable of inhibiting the growth of prostate, breast, and colon cancer cells by suppressing pAkt, pERK, NF- κ B, and glucose metabolism.⁴⁻⁷ This is consistent with our findings where we found that the experimental exposure resulted in reductions in expression of pAKT in A549 cells and in pS6 from the LLC tumor tissues. Additionally, we also observed a 71% reduction in PDK1 protein in the tumor tissue from the experimental exposure group compared with that of control (Figure S1). PDK1 is responsible for phosphorylating Akt at Theronine 308 position when stimulated by insulin or growth factors.²³ Together, these data further suggest that the tumor growth inhibition seen in the experimental

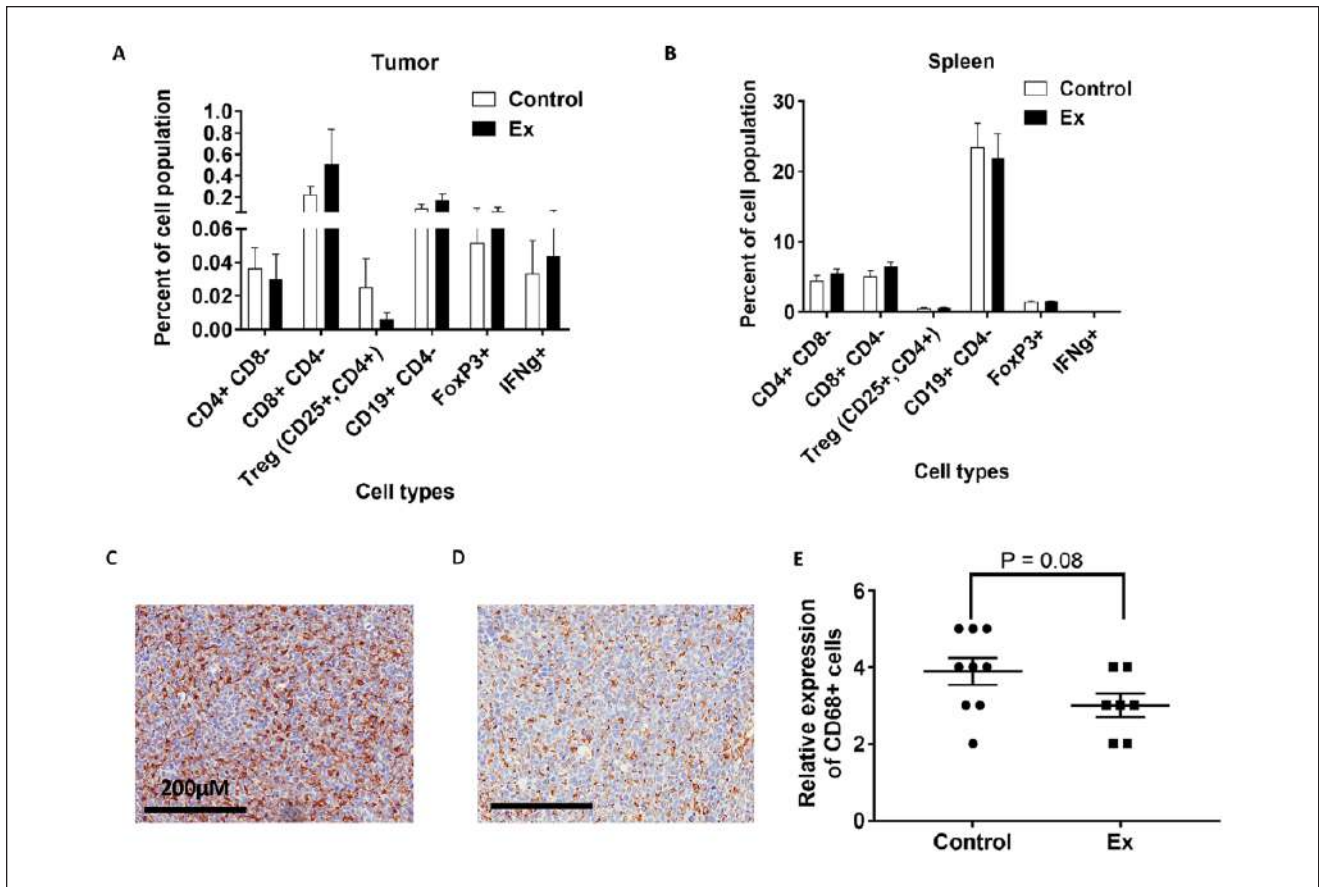


Figure 5. Immune modification in mice with LLC. (A) Tumors and (B) spleens of mice with LLC. The data suggest that experimental exposure (Ex) increased the number of CD8+ cytotoxic T cells while suppressing the number of regulatory T (Treg) cells, which are known to support the growth of tumor cells. Stains of tumor-infiltrating macrophages from (C) control and (D) Ex exposure mice for CD68. (E) Quantification of CD68+ cells in the tumors of the control and Ex exposure mice.

exposure group may in part be due to downregulation of the PI3K/mTOR pathway.

Additionally, Gronowicz et al showed that Therapeutic Touch reduced the metastatic potential of breast cancer and significantly decreased the amount of IL1 α , IL1 β , MIP, and MIG in the serum and CD11b+ macrophages in popliteal lymph nodes of mice injected with breast cancer 666c14 cells.³ In our study, we showed that the experimental exposure significantly inhibited the growth of LLC tumors when the exposure was started in the mice carrying just palpable or small tumors. In contrast, limited impact on the tumor growth was observed in mice when the exposure was started after more substantial tumor growth. Given that immune therapy generally works more efficiently in tumors that contain high numbers of immune infiltrating cells, which is typically found with early-stage tumors,²⁴ perhaps the anti-tumor effect of the experimental exposure was mediated through immune modification. Indeed, the experimental exposure significantly reduced the serum level of MCP-1, a chemokine known to be associated with increased

proliferation and metastasis of various cancers including NSCLC,^{25,26} and resulted in reductions in IL-6 and tumor necrosis factor. We also found that the experimental exposure marginally reduced tumor-infiltrating CD68+ macrophages (*P* = .08) and resulted in reductions in Tregs and PD-L1 expression. However, due to the small sample size, large variance in the control group, and some marginally statistically significant effects these findings should be interpreted with caution.

Our findings suggest that the experimental exposure not only directly acted on tumor cells but also moderately modulated the immune system in tumor-bearing mice. A strength of these series of studies was our ability to replicate the findings when the experimental exposure was started when the tumors were still small. In light of the association of MCP-1 abundance and tumor-infiltrating macrophages with stimulation of tumor growth and metastasis for various cancer types, including lung cancer, and that LLCs are known to be immunogenic, our findings suggest that in-depth mechanistic research is warranted to

further study this type of treatment. However, until clinical evidence is supportive, patients should not be encouraged to seek out biofield therapies as a stand-alone treatment and should always seek conventional cancer treatments to manage their disease.³

There are several limitations in this study. Most important, we were not able to implement any measurements of electromagnetic fields or biophoton emissions from SLH. It is well accepted that the human body emits EMFs and these fields are intricately involved in maintenance of normal function of many organ systems and overall homeostasis. The EMFs emitted by the heart and brain are measured using electrocardiograms and electroencephalograms, respectively, among other technologies. A human EMF can also be measured in a number of other ways, including examination of the emission of biophotons from the body.²⁷ EMFs are not unique to humans, or even mammals, and can be measured in all living organisms.²⁸ It is interesting to note that EMFs are now being used in conventional cancer treatment settings. For example, the US Food and Drug Administration approved the use of low-frequency alternating electric fields for the treatment of refractory glioblastoma multiforme, and for treatment of other cancers.^{29,30} EMFs also have modulated tumor growth, angiogenesis, and tumor necrosis factor in animals,³¹ as well as inhibited Eph4-MEK-Bcl2 breast tumor growth in mice via induction of apoptosis.^{5,32} In addition, the electroencephalographic (EEG) pattern of SLH has been studied and recorded while he engaged in a session,^{9-11,33} and the EEG-based digitized EMF generated through his pattern has been applied to melanoma cells *in vitro* and found to decrease cell proliferation.³⁴ Additionally, when researchers applied a similar EMF pattern to syngeneic C57b mice implanted with B16-BL6 melanoma cells, it resulted in smaller tumors than in sham-treated controls.^{14,19} It is, therefore, logical to hypothesize that a plausible mechanism of the antitumor effect of the experimental exposure was mediated, at least in part, through a unique EMF pattern. However, this remains speculation, as the prior study examining the EEG-based digitized EMF³⁴ was not based on the actual EMF emitted from SLH during a healing session and EMFs were not measured in the current studies. In order to better understand the mechanisms whereby humans may affect tumor growth, it is critical that future studies measure the purported emissions from the body and conduct experiments to manipulate said emissions (eg, blocking or enhancing experiments). In addition, other unmeasured mechanisms might also be part of the effect. For example, another plausible mechanism could be through modulation of the sympathetic nervous system (SNS). Exposure to a “healer” could result in a calming effect on the subject and possible reductions in SNS activation could lead to beneficial changes in the tumor microenvironment.³⁵ Future studies

should explore SNS activation and collect behavioral data. Another limitation was the close proximity of the experimental and control conditions. However, this would have resulted in an augmented effect in the control condition, diminishing the likelihood of observing statistically significant group differences. In the current case, close observation of the experimental condition outweighed the potential contamination of the groups. Future research should ensure a minimum of 20 feet between conditions. This study also only examined one *in vivo* lung cancer model. It is not clear if the current findings would generalize to other preclinical cancer models. Moreover, our trial was limited to testing the abilities of only one individual. Future research needs to include other people trained in biofield therapies and to explore the ability to train novice people. Therapeutic Touch, Healing Touch, Reiki, and Qigong all have formal training programs and this approach could be explored. Finally, it is of utmost importance for future studies to examine the EMF and biophotons emitted by SLH and others with the same purported ability to correlate the specific EMF configuration with the physiological changes in the target animal. Further characterization of mechanisms should also be explored by using EMF shielding material or by blocking specific pathways such as PI3k/mTOR pathway, MCP-1, and/or tumor-infiltrating macrophages. This would allow for more precision when isolating a specific mechanism of human emitted EMFs.

In summary, we showed for the first time that experimental exposure to a purported biofield therapy could potentially suppress the growth of NSCLC cells and mouse LLC syngeneic tumor possibly by modulating immune system and inhibiting inflammation. Given the immune system plays a significant role in tumor growth and immune therapy has significantly prolonged the survival of patients with various cancers including lung cancer, a better understanding of whether human-emitted EMF or other biofield mechanisms can alter the immune system and tumor growth suppression deserves further investigation.

Author Contributions

PY and LC designed the research; YJ, PR, MG, DC, SLH, and LC performed the experiments; PY, YJ, and MG analyzed the data; YJ, LC, and YP wrote and reviewed the manuscript. All authors contributed to the manuscript at various stages.

Declaration of Conflicting Interests

The author(s) declared the following potential conflicts of interest with respect to the research, authorship, and/or publication of this article: SLH has a private practice in Sugar Land, Texas, and is the president of the Sean Harribance Institute for Parapsychology, Inc. He is also the honorary director of the Sean Harribance Institute for Parapsychology Research, a 501(c)(3) corporation.

Funding

The author(s) disclosed receipt of the following financial support for the research, authorship, and/or publication of this article: This project was supported by Black Beret Life Sciences, Marie Bosarge, and the NIH/NCI under Award Number P30CA016672.

References

- Hammerschlag R, Jain S, Baldwin AL, et al. Biofield research: a roundtable discussion of scientific and methodological issues. *J Altern Complement Med.* 2012;18:1081-1086.
- Jain S, Hammerschlag R, Mills P, et al. Clinical studies of biofield therapies: summary, methodological challenges, and recommendations. *Glob Adv Health Med.* 2015;4(suppl):58-66.
- Cohen L, Chen Z, Arun B, et al. External qigong therapy for women with breast cancer prior to surgery. *Integr Cancer Ther.* 2010;9:348-353.
- Gronowicz G, Secor ER Jr, Flynn JR, Jellison ER, Kuhn LT. Therapeutic Touch has significant effects on mouse breast cancer metastasis and immune responses but not primary tumor size. *Evid Based Complement Alternat Med.* 2015;2015:926565.
- Yan X, Shen H, Jiang H, Hu D, Wang J, Wu X. External Qi of Yan Xin Qigong inhibits activation of Akt, Erk1/2 and NF- κ B and induces cell cycle arrest and apoptosis in colorectal cancer cells. *Cell Physiol Biochem.* 2013;31:113-122.
- Yan X, Shen H, Jiang H, et al. External Qi of Yan Xin Qigong Induces apoptosis and inhibits migration and invasion of estrogen-independent breast cancer cells through suppression of Akt/NF- κ B signaling. *Cell Physiol Biochem.* 2010;25:263-270.
- Yan X, Li F, Dozmorov I, et al. External Qi of Yan Xin Qigong induces cell death and gene expression alterations promoting apoptosis and inhibiting proliferation, migration and glucose metabolism in small-cell lung cancer cells. *Mol Cell Biochem.* 2012;363:245-255.
- Yan X, Shen H, Jiang H, et al. External Qi of Yan Xin Qigong induces G2/M arrest and apoptosis of androgen-independent prostate cancer cells by inhibiting Akt and NF- κ B pathways. *Mol Cell Biochem.* 2008;310:227-234.
- Roll WG, Persinger MA, Webster DL, Tiller SG, Cook CM. Neurobehavioral and neurometabolic (SPECT) correlates of paranormal information: involvement of the right hemisphere and its sensitivity to weak complex magnetic fields. *Int J Neurosci.* 2002;112:197-224.
- Persinger MA, Saroka KS. Protracted parahippocampal activity associated with Sean Harribance. *Int J Yoga.* 2012;5:140-145.
- Kelly EF. On grouping of hits in some exceptional psi performers. *J Amer Soc Psychological Res.* 1982;76:101-142.
- Persinger MA. The Harribance effect as pervasive out-of-body experiences: NeuroQuantal evidence with more precise measurements. *NeuroQuantology.* 2010;8(4):444-465.
- Zhuang L, Xu L, Wang P, et al. Na⁺/K⁺-ATPase α 1 subunit, a novel therapeutic target for hepatocellular carcinoma. *Oncotarget.* 2015;6:28183-28193.
- Hu JH, St-Pierre LS, Buckner CA, Lafrenie RM, Persinger MA. Growth of injected melanoma cells is suppressed by whole body exposure to specific spatial-temporal configurations of weak intensity magnetic fields. *Int J Radiat Biol.* 2010;86:79-88.
- Tibes R, Qiu Y, Lu Y, et al. Reverse phase protein array: validation of a novel proteomic technology and utility for analysis of primary leukemia specimens and hematopoietic stem cells. *Mol Cancer Ther.* 2006;5:2512-2521.
- Bartkowiak T, Singh S, Yang G, et al. Unique potential of 4-1BB agonist antibody to promote durable regression of HPV+ tumors when combined with an E6/E7 peptide vaccine. *Proc Natl Acad Sci U S A.* 2015;112:E5290-5299.
- Cappella P, Gasparri F. Highly multiplexed phenotypic imaging for cell proliferation studies. *J Biomol Screen.* 2014;19:145-157.
- Pall ML. Electromagnetic fields act via activation of voltage-gated calcium channels to produce beneficial or adverse effects. *J Cell Mol Med.* 2013;17:958-965.
- Buckner CA, Buckner AL, Koren SA, Persinger MA, Lafrenie RM. Inhibition of cancer cell growth by exposure to a specific time-varying electromagnetic field involves T-type calcium channels. *PLoS One.* 2015;10:e0124136.
- Pokorny J, Foletti A, Kobilkova J, et al. Biophysical insights into cancer transformation and treatment. *ScientificWorldJournal.* 2013;2013:195028.
- Yoshimura T, Robinson EA, Tanaka S, Appella E, Leonard EJ. Purification and amino acid analysis of two human monocyte chemoattractants produced by phytohemagglutinin-stimulated human blood mononuclear leukocytes. *J Immunol.* 1989;142:1956-1962.
- Gronowicz G, Secor ER, Flynn JR, Kuhn LT. Human biofield therapy does not affect tumor size but modulates immune responses in a mouse model for breast cancer. *J Integr Med.* 2016;14:389-399.
- Du J, Yang M, Chen S, Li D, Chang Z, Dong Z. PDK1 promotes tumor growth and metastasis in a spontaneous breast cancer model. *Oncogene.* 2015;35:3314-3323.
- Budhu S, Wolchok J, Merghoub T. The importance of animal models in tumor immunity and immunotherapy. *Curr Opin Genet Dev.* 2014;24:46-51.
- Fridlender ZG, Kapoor V, Buchlis G, et al. Monocyte chemoattractant protein-1 blockade inhibits lung cancer tumor growth by altering macrophage phenotype and activating CD8⁺ cells. *Am J Respir Cell Mol Biol.* 2011;44:230-237.
- Qian BZ, Li J, Zhang H, et al. CCL2 recruits inflammatory monocytes to facilitate breast-tumour metastasis. *Nature.* 2011;475:222-225.
- Van Wijk R, Van Wijk EPA, van Wietmarschen HA, Greef JVD. Towards whole-body ultra-weak photon counting and imaging with a focus on human beings: a review. *J Photochem Photobiol B.* 2014;139:39-46.
- Zhou SA, Uesaka M. Bioelectrodynamics in living organisms. *Int J Eng Sci.* 2006;44:67-92.
- Stupp R, Taillibert S, Kanner A, et al. Effect of tumor-treating fields plus maintenance temozolomide vs maintenance temozolomide alone on survival in patients with glioblastoma: a randomized clinical trial. *JAMA.* 2017;318:2306-2316.
- Rick J, Chandra A, Aghi MK. Tumor treating fields: a new approach to glioblastoma therapy. *J Neurooncol.* 2018;137:447-453.

31. Crocetti S, Beyer C, Schade G, Egli M, Frohlich J, Franco-Obregon A. Low intensity and frequency pulsed electromagnetic fields selectively impair breast cancer cell viability. *PLoS One*. 2013;8:e72944.
32. Tatarov I, Panda A, Petkov D, et al. Effect of magnetic fields on tumor growth and viability. *Comp Med*. 2011;61:339-345.
33. Hunter MD, Mulligan BP, Dotta BT, et al. Cerebral dynamics and discrete energy changes in the personal physical environment during intuitive-like states and perceptions. *J Consciousness Exploration Res*. 2010;1:1179-1197.
34. Karbowski LM, Harribance SL, Buckner CA, et al. Digitized quantitative electroencephalographic patterns applied as magnetic fields inhibit melanoma cell proliferation in culture. *Neurosci Lett*. 2012;523:131-134.
35. Cole SW, Nagaraja AS, Lutgendorf SK, Green PA, Sood AK. Sympathetic nervous system regulation of the tumour micro-environment. *Nat Rev Cancer*. 2015;15:563-572.